

Evaluation of the usability of a rapid flood model

Master Thesis Report



June 2013

Author:
Ilhame Oujamaa

Master Thesis

Evaluation of the usability of a rapid flood model



Ilhame Oujamaa

Delft, June 2013

This research has been done for the partial fulfillment of requirements for the degree of Master of Science in the field of Civil Engineering at the Delft University of Technology, Delft, The Netherlands

Graduation Committee:

Prof. drs. ir.J.K. Vrijling	Delft University of Technology - Hydraulic Engineering Section
Prof. dr. ir. S.N. Jonkman	Delft University of Technology - Hydraulic Engineering Section
Dr. ir. H.C. Winsemius	Deltares
Dr.ir. M. van Ledden	Delft University of Technology - Hydraulic Engineering Section
Dr. R.C. Lindenberg	Delft University of Technology - Optical & Acoustic Remote Sensing

Preface

This report marks the end of my study Hydraulic Engineering at the faculty of Civil Engineering at the Delft University of Technology.

First I would like to thank my commission members for their support and contribution throughout this thesis. Special thanks go to Hessel Winsemius from Deltares for his guidance as well as his enthusiasm during this period.

I would like to express my gratitude to some people that supported me through my master thesis. First of all, I would like to thank my siblings, Youssef, Laila and Nadia, for always encouraging me and being there for me no matter what.

Furthermore I would like to thank my friends and my housemates for supporting me through this process with long talks, drinks and laughs. Special thanks go to my two girls, Ouiam and Frauke, who have been there from the first week in Delft. Delft would not have been the same without you two. Matthieu , thank you for your support and encouragement during this period.

Summary

Background

The fight against floods is a battle that has been going on for millennia. Floods are one of the most devastating natural disasters, hitting various regions in the world each year. In the last decades the damage and the loss of human lives caused by floods has increased rapidly. Due to the large potential damage caused by floods the need for preparatory tools, like flood models and flood maps, for real-time monitoring and forecasting of floods has increased.

Objective

A major problem is that with an upcoming flood, there is often little insight into how and when the flood will proceed, especially if preparatory tools are not available. Rapid flood modeling can assist in decision making and emergency response during threatening flood situations. The concept of a rapid flood is a model which makes prediction of a flood event in 1) a short period with the use of 2) publicly available data 3) for any flood prone area in the world. This thesis evaluates the usability of a rapid flood model for river flooding and crisis management.

Methods

To find out what the contribution is of using publicly available data on a flood prediction, three case studies are done to determine which parameters and conditions of a flood event influence the prediction the most. The types of areas and rivers are distinguished by characteristics of the terrain and the rivers, using the river classification scheme of Rosgen (1994). In this study, four terrain types are examined, mountainous terrain, hilly terrain, delta with small sloped terrain and delta with relatively flat terrain.

In the first two cases, the parameters and conditions, the river characteristics, the type of land use, the varying upstream discharges and downstream water levels, are examined on the influence of the prediction of a flood. The prediction of a flood consists of the following:

- flood extent (where the flood will occur)
- flood depth (the severity of the flood)
- propagation of the flood over time (when the flood will occur)

The influence of the parameters and conditions is tested for a simple one dimensional (1D) flow schematization and for an elaborated two dimensional (2D) flow schematization. In the third case publicly available data is used for these parameters and conditions to simulate the 2011 Thailand flood event which is compared to satellite images of the flood event.

Results

In the first case study, the 1D flow schematization, the most influential parameters for the types of terrains are listed in Table 0-1:

Table 0-1 The most influential parameters for the 1D flow case study per type of river area

Type of river area	Mountainous terrain	Hilly terrain	Delta terrain with small slope	Delta with relatively flat terrain
Classes	<i>Aa+</i>	<i>B</i>	<i>C</i>	<i>DA</i>
Water level in the flood plains	<ul style="list-style-type: none"> • Floodplain roughness • Width channel 	<ul style="list-style-type: none"> • Floodplain roughness • Bed level of channel 	<ul style="list-style-type: none"> • Floodplain roughness • Width floodplain • Slope of terrain 	<ul style="list-style-type: none"> • Floodplain roughness • Width floodplain • Slope of terrain
Flood wave celerity	<ul style="list-style-type: none"> • Floodplain roughness • Width floodplain • Slope of terrain 	<ul style="list-style-type: none"> • Floodplain roughness • Width floodplain • Bed level of channel 	<ul style="list-style-type: none"> • Floodplain roughness • Width floodplain • Slope of terrain 	<ul style="list-style-type: none"> • Slope of terrain

The Thailand area, the third case study, is a relatively flat delta terrain. Using the classification of Rosgen's, the area is classified as classes C and DA. For the 2D flow case, the focus is on examining more parameters and conditions for these two types of areas. In the 2D flow case, the most influential parameters and conditions are listed in Table 0-2:

Table 0-2 the most influential parameters for the 2D flow case study

Type of river area	Delta terrain with small slope		Delta with relatively flat terrain	
Classes	C		DA	
Slope perpendicular to the channel	No slope	Small slope	No slope	Small slope
Water depth	<ul style="list-style-type: none"> • Upstream boundary condition • Floodplain roughness 		<ul style="list-style-type: none"> • Upstream boundary condition • Floodplain roughness 	<ul style="list-style-type: none"> • Upstream boundary condition • Floodplain roughness • Channel roughness
Propagation of the flood	<ul style="list-style-type: none"> • Upstream boundary condition • Floodplain roughness 		<ul style="list-style-type: none"> • Upstream boundary condition • Width channel 	<ul style="list-style-type: none"> • Upstream boundary condition • Floodplain roughness • Width channel
Flood extent	<ul style="list-style-type: none"> • Peak upstream boundary condition 		<ul style="list-style-type: none"> • Tail upstream boundary condition 	

Besides the flood depth and propagation of the flood, the flood extent is examined in the 2D flow case. For the prediction of the flood extents, the most influential condition is the upstream boundary. For delta terrains with a small slope, class C, the peak discharges have the most influence. But for flatter terrains, class DA, the tail of the discharges has a more impact than the peak discharges. It appears that in the flatter areas the river capacity depends not on the peak but more on the total volume. When this capacity is reached, the subsequent discharge causes an increase in the flood extent.

In the 1D flow case the two delta scenarios, classes C and DA, have similar influential parameters. The 2D flow case shows that the two areas differ a lot more than the 1D flow suggests. The flatter area (class DA) has more parameters and conditions that have a high influence on the prediction of a flood event than the area with a small slope, class C.

The third case, the 2011 Thailand flood event, showed that a satisfying initial flood prediction can be observed compared to the actual flood event. Especially the propagation of the flood shows a good fit with the satellite images. The simulated flood maps match the satellite images during the 4 months, mid-August till mid-November. In mid-August the flood starts in the north and travels towards the south during three months at the same rate as in the satellite images.

For the flood extent, the overall simulations give a reasonably good fit, but in certain areas the flood is over or underestimated. In the north of Thailand, a delta area with a small slope, the simulations give a good replica of the satellite images. In the south, a delta area with relatively flat terrain, there are a few areas where overestimation and underestimation of the flood extent can be found. In the south it also noticeable that in the last month, the flood waters start to retreat in the satellite images. The simulations also show a retreating flood extent, but at a much slower rate.

The flood depth was not examined for the third case study. The reason for this is that there exists no publicly available data on the real flood depths during the 2011 flood event in Thailand.

Conclusion and discussion

This study shows that a rapid model, with use of publicly available data can simulate a flood event for any flood prone area in the world. This study also shows that the most influential data differs with the type of area considered. This gives an insight into which data available resources, both time and money, should be spend on if the data is not publicly available or more details are needed.

The main conclusions and the discussion in this study are listed in the following:

- The rapid model can be setup for any flood prone area in the world in 1 or 2 days by an experienced modeler. The time to produce a prediction depends on the amount of details included in the model, and hence the desired accuracy of the prediction. In case more details (data) are used to increase the accuracy, the disadvantage is that the computation and simulation time of the model also increases.
- There is an abundant amount of publicly available data for the rapid flood model. Most of the data needs to be processed and formatted with different methods and equations before they can be used for the rapid flood model. The rapid flood model can potentially be applied for any flood prone area in the world as data used are publicly and globally available.
- The terrains types have a large influence on the usability of the rapid flood model. The classification of rivers and areas by Rosgen, 1994 is used to identify these areas into mountainous, slightly hilly, delta small slope and deltas with flat areas. The applicability of the model depends on which type of river area, the area of interest belongs to. Which methods are suitable for the data and which variables have the most influence on the prediction, depends on the type of river and area. For the four classifications tested in this study, the data for the most influential parameters and conditions are available publicly.

Recommendations

- Splitting the rapid model into multiple rapid flood models for different types of areas would improve the prediction of a flood. The north and the south area in the Thailand case can be seen as two different types of areas. By using different selected data for the two areas, the prediction of the flood event can be improved. Identifying the type of river areas is an important aspect when the rapid flood model is used for new areas.
- The results of the rapid model are compared visually to satellite images. In future research a quantitative method should be applied to compare the results so that the size of the type I and II errors can be identified. This can give a better insight into the performance of the rapid flood model.
- Including new and updating data should be an ongoing process for the rapid flood model. New data that can have a large influence on the improvement of the prediction are the implementation of hydraulic structures. If these can be included into the rapid flood model, this can solve some of the problems, like the distribution of the discharge of diverging rivers. Updating the data is also a necessity. The available data online keeps growing and expanding and the rapid flood model should be kept up to date.
- Implementation of flood prevention measures
The current rapid flood model is limited to give a prediction of a flood event for crisis management. It would be an added value if the rapid flood model can also be used to evaluate measures to prevent or delay the flood or reduce the consequences of the flood.

Content

Preface	v
Summary	vi
Content	x
1. Introduction.....	1
1.1 Background	1
1.2 Motivation.....	1
1.3 Goals and principles of a rapid flood model	1
1.4 Problem description	2
1.5 Objective and research questions	2
1.6 Methodology.....	3
1.6.1 Flood event information	3
1.6.2 Case studies part.....	3
1.7 Reader's guide.....	4
2. Information for the simulation and prediction of a flood event	5
2.1 Introduction	5
2.2 Origin of flood events	5
2.2.1 High discharges from upstream.....	5
2.2.2 Flash flood	6
2.2.3 High water from downstream	6
2.2.4 Flood prone areas	7
2.3 Prediction of a flood event	7
2.3.1 Users	7
2.3.2 Types of flood maps.....	8
2.3.3 Information on flood maps	9
2.3.4 Scale of flood map	9
2.3.5 Errors in prediction of the flood	10
2.3.6 Summary	11
2.4 Simulation of a flood event.....	12
2.5 Summary.....	15
3. General data for flood models.....	17
3.1 Data categorization	17
3.1.1 Event data	17

3.1.2	Data to characterize area	19
3.2	Methods to process data	22
3.2.1	Classification of rivers	22
3.2.2	Event data	24
3.2.3	Data to characterize area	26
3.3	Summary	29
4.	Study case: 1D flow	30
4.1	Introduction	30
4.2	Types of areas	30
4.3	Schematization for 1D flow	32
4.3.1	Equations	32
4.3.2	Values for the classes	34
4.4	Methodology	36
4.5	Results of simulation 1D flow	36
4.5.1	Introduction	36
4.5.2	Classification ratios	37
4.5.3	Real rivers	39
4.5.4	The water depth in the flood plains	40
4.5.5	The flood wave celerity in the flood plains	48
4.6	Conclusion	53
5.	Hypothetical case study (2D-flow)	55
5.1	Introduction	55
5.2	The simulations for 1D/2D flow	56
5.2.1	Schematization for the flood simulations	56
5.2.2	The output of the flood simulations	57
5.2.3	River classes	61
5.2.4	The conditions and characteristics of the flood events	62
5.3	Results of the simulations	67
5.3.1	Results for class C	67
5.3.2	Results for class DA	71
5.3.3	Differences between class C and class DA	76
5.4	Conclusion	80
5.4.1	Comparison with 1D flow	80
5.4.2	Recommendations for the 2D flow	82

6.	Case study: the 2011 Thailand flood event	83
6.1	Introduction	83
6.2	Available data for 2011 Thailand flood event	83
6.2.1	Topographic information	83
6.2.2	Water system	89
6.2.3	Precipitation	93
6.2.4	Overview of available data	96
6.2.5	Validation methodology and validation data	97
6.3	Selection of input data	100
6.3.1	Introduction	100
6.3.2	Selection of the data sources	101
6.3.3	Simulation with the combined selected data	106
6.4	Results of the rapid flood model for the three month period	108
6.4.1	Simulation for mid-September	108
6.4.2	Simulation for mid –October	114
6.4.3	Simulation for mid –November	118
6.5	Conclusions and discussion	122
6.5.1	Conclusion	122
6.5.2	Discussion	123
7.	Conclusions and recommendations	126
7.1	Summarized main conclusions	126
7.2	Answering research question	127
7.3	Recommendations	132
7.3.1	Improving the current rapid flood model	132
7.3.2	Including new data into the rapid flood model	133
7.3.3	Further developments of the rapid flood model	133
	References	140
	Appendix	143

1. Introduction

1.1 Background

Flooding of areas is a natural hazard that has been occurring for millennia. In the recent decades the damage and the loss of human lives caused by flood has increased rapidly due to increased population and economic growth, in particular in flood-prone areas such as floodplains and deltas.

Between 1998 and 2009 Europe suffered over 213 major damaging floods. In this decade floods in Europe have caused 1126 deaths, dislocation of half a million people and at least €52 billion insured economic loss (European Environment Agency, 2010). Europe adopted a new Directive (2007/60/EC) requiring EU members states to assess if the water courses and the coast lines are at risk of flooding by establishing flood hazard estimates.

The increase in flood risk is predominantly a result of three issues. Increase in flood hazard due to urbanization (Nirupama and Simonovic, 2006), climate change (Nicholls et al., 1999) and increase of potential damage due to economic growth (Kellenberg and Mobarak, 2008).

Urbanization results in three consequences that can lead to more frequently flooded areas:

1. Subsidence due to abstraction of water and high rise buildings,
2. Increase in the precipitation run-off due to urbanization, resulting in
3. Decrease in storage and conveyance of the precipitation.

The impact of climate change on flood sensitive areas is due to increase of sea level and the change in precipitation intensity.

1.2 Motivation

Floods are one of the most devastating natural disasters, hitting various regions in the world each year. In the last decades the damage and the loss of human lives caused by floods has increased rapidly. Due to the large potential damage caused by floods the need for preparatory tools, like flood models and flood maps, for real-time monitoring and forecasting of floods has increased.

As mentioned here above in Europe measures are taken to assess the flood risks. Unlike in Europe, in many flood prone areas in the world flood information is not readily available. One of these countries is Thailand. The flooding in Thailand during the 2011 monsoon season is the motivation for this study. A large amount of companies and research institutes were invited to help with analyzing the situation. To be able to make decisions during this flood crisis about for instance temporary embankments and possible evacuations with no flood model being available, there was an urgent need to develop a flood model in a short amount of time.

1.3 Goals and principles of a rapid flood model

In this paragraph a short description is given to understand the concept of a rapid flood model for further reading. The idea of rapid flood modeling is not to create the best model to predict floods. The concept is to create a model that enables the prediction of the evolution of a flood event in a short amount of time using certain assumptions and accepting limited accuracy in relatively unknown area.

In the case of an expected flood, the rapid flood model provides information about the magnitude of the flood and other information needed for decision making, see chapter 2, to help the crisis management to prepare measurements or evacuation plans.

The rapid part of the rapid flood model refers to a fast set-up of the model. In this study the focus will be on gaining the information for a flood model and simulating the flood in a short amount of time.

1.4 Problem description

A large number of studies have been done on the subject of flood events and flood model accuracy. In most of these studies different models have been used and compared to determine which models give the best results. In some studies the accuracy is evaluated on the type of models used (Apel et al., 2008; de Moel et al., 2009; Horritt and Bates, 2002). In other studies the sensitivity of certain components are also been investigated, like the use of coarse DEM or roughness coefficient (Bates and De Roo, 2000; Cook and Merwade, 2009; Finnegan et al., 2005; Kiss, n.d.; Leon et al., 2006; Sanders, 2007; Schumann et al., 2007). In the sensitivity studies usually one component, such as roughness coefficient or DEM accuracy, is studied and not the sensitivity between different components. So far there is not a clear picture about the sensitivities between the components and which component is most relevant to create an accurate prediction of a flood event for a certain type of area. The studies of flood events are usually done for a specific case, where a flood event is occurred. This makes the results of these studies case based and only relevant for that specific area. This is the reason that the focus of this study is on the sensitivity for different types of areas.

One of the time consuming aspects of deriving a flood model is gathering data to provide a prediction for a flood event in short amount of time. Deckers et al. (2009), mention that the data gathering is a difficult task, being time consuming, costly and sometimes even impossible. Even when locally obtained data is available, the completeness and the accuracy can be insufficient.

In the last two decades the amount of online data has grown rapidly. In the situation where local data is not available the use of publicly available data, e.g. satellite remote sensing data can be a useful method to gather information for flood prognoses. However these data have a certain accuracy, which should be taken into consideration. It is not clear if a prediction of a flood event can be simulated based only on publicly available data. Assumptions or methods need to be derived for certain data that is not publicly available.

1.5 Objective and research questions

The objective of this study is:

Evaluate the usability of a rapid flood model

The research questions are derived from the literature study and from consulting the experts involved in the Thailand flood event 2011. The three main research questions are:

1. Which publicly available data and methods can be used for the simulation and prediction of a flood event?
2. Which parameters and conditions have the largest influence on the simulation and the prediction of a flood event?
3. Is the rapid flood model a feasible tool to be used for urgent prediction of a flood event for the purpose of crisis management?

To be able to answer the main research question, these sub-questions need to be answered first:

- 1.1 *What kind of information is required for the simulation and prediction of a flood event?*
- 1.2 *Which publicly available data sources can provide the required information for the simulation and prediction of a flood event?*

- 2.1 *Which parameters and conditions have the largest influence on the simulation and the prediction of flood event using 1D flow schematization?*
- 2.2 *Which parameters and conditions have the largest influence on the simulation and the prediction of flood event using a 2D flow schematization?*

When the publicly available data for a rapid simulation and prediction of a flood event and the parameters to be derived from the data sources with the largest influence on the credibility on the prediction of a flood event are determined this information is used to make a rapid prediction of the 2011 flood event in Thailand:

- 3.1 *Is a prediction with a rapid flood model possible in a short amount of time?*
- 3.2 *Is there enough data publicly available in real time to be able to use rapid flood models in crisis management?*
- 3.3 *Is the rapid flood model applicable for any flood prone area in the world?*

1.6 Methodology

This study consists of two parts, the data needed for a flood event and the tests with the case studies. In this study the focus is on prediction of river flooding for crisis management.

1.6.1 Flood event information

The first part of this study is focused on the information around floods. In this part an evaluation of different flood maps and flood models is done. The information needed to create the maps and models as well as the outcome of the maps and models will be discussed.

Furthermore, the availability of publicly data for the information needed for flood maps and flood models, determined in the previous section, is clarified. The methods and approaches to process and to convert this information into data that can be used in flood maps and models are investigated.

1.6.2 Case studies part

In the second part of the study three case studies are prepared. The first two are hypothetical case studies where the case is fictional and the objective is to determine the parameters to be derived from the data sources that have the most influence on the simulation of a flood event. The third case is a real case based on the 2011 Thailand flood event, where the publicly available data is used for a real flood event.

Case study 1: The sensitivity of different river areas for 1D flow will be investigated. The 1D flow refers to cross section of the schematization of the rivers. The variety of rivers and their floodplains makes it interesting to investigate the influence of these different components on the flood depth and the propagation of the flood. With calculations for different terrains, the sensitivity of the components of a river, the area and the floodplains on the flood levels are tested.

Case study 2: This case is the 1D/2D flow case study. In this case the influence of two types of landscape characteristics, the related components and conditions of the flood event are investigated. The influence on the flood depth, the propagation of the flood and the flood extent is analyzed. The flood extent is an extension of the 1D flow analysis and can only be investigated in 2D because of its

spatial dimension. Here the influence on two types of river areas is determined and the differences between the two types of river areas are investigated.

Case study 3: The last case study is based on the 2011 Thailand flood event. With the knowledge gained from the analysis of the 1D flow and the 1D/2D flow case studies, the influences on a flood prediction are determined. The aim is to use this knowledge and make a “prediction” of the 2011 Thailand flood event with the use of only publicly available data that fits the real flood event.

1.7 Reader’s guide

In the chapter 2 the information on floods, flood maps and flood models is given. Chapter 3 consists of the information from publicly available data and gathering and processing this data for a rapid flood model. Chapters 4, and 5 the influence of different parameters to be derived from the data sources is investigated for 1D and a 1D/2D schematization. In chapter 6 the information provided from the first five chapters are used for the Thailand case study. Finally in chapter 7 the conclusion of this study and the recommendations for further studies are listed.

2. Information for the simulation and prediction of a flood event

2.1 Introduction

Flood information is valuable information to have. By real-time monitoring, forecasting of floods and historical information an insight in the anticipated flood events can be compiled. Planning and taken precautionary measures against floods can only be done by deciphering the causes. In this chapter the steps needed to be taken to be able to make a prediction of a flood event are described.

First the different types of flood events are introduced in chapter 2.2. Next the flood tools to evaluate and predict a flood event are discussed in chapter 2.3 and in chapter 2.4 the different types of flood models are evaluated. In chapter 2.5 a summary of the information and tools for a prediction of a flood event will be used in this study are explained.

2.2 Origin of flood events

Flood events can have several origins in different areas. The origin of an event characterizes part of the flood event, the flood extent and even the consequences. In this chapter the flood event origins are described. There can be distinguish in the origin of flood events, flooding due to high waters in the river and spilling of the levees and flooding due to breaching of levees.

Here the focus will be on three origins of flood events due to high water in the river causing over spilling of levees.

In Figure 2-1 the origins that can cause overflow are drawn; the high discharges from upstream of the river, the increase in water level downstream of the river and the increase in precipitation in the flood prone area. After description of the origin of the flood event, the types of areas where flood events occur, flood prone areas are described.

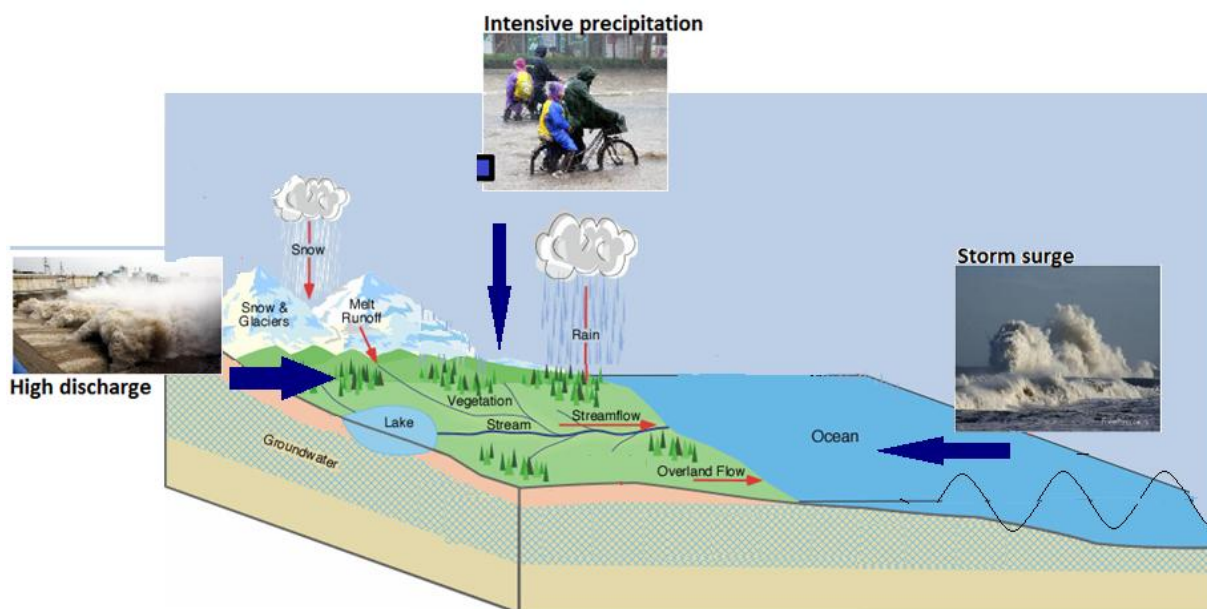


Figure 2-1 Origins of flood events

2.2.1 High discharges from upstream

High discharges in the upstream part of a river can cause high water levels in the river. When these discharges are high enough they can cause be over spilling of the levees. The high discharges can be caused by intensive precipitation in the catchment areas of the upstream river or melting of snow

and ice on higher grounds. This abundance of water can make it down the river in two ways, regulates or unregulated. To manage these high discharges and to prevent high water levels in the river, reservoirs are built in the upstream area of large rivers. Besides regulating the large discharges it's also a possibility to ensure water for several other needs, e.g. supply drink water, irrigation and produce energy. The reservoir can retain the large water quantities and release it or in smaller amounts or when the water levels in the river are very low. The problems of flooding arise when the reservoir is at maximum capacity and needs to discharge the water to the river when the water level in the river is already high or the discharging of water takes place for a long time, so that the water levels in the river approach flooding levels.

The maximum capacity of the reservoirs is usually known information. This makes it easier to predict what the discharges can be when a reservoir is at its maximum capacity and needs to discharge its water to the river. It is harder to predict the precipitation and quantity of melting snow and ice in the upstream area and the corresponding discharges.

2.2.2 Flash flood

In the flood prone area when intensive precipitation is occurring and the water cannot be disposed through channels or drainage network to the river, the water will be remain in that area, causing a flood area. This can be the cause of the drainage network to be insufficient or outdated.

Another cause in urban areas is the decrease room for storage and an increase in run-off (Booth and Jackson, 1997). Large parts in urban areas are paved, decreasing the infiltration of water in to the ground and enables the water to be stored in the ground. The increase in run-off is also caused by more paved surface.

So to be able to predict the intensive precipitation and the consequences, due to storage and run-off is information that is hard to be determined. In practice assumptions are made to make a prediction of these events caused by intensive precipitation. Hydrological models are not used to make prediction of this event in this study, this will be explained further in chapter 2.4.

2.2.3 High water from downstream

High water levels at the downstream area of the river cause by the downstream boundary can have different causes: high water levels due to high tide and due to storm surge and the combination of the two. As a result of strong winds on the ocean, storm surges and high waves may occur. High waves are a hazard for the sea defenses.

Storm surges are caused by high winds pushing the water of the sea surface, causing the water to pile up at the coast. The piled up water penetrates into the river. The extension of the infiltration of the water into the river depends on the area downstream of the river.

The higher sea level due to storm surge or high tide result also in the hinder of the discharge of rain and river discharge water, which can cause overtopping

In this study the focus will be on the storm surge penetrating and the high tide that may cause high water levels in the river and result in flooding. The hazard of high waves that can cause flooding due to damaging the sea defense structures is not taken into consideration in this study.

2.2.4 Flood prone areas

Anywhere on earth flood events can occur. An area which has not been flooded in the past is not



Figure 2-2 A call to 911 to report flooding

excluded from possibly flooding in the future. Yet from historical flood events give a good insight into flood prone areas. But different types of flood events, described in previous chapters, affect different areas. Floods commonly occur in areas adjacent to streams and rivers or a coastal area and even in mountain areas. The lateral two flood areas flooding can happen rapidly with a warning of only a few hours to the public and in some cases no warning, figure 2-2.

The flood prone areas are often low lying areas and below sea level but this is not always the case. So to assess the types of most flood prone areas in the world, the areas are classified into the following:

- Flat terrain
- Delta terrain
- Hilly terrain
- Mountainous terrain

Depending on the characteristics of these four areas the flood can come from all three sources, which are mentioned in the previous three chapters 2.2.1, 2.2.2 and 2.2.3 or a combination of the three.

2.3 Prediction of a flood event

To be able to make a prediction on a flood event the use of a flood map is very useful. A flood map can give a good insight in which areas are flood-sensitive and what the consequences of a possible flood event. In this chapter the users of flood maps will be addressed and their purpose for the flood map, chapter 2.3.1. After this the types of flood maps, chapter 2.3.2 and the information needed to be gained from a flood map and needed for a flood map are discussed in chapter 2.3.3. Next the kinds of decisions that can be made based on a flood map are evaluated in chapter 2.3.4. Finally in chapter 2.3.6 the choices for this study derived from the previous chapters are explained.

2.3.1 Users

Each user has different demands for a flood map. This makes it critical to know for which purpose or user you are developing a flood map. In general the following purposes should be taken into consideration (*Workshop on Flood Maps, 2006*):

- Inform the public (awareness)
- Preventive land-use management
- Constructions for precautionary measurements
- Flood prediction and warning
- Prevention and control of disaster
- Flood insurances

The stakeholders can be divided into two groups, the private bodies and on the other hand the authorities and the public bodies.

Table 2-1 Different users of flood maps, their purposes and an example.

Stakeholders	Purpose	Example
Private bodies		
House owners	Informative Flood insurances	Precautions for building in risk areas
Insurances	Flood insurances	Insure households and businesses
Industry	Flood insurances	Storage of potential hazard materials
Authorities/public bodies		
Government	Constructions precautionary measurements	Prediction
Spatial planning (regional/local)	Preventive land-use management	No new urban planning in flood plains
Flood protection agencies, water management	Prevention and control of disaster	Plan/realization protection works
Flood management, emergency management	Flood prediction and warning	Develop emergency systems

As can be seen in the Table 2-1 the private bodies are more interested in flood insurances and the authorities/public bodies are interested in preventing the flood from occurring and preventing damage.

2.3.2 Types of flood maps

The variety of concepts used for flood mapping is large. Therefore it is important to define which aspects are considered in a flood map. Only in Europe alone different conditions exist in different regions, so also different approaches have been developed. However most flood mapping approaches are limited to identify flooded areas for certain flood scenarios and in some cases additional information is given, e.g. maps that illustrate the consequences of inundations. Many authors have defined concepts of flood maps. Among these authors, Merz et al., 2007 proposes systematic concept and definitions for flood mapping.

Table 2-2 Systematic flood mapping increasing information down table (Merz et al., 2007) [give examples with pictures]

Type of flood map	Definition
Flood danger map	Shows the spatial distribution of the flood danger without information about the exceedance probability
Flood hazard map	Shows the spatial distribution of the flood hazard, i.e. information on flood intensity and probability of occurrence for single or several flood scenarios
Flood vulnerability map	Shows the spatial distribution of the flood vulnerability, i.e. information about the exposure and/or the susceptibility of flood-prone elements (population, built environment, natural environment)
Flood damage risk map	Shows the spatial distribution of the flood damage risk, i.e. the expected damage for single or several events with a certain exceedance probability

2.3.3 Information on flood maps

The flood maps in Table 2-2 show increase in information downwards. The first two flood maps show the intensity and extension of the flood. The lateral two, vulnerability and damage risk map give besides the intensity and extension also information about the consequence of a flood event. The lateral two maps are a combination of the flood extents and the consequence. In the vulnerability map the consequence is the exposure of the flood on different elements, e.g. population, buildings and environment. In the flood damage risk map, the consequence is the exposure to the elements expressed in damage, related to the land-use.

All the flood maps have one or more of the following information:

- Flood extent
- Inundation depth
- Flow velocity
- Duration
- Propagation of water front
- Rate of water rise
- Return period of high water

With the lateral two flood maps having extra information:

- Population in area
- Type of land use
- Economic value of land

The most important information on a flood map is the extension; this information is on every map, with additional information about the flood event. In Europe the flood extent maps are most commonly used flood maps, about 80% of the countries (de Moel et al., 2009). The next most common parameter used in addition to the flood extent is the flood depth. Some countries have additional information like flow velocity (Switzerland and Luxembourg) or propagation (Netherlands and Hungary) but this is rare.

2.3.4 Scale of flood map

As in chapter 2.3.1 is mentioned, flood maps have different purposes. The purposes named in that chapter demand different kind of information from the flood maps. This is not only dependable on the information on the flood map but also on two other aspects: The spatial and time scale.

Spatial scale of flood map

The spatial scale of flood map is dependable on the user and the purpose of the flood information on the map. The three most common scales for flood maps are shown in Table 2-3. The spatial scales are categorized into the three types of flood maps discussed in chapter 2.3.2 and the focus of the map is clarified (EXCIMAP, 2007).

Table 2-3 Spatial scales for a flood map

	Flood danger/ hazard map	Flood vulnerability map	Flood damage risk map
Scale	1:100.000 - 1:1.000.000	1:100.000 - 1:10.000	1:10.000 - 1:2.000
Accuracy	Very low	Low	High
Covered areas	National or supra-regional	Regional level	Local level
Focus			
Stakeholder	National spatial planning Public at large	Regional spatial planning	Local spatial planning Insurance
Example of purpose	General flood extent	Assets at risk	Probable loss

Time scale of flood map

The information of a flood map is also dependable on the time scale. The difference on the two time scales is that the long term can be used to plan prevention, spatial solutions and crisis management. The short term scale needs to give information to set in motion the crisis management, like control of disaster and warning.

Table 2-4 Time scales for a flood map

	Flood map information	Purposes	Decisions
Long term	Return period Flood extent Inundation depth Flow velocity Duration	Prevention Land use Meerlaagse veiligheid Spatial solution Crisis management	Plan/realization protection works No new urban planning in flood plains
Short term	Flood extent Inundation depth Propagation of waterfront	Prevention Control of disaster Flood prediction Warning	Crisis management Sand backs Deliberate inundation of certain areas Evacuation

2.3.5 Errors in prediction of the flood

A flood map gives information that is based on a prediction. The various information a flood map gives is discussed in chapter 2.3.3. A prediction of a flood event can be wrong e.g. the duration of a flood can be much longer than was given in the prediction. Table gives the different types of flood map. However the most important information of the flood is the extension of the flood, this is the information all the flood maps possess. In this chapter the errors on this information is discussed.

All the flood maps indicate the places where floods can occur and where they do not. There are two types of errors when a real flood event occurs and the prediction is not correct, Table 2-5 shows the different outcomes.

Table 2-5 Real flood event compared to the prediction of flood event

		Reality	
		Flood occurs	Flood does not occur
Prediction	Flood occurs	No error	Error (Type I)
	Flood does not occur	Error (Type II)	No error

The two errors that may occur are, the prediction of a flood does not occur in a real flood event and in a real flood event a flood occurs when the prediction did not predict a flood. These errors are named Type I and Type II errors. The consequence of these errors can be looked at in an economic view and a credibility view.

Duckstein and Kisiel (1971) have looked at the economic loss due to this error. Type I error is seen as costs for the producer and type II for the consumer. From an economic point of view in the case of flood event and type I error takes place, the costs for the public bodies, Table 2-1 due to investment to plan and realization protection works, develop emergency systems and no new urban planning in flood plains, have been made for nothing. For the consumer, the population, the property owners

and business the occurring of a type II error is catastrophic. Not being prepared for a flood can have large impact on the economic consequence of a flood (Hoss et al., 2011).

For the credibility point of view, this will be damaging if error type I occurs. Type I error is also called a "false alarm". The most famous type I error is case of crying wolf by the shepherd. By alarming the people with false alarm a numerous times, when it did happen the people were sick of being alarmed wrongly and didn't responds at all.

So both errors need to be avoided as much as possible. The problem is that measures to reduce one of the error types has the unfortunate consequence of increasing the risk of the other error type (Belknap et al., 1996). This seems logical, by setting a lower threshold on naming areas flood plains, results in an increase in the number of flood plains. This will decrease the number of areas where no flood occurs and also the type II error. But the number of areas named flood plains in the prediction, and actual not flooding during a real event increases, result in the increase of type I error.

2.3.6 Summary

In the previous sections the different types of flood maps and the corresponding information has been discussed. In this chapter the choice on what kind of flood map is been used for this study is made. This section is the beginning of answering the sub question:

1.1 What kind of information is required for the simulation and prediction of a flood event?

The kind of information required depends on the type of user, the type of flood map, the information of the flood map and the decisions need to be made with the flood map.

Chapter 2.3.1 shows that the users can be divided into two groups, the private bodies, who are more interested in flood insurances and the authorities/public bodies, who are more interested in the preventing floods and the associated damage. This studies focus is on the user flood management and emergency management which are part of the authorities/public bodies. The purpose of this study is to design an efficient way to produce flood prediction and warning system.

The type of flood maps that have been discussed in chapter 2.3.2 have all one aspect in common, all the maps show the spatial distribution of the flood danger with extended information. Except for the type of flood map chosen to be used in this study, the Flood danger map. This is the only map with only a spatial distribution of the flood danger. The extended information needed for the other type of maps gives more information about the flood event but this extended information is also something that takes resources (time and money) to be gathered. In this study the assumption is that the resources are little and that only the essential components should take up any resources.

As mentioned above, the different types of flood maps give different kind of information. The chosen map is the flood danger map where the spatial distribution of the flood danger is the only information. The flood danger map can be seen as the all the information mention in chapter 2.3.3 i.e.:

- Flood extent
- Inundation depth
- Flow velocity
- Duration
- Propagation of water front
- Rate of water rise
- Type of land use

To keep this study's goal on the use of limited resources, the flood extent, the propagation of the flood and the inundation depth are the flood map information that will be used.

The spatial and time scale of the map is chosen based on corresponding with the chosen purpose of the flood map, chapter 2.3.1: produce flood prediction and warning map. The corresponding spatial scale is the scale between 1:100.000 and 1:1.000.000. This fits the type of flood map that is chosen. And the corresponding time scale is the short term scale, which focuses on the crisis management, like control of disaster and warning.

The two type of errors discussed in chapter 2.3.5 are the best way to check the flood maps potential which involves the flood extent and the inundation depth.

2.4 Simulation of a flood event

For engineers and managers a fast estimation of the reach of flood inundation is a major task, which is increasing in frequency (Anderson et al., 1996). Observations of flood inundation are not available for most rivers in the world. To determine areas of flood a resort to some kind of 'predictive' model has to be made. The amount of available 'predictive' models is large. These models range in complexity from a simple intersection between water surface with a digital elevation model (DEM) (for example Priestnall et al., 2000) to a full 2D solution of the Navier-Stokes equations with turbulence closure (for example Younis et al., 1996).

Table 2-6 shows different models used in papers. The models are compared for the following points:

- Channel routing:
Describes the method to calculated the flow in the channel
- Floodplain routing:
Describes the method to calculated the flow in the channel
- Discretisation:
Schematization of the models
- Application:
Example of use of the model in a scientific article

Table 2-6 Comparison 'predictive' models with modeling flood inundation and standard hydraulic models. Complexity increases down table (Bates and De Roo, 2000)

Type of model	Channel routing	Floodplain routing	Discretisation	Application
Planar water surface	None	None	All areas below the planar surface are considered flooded	Applied to DEM generated by the UK Environment agencies LiDAR data collection program (e.g. Priestnall et al., 2000)
Storage cell	Uniform flow formula (Manning equation) using designated channel cells	Uniform flow formula (Manning equation)	Valley is split into channel and single cells present the right and left floodplains	Applied to the river Culm, UK (e.g. Romanowicz et al., 1996)
Storage cell	1D kinematic wave solved using explicit finite difference procedure using designated channel cells	Uniform flow formula (Manning equation)	Raster-based derived automatically from a DEM	Applied to a reach of 35km of the river Meuse(e.g. Bates and De Roo, 2000)
1D models	Full solution of the 1D St. Venant equations.	Full solution of the 1D St. Venant equations.	Treats domain as a series of cross sections perpendicular to the flow direction. Areas between cross sections are not explicitly represented	Applied to the lower river Thames UK(e.g. Ervine and MacCloed, 1999 as cited by Bates and De Roo, 2000)
2D models	Full solution of the 2D St. Venant equations with turbulence closure	Full solution of the 2D St. Venant equations with turbulence closure	Structured grids (finite difference methods) or unstructured grids (finite volume and element methods) using a variety of geometries.	Applied to five river reaches between 0.5 and 60 km in length(e.g. Bates et al., 1998 as cited by Bates and De Roo, 2000)

In this section the simplest model, the altitude model, and a more complex one, the SOBEM model, will be compared. These models are different in the way that they are setup, the data that they need and the outcomes. Therefore they also have different drawbacks.

The altitude model is a simple way of creating a flood map. It's a linear interpolation from measured water levels in channels. For example the water levels at gauge stations are linear interpolated at every point between the gauges, creating a uniform sloping flood level. This level is intersected with the DEM. Each level on the DEM below this flood level can be considered a flooded area.

The SOBEK model is 1D for the channel routing and 2D for the floodplain routing. The channel hydraulic model is a 1D model where a cross section of the channel perpendicular to the flow direction, is used to determine the water level in the channel. This water level is then used for the flood plains which are modeled in 2D with the shallow water Navier-Stokes equations.

All these aspects of the flood models are shown in Table 2-7.

Table 2-7 Steps to setup and run a flood model

Name model	Altitude model	SOBEK model	Notes
Scenario definition	Historical events Synthetic events	Historical events Synthetic events	Events contain: - Water levels - Boundary conditions - Upstream (reservoir) - Downstream(tide) - Precipitation
Data used	DEM Water levels	DEM Water levels River parameters(width, height, slope) Roughness coefficient (channel, flood plains) Precipitation	Data source: - Gauge measurements - Satellite data - Laser scanner data
Data preparation	DEM filtering (Wavelet, Fourier) Return periods	DEM filtering (Wave let, Fourier) Return periods	
Calibration	None	Determination unknown parameters by comparing results of the model with measured data	
Simulation	Several water levels	Several scenarios	SOBEK time consuming
Flood map parameters	Flood extent Inundation depth	Flood extent Inundation depth Flow velocity Duration Propagation water front Rate water rise	

The altitude model is the simplest flood model. The amount of data needed is also far less than the other models. This makes the outcome usually also less reliable. Due to no restriction in the volume of the flood plains this results in huge and unrealistic flood plains. This has also to do with the fact that dikes are usually neglected. The presents of dikes are hardly present in a DEM. Due to simplicity of the model the dynamics of the flood process are completely ignored. In figure 2.3 a flood map of an altitude model is shown as an example. All the levels below a certain water level are considered flooded. This doesn't reflect a realistic flow path.

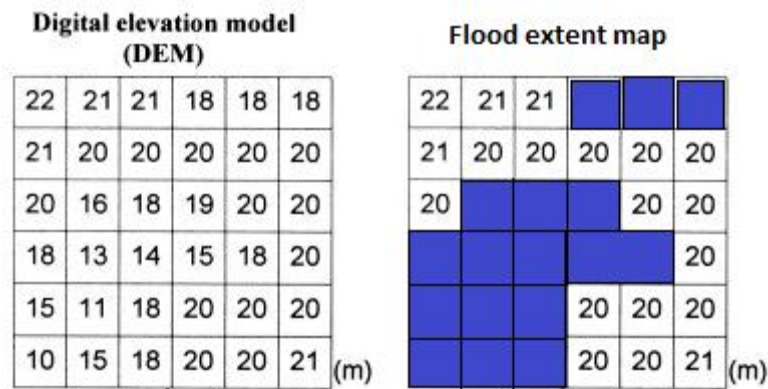


Figure 2-3 Flood extent map from DEM all levels below 20 m are inundation areas

The points where the SOBEK model has its drawback and what is actually contradiction are the points: the data used the calibration, the simulation and the flood map characteristics.

Gathering the data that is used, is a difficult task, which is time consuming, costly and sometimes impossible (Deckers et al.,

2009). With this said the second point, the calibration of the model, becomes more difficult when there is insufficient data. The assumptions have to be reconsidered and modified. The amount of data that is needed in the SOBEK model makes the processing time and the simulation time increase. The contradiction between the calibration and the simulation makes the process of gathering data one of the most important ones in the flood modeling system.

2.5 Summary

In the previous chapters the variety in flood information, flood events, flood maps and flood models is been addressed. Due to the large variety in information, there is a need to summaries the choices and restrict the variety of the information. In this chapter the choices and the restrictions of the variety of information that is going to be used in this study is described.

The flood events that will be considered in this paper are the floods caused by river flooding and other causes will be left out e.g. tsunamis. This study is restricted to floods causing river flooding by failing of the embankment or due to overtopping of the embankment or due to levee breaching. In this study the failing of the embankments can only be caused by high discharges from upstream of the river and high water levels from downstream of the river. This excludes the precipitation because of the complexity of a hydrological model e.g. the input of the rain, the run-off, the storage of water in the ground. The following types of information needed for a flood prediction:

- Origin of the flood event
 - o High discharges
 - o Intensive precipitation
 - o Sea conditions
- Type of terrain
 - o Slope
 - o Land use
- River information
 - o Location
 - o Geometry (width, depth, slope etc.)

As it stated in the introduction of the Methodology in chapter 1.6, the majority of the research done on flood events is based on the accuracy of a certain model or of a certain area. Therefore all the flood prone areas described in chapter 2.2.4 will be a subject in this study. These areas are the flat, delta and mountainous terrains.

Table 2-8 shows the choices made for the user, the type of flood map, the flood information, the spatial and time scale and the errors.

Table 2-8 Type of choices for the flood map for this study

Flood map information		Additional information	
User	Flood management, emergency management	Purpose Example	Flood prediction and warning Develop emergency systems
Type of flood map	Flood danger map	Definition	Shows the spatial distribution of the flood danger without information about the exceedance probability
Flood information	Spatial information		Flood extent Inundation depth
Spatial scale	1:100.000 - 1:1.000.000	Accuracy Covered areas	Very low National or supra-regional
Time scale	Short term		
Error	Type error I and II	Decisions	Crisis management Sand bags Deliberate inundation of certain areas Evacuation

In chapter 2.3 the variety of flood maps is discussed. In the first paragraph of this chapter the users are described. In this study the focus is on the user, the flood prediction and emergency management with the purpose of flood prediction and warning. This user's focus is on the type of flood danger map that shows the spatial distribution of the flood danger without information about the exceedance probability. The information of the flood maps required to make a prediction of a flood event is the flood extent and there is no additional information used in the flood maps like population, type of land use or economic value of the area. The information on the flood map is chosen to be restricted to the flood extent and the flood depth, these are the most common used parameters in Europe (de Moel et al., 2009).

According to *Handbook good practice for flood mapping in Europe* (EXCIMAP, 2007) the appropriate scale for a flood danger map to display the flood extent is in the order of 1:1.000.000. The accuracy is low for this scale but can give enough information on a national or river basin scale about a flood event. For the information on the flood extent and the flood depth the scale is sufficient.

The choice for the flood model is made based on the balance between the accuracy and the needed data for the model. The SOBEK model is a model that has its disadvantage in the large variety in data needed, but due to its 1D/2D characteristics it is a good compromise.

With the choices made in this chapter on the information for the simulation and prediction of a flood this study will have both a general and in some aspect a more specific look on flood events. The general part in the study will not focus on one area specific but try to specify the sensitivity analysis for different types of terrains and taking different types of flood events into consideration. The choice for the use of the flood danger map and the 1D-2D SOBEK model as the flood model excludes some aspects in this study. But this will make this study more focused on the general part, an analysis on the important data for a flood prediction for not a flood prone area or flood event.

3 General data for flood models

Eventually, the model that will perform the best will be the simplest one that supplies the information required by the user whilst realistically fit the available data. For flood models high quality data are often unavailable, especially in data-poor developing countries. In this chapter the needed data for a flood model will be discussed. In chapter Data categorization 3.1 the data needed for a prediction of a flood event will be discussed. Chapter 3.2 presents methods to process the data so it can be used for the prediction of the flood model. Chapter 3.3 gives a summary of the available data and methods to simulate and predict a flood event.

3.1 Data categorization

The data needed for a flood map can be divided into two groups, the data to create flood events and the data to characterize the area.

Data to create events:

- Water levels in channels and rivers
- Boundary conditions
 - o Upstream (discharge)
 - o Downstream (sea level)
- Precipitation

Data to characterize area:

- Flood plains
 - o DEM
 - Surface elevation
 - Line elements
 - Dykes
 - Roads
 - o Type of areas
 - Roughness coefficient
- River parameters
 - o Location
 - o Width
 - o Depth
 - o Slope
 - o Roughness coefficient

3.1.1 Event data

Gauge station measurements are the most common way to obtain data for discharges and water levels for rivers and precipitations. A few hydro-meteorological agencies are releasing this information via the internet, but most information has to be paid for. According to Fekete and Vörösmarty, 2002 the amount of monitoring stations is decreasing in the last decades. Figure 3-1 shows the distances between stations, black colored means stations close to each other and white colored is distance of 2000 km between stations. There is a clear rapid drop of stations since 1975.

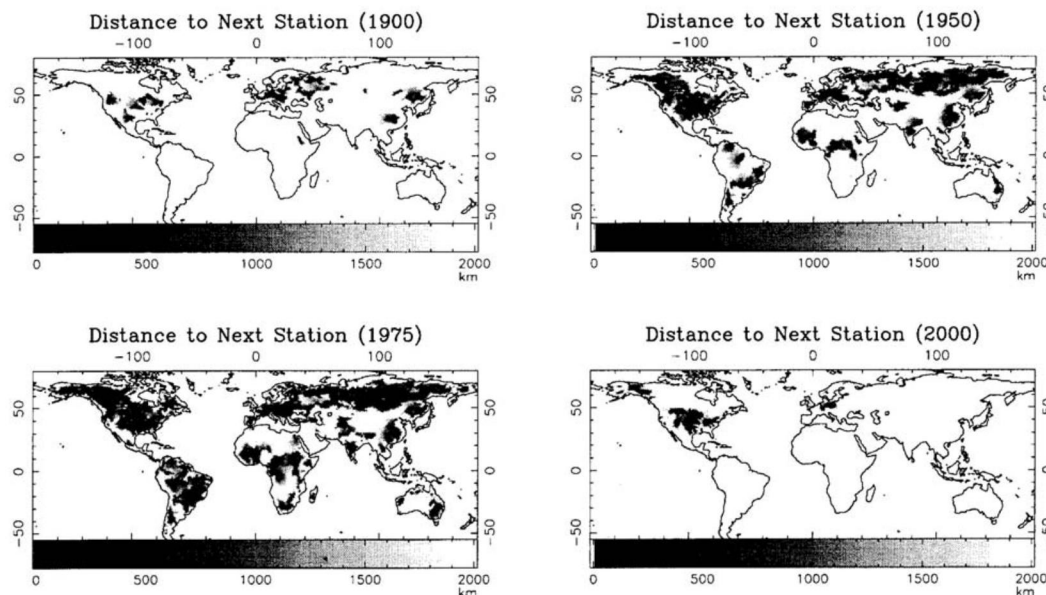


Figure 3-1 Distance to next downstream gauging station. Darker color means closer stations, while the lighter colors means increasing distance to the nearest downstream stations, which blends into the white colored unmonitored landmass (Fekete and Vörösmarty, 2002)

Even when the measured data is obtained, it can still contain errors, voids where the user has to make assumptions or interpolate (Mc Gahey et al., 2008). For most rivers in the world measured data are not easily available or are very costly.

River data

On the Wikipedia page for the large rivers in the world some values can be found, like average annual discharge, maximum discharges (“List of rivers by discharge - Wikipedia, the free encyclopedia,” n.d.) average depths and average widths. These discharges can be used to create synthetic events.

The discharge of a reservoir can be used if available for the upstream boundary. In this study the focus is on prediction of a flood event. This means that using the average values of the discharges is not efficient enough to create an event where flooding will occur. The use of the extreme data, like highest discharge ever measured or the maximum spilling capacity of a reservoir would be more appropriate.

Ocean and sea data

For the downstream boundary the tidal information and the water level at sea are important data to obtain. For certain areas, like USA, Europe and Australia the tide information can be found online on governmental sites. In other areas the use of surf sites can be helpful to get this information (e.g. “Surf Forecast and Surf Reports Worldwide | Surf-forecast.com,”).

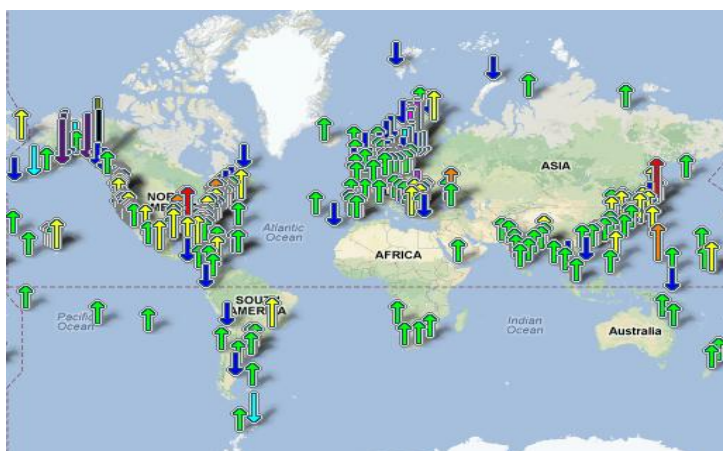


Figure 3-2 Station measuring sea water levels (“Sea Level Trends,” 2012)

On the site of Sea Level Trends, 2012 the sea water levels and the trends of the last century are given. The site contains information of over 200 station spread all over the world, figure 3.2. Because it’s the

prediction of a flood event we should take the sea water level rise into account.

Precipitation

As is mentioned in chapter 2.2.2 to predict the intensive precipitation and the consequences, due to storage and run-off is information that is hard to determine. But GLDAS (Global Land Data Assimilation System) provides among other information the precipitation data, in the form of rainfall rate, surface runoff and subsurface runoff. The data are archived and distributed by the Goddard Earth Science (GES) Data and Information Services Center (DISC) as part of the activities of NASA's Science Mission Directorate. The data can be downloaded from the website [http://hydro1.sci.gsfc.nasa.gov/thredds/catalog/GLDAS_NOAH025SUBP_3H/catalog.html] for the periods between 2000 en 2013. The data gives global daily, 12 hourly and three hourly outputs on a grid size of 0.25 geographic decimal degrees coordinate (long, lat).

3.1.2 Data to characterize area

There are two ways to obtain data to characterize the area, by in-situ measurements and using on-line data. From the previous chapter it became clear that for in-situ data the availability is limited and costly. The on-line data will be researched in this chapter. There are three different on-line data that are going to be discussed.

First online-data is the altimetry data to determine the DEM, the heights of the water levels, the height of the river banks and the slopes of the floodplains.

The second is the image data, which can be used to confirm the location of the river and gain more information about the river characteristics, like width and floodplain extent.

The third is the products that use the combination of the previous two data and other sources to create a product with more detailed information.

In Table 3-1 the available data online are listed. Only free of charge data is reviewed.

Table 3-1 Overview of available on-line data

	Application	Spatial resolution	Website
Altimetry	SRTM	90 m	http://dds.cr.usgs.gov/srtm/
	ASTER GDEM	30 m	www.gdem.aster.ersdac.or.jp/search.jsp
Image data	LandSat	30 m	http://glovis.usgs.gov/
	MODIS	250m, 500 m, 1000 m	http://modis.gsfc.nasa.gov/data/
Product of combined sources	Dartmouth	-	http://csdms.colorado.edu/pub/flood_observatory/MODISlance/
	OpenStreetMap	-	www.openstreetmap.org/
	LEGOS	-	www.legos.obs-mip.fr/soa/hydrologie/hydroweb/Page_2.html

Altimetry

The spatial resolution of the SRTM and ASTER GDEM is respectively 90m and 30m (Frey and Paul, 2012; Reuter et al., 2009). The drawback of using ASTER GDEM is that the data is obtained in more than seven years. The data used is an average mean value over this long period. The acquisition period data for the SRTM is shorter. This was done in 11 days (11-22 February 2000). But the uncertainties for SRTM are that there are voids in the data. These voids are filled with artificial data by interpolating or other sources that don't have a date.

A disadvantage of ASTER GDEM is that it can't penetrate through clouds (Frey and Paul, 2012). Therefore ASTER GDEM shows in certain areas more details than the SRTM but can be consistently poor quality due to cloud cover.

These disadvantages translate to the accuracy of these two altimetry data sources. Table 3-2 shows the absolute and relative accuracy.

Table 3-2 Accuracy of the SRTM and ASTER GDEM data ("SRTM Statistics," 2012 and ASTER Validation Team, 2011)

Altimetry	Spatial resolution	Accuracy				Level of accuracy = $1-\alpha$
		Absolute		Relative		
		Vert.	Hor.	Vert.	Hor.	
SRTM	90 m	16 m	20 m	10 m		90%
ASTER GDEM	30 m			20 m	30 m	95%

The SRTM accuracy is much higher than the accuracy of ASTER GDEM. For this study the focus is on the relative vertical accuracy. The absolute accuracies are not taking into consideration in this study, due to that the whole area which is examined will be having the similar absolute accuracy. This is especially the case when using the flood extend. If the flood depth is also been used, the absolute accuracy starts to play a role, see Figure 3-3.

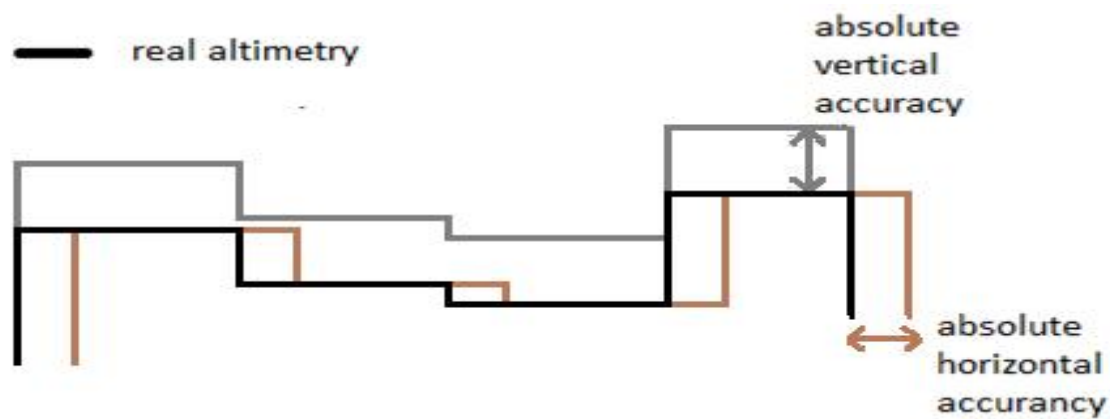


Figure 3-3 A bottom profile (black line) with the absolute and relative accuracy errors (brown, grey and red line)

In Hirt et al., 2010 the vertical accuracy of the SRTM and ASTER GDEM data was tested based on a set of geodetic ground control point. These were much lower than the values given by SRTM Statistics, 2012 and *ASTER Validation Team, 2011*. But the in Hirt et al., 2010 is also mentioned that the values for vertical accuracy vary as a function of the terrain type and shape. In mountainous terrain these values were much larger than for relatively flat terrains. Figure shows the normal distribution of accuracy. In the blue area is where the mountainous terrains accuracy lies, this is larger than the accuracy given in Table 3-2. This should be taken into consideration for the 2011 flood event in Thailand in chapter 6.

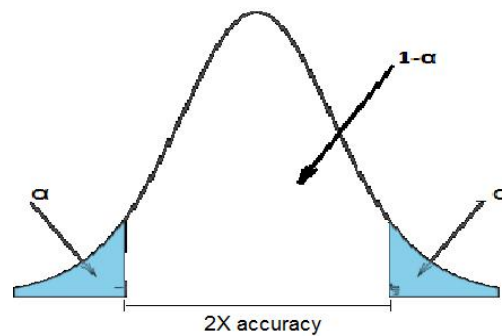


Figure 3-4 Normal distribution of the vertical accuracy

Image data

The image data are created out of several bands, with different wavelengths. Each wave length has its one specification and is useful to distinguish different things. For example band 3 is useful to distinguish vegetation and band 6 to measure surface temperature. By combing different bands clear distinguish can be made for example of water and land.

LandSat acquisition period is from 1972 till 2011. A global archive is available sorted by date, by satellite and sensor. MODIS only disadvantage is that the spatial resolution is coarse.

Product of combined sources

By combining the information from the different on-line sources, a fuller picture of the area can be compiled.

Dartmouth flood observatory that uses space-based information to create information for international flood detection, response and assessment. There are three products with global coverage from 1985 till now;

1. NASA NRT Experimental Flood Maps;
These are near real-time maps of current flood water. Only few hours after the Aqua satellite flies over the area a flood map is created.
2. The GIS data;
Those are previous mentioned maps transformed to an archive
3. Surface Water Record;
This information can be used when there are no measurements of flooding.

Dartmouth has the NASA NRT and Surface Water Records products available for some parts of the world.

OpenStreetMap is an open source where everybody in the world can improve and contribute to development. This creates a detailed map but the origin of the data is unclear. These images can be used to check and clarify assumptions.

The LEGOS program uses a number of satellite data. By combing the information from different satellites a large contribution is made on mapping lakes, reservoirs, rivers and floodplains with the related altimetry. This product is available for some parts of the world.

3.2 Methods to process data

In the previous chapter different potential online data is discussed. The data obtained from these sources, is either not complete or has to be modified to be used for the rapid flood model. First the use of classification of rivers is explained, next the methods to process the event data and the data to characterize area.

3.2.1 Classification of rivers

In Rosgen, 1994 a large scale of classification of natural rivers are given. In Figure 3-5 the streams are classified based on the dominant slope range, the cross-section and the plan view of the stream. There are seven major classes in this classification of Rosgen, 1994, specific based on the dominant slope range. There are two classes that are a combination of one of the seven major classes.

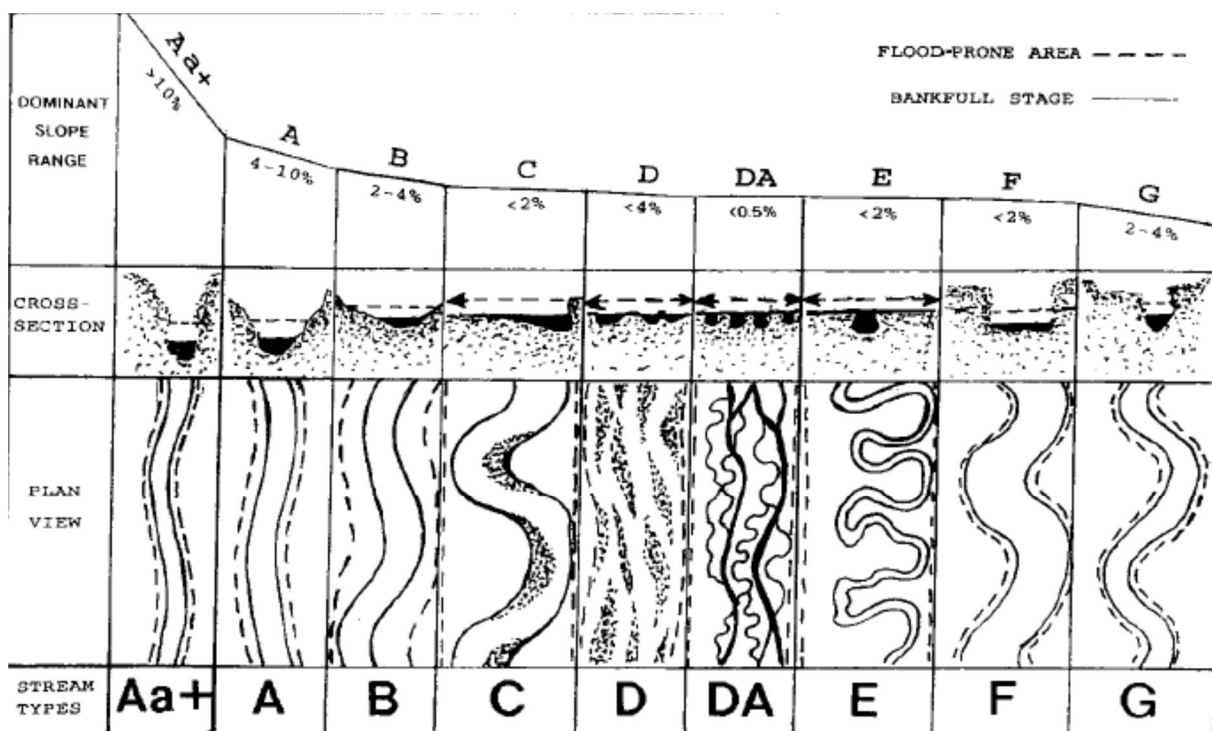


Figure 3-5 Longitudinal, cross-sectional and plan views of stream types(Rosgen, 1994)

Figure 3-5 shows besides the lateral characteristics more characteristics for the classification: entrenchment ratio, sinuosity, the width/depth ratio and the slope. These classifications are based on the morphology of rivers. This makes the characteristic, the cross-section also dependable on the bed material.

Dominant Bed Material	A	B	C	D	DA	E	F	G
1 BEDROCK								
2 BOULDER								
3 COBBLE								
4 GRAVEL								
5 SAND								
6 SILT/CLAY								
ENTRH.	<1.4	1.4-2.2	>2.2	N/A	>2.2	>2.2	<1.4	<1.4
SIN.	<1.2	>1.2	>1.4	<1.1	1.1-1.6	>1.5	>1.4	>1.2
W/D	<12	>12	>12	>40	<40	<12	>12	<12
SLOPE	.04-.099	.02-.039	<.02	<.02	<.005	<.02	<.02	.02-.039

Figure 3-6 Classification of channels with the important parameter, the bed material (Rosgen, 1994)

The entrenchment ratio is the ratio between the flood-prone area and the bank-full width. This results in an elevation in the water level. These water levels have been compared to field observations and this shows that this elevation to be a frequent flood (50 year return period) or less, rather than a rare flood elevation (Rosgen, 1994). The larger the entrenchment ratio, the more the floodplains are developed, see Figure 3-7.

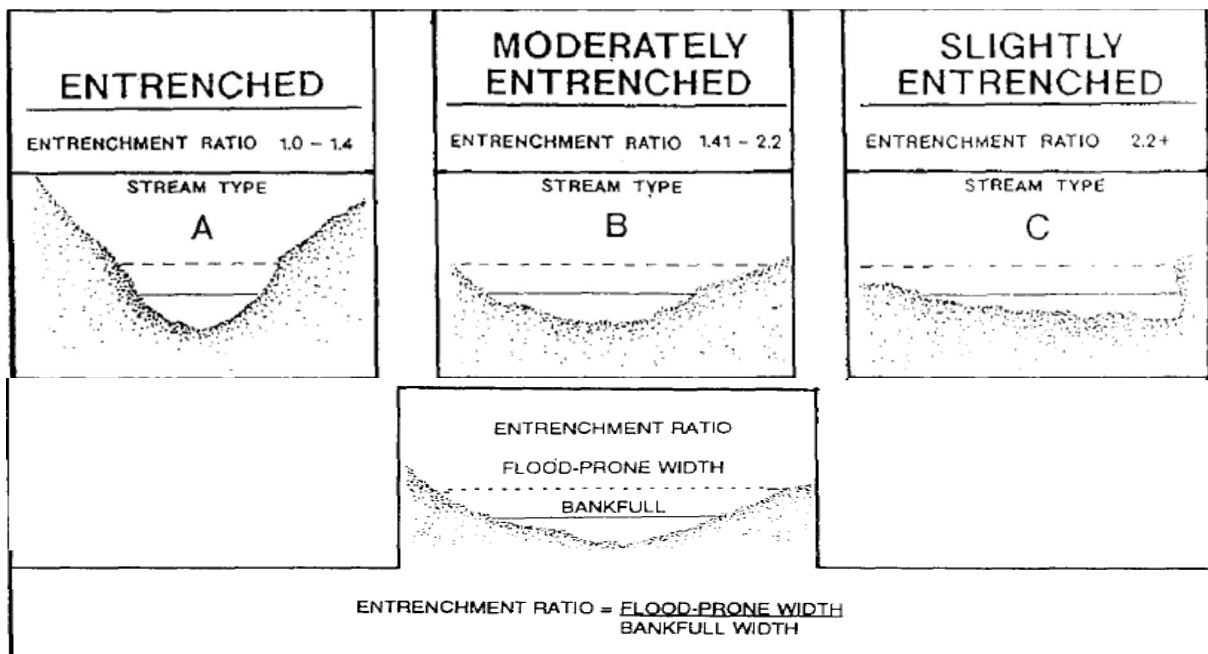


Figure 3-7 Entrenchment ratio for class A, B and C (Rosgen, 1994)

The sinuosity is a ratio of the length of the channel to the area length. It can also be seen as a ratio between the area slope and the channel slope. When this ratio approaches to the value of one than the channel is a straight line. The entrenchment ratio depends generally on the grain and particle size, a decrease in bed material size corresponds in an increase in sinuosity (Rosgen, 1994).

The width/depth ratio is definition for the deepness or shallowness of the channel. Given you have one of the two parameters; the other parameter can be calculated with the ratio.

These classifications can be very helpful for situations where the obtained-data is incomplete or no data is available. In the next section of this chapter the use of the online data and characteristics will be used to obtain information that can be used for a flood model.

Real rivers

The classification of the rivers by Rosgen, 1994 is based on natural rivers. Rivers that are found for example in The Netherlands do not fit this classification because of the interference by humans. By changing the course of the river, dredging the rivers and building dykes to decrease the chance on floods the characteristics of these rivers are changed and do not fit the classification.

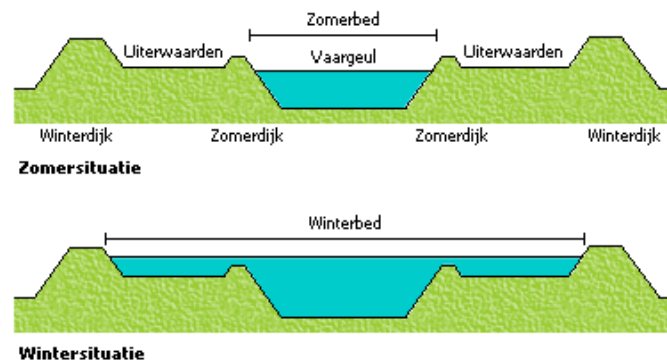


Figure 3-8 Cross section of a river with dykes in the Netherlands

3.2.2 Event data

The event data contains three types of data needed for a flood model:

1. Water levels
2. Upstream boundary conditions (discharge)
3. Downstream boundary conditions (sea water level with tide and wind-set up)

Water levels

The water levels in the channel are harder to obtain. The best way when there is no information is to use the characteristics for width/depth ratio of the classification.

Upstream boundary conditions

The average discharges as mention in section 3.1.1 can be obtained for large rivers from online data, like Wikipedia. But due to the focus of this study on flood events, the need for an extreme discharge is necessary. By using the entrenchment ratio of the classifications, a flood discharge can be calculated. The entrenchment ratio is based in the width of the flood prone and the bank-full width. When calculating the bank-full discharge with a simplified Manning's equation, a flood event discharge can be estimated.

$$Q_{bank-full} = B_c * \frac{1}{n_c} * h_c * R_c^{2/3} * \sqrt{i_b}$$

$$Q_{flood} = B_f * \frac{1}{n_c} * h_f * R_f^{2/3} * \sqrt{i_b}$$

With assumption;

$$R_f = \frac{B_f * h_f}{B_f + 2 * h_f} \approx h_f$$

$$R_c = \frac{B_c * h_c}{B_c + 2 * h_c} \approx h_c$$

The discharges become:

$$Q_{bank-full} = B_c * \frac{1}{n_c} * h_c * h_c^{2/3} * \sqrt{i_b}$$

$$Q_{flood} = B_f * \frac{1}{n_c} * h_f * h_f^{2/3} * \sqrt{i_b}$$

When the discharges increase in the channel, the channel width increases from a bank-full to a flood-prone width and the water level increases. But the rate in which the width increases is larger than for the water level (except for class A, where the water level in the channel increases faster than the channel width).

With assumption:

$$\frac{h_f}{h_c} \ll \frac{B_f}{B_c}$$

The ratio between the bank-full and the flood discharge becomes,

$$\frac{Q_{flood}}{Q_{bank-full}} = \frac{B_f * \frac{1}{n_c} * h_f * h_f^{2/3} * \sqrt{i_b}}{B_c * \frac{1}{n_c} * h_c * h_c^{2/3} * \sqrt{i_b}} = \frac{B_f * h_f * h_f^{2/3}}{B_c * h_c * h_c^{2/3}} \approx \frac{B_f}{B_c}$$

This is the same as the entrenchment ratio. In the case of no information is available on the flood discharges, the classification can be used to calculate the bank-full discharge and with the entrenchment ratio the flood discharge can be calculated:

$$Q_{flood} = Q_{bank-full} * entr.ratio$$

With:

- $Q_{bank-full}$ = Discharge of bank full river
- Q_{flood} = Discharge of a flood – prone river
- $entr.ratio$ = Entrenchment ratio
- B_c = Bank – full width of the river
- B_f = Flood – prone width of the river
- n_c = Roughness coefficient
- h_c = Bank – full water level in the river
- h_f = Flood – prone water level in the river
- R_c and R_f = Hydraulic radius
- i_b = Bottom slope of the river

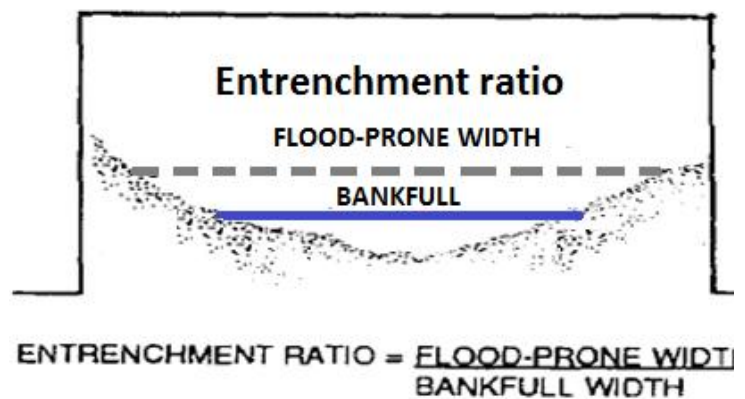


Figure 3-9 The entrenchment ratio is ratio between flood-prone width and the bank-full width

3.2.2.1 Downstream boundary conditions

For the upstream boundary conditions there are three parts that play a role:

1. Sea water level
2. Tide
3. Storm surge

The sea water level can be obtained from the site Sea Level Trends, 2012. When a station is not near the estuary of the river, there is the option to take to stations between the point of interest and either take the average or interpolate between the two stations, depending on the distance between the points.

The tide information of the sites mentioned in the section 3.1.1 can be used and do not need any processing or alternations.

The storm surge, or also called wind setup can be calculated using the next formula:

$$\frac{\Delta S}{\Delta x} = C_2 * \frac{u^2}{g * d}$$

With

$\Delta S =$ Wind setup [m]

$\Delta x =$ distance wind travel [m]

$C_2 =$ constante $\approx 4 * 10^{-6}$ [-]

$d =$ average water depth [m]

$g =$ gravity [m/s²]

$u =$ wind velocity [m/s]

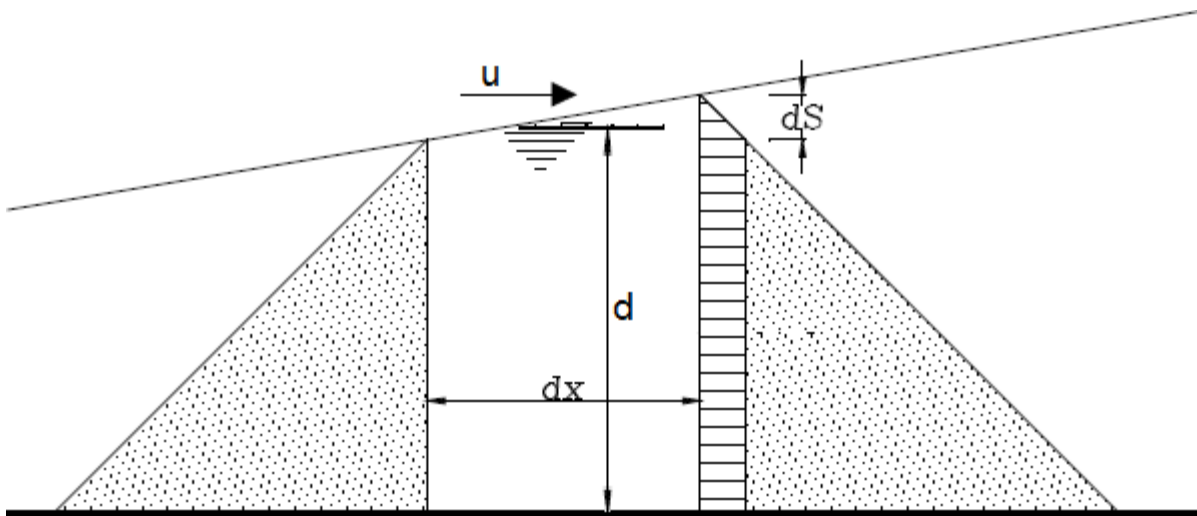


Figure 3-10 Wind set-up by storm surge (Molenaar et al., 2008)

As for the wind velocity, this depends really on what kind of storm is taken into consideration e.g. with return period of 1 year (monsoon) or 50 year return period.

3.2.3 Data to characterize area

DEM

The choice between the SRTM DEM and ASTER GDEM has to be made depends on the region that is looked at. The SRTM height at vegetated areas are systematic to high and the voids in mountain terrain (Hirt et al., 2010). ASTER GDEM is a very high grid resolution but in Hirt et al., 2010 is shown that in comparison with GPS measurements the errors can be large.

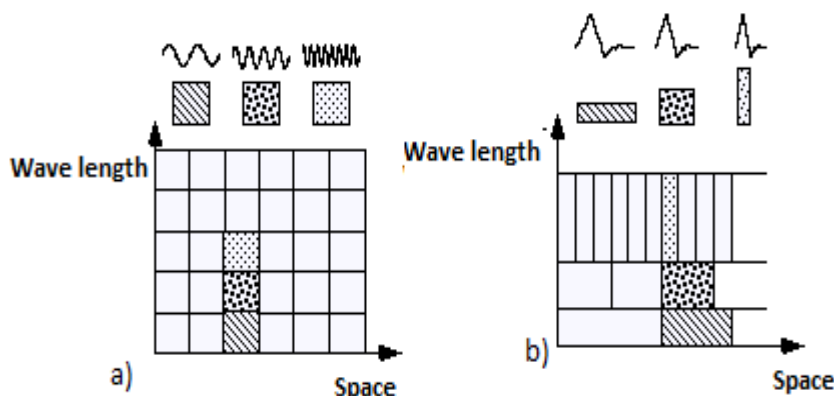


Figure 3-11 Space-wave length tiles for a) Fourier basis functions b) Wavelet basis functions

Once a DEM has been chosen a filter has to be applied to clear out any noise and voids. There are several filter methods to smooth out the DEM. The most used filters are based on Fourier or Wavelet filter method. Both methods' basis

functions are localized in frequency. The difference is that the individual wavelet functions are localized in space, the Fourier sine and cosine functions are not.

The wavelet has an endless set of possible basis function, not like Fourier that has a distinct set (sine and cosine functions). This makes the wavelet analysis favorite by giving immediate access to information ("An Introduction to Wavelets: Wavelet versus Fourier Transforms," n.d.).

River

Location

To determine the location of the channels can be done in several ways.

In the literature a number of algorithms are presented to automate determine the drainage network from a DEM. This network forms the basis to determine sub-catchments and river networks. The basis for this method is that water flows downwards on the surface in the direction of the steepest slope. When the flow direction is determined for each point (or a grid cell) of the catchment area, the flow network of the catchment is determined. With a chosen threshold, the cells whose catchment areas exceed a certain size, the network of watershed is determined. The eight flow direction (D8) is an approach to the model watershed drainage structure (Tribe, 1992). Each cell grid has eight possible flow directions, Figure 3-12.

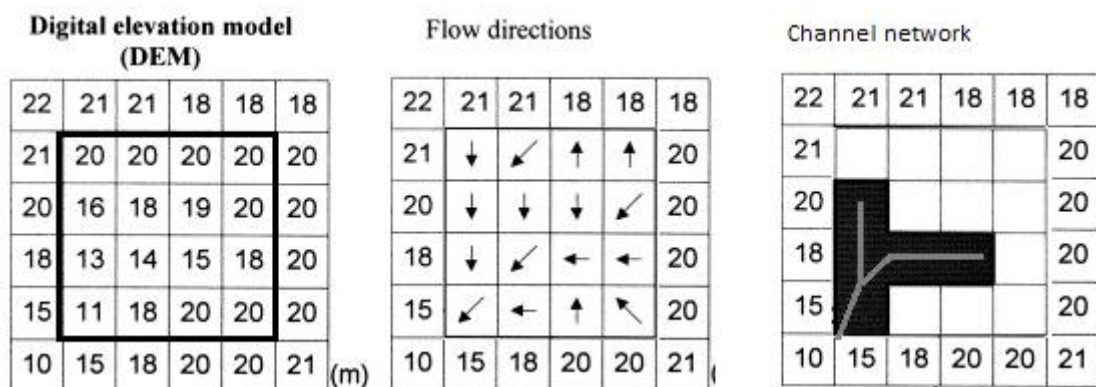


Figure 3-12 Using a DEM to determine the flow directions and the channel network

The D8 model gives unrealistic flows when it's a divergent or plane area. Due to the only eight directions the drainage lines are all parallel orthogonal or diagonal flow lines. This does not reflect the realistic flow lines. This should be visual checked with other data, for example OpenStreetMap.

Depth

In the paper of Leon et al., 2006 the measured discharges in the upper Negro River (Amazon Basin, Brazil) were compared to the heights derived from online satellite data. The water levels were obtained by so called virtual stations. The virtual stations are chosen where the satellite measurements are available and the river intersects. These water levels at the virtual stations were used to determine the discharge using the full dynamic flow, Saint-Venant equation (Boroughs and Zagona, 2002 as cited in Leon et al., 2006). Figure 3-13 shows satellite orbits, the white lines, intersecting with the river, in black and creating a virtual station, the red rectangles.

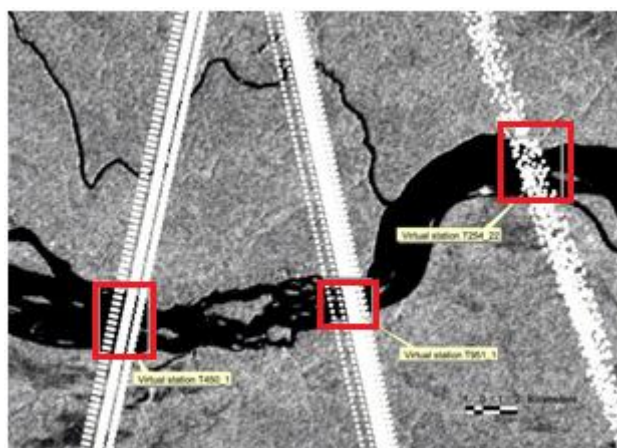


Figure 3-13 Virtual stations, the red rectangles, based on the intersection between the channel, in black, and the satellite orbits, the white lines

Due to seasonal variety (wet and dry season) large variety was found in the water height. The water heights obtained from the virtual stations were compared with the related discharges for the same period. With this selection the discharges estimations obtained from the virtual stations have an error less than 10% compared to gauge measurements.

For the seasonal variety one should or sort the satellite data per period, separating the data into dry and rainy season, or separate relative larger width from sequence virtual stations. Both methods will give an insight into the bank-full characteristics of the river. The definition of the bank-full in the literature varies. The term for this is closely related to terms river floodplains and benches (Williams, 1978). In Williams, 1978 three general descriptions to define a bank-full are given. The best suited for this study is the cross sections (looking at the width/depth ratio). The method to determine the width from the previous section can now be used to determine the depth.

Width to Depth Ratio

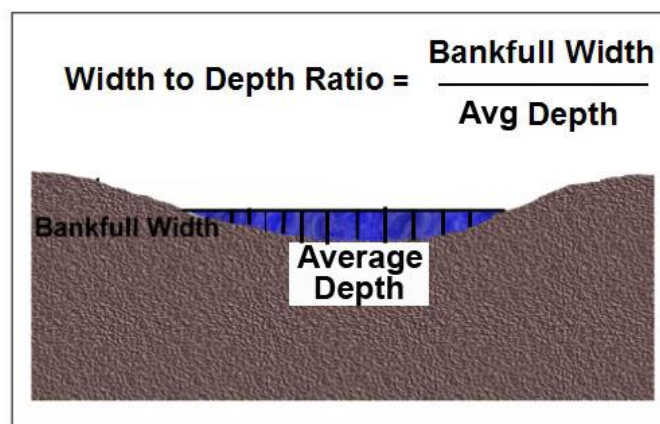


Figure 3-14 Width to depth ratio with bank-full width [http://www.fgmorph.com/fg_3_19.php]

Width

The application by Leon et al., 2006 mention in the previous section can also be used to determine the width of the rivers. By using a buffer zone around the river vector obtained in the paragraph location for example 500 m (Koudijs, 2012) and using satellite data with a smaller spatial,

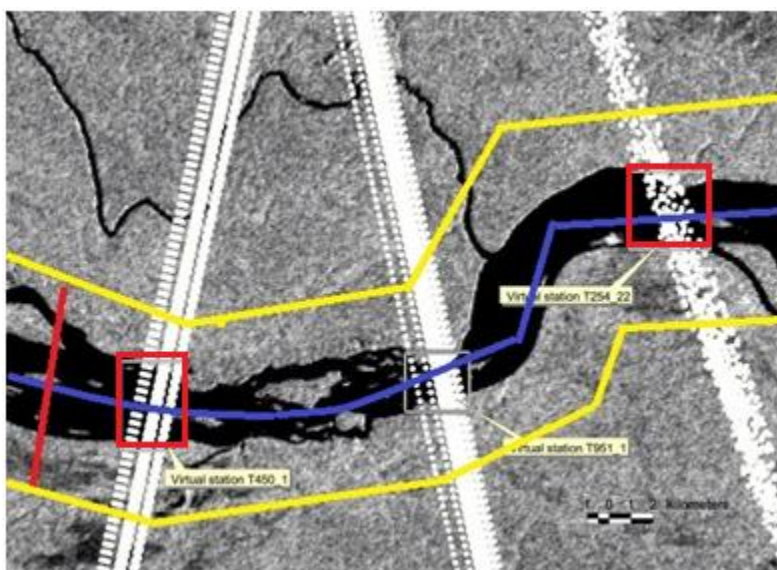


Figure 3-15 Buffer zone for the Upper Negro River

like the ASTER GDEM, a river width can be determined. The choice of the size of the buffer length depends on two aspects: 1) An estimation of the size of the actual river and 2) which satellite data is used with its spatial resolution. Figure 3-15 shows an example of a buffer zone for the Upper Negro River.

In this case the seasonally changes also will have impact on the results. In the rainy season the width of the river can be much larger than in the dry season. This can result in a large difference in width for two

sequence virtual stations. Another point that needs to be addressed is that in Leon et al., 2006 the upper part of the Negro River was tested for the method. When for a river the downstream characteristics need to be determined, the tidal penetration inland and storm surge should be taken into account.

The chosen period for the satellite data that is used in the virtual stations, the tidal heights in that period should be checked. So if there are sequence virtual stations with extreme differences it might be explainable due to the tidal elevations.

3.3 Summary

In this chapter methods are discussed to derive the DEM and the river location, depth and width. Typically these parameters are derived one after the other: The filtered DEM is used to derive the location of the river. Next this location is used to determine the depth and the width of the rivers. If one of the two can be determined with satellite images by using a depth-width ratio, the other component can be determined. This means that all methods described above depend on the accuracy of the previous steps.

The river location and width can be derived in a second manner using the image data, LandSat or MODIS and the products of Dartmouth, OpenStreetMap and LEGOS.

In combination with the classification of the rivers (Rosgen, 1994) these methods can result in enough data to be able to use in a flood model for a flood prediction. The accuracy of these methods need to be researched, this will be done by means of the three case studies in the following chapters.

4. Study case: 1D flow

4.1 Introduction

The different components of flood information have been discussed in chapter 2. In this chapter the components that determine the 1-dimensional flow in the channel are described and analyzed. The objective for this chapter is to determine the relevant components for river and flood plain areas with varying characteristics. To work towards this objective this chapter is divided into the following segments. In chapter 4.2 the different classes of areas for the rivers and the flood plains are described. In chapter 4.3 the equations and the assumptions for the calculations are clarified. Chapter 4.4 the methodology for deriving the relevant components for the river channels and the floodplains is explained. The methodology used is a sensitivity analysis with the components if the channel and the floodplain. Chapter 4.5 the result of the calculation for the classes and all the components are presented. In the last chapter, chapter 4.6 the conclusions for the relevant components for the different river and flood plain areas are discussed.

4.2 Types of areas

In chapter 2.2.4 different flood prone areas are described. The areas with that are chosen for this study are:


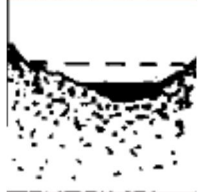


- Mountainous areas with slopes larger than $1 \cdot 10^{-2}$
- Hilly areas with slopes between $1 \cdot 10^{-2}$ and $4 \cdot 10^{-2}$
- Delta areas with slopes between $4 \cdot 10^{-2}$ and $2 \cdot 10^{-2}$
- Flat areas with slopes smaller than $2 \cdot 10^{-2}$

The areas differ in the slopes, the cross sections of the channel and the floodplains. In the sensitivity study the terrains have different combinations of slopes and cross sections characteristics. With these varying values for the different terrains, these areas can be classified.

The mountainous area has the largest slope, the flat area the smallest slope and the delta area has a slope in between the two extremes. These classifications can also be seen as the different cross sections of one river, with class Aa+ being a cross section presenting up streams of a river, the class DA as down streams of a river and the classes B and E as sections in between.

To characterize the type of rivers, the river characteristics are used, as described in chapter 3. In this classification the rivers are divided according to their dominant slope range, width-depth ratio, entrenchment ratio and type of cross section (Rosgen, 1994). From this classification four classes are chosen to be tested.

Table 4-1 Classification for types of area varying in slope, width-depth ratio and cross-section [draw better pictures]

Class	Aa+	B	C	DA
Dominant slope range	<10%	2-4%	<2%	<0.5%
Width-depth ratio	<12	>12	>12	<40
Entrenchment ratio	<1.4	1.4-2.2	>2.2	>2.2
Cross-section				
Flood prone area	Mountainous area	Delta area	Delta area	Flat area

The classes are sorted with one of the flood prone areas from chapter 2.2.4 based on the dominant slope range.

To be able to calculate which components are relevant for the four types of areas, a simplification needs to be made for these cross-sections. Figure 4-1 shows the simplified schematization of the cross-section.

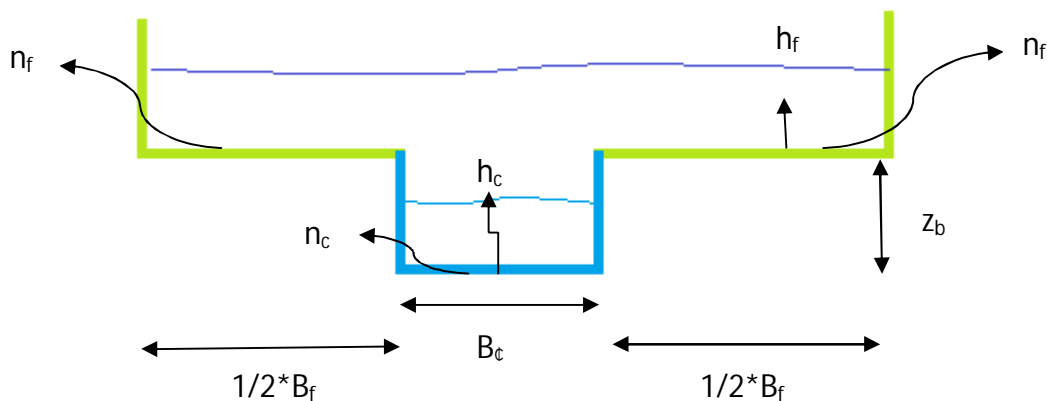


Figure 4-1 Schematization of the cross section of a river and flood plain area

The schematization distinguishes the characteristics for the channel in blue (variables with subscript c) and flood plain in green (variables with subscript f).

n_f =Manning coefficient for floodplains [$s/m^{1/3}$]

n_c =Manning coefficient for channel [$s/m^{1/3}$]

B_f =width of floodplains [m]

B_c =width of channel [m]

h_c =water level in channel[m]

h_f =water level in floodplain[m]

z_b =bottom level of the channel

The components described here above have different values for each of the classes. In the chapter 4.3.2 the chosen values for these components of the channel and the floodplains will be given.

4.3 Schematization for 1D flow

The investigation in the sensitivity of the components of the channel and of the floodplains on the water level of the floodplain, a simple rectangular channel and rectangular floodplain is used as drawn in Figure 4-1. In this chapter the used equations will be explained. Also the assumptions that have been made to be able to derive an equation for the water level of the floodplain. Furthermore the chosen values for the components of the channel and the floodplains for the different classes are given.

4.3.1 Equations

For the calculation of the flow in the channel and the flow in the flood plains the following equations are used. The total discharge is the discharge that goes through the channel together with the discharge that goes through the floodplains:

$$Q_{tot} = Q_f + Q_c$$

Equation 4-1

With the Manning equation, the discharge through the channel is:

$$Q_c = B_c * h_c * \frac{1}{n_c} * R_c^{2/3} * i_b^{1/2}$$

Equation 4-2

The discharge through the floodplain is:

$$Q_f = B_f * h_f * \frac{1}{n_f} * R_f^{2/3} * i_b^{1/2}$$

Equation 4-3

Where the hydraulic radius for the floodplain is:

$$R_f = \frac{B_f * h_f}{B_f + 2 * h_f}$$

Equation 4-4

With the assumption that the water level in the floodplain increases simultaneously the water level in the channel,

$$h_c = h_f + z_b$$

The hydraulic radius for the channel becomes:

$$R_c = \frac{B_c * h_c}{B_c + 2 * h_c} = \frac{B_c * (h_f + z_b)}{B_c + 2 * (h_f + z_b)}$$

Equation 4-5

The assumptions that are made to be able to use these formulas are:

1. $i_b = i_w$
2. $h_f \ll z_b$ and $h_f \ll B_f$
3. if $Q_c > Q_{tot}$ than $h_f = 0$

With the first assumption a uniform stationary flow is applied, the waterline (energy slope) is equal to the bottom slope. The advantage of this approach is that only one upstream boundary condition is

required. The disadvantage of this approximation it is not applicable for bottom slopes that are close to zero and for areas where significant impact of backwater is expected.

In the second assumption the water level in the flood plain is considered much smaller than in the channel, making the water level in the channel h_f equal to the bed level of the channel z_b .

By assuming the level of the floodplain to be smaller than the bottom of the channel, the hydraulic radius for the channel R_c can be simplified:

$$R_c = \frac{B_c * h_c}{B_c + 2 * h_c} = \frac{B_c * (h_f + z_b)}{B_c + 2 * (h_f + z_b)} \approx \frac{B_c * z_b}{B_c + 2 * z_b}$$

Equation 4-6

And the assumption that flood plain level is smaller than the width of the flood plain makes the wetted perimeter for the flood plain:

$$R_f = \frac{B_f * h_f}{B_f + 2 * h_f} \approx h_f$$

Equation 4-7

The thirds assumption assumes that the water entering the flood plains can only come from the overcapacity of the channels discharge. So if the maximum capacity of the channel is not reached, there is no flood plain under water.

To be able to investigate the sensitivity of the water level in the flood plains, the equations are rewritten:

$$h_f^{5/3} = \frac{Q_{tot} - B_c * z_b * \frac{1}{n_c} * i_b^{\frac{1}{2}} * R_c^{\frac{2}{3}}}{B_f * \frac{1}{n_f} * i_b^{\frac{1}{2}}}$$

Equation 4-8

And the equation is divided into three terms:

$$h_f^{5/3} = \frac{Q_{tot}}{B_f * \frac{1}{n_f} * i_b^{\frac{1}{2}}} - \frac{B_c * z_b * \frac{1}{n_c} * R_c^{\frac{2}{3}}}{B_f * \frac{1}{n_f}} = \left[\left(\frac{Q_{tot}}{i_b^{\frac{1}{2}}} \right) - \left(B_c * z_b * \frac{1}{n_c} * R_c^{\frac{2}{3}} \right) \right] \frac{1}{B_f * \frac{1}{n_f}}$$

Equation 4-9

1^e term 2^e term 3^e term

The first term in the equation above represents the forcing term, the second term is the channel characteristics term and the third term is the floodplain characteristics term.

The solution for h_f becomes:

$$h_f = \left[\left[\left(\frac{Q_{tot}}{i_b^{\frac{1}{2}}} \right) - \left(B_c * z_b * \frac{1}{n_c} * R_c^{\frac{2}{3}} \right) \right] \frac{1}{B_f * \frac{1}{n_f}} \right]^{3/5}$$

Equation 4-10

1^e term 2^e term 3^e term

The sensitivity of all the components has been tested on the water level in the floodplains by using different values of the components and checking the sensitivity of this component on the water level in the floodplain. The components are the parameters in the equations described here above, i.e. the width, (B), the slope (i_b) and the Manning's roughness coefficient (n). This has been done for all four classified river and flood prone areas for all the components.

In the previous section the solution for the water level of the floodplains with the use of the Manning's equation is solved. In chapter 2.3.3 the flood depth and the propagation of the flood have been assigned as the information needed for a prediction of a flood event. To calculate the propagation of the flood in this 1D flow schematization, the kinematic flood wave propagation theory is used:

$$c = \frac{1}{B_f} \frac{\partial Q_{tot}}{\partial h_f}$$

Equation 4-11

Where

c = flood wave celerity[m]

B_f = storage width of the floodplain [m]

Q_{tot} = total discharge [m^3/s]

h_f = water depth in the floodplains [m]

$$\frac{\partial Q_{tot}}{\partial h_f} = \frac{\partial(Q_f + Q_c)}{\partial h_f} = \frac{\partial Q_c}{\partial h_f} + \frac{\partial Q_f}{\partial h_f}$$

Equation 4-12

$$\frac{\partial Q_c}{\partial h_f} + \frac{\partial Q_f}{\partial h_f} = \frac{5}{3} * B_c * (h_f + z_b)^{2/3} * i_b^{1/2} * \frac{1}{n_c} + \frac{5}{3} * B_f * h_f^{2/3} * i_b^{1/2} * \frac{1}{n_f}$$

Equation 4-13

With

$$h_f + z_b \approx z_b$$

The celerity of the flood wave becomes;


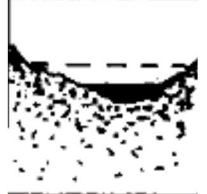
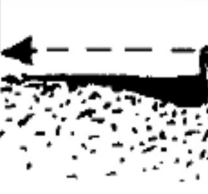
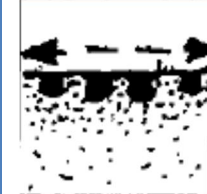
$$c = \frac{5}{3} * \frac{B_c}{B_f} * z_b^{2/3} * i_b^{1/2} * \frac{1}{n_c} + \frac{5}{3} * h_f^{2/3} * i_b^{1/2} * \frac{1}{n_f}$$

Equation 4-14

4.3.2 Values for the classes

The chosen ranges in the schematization for the components of the flow in the channel and the flood plain are given for each of the four classes in Table 4-2. The range is determined by using the classifications by Rosgen, 1994. The ranges for the width, the depth and the slope are clearly identified in this paper. The values for the Manning's coefficient are determined by a general value for natural rivers and are equal for all classes, see the appendix. For the values of the discharges the entrenchment ratio is used. The entrenchment ratio is defined as ratio between the flood-prone width and bank-full width. By calculating the channel discharge and multiplying this with the entrenchment ratio, a total discharge is created that causes a flood that can occur in that area, this method is explained in chapter 3.2.2.

Table 4-2 Values for the components of the flow for the channel and flood plains in the schematization

Class	Aa+	B	C	DA
Slope	>10%	2-4%	<2%	<0.5%
Width-depth ratio	<12	>12	<12	<40
Entrenchment ratio	<1.4	1.4-2.2	>2.2	>2.2
Cross-section				
Schematization	$i_b=0.04-0.1$	$i_b=0.02-0.04$	$i_b=0.005-0.02$	$i_b=0.001-0.005$
	$B_c < 12 * z_b$	$B_c > 12 * z_b$	$B_c < 12 * z_b$	$B_c < 40 * z_b$
	$z_b=5-10$ m $B_c=10-30$ m $B_f=25-50$ m $n_c=0.03-0.05$ $n_f=0.035-0.07$ $Q_{tot}=2500-3500$ m ³ /s	$z_b=1-5$ m $B_c=50-100$ m $B_f=50-100$ m $n_c=0.03-0.05$ $n_f=0.035-0.07$ $Q_{tot}=2500-4500$ m ³ /s	$z_b=1-5$ m $B_c=10-50$ m $B_f=50-150$ m $n_c=0.03-0.05$ $n_f=0.035-0.07$ $Q_{tot}=1000-3000$ m ³ /s	$z_b=1-5$ m $B_c=50-100$ m $B_f=100-200$ m $n_c=0.03-0.05$ $n_f=0.035-0.07$ $Q_{tot}=1500-3000$ m ³ /s
Average values	$i_b=0.07$ $z_b=7.5$ m $B_c=20$ m $B_f=40$ m $n_c=0.04$ $n_f=0.0525$ $Q_{tot}=3100$ m ³ /s	$i_b=0.03$ $z_b=3$ m $B_c=75$ m $B_f=75$ m $n_c=0.04$ $n_f=0.0525$ $Q_{tot}=3500$ m ³ /s	$i_b=0.0125$ $z_b=3$ m $B_c=30$ m $B_f=100$ m $n_c=0.04$ $n_f=0.0525$ $Q_{tot}=2000$ m ³ /s	$i_b=0.003$ $z_b=3$ m $B_c=75$ m $B_f=125$ m $n_c=0.04$ $n_f=0.0525$ $Q_{tot}=2200$ m ³ /s

The sensitivity analysis has been performed by keeping all, except one, components constant at the minimum value, and selecting five values for the remaining component between the maximum and minimum value of its range. For the values between the minimum and maximum, a uniform distribution is used.

An example is given in table 4-3, where the slope is varied and the other components are attributed the minimum value. This is done for all the components and for all classes. One component is an exception, for the discharge is the average value and not the minimum value used. By using a larger value than the minimum discharge a larger flood occurs.

Table 4-3 Example of calculations of Class Aa+ with average values of the components and varying values of i_b

Class Aa+	
Minimum values	$z_b=5$ m $B_c=10$ m $B_f=25$ m $n_c=0.03$ $n_f=0.035$ $Q_{tot}=3100$ m ³ /s
Varying component i_b	$i_b = 0.001$ $i_b = 0.002$ $i_b = 0.003$ $i_b = 0.004$ $i_b = 0.005$

4.4 Methodology

In this chapter the methodology used to determine the relevant components of the channel and the floodplains for the water level in the floodplains is described. Before the sensitivity analysis of the components, an analysis to distinguish the classes not only by their classification values but also by the ratio of the terms. It's essential to be able to classify real rivers into these classes, without the exact values of the components of the real rivers matching the components of the classes.

First the Equation 4-10 is used to determine the differences between the classes by withdrawing the influence of the third term, the floodplain characteristics. By taking the third term equal to one, Equation 4-10 becomes Equation 4-15. In the first sensitivity analysis the first and the second term are the only terms used.

$$h_f^{5/3} = \left[\left(\frac{Q_{tot}}{i_b^{1/2}} \right) - \left(B_c * z_b * \frac{1}{n_c} * R_c^{2/3} \right) \right]$$

Equation 4-15

To distinguish the differences between the classes, the first two terms, the forcing term and channel characteristics term are the terms most important. This analysis shows the difference in the four classes by comparing the first and the second term. The comparison is done by looking at the absolute values of the two terms but also the ratio of the two terms.

Next the real rivers are also compared to the results of the analysis of the first two terms of Equation 4-15. For the three real rivers the values of the components are derived from different sources and the values of the first two terms and the ratio between the two terms are compared to the results of the classes. For the sensitivity analysis of the components, classifying the real rivers into the classes is an important step. If the real rivers fit the classification, this proves that the results of the sensitivity analysis can also be applied to real rivers.

To be able to determine the relevant components for each of the four classes a sensitivity analysis on the components of the classes is been carried out. By varying the values of the components i_b , z_b , B_c , B_f , n_c , and n_f , the influence of these components on the water level of the floodplains can be determined.

With the results of this sensitivity analysis, the influence on the water level of the floodplain due to uncertainties of a component can be derived. The difference in the water level can be seen as the expected error when values of a component are unknown or uncertain for each class.

This method is also used to analyze the influence on the celerity of the flood wave due to uncertainties of the parameters.

4.5 Results of simulation 1D flow

4.5.1 Introduction

The result from the calculation will be presented and analyzed for each class separately. The Manning's equation, Equation 4-10 from the previous paragraph, is stated here below, divided into three terms, the first is the forcing term, the second term is the characteristics of the channel and the third term is the floodplain characteristics.

$$h_f^{5/3} = \left[\left(\frac{Q_{tot}}{i_b^{1/2}} \right) - \left(B_c * z_b * \frac{1}{n_c} * R_c^{2/3} \right) \right] \frac{1}{B_f * \frac{1}{n_f}}$$

1^e term
 2^e term
 3^e term

Equation 4-10

All three terms in Equation 4-10 contribute to the water level of the floodplain h_f .

The first term, the forcing term, contains two components the discharge and the slope. The first term is a measure for how fast the water flows through the area, the residence time. An area with a small slope (i.e. a flat terrain) and a large discharge can have a similar residence time as a large slope (i.e. a steep terrain) with a small discharge. Therefore the first term gives insight into the different classes not only their variable slopes and discharge but the size of the forcing of the system.

The second term contains only characteristics of the channel. This term gives insight into the flow capacity of the channel. Large and deep rivers have a relatively large value for the second term compared to small and narrow rivers.

The third term gives insight in the floodplain characteristics. To be able to qualify the first two terms the values for the third term will be assumed to be equal to one, chapter 4.5.2. After this the real river will be sorted into the classification, chapter 4.5.3. After evaluating the results for the classes, the third term will be analyzed separately. This approach will solve all the three terms in Equation 4-10 to derive the sensitivity of the components on the water level in the floodplain.

4.5.2 Classification ratios

The results of the different classes are displayed into one graph, Figure 4-2. In Figure 4-2 on the vertical axes is the first term of the Equation 4-10 the forcing term. The second term of the Equation 4-10, the channel characteristics is on the horizontal axis. The third term is left out by assuming it to be equal to one. The reason for leaving out the third term is that the third term components do not have a presented value for the classification. The values for these terms are subjective but have a large impact on the results. By leaving this term out the results focus is on the first two terms.

Figure 4-2 shows the positions of the four classes relative to each other. The closer the class is to the horizontal axes the larger the first terms is and the first term takes a dominating role. The more the class is towards the right the more influence the second term has. The influence on the water level of the floodplain is approximated by the first term minus the second term. This is an approximation due to the third term being left out. Therefore a relative large the first term results in an increase of the water level of the floodplain and a relative large second term results in a decrease of the water level of the floodplain.

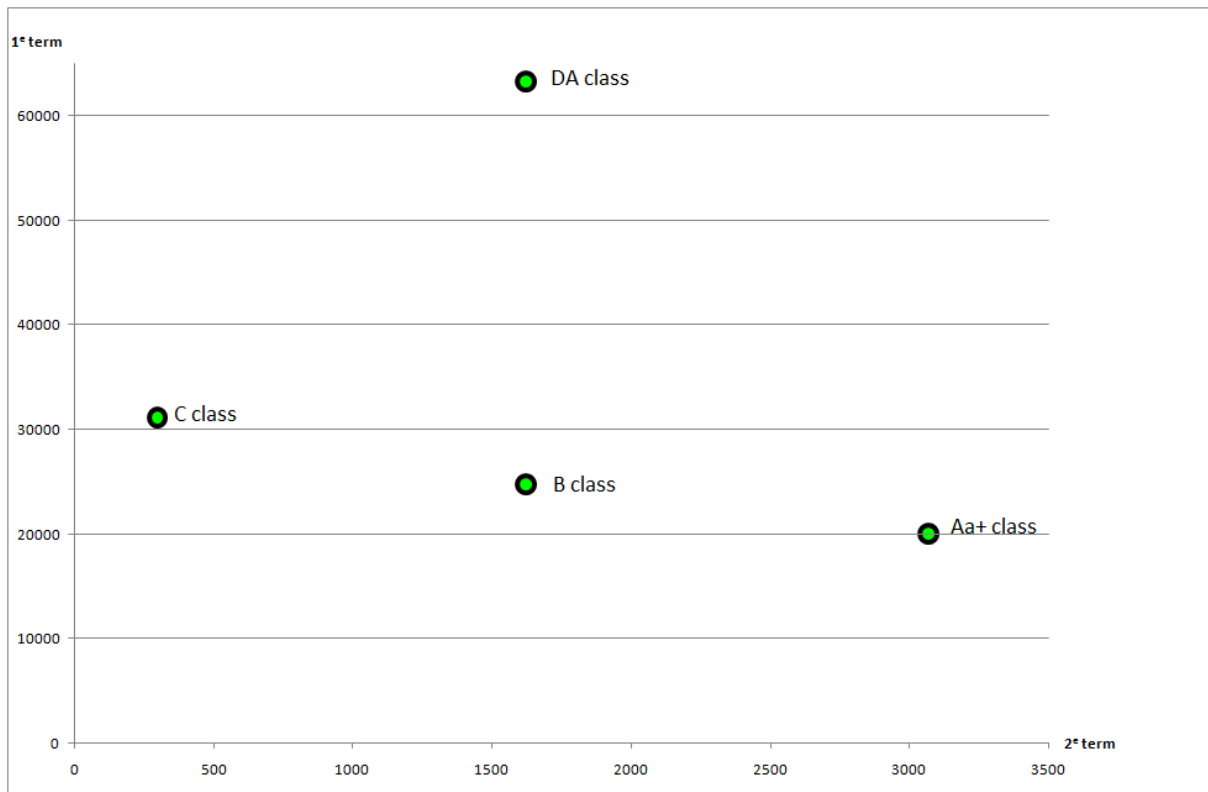


Figure 4-2 Values of first term on the vertical axes, $\frac{Q_{tot}}{i_b^2}$ and second term on the horizontal axes, $B_c * z_b * \frac{1}{n_c} * R_c^{\frac{2}{3}}$ of Equation 4-10 for all classes

In Figure 4-2 the minimum values are used for each of the classes. This figure covers on the vertical axes the forcing term, dependable on the slope and the discharge. For the classes Aa+, B, C and DA, the slopes are respectively 0.04, 0.02, 0.005 and 0.001. Although the first term covers as well as the slope as the discharge, this figure shows that the slope is an important component for the forcing term. An increasing slope results in decrease in the first term, regardless of the discharges.

On the horizontal axes is the second term, the channel characteristics. Here the flow capacity of the river (i.e. the bank-full discharge) determines the position of the class in the figure.

Here both values for the first and second term have been evaluated. The next step is to look at the ratio between these two terms.

$$Ratio\ term = \frac{1^e\ term}{2^e\ term} = \frac{\frac{Q_{tot}}{i_b^2}}{B_c * z_b * \frac{1}{n_c} * R_c^{\frac{2}{3}}}$$

Equation 4-16

The ratio is a better result to classify these rivers than to just take the difference between the first and second term of Equation 4-10. The reason for this is that the classes are defined by certain values and ratio's (i.e. the slopes, the width-depth ratio and the entrenchment ratio). When using the Equation 4-10, the components are divided into two terms, the forcing and the channel characteristics. Figure 4-2 shows that by comparing these two terms the difference in classes can be seen. But due

Table 4-4 Ratio of the first and the second term for all classes

Class	First term	Second term	Ratio
Aa+	20.000	3.000	7
B	25.000	1.600	15
C	31.000	300	105
DA	63.000	1.600	39

to the fact that the classes are defined by values and ratio's, Figure 4-2 shows the value differences between the classes but by taking the ratio between the two terms this gives a different and a more general classification. Table 4-4 gives the ratio between the two terms.

The larger the ratio between the first and the second term is the more influence the first term has on the water level in the floodplains.

4.5.3 Real rivers

Because the classifications used here are based on theoretical rivers and floodplains, the values for these terms are subjective. To have an insight on these two terms, the real rivers have been evaluated and compared to the result presented in Figure 4-2 and in Table 4-4. The sections of the rivers that have been chosen are the Meuse River, the Rhine River and the Nile River.



Figure 4-3 The Meuse river at Maastricht

The values of the Meuse are derived from Spaargaren, 2002 and can be found in the appendix. The Meuse is a river of a length of 950 km. For the classification of the river Meuse, the part between Maastricht and Venlo (length of approximately 75 km) has been taken into consideration. This can be seen as the downstream part of the river and relatively flat.

The second river that has been compared is the Rhine. The Rhine is a river with a total length of 1233 km and is one of the longest rivers in Europe ("Middle Rhine - Wikipedia, the free encyclopedia," 2012). The section Middle Rhine is being evaluated here. The Middle Rhine is the part of the Rhine in Germany from Bingen until Bonn with a length of 150 km. This can be seen as the upstream part of the river with a relatively steep slope, as it is a mountainous area.



Figure 4-4 View of the Rhine from the source till the estuary. The yellow section is the Middle Rhine.



Figure 4-5 The Nile River, with in blue the upper-middle part between Aswan and Edfou

The other river to be examined and to be classify is the Nile, the largest rivers in the world, with a total length of 6671 ("Nile River," n.d.). For the Nile River, the upper-middle part between Aswan and Edfou with a length of 115 km has been reviewed. This can be seen as the upper-middle part of the river with a relatively flat terrain.

The final river to be examined and to be classify is the Chao Phraya, the largest river in Thailand, with a total length of 372 km. The Chao Phraya can be seen a river in a relatively flat terrain.

The values which have been used to calculate the values for the first and second term of Equation 4-10 for these rivers can be found in the appendix.

Table 4-5 Values for the first and second term (Equation 4-10) and the ratio (Equation 4-16) of these two terms for the three real rivers

River	First term	Second term	Ratio term	Best Class fit
Meuse	12.000.000	120.000	103	C
Middle Rhine	6.000.000	600.000	10	Aa+
Nile	97.000.000	2.000.000	45	DA
Chao Phraya	89.300.000	1.150.000	77	DA/C

Table 4-5 shows the values for the first and the second term, the ratio term (the ratio between the two terms Equation 4-16) and the best class fit. First the values for the first two terms of Equation 4-10 will be evaluated.

The values that are presented in Table 4-4 for the first two terms do not fit the real river values. The values for the first and the second term in Table 4-5 are almost 1000 times larger than the values in Table 4-4. But when the ratio terms are compared, the real rivers match the description of the classes. Therefore the best class fit is based on the ratio term and not on the absolute values of the first two terms.

The classes that are best fitted with the real rivers match also the description of these real rivers. The chosen section of the Meuse River fits the description of a downstream section of the river in a relatively flat terrain. The values for the discharge and the width and depth of the channel do not fit any of the description of a class as it's been determined here. But with the ratio term (Equation 4-16) equal to 100 for the Meuse River, this fits the Meuse River into the classification of the class C. This can also be determined for the chosen section of the Middle Rhine River. The description is an upstream section of the Rhine River in a relatively steep area, as it is in the mountainous terrain. The ratio term of 10 fits the Aa+ class, which is for mountainous areas. The section of the Nile River is described as the section between the downstream and upstream of a river. But due to a relative extreme small slope the ratio of the section the Nile River is in the class DA. The class DA is described as a class for downstream areas, but when a terrain is extreme flat in combination with the values for the other components this can still be classified as a class DA. The Chao Phraya is a river that cannot be classified to one class. The ratio value of the first two terms is right between class C and DA. This should be taken into account in the third case study.

For the real rivers that have been checked to fit a class the ratio term is an important parameter for classification. This makes it possible to classify the river into one of the four classes. In the next chapter the sensitivity of the components of the classes on the water level of the floodplains will be analyzed. With the result of this chapter, fitting the real rivers into one of the four classes, the sensitivity analysis of the components will also be applicable to the real rivers.

4.5.4 The water depth in the flood plains

The next step is to determine the components that are relevant for the water level of the floodplain of certain terrains. This is done by taken a uniform distribution for the components, i_b , z_b , B_c , B_f , n_c and n_f for all five classes. This gives insight into the sensitivity of each component on the water level of the flood plains. All the three terms from Equation 4-10 are taken into account.

As in the previous chapter the exact values of these terms are subjective. With the uniform distribution of the components, the changes of the components step by step results in the change in the water level of the floodplain also step by step. The interest goes to the change in the water level in the floodplains due to these components and also the magnitude of the change. This gives an insight into the magnitude of the error that can be made by each component.

These results will be presented in graphs where the change in the water level in the floodplains due to varying values of the components can be seen on the two axes. The graphs are presented with on the vertical axes the first term of Equation 4-10 times the third term. This gives an insight into the influence of the forcing term and the flood plain characteristics on the water depth in the floodplain.

$$\text{vertical axes} = \frac{Q_{tot} / i_b^{\frac{1}{2}}}{B_f * \frac{1}{n_f}} [m^{5/3}]$$

Equation 4-17 First term divided by the third term of Equation 4-10

On the horizontal axes is the second term of Equation 4-10 times the third term. This gives an insight into the influence of the channel characteristics and the flood plain characteristics on the water level of the floodplain.

$$\text{horizontal axes} = \frac{B_c * z_b * \frac{1}{n_c} * R_c^{\frac{2}{3}}}{B_f * \frac{1}{n_f}} [m^{5/3}]$$

Equation 4-18 Second term divided by the third term of Equation 4-10

The graphs are presented in the way that all values of the components are plotted in one graph for each class. The light blue circle is the point where each component has a minimum value. From this point the varying values of the components show the influence that the component has on the water level of the floodplains. Each component has individual color and five different. The shapes present the values from minimum to maximum value, a diamond, a square, a triangle, a star and a circle.

In the graphs the black lines give the change in the water level of the floodplain. This way the magnitude of the change in the water level of the floodplain can be seen due to the varying values of the components. The bolt dark line is the threshold for flooding, it has also an indication of $h_f=0$, meaning all points below this line, flooding does not occur. The next line is the line of $h_f=1$ m, where the points on this line having all have a water level in the floodplains of 1 m. The other black lines present the water level in the floodplains of $h_f=1,5$ m, $h_f=2$ m and $h_f=2,5$ m.

Difference in water depth in the floodplains

The different values for the components, i_b , z_b , B_c , B_f , n_c and n_f , result in different values for the water depth in the floodplains. To determine the influence of each component on the water depth of the floodplains, the difference in value for the water depth for the minimum and the maximum value of a component is taken. This gives insight into the size of the influence of that component. When the difference is small, that component has little influence, while when the difference is large the influence is high.

Angle of water depth values

In the previous section, section 4.5.3, is shown that the ratio term between the forcing term (1e term) and the channel characteristics (2e term) is of importance. The absolute results for the water depth in the floodplains are analyzed by looking at the difference in the water depth in the floodplains, but the ratio between the two terms is also of importance. The ratio between these two terms is expressed in an angle. The absolute values of the water depth in the floodplains are the results of the chosen range for the components, l_b , z_b , B_c , B_f , n_c and n_f . If the range for a component was smaller or larger, the difference for the water depths would be smaller or larger. Figure 4-6 shows two sets of ranges for one component, in brown the smaller range and in blue the larger range. With the larger range the difference in the water depth is larger, this is the reason the angle is taken into account because for both ranges the angle is the same.

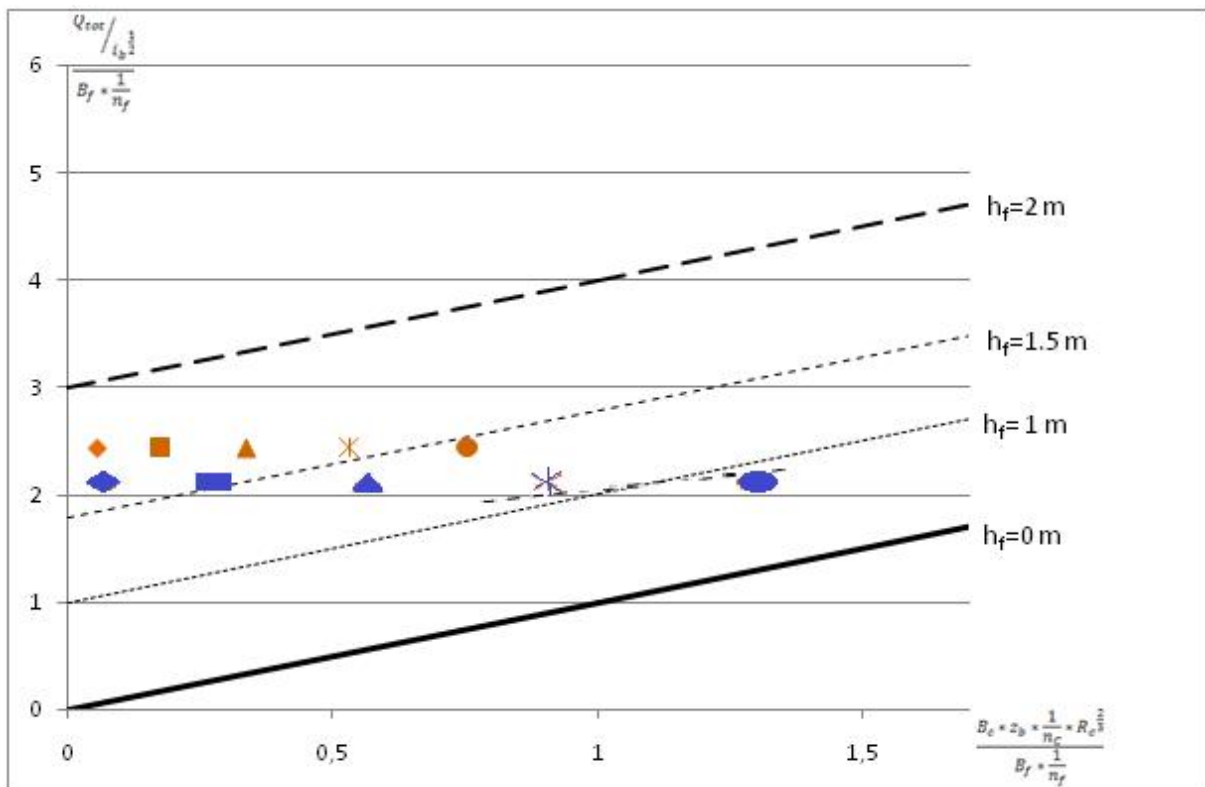


Figure 4-6 Example of the angle of the water depth in the floodplains

The angle is taken relative to the angle of the black lines, which indicates a constant water depth in the floodplains. Figure 4-7 shows the angles are indicate a significant influence or no influence. If the components lines would follow the black dotted lines(0°), the influence of that component would be zero, because the black lines represent a constant value in the water depth of the floodplains. If the components lines would be perpendicular to the black lines(90° or -90°) the influence is the highest, because this indicates the largest change. The negative angle represents a decrease in the water depth and a positive angle an increase in the water depth.

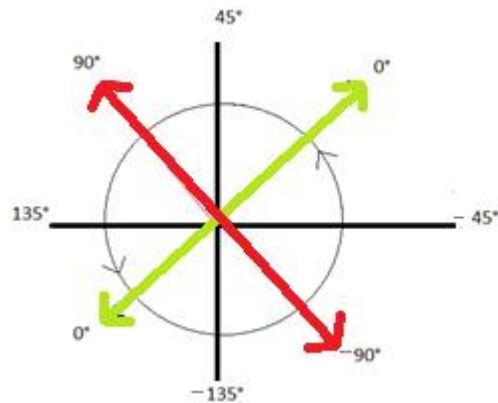


Figure 4-7 The angle of the components

All four classes will be presented here, starting with the class Aa+, the mountainous terrain, then the class B and C, the terrains with small slope, and followed by the class DA, the flat terrain. The scale of the graphs has been kept the same for all classes.

Class Aa+

In Figure 4-8 the results for the uniform distribution of the components for class Aa+ are shown.

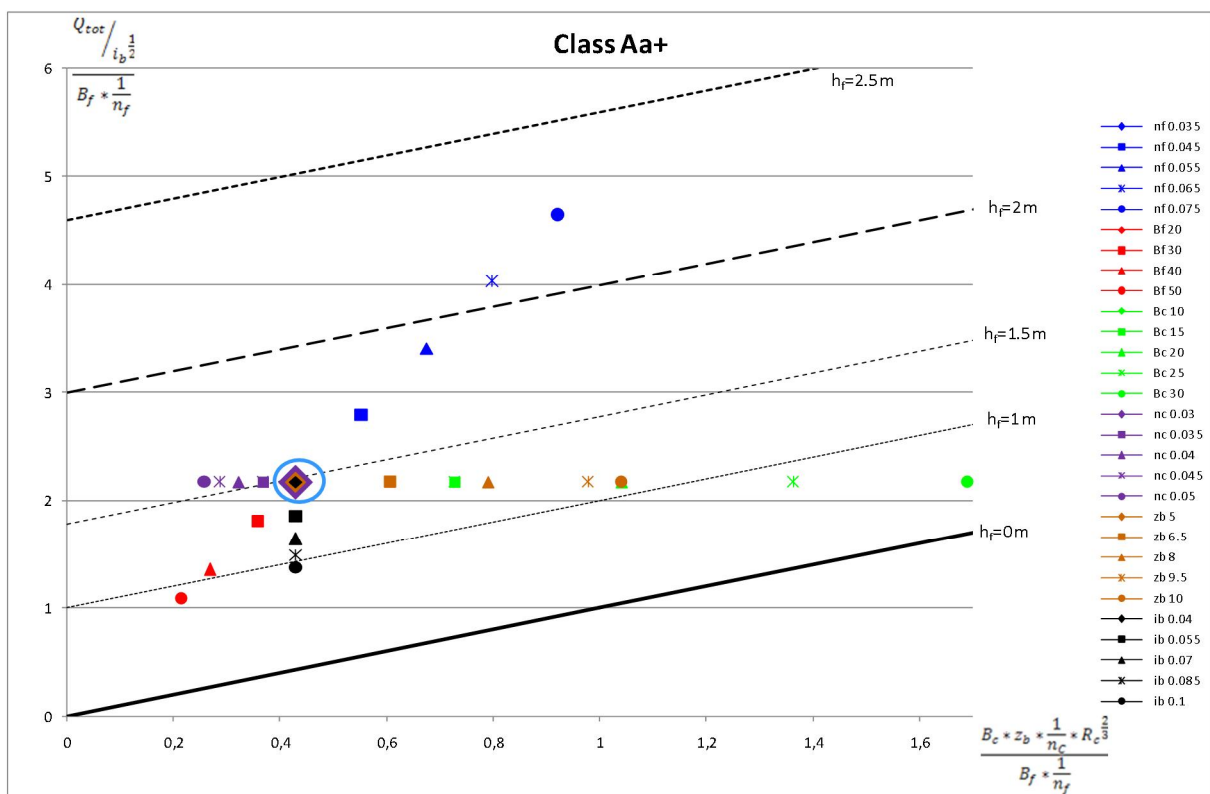


Figure 4-8 The effect of a uniform distribution of the components on the water level of the floodplains for class Aa+.

Figure 4-8 shows that the components n_f , B_c and z_b have the largest spread. It is important the clear that not only a large spread implies a large influence on the water level of the floodplain but also the angle.

The influence of the components on the water level of the floodplain can be measured through the angle with the black lines and the size of the spread. This shows again that the ratio between the first and second term are important and not only the exact values of these terms.

Table 4-6 shows the difference of the actual water level in the floodplains with the minimum and maximum values of the components and the angle due to range of the chosen values for the components.

Table 4-6 The values for the water level of the floodplain due to change in values of the components for class Aa+

class Aa+				
Component	hf for minimum component value [m]	hf for maximum component value [m]	Difference [m]	Angle [°]
n_f	1.39	2.20	0.81	34
B_f	1.39	0.92	-0.47	-136
B_c	1.39	0.64	-0.75	-45
n_c	1.39	1.48	0.08	135
Z_b	1.39	1.08	-0.32	-45
i_b	1.39	0.97	-0.43	-135

The component that has negligible influence on the water level of the floodplains is the component n_c . The components n_f and B_c have the most influence on the water level. The other components, B_f , Z_b and i_b have a small influence close to 0.5 m.

For the components B_f , B_c , Z_b and i_b the increasing value results in decrease of water level of the floodplain. This can be also derived from Equation 4-15. These components are the denominators in the equation, so increasing these components results in a decrease of the output of the equation.

Class B

Figure 4-9 shows the results for the uniform distribution of the components for class B .

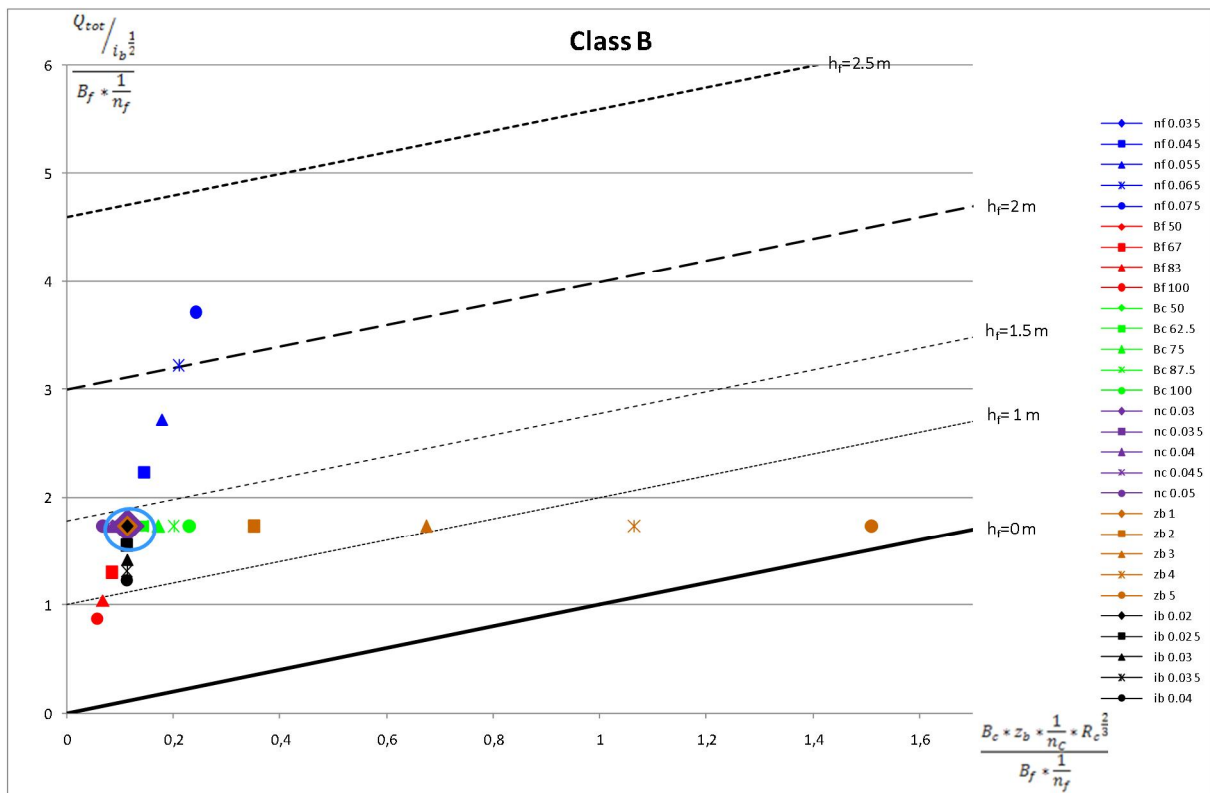


Figure 4-9 The effect of a uniform distribution of the components on the water level of the floodplains for class B.

For class B similar results can be seen as in class Aa+, except that the spread in the graph is smaller for most of the components. But as mentioned in the previous class, the spread and the angle have influence on the water level of the floodplain. The spread for the component n_f in class Aa+ is larger than in class B but the angle of n_f in class B is 41° and in class Aa+ the angle is 34° . The angle in class B is larger, making the influence of the component n_f in class B larger than appears in Figure 4-9.

Table 4-7 shows the difference in the water level for the varying components. Here the two components n_f and z_b have the most influence on the water levels in the floodplain. And the components B_c and n_c have the least. These values for the components B_c and n_c are so small that this can be neglected.

Table 4-7 The values for the water level of the floodplain due to change in values of the components for class B

class B				
Component	hf for minimum component value [m]	hf for maximum component value [m]	Difference [m]	Angle [°]
n_f	1.34	2.11	0.77	41
B_f	1.34	0.88	-0.45	-139
B_c	1.34	1.28	-0.06	-45
n_c	1.34	1.36	0.02	135
z_b	1.34	0.41	-0.93	-45
i_b	1.34	1.07	-0.27	-135

Class C

Figure 4-10 shows the results for the uniform distribution of the components for class C.

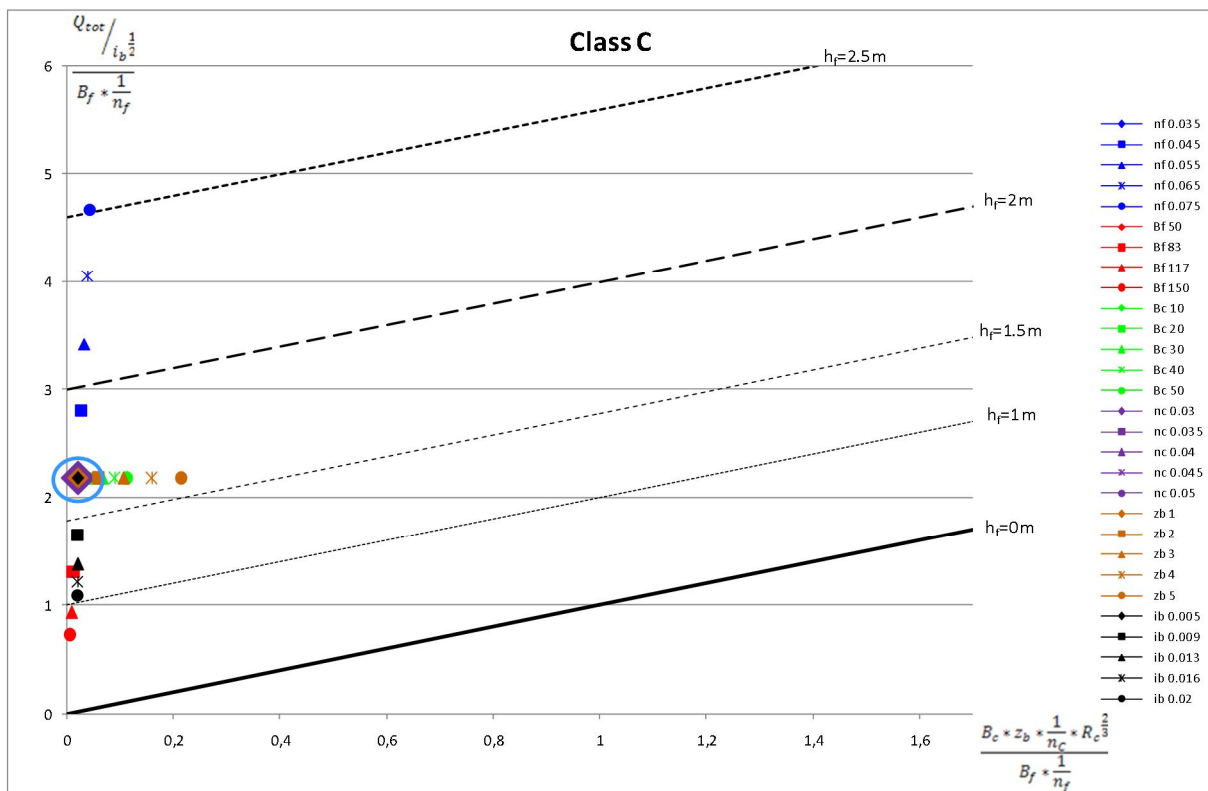


Figure 4-10 The effect of a uniform distribution of the components on the water level of the floodplains for class C.

In the previous classes the components could be divided into three groups; high influence, small influence and negligible influence. In class C the components can be divided into two groups, the group that is negligible and the group that has a large influence on the water level of the floodplain. The first group contains the following components n_c , B_c and z_b . In the second group the other components, n_f , B_f and i_b . The component n_f has the largest difference in the water depth and also the angle is to be larger than for the other classes, this results in the largest difference in the water level of the floodplain.

Table 4-8 The values for the water level of the floodplain due to change in values of the components for class C

class C				
Component	hf for minimum component value [m]	hf for maximum component value [m]	Difference [m]	Angle [°]
n_f	1.59	2.51	0.92	45
B_f	1.59	0.82	-0.77	-135
B_c	1.59	1.54	-0.04	-45
n_c	1.59	1.59	0.00	135
z_b	1.59	1.50	-0.09	-45
i_b	1.59	1.04	-0.55	-135

Class DA

Figure 4-11 shows the results for the uniform distribution of the components for class DA.

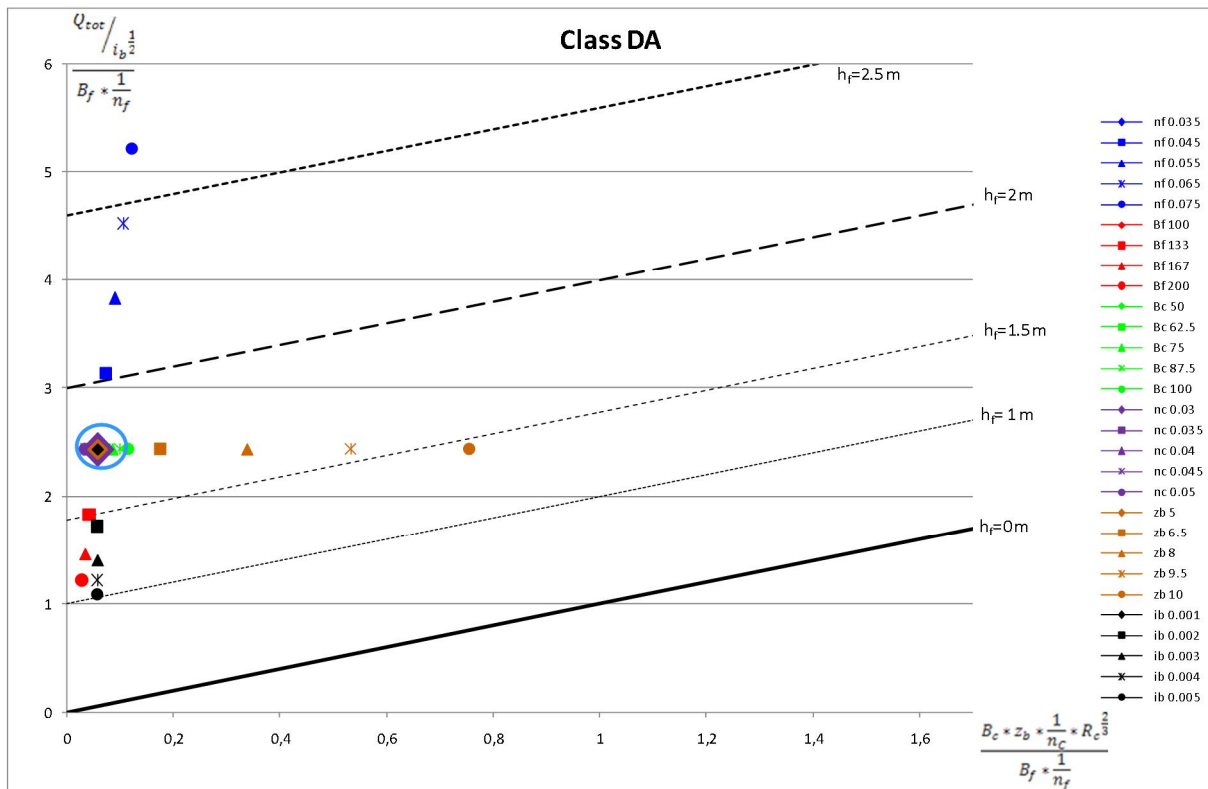


Figure 4-11 The effect of a uniform distribution of the components on the water level of the floodplains for class DA.

Figure 4-11 shows a large spread of various components. As mentioned before, not only should the spread of the components but also the angle of the components be taken into account.

Table 4-9 shows that the river characteristics B_c , n_c and z_b are so small that these can be neglected. The components n_f , B_f and i_b and have the largest influence on the water level of the floodplains. In this class the components can be divided into two groups, a group that influence the water level of the floodplain and a group that can be neglected.

Table 4-9 The values for the water level of the floodplain due to change in values of the components for class DA.

class DA				
Component	hf for minimum component value [m]	hf for maximum component value [m]	Difference [m]	Angle [°]
n_f	1.68	2.66	0.97	44
B_f	1.68	1.11	-0.57	-136
B_c	1.68	1.66	-0.02	-45
n_c	1.68	1.69	0.01	135
z_b	1.68	1.37	-0.32	-45
i_b	1.68	1.02	-0.66	-135

For each class the relative components that influence the water level of the floodplain and the components that can be neglected are pointed out. In the next table the classes and the components will be compared on the difference in the water level of the floodplain and the angle.

Table 4-10 All classes with the difference in the water level of the floodplain for the uniform distribution of the components and the angle of the components

All classes	Aa+		B		C		DA	
Component	Difference [m]	Angle [°]	Difference [m]	Angle [°]	Difference [m]	Angle [°]	Difference [m]	Angle [°]
n_f	0.81	34	0.77	41	0.92	45	0.97	44
B_f	-0.47	-136	-0.45	-139	-0.77	-135	-0.57	-136
B_c	-0.75	-45	-0.06	-45	-0.04	-45	-0.02	-45
n_c	0.08	135	0.02	135	0.00	135	0.01	135
z_b	-0.32	-45	-0.93	-45	-0.09	-45	-0.32	-45
i_b	-0.43	-135	-0.27	-135	-0.55	-135	-0.66	-135
Influence								
High	n_f, B_c		n_f, z_b		n_f, B_f, i_b		n_f, B_f, i_b	
Small	B_f, i_b, z_b		B_f, i_b					
Negligible	n_c		B_c, n_c		B_c, n_c, z_b		B_c, n_c, z_b	

At the bottom of Table 4-10 the components are divided into one of the three groups, being a component that has a high influence on the floodplain water levels, having a small influence and being negligible. For the classes the DA and C the group distribution is the same. In these classes there are two groups. The components are either components that have high influence on the floodplain water levels or can be neglected.

For the other two classes, there are only two components that fit the same group. The roughness coefficient for the floodplain (n_f) has high influence on the water levels and the roughness coefficient for the channel (n_c) is negligible in both classes.

4.5.5 The flood wave celerity in the flood plains

The next step is to determine the components that are relevant for the flood wave celerity of the floodplain of certain terrains. This is done with the same method as in the previous section for the water depth in the floodplains. By taken a uniform distribution for the components, i_b , z_b , B_c , B_f , n_c and n_f for all five classes. This gives insight into the sensitivity of each component on the flood wave celerity in the flood plains. Equation 4-14 is used to determine the influence of the parameters on the flood wave celerity.

$$c = \frac{5}{3} * \frac{B_c}{B_f} * z_b^{2/3} * i_b^{1/2} * \frac{1}{n_c} + \frac{5}{3} * h_f^{2/3} * i_b^{1/2} * \frac{1}{n_f}$$

Equation 4-14

Class Aa+

Figure 4-12 shows the results for the uniform distribution of the components for class Aa+.

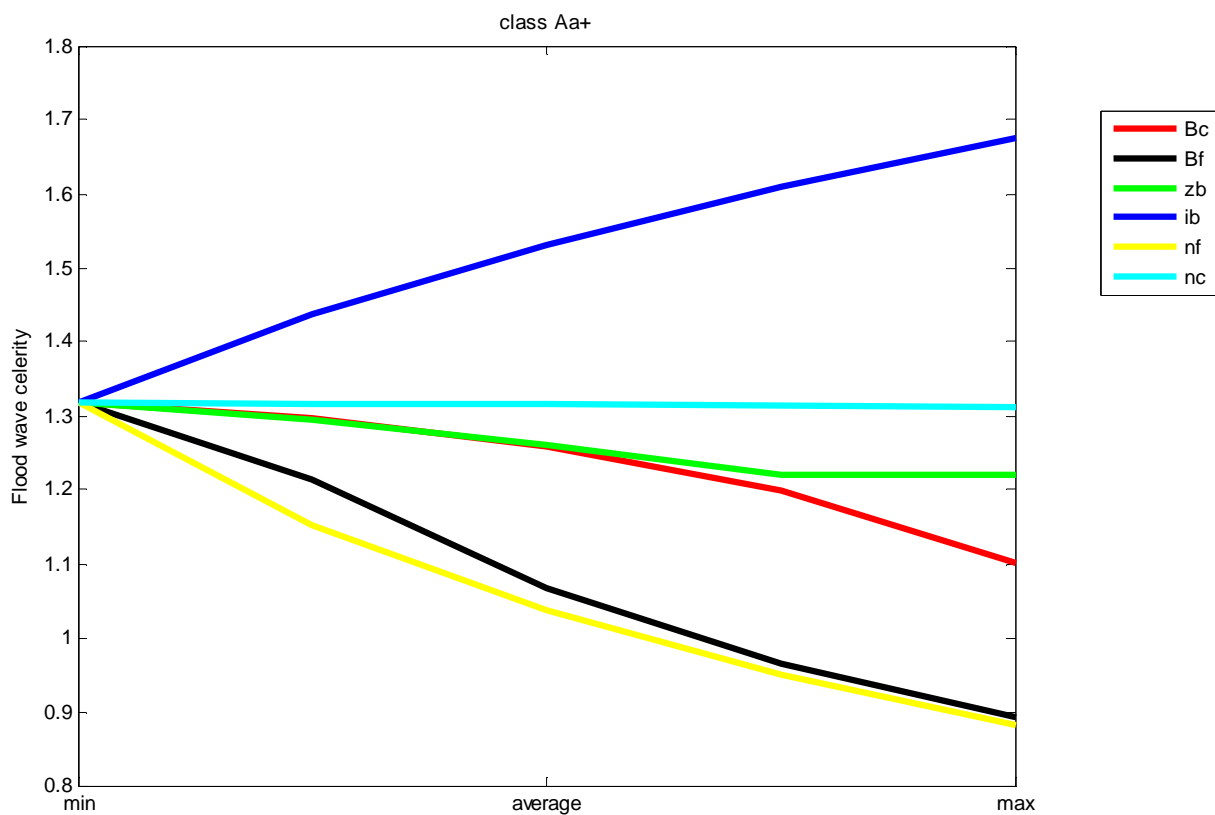


Figure 4-12 The effect of a uniform distribution of the components on the flood wave celerity of the floodplains for class Aa+

Table 4-11 shows the difference of the flood wave celerity in the floodplains with the minimum and maximum values of the components.

Table 4-11 The values for the flood wave celerity due to change in values of the components for class Aa+

class Aa+			
Component	c for minimum component value [m/s]	c for maximum component value [m/s]	Difference [m/s]
n_f	1.32	0.88	-0.44
B_f	1.32	0.89	-0.43
B_c	1.32	1.10	-0.22
n_c	1.32	1.31	-0.01
z_b	1.32	1.22	-0.10
i_b	1.32	1.68	0.36

The component that has negligible influence on the flood wave celerity of the floodplains is the component n_c . The components n_f , B_f and i_b have the most influence on the flood wave celerity. The other components, B_c and z_b have a small influence.

For the components, n_f , B_f , B_c , z_b and n_c the increasing value results in decrease of the flood wave celerity of the floodplain. Except for the component i_b . An increase in this components result in the increase of the flood wave celerity.

Class B

Figure 4-13 shows the results for the uniform distribution of the components for class B.

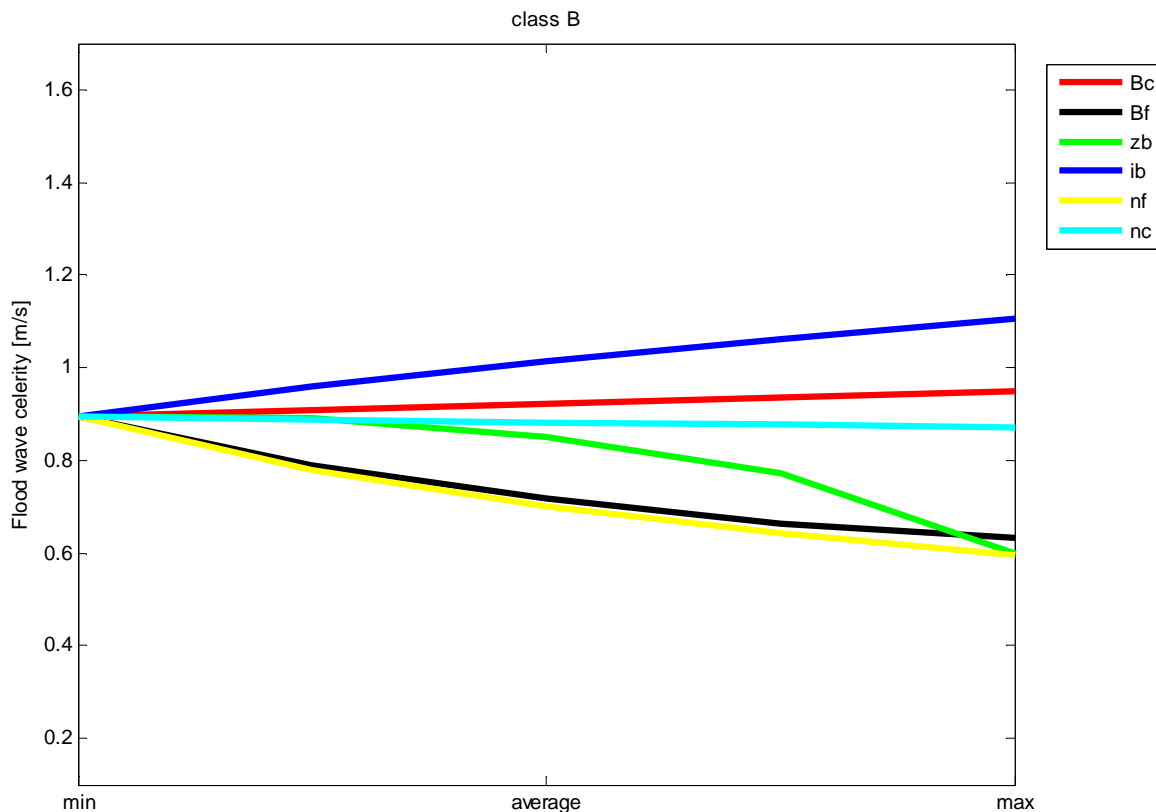


Figure 4-13 The effect of a uniform distribution of the components on the flood wave celerity of the floodplains for class B

Table 4-12 shows the difference of the flood wave celerity in the floodplains with the minimum and maximum values of the components.

Table 4-12 The values for the flood wave celerity due to change in values of the components for class B

class B			
Component	c for minimum component value [m/s]	c for maximum component value [m/s]	Difference [m/s]
n_f	0.60	0.90	-0.30
B_f	0.63	0.90	-0.26
B_c	0.90	0.95	0.05
n_c	0.87	0.90	-0.02
z_b	0.60	0.90	-0.30
i_b	0.90	1.10	0.21

The components that have negligible influence on the flood wave celerity of the floodplains are the component n_c and B_c . The components n_f , B_f , z_b and i_b have the most influence on the flood wave celerity.

For the components, n_f , B_f , z_b and n_c the increasing value results in decrease of the flood wave celerity of the floodplain. Except for the component B_c and i_b . An increase in these components results in the increase in the flood wave celerity.

Class C

Figure 4-14 shows the results for the uniform distribution of the components for class C.

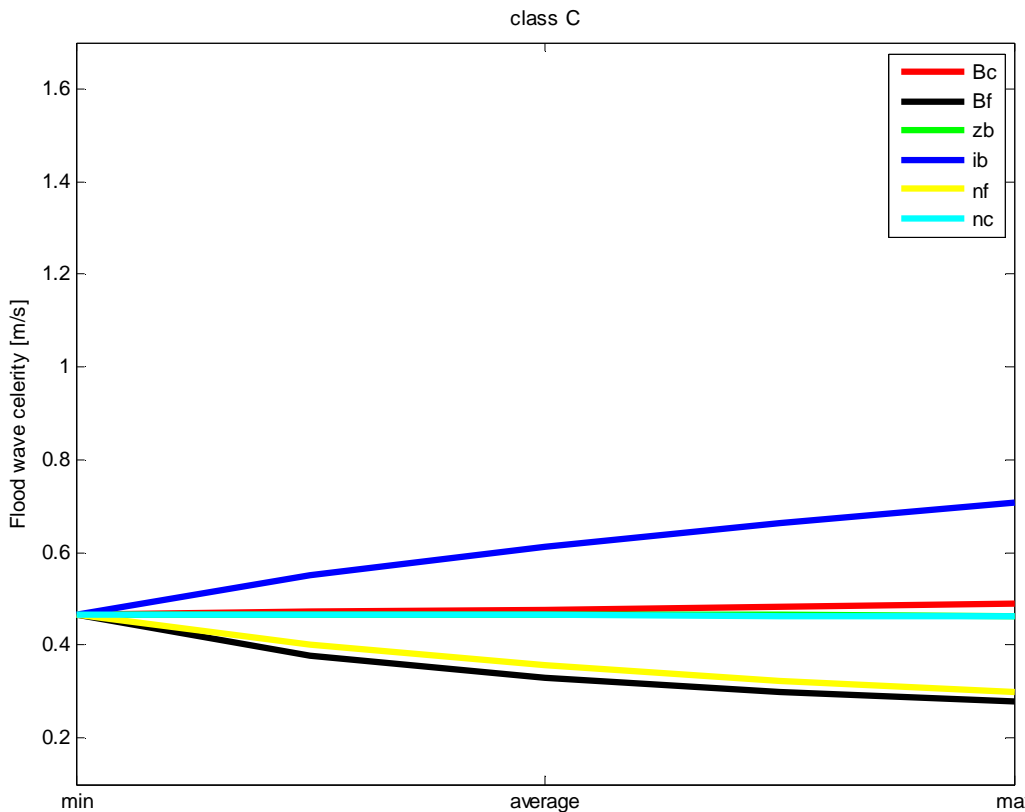


Figure 4-14 The effect of a uniform distribution of the components on the flood wave celerity of the floodplains for class C

Table 4-13 shows the difference of the flood wave celerity in the floodplains with the minimum and maximum values of the components

Table 4-13 The values for the flood wave celerity due to change in values of the components for class C

class C			
Component	c for minimum component value [m/s]	c for maximum component value [m/s]	Difference [m/s]
n_f	0.30	0.47	-0.17
B_f	0.28	0.47	-0.19
B_c	0.47	0.49	0.02
n_c	0.47	0.47	0.00
z_b	0.47	0.47	0.00
i_b	0.47	0.71	-0.24

The component that has negligible influence on the flood wave celerity of the floodplains is the component n_c , B_c and z_b . The components n_f , B_f and i_b have the most influence on the flood wave celerity.

For the components, n_f , B_f and B_c , the increasing value results in decrease of the flood wave celerity of the floodplain. For the component B_c and i_b . An increase in these components results in the increase in the flood wave celerity. The components, z_b and n_c show that any change in the values of these components show no change in the flood wave celerity.

Class DA

Figure 4-15 shows the results for the uniform distribution of the components for class DA.

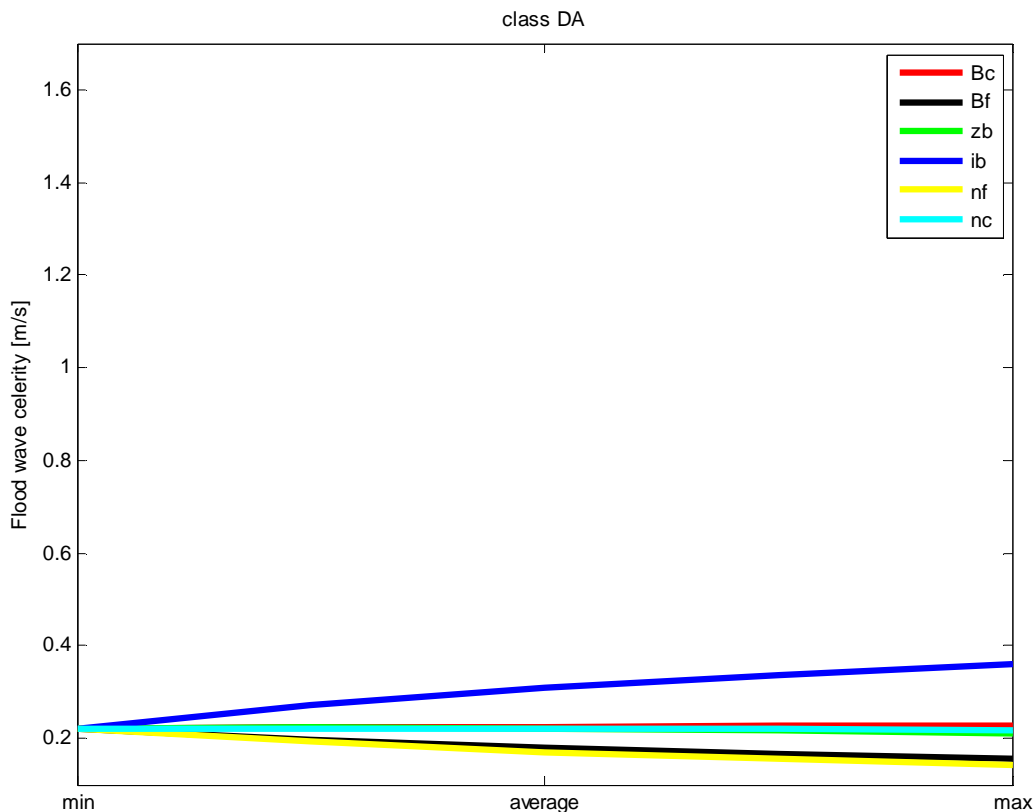


Figure 4-15 The effect of a uniform distribution of the components on the flood wave celerity of the floodplains for class DA

aximum values of the components.

Table 4-14 shows the difference of the flood wave celerity in the floodplains with the minimum and maximum values of the components.

Table 4-14 The values for the flood wave celerity due to change in values of the components for class DA

class DA				
Component	c for minimum component value [m/s]	c for maximum component value [m/s]	Difference [m/s]	Angle
n_f	0.14	0.22	-0.08	-62,90
B_f	0.16	0.22	-0.07	0,00
B_c	0.22	0.23	-0.01	-0,01
n_c	0.22	0.22	0.00	-7,69
z_b	0.21	0.22	-0.01	-0,17
i_b	0.22	0.36	-0.14	-88,35

The component that has negligible influence on the flood wave celerity of the floodplains is the component n_c , B_c and z_b . The component i_b has the most influence on the flood wave celerity. The components n_f , and B_f have a small influence on the celerity.

For the components, n_f , B_f and B_c , the increasing value results in decrease of the flood wave celerity of the floodplain. For the component B_c and i_b . An increase in these components results in the increase in the flood wave celerity. The components, z_b and n_c show that any change in the values of these components result in no change in the flood wave celerity.

For each class the relative components that influence the flood wave celerity and the components that can be neglected are pointed out. In the next table the classes and the components will be compared on the differences in the flood wave celerity.

Table 4-15 The difference in the flood wave celerity for varying values of the components for call classes

All classes	Aa+	B	C	DA
Component	Difference [m/s]	Difference [m/s]	Difference [m/s]	Difference [m/s]
n_f	-0.44	-0.30	-0.17	-0.08
B_f	-0.43	-0.26	-0.19	-0.07
B_c	-0.22	-0.05	-0.02	-0.01
n_c	-0.01	-0.02	0.00	0.00
z_b	-0.10	-0.30	0.00	-0.01
i_b	-0.36	-0.21	-0.24	-0.14
Influence				
High	n_f, B_f, i_b	n_f, B_f, z_b	n_f, B_f, i_b	i_b
Small	B_c, z_b	i_b		n_f, B_f
Negligible	n_c	B_c, n_c	B_c, z_b, n_c	B_c, z_b, n_c

At the bottom of Table 4-15 the components are divided into one of the three groups, being a component that has a high influence on the flood wave celerity, having a small influence and being negligible.

The components n_f and B_f have a high influence on the flood wave celerity for the classes Aa+, B and C. The component i_b has a high influence in the classes Aa+, C and DA. The two components B_c and n_c have for three of the four classes, a negligible influence.

4.6 Conclusion

In this chapter the objective is to determine the sensitivity of the components on the water level of a floodplain and the flood wave celerity for different terrains in 1D flow. To be able to draw general conclusions, four types of terrains were chosen to be investigated. The types of terrains were sorted into four classes with each class having its own characteristics for the channel and for the floodplain. For the calculations the Manning equation has been used and rewritten. For the water depth in the floodplains, the equation consisted out of three terms, the forcing term, the channel characteristics term and the floodplain characteristics term. Each term consist of components. Each component has been given a uniform distribution. For each value of all six components the effects on the water level of the floodplain and on the flood wave have been calculated. From the results for the water depth in the floodplains it became clear that the calculated values of the terms are subjective. The ratio between the terms showed another dimension to the classification. So now the classification is not only on the exact values of the components it also to be able to classify a river on the ratio between the two first terms derived from the Manning's equation.

The following step was to evaluate the results. By taking three rivers sections and testing them on the same calculation as the classified channels, the classification by ratio could be tested on real rivers. The results showed that the description of the real river matches the classification in chapter 4.5.2.

After deriving the ratio of the terms for each class, the sensitivity of the components needed to be analyzed. The absolute values of the components did not give a clear picture of the influence of the components on the water levels. Here just as in the classification of the real rivers the ratio between the terms was also of importance. The ratio for the components is expressed in an angle. By taken the angle into consideration, the chosen values are an indication and not deterministic solution for the size of the sensitivity of the floodplain water levels.

This results in dividing all components into three groups for each class. The components are divided into a high influence, a small influence and a negligible influence on the water level of the floodplain and the flood wave celerity.

Table 4-16 For each class the components are divided into three groups according to their influence on the water level of the floodplains and their influence on the flood wave celerity

	Classes	Aa+	B	C	DA
	Influence				
Water level of the flood plains	High	n_f, B_c	n_f, z_b	n_f, B_f, i_b	n_f, B_f, i_b
	Small	B_f, i_b, z_b	B_f, i_b		
	Negligible	n_c	B_c, n_c	B_c, n_c, z_b	B_c, n_c, z_b
Flood wave celerity	High	n_f, B_f, i_b	n_f, B_f, z_b	n_f, B_f, i_b	i_b
	Small	B_c, z_b	i_b		n_f, B_f
	Negligible	n_c	B_c, n_c	B_c, n_c, z_b	B_c, n_c, z_b

The results for the water depth in the floodplains are that the components of the classes C and DA can be divided into the same groups, highly sensitive and negligible. And the classes Aa+ and B have hardly any similarities, except for the n_f having the most influence and the n_c having a small influence on the floodplain water level.

Similar results are found for the flood wave celerity. For class C, exactly the same influences are found for each component. For the other classes, the components with a small influence on the flood wave celerity are exactly the same. If the group of high and small influence is taken together as the group with influence, the result for the tests for the water depth of the floodplains is the same as the tests for the flood wave celerity.

The test on the real rivers makes the sensitivity analysis on the components a general analysis. By dividing the rivers into the channel classification with use of the ratio of the terms of rewritten Manning equation, the classification indicated which components are of importance and which components can be neglected. Taken the section of the river the Maas, that was classified into the DA class, the sensitivity analysis shows that for this river section the n_f , B_f and i_b are important parameters and that the B_c , n_c , z_b accuracy is of less importance.

The result of the sensitivity analysis gives each component for each class a label of highly influence, small influence and negligible. These labels can be interpreted as expected respectively a large, small and negligible error on the water level in the floodplains and the flood wave celerity due to uncertainties in the value of the components. By using this sensitivity analysis the resources (time and funds) for gathering data can be more focused on the important components and less on the negligible components.

To be able to use the Manning's equation for this analysis, certain assumptions are made. The first assumption, the bottom slope is equal to the water line, excludes the phenomena backwater curves in this analysis. While for large discharges this is a phenomenon that can influence the water levels in the channel and thereby also the water levels in the floodplains.

The second assumption that the water level in the floodplain is small compared to the bottom level of the channel is not always applicable for the classes C and DA.

The other assumption is that there is only the upstream boundary and no downstream boundary. This excludes the flooding that can occur from the downstream boundary as is mentioned in chapter 2.2.3.

These assumptions should be taken into consideration when using this sensitivity analysis to ignore certain components.

5. Hypothetical case study (2D-flow)

5.1 Introduction

In the previous chapter the sensitivity of a flood simulation of a channel and the floodplains has been examined in a 1D flow for a number of landscape characteristics. In this chapter the schematization is expanded to a 1D/2D model to include the development of the flood event as a function of time and space. This expansion of the schematization gives an insight in not only the water depth and celerity in the channel and the flood plains but also in how different components influence the propagation of the flood and how the flood develops over an area.

In chapter 2.3.3 the types of information of flood simulations are discussed. In chapter 4, the 1D flow study case, the water depth and the celerity in the floodplains has been analyzed for the 1D flow. The missing information that is considered vital in chapter 2.3.3 is the water depth, the flood extent, the propagation of the water front in space and time. This information can only be investigated in a 2D schematization.

This chapter is divided into four sections. In section 5.2 the set-up and the varying simulation conditions are described. In section 5.3 the results of the simulations are analyzed. In section 5.4 the conclusion of the results for the 1D and 2D flow study cases are discussed.

5.2 The simulations for 1D/2D flow

The objective of this analysis is to determine the sensitivity of a flood event with respect to the following:

1. conditions and characteristics of the event,
2. characteristics of the river
3. characteristics of flood plain surrounding.

To determine a 2D inundation the SOBEK 1D/2D is used. The 2D flow is fully integrated with the 1D flow. The 1D flow simulates the flow in the channels and the 2D flow simulates the overland flow. The simulations are based upon the complete Saint Venant equations.

In section 5.2.1 the three outputs of the flood simulation are described. The methods to determine the influence of this output are described as well in section 5.2.1. In section 5.2.2 the two types of river classes are explained. The varying conditions and characteristics of the flood event simulations are described in section 5.2.3.

5.2.1 Schematization for the flood simulations

Spatial schematization

For the schematization of the 1D/2D flow, an area of 200 by 300 km is chosen. The size of the chosen area is similar to the size of the area that will be investigated in the third case study, the Thailand case.

The area is divided into grid cell with a size of 1 by 1 km. In the middle of the area a channel is running from north to south, this is schematized as the 1D flow.

At the north end of the channel, the upstream boundary is situated where a certain discharge is released. This discharge may be the result of intensive precipitation in the upstream catchment area or melting of snow and ice on higher grounds, as described in section 2.2.1.

At the south side of the channel, the downstream boundary is situated where a water level boundary condition is imposed. This water level represents the water levels at the sea side, due to the tide or a storm surge (see section 2.2.3).

Figure 5-1 shows the schematization in SOBEK of the area with the channel in the middle (in blue), the boundary conditions (pink squares) and the grid cells (black lines). The area has a slope from north to the south. The color of the grid cell indicates the surface level (the z-coordinate) with the darker brown cells being higher surface levels and the lighter brown lower surface levels.

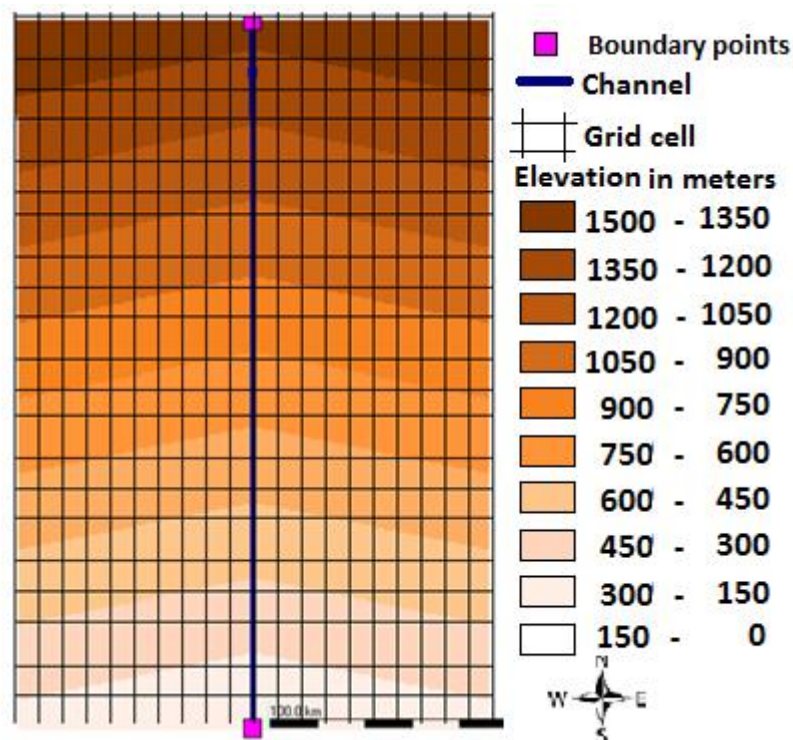


Figure 5-1 Schematization in SOBEK of the area of 200 by 300 km with a slope from north to south of 0.005; the channel situated in the middle in blue, the boundaries at the north and south side of the channel in the pink squares and the black lines dividing the grid cells.

Time schematization

In section 4.5.4 and 4.5.5, for each class calculations have been made for the following:

1. The water depth in the flood plains
2. The flood wave celerity in the flood plains

The flood wave values for the extreme cases vary between 1.33 and 0.22 m/s. In these extreme cases, the waves need a period of respectively 62 and 380 hours to flow through the 300 km long area. The simulations are run for 216 hours (a period of 9 days). The reason for shortening the simulation period is because of the elaborated 2D flow simulations. Here the choice is to examine large amount of simulations instead less simulations with longer simulation period.

5.2.2 The output of the flood simulations

By using a 1D/2D schematization the information, the simulations are expanded compared to the 1D flow. For this analysis the chosen information of flood simulation to be analyzed is:

1. Water depth in the flooded area
2. The onset time of flooding
3. Flood extent

First the three types of output of the simulations are discussed. Next the methods to compare the simulations to each other are discussed.

Water depth in the flooded area

The flood depth has been examined in the previous chapter, 1D simulation. It is interesting to analyze if the sensitivity of the tested parameters will be valid for both the simple 1D flow and 1D/2D flow.

Figure 5-1 shows the grid cells with the information of the surface level. These grid cells can contain other information. In this case it can be the maximum water depth during a simulation. The

sensitivity of the water depth is studied by establishing the maximum water depth during each simulation for each grid cell. The differences in the outputs of the simulations are compared.

The grid cells that are not flooded are not part of this analysis. Only the cells that are flooded are compared. By excluding the grid cells that are not flooded in every test, the inactive (i.e. fully dry) cells are prevented to render the comparison method too positive.

The onset time of flooding

The onset time of flooding is not exactly the same as the propagation of flooding, but the onset time of flooding is a measurable indicator for the propagation of flooding. By comparing the first time each grid cell is flooded for different simulations, it can be determined if a flood propagates faster in one simulation than the other.

As for the case of water depth, instead of subtracting the onset time of flooding of each grid cell, only the grid cells that are flooded in both simulations are taking into consideration.

Flood extent

In the information types described above, it is mentioned that the inactive grid cells are not taken into account. By excluding these cells the spatial change in the flood event would be left out. To take this into account, the flood extent is analyzed separately.

Each grid cell is given the value 1, indicating if it is flooded at some moment during the simulation, or 0 if it is not flooded. When the simulations are compared with each other, by subtracting these given values from each other, the comparison figure will indicate the value 1, 0 or -1. Figure 5-2 gives an example.

In the figures for the flood extent the grid cell values are indicated with a color, -1 are blue, 0 is white and 1 is red.

Figures who are mainly blue, indicate an increase in the flooded area with respect to the reference simulation. This figure shows an extent of flooded area. Figures who are mainly red indicate a decrease in flooded area. The mix of the red and blue grid cells is also a possible outcome of the comparison. This outcome shows that the flood extent shifts from one area to another.

Method to define the sensitivity of the flood simulation

Due to the large amount of simulations and different flood events, the simulations are difficult to compare in only absolute terms. Therefore two methods are explained here to define the sensitivity of the simulated variable.

The first method is by visual examination of the plotted differences between the spatially output of the simulations. By subtracting the spatial outputs of two simulations, the differences in the output can be spatially plotted, see Figure 5-3.

Test X		
1	1	0
0	1	1
0	0	1

Test Y		
0	1	1
0	0	1
1	1	0

Test X-Y		
1	0	-1
0	1	0
-1	-1	1

Figure 5-2 Example of two tests; test X (the reference simulation) and test Y; The grid cells indicate if they are flooded (1) or not (0). The difference of the tests X and Y indicate if in both simulations the grid is flood (0 and white), only flooded in test X (1 and red) or only flooded in test Y (-1 and blue).

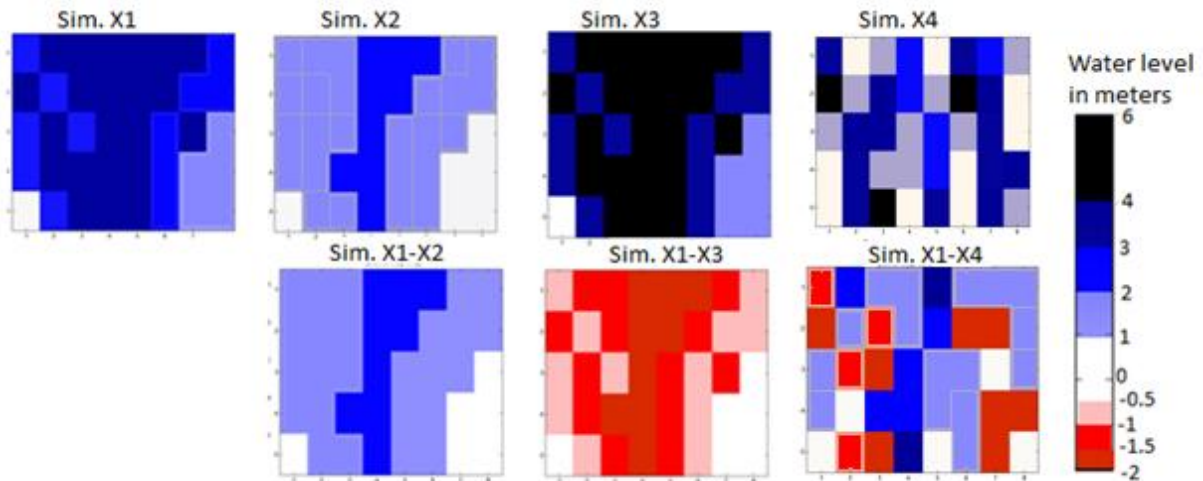


Figure 5-3 An example of the spatially plotted water depth of two simulations. And the spatially plotted difference of reference simulation X1 and simulations X2, X3 and X4. Each grid cell has a water level with related shade of blue or red.

In case of large differences between the two outputs of the simulations, in the plot of the subtracted outputs the large differences can be visually spotted. The large differences in the subtracted plots indicate that the difference between the two simulations (e.g. the conditions, channel characteristics or type of class, this is explained in the next section) has a large impact on the output of the simulation and can be classified as a high influential variable.

In the case of small differences in the subtracted plots, these are difficult to be examined visually. Therefore the simulations are examined not only visually, but also with a second method by using the empirical cumulative distribution of the spatial simulation outputs. The latter method determines the differences in the median and the standard deviation of the simulation outputs. The median gives insight into the differences in absolute terms, while the standard deviation is equivalent to the spread of the results.

Figure 5-4 shows the cumulative distribution of the four simulations in Figure 5-3. The figure shows that the distributions illustrate clearly that the outcome vary mainly in shape (angle of the line) and location on the x-axis (horizontal displacement).

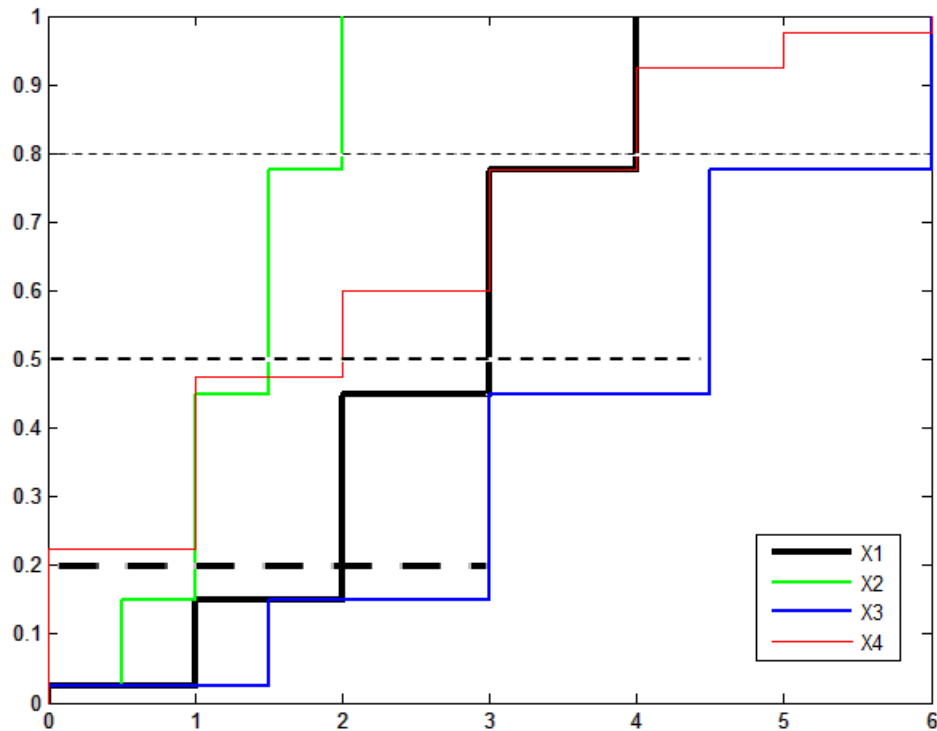


Figure 5-4 an example for the cumulative distribution of the four examples

To determine the differences in the cumulative distribution, the median and the angle of the considered case and the reference case are compared. By using the angle of the line between the 0.2 and 0.8 probability of exceedance, the tails are left out and the spread is approached.

The difference in the simulation outputs by an altered variable simulation compared to the benchmark simulation can be formulated as function of the median and the angle of the empirical cumulative distribution:

$$Factor\ of\ difference = \left| \frac{m_{benchmark\ case} - m_{test\ X}}{m_{benchmark\ case}} \right| + \left| \frac{\theta_{benchmark\ case} - \theta_{test\ X}}{\theta_{benchmark\ case}} \right|$$

$$F_{difference} = |\Delta_{median}| + |\Delta_{angle}|$$

$m_{benchmark\ case}$ = median of the spatial cumulative distribution for the benchmark case

$m_{test\ X}$ = median of the spatial cumulative distribution for test X

$\theta_{benchmark\ case}$ = angle of the spatial cumulative distribution for the benchmark case

$\theta_{test\ X}$ = angle of the spatial cumulative distribution for test X

With the combination of the visual examination and the factor of difference, the influence factor is determined:

$$Factor\ of\ influence = \begin{cases} 0, & F_{difference} = 0 \\ 1, & 0 \leq F_{difference} \leq 0.25 \\ 2, & 0.25 < F_{difference} \leq 0.50 \\ 3, & 0.50 < F_{difference} \end{cases}$$

With the factor of influence:

0. No influence
1. Negligible influence
2. Small influence
3. Large influence

This factor is used to get an idea of the influence of the different components on the flood event. When the factor of differences is determined for a test, the visual examination in combination with the factor determines whether that component has large or low influence on the flood event.

For the normal distributions in Figure 5-4, the factor of difference and the factor of influence are determined in Table 5-1.

Table 5-1 an example of the normal distribution: the median, the angle, the factor of difference and the factor of influence for five normal distributions

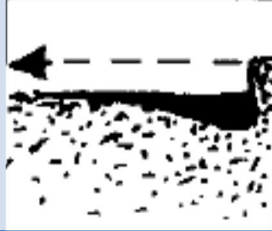

Normal distribution	Median	Angle				
X1	3	45.0	Δ_{median}	Δ_{angle}	$F_{difference}$	Factor of influence
X2	2.25	53.1	0.25	0.18	0.43	2
X3	4.5	33.7	0.50	0.25	0.75	3
X4	1.5	63.4	0.50	0.41	0.91	3

The factor of difference of the cumulative distribution is used for the outputs, the water depth and the propagation of the flood.

5.2.3 River classes

In chapter 4.5.3 the river Chao Phraya is classified as a class between the classes C and DA. For this reason the sensitivity of 1D/2D flow for these two classes is investigated in this chapter. The difference between these two classes is shown in Table 5-2.

Table 5-2 Differences between the classes C and DA with the range in values for the parameters

	Class C		Class DA	
				
Bed slope: i_b [-]	0.005		0.0005	
Discharge [m^3/s]	2200		2500	
Parameters	Minimum	Maximum	Minimum	Maximum
Width of channel: B_c [m]	10	50	50	100
Roughness coefficient of channel: n_c [$s/m^{1/3}$]	0.03	0.05	0.03	0.05
Roughness coefficient of floodplain: n_f [$s/m^{1/3}$]	0.035	0.07	0.035	0.07
Bed level: z_b [m]	1	5	1	5

This 2D flow case study is to examine the differences in the sensitivity for the two classes for the different flood events, described in the next section.

5.2.4 The conditions and characteristics of the flood events

The objective of this analysis is to determine the sensitivity of the output of flood simulation, with respect to certain conditions and characteristics of the event, as well as characteristics of the river and the flood plain surroundings. The difference between the characteristics of the river and the floodplains of the class C and DA are described in Table 5-2. The conditions and the characteristics of the events are described and specified in the three tests for both classes, class C and DA:

- Tests 1: Varying boundary conditions
- Tests 2: Slope in the perpendicular direction to the channel
- Tests 3: Varying parameters to characterize the channel and flood plain

Test set 1, with varying types of boundary conditions is the benchmark test set for the other test sets.

In the test set 2, the test set 1 is extended by keeping all variables the same as for tests 1 but by altering the slope in the perpendicular direction to the channel.

In the test set 3, the parameters to characterize the channel and the floodplains are altered while keeping all other variables the same as for test sets 1 and 2. So for test set 3 the test sets 1 and 2 are benchmark tests.

The conditions for the tests are explained in the following section. An overview of all the simulations of the tests and the corresponding conditions can be found in the Appendix.

Tests 1: Varying boundary conditions

In chapter 3.2.2 the difficulty of obtaining the boundary conditions, which are part of the event data are discussed. It was established that maximum and average annual discharges and water levels can be obtained from publicly available data, but these values need to be used to create synthetic events to simulate a historical or a future event.

The sensitivity of the boundary conditions is tested by creating several synthetic events and comparing the outputs of the simulations with the method to define the sensitivity of the flood simulation as described in section 5.2.1. For the upstream and the downstream boundary conditions, three types of events have been created: by altering either the up- or the downstream conditions and keeping all the other variables equal.

The three simulations tested for each of the two boundary conditions are:

Tests 1-1: Varying upstream boundary conditions

- A. Constant discharge in time
- B. Triangular shaped discharge in time
- C. Parabolic shaped discharge in time

Tests 1-2: Varying downstream boundary conditions

- A. Constant water level in time
- B. Tidal amplitude
- C. Storm surge
- D. Combination of tide and storm surge

Tests 1-3: Delay in the boundary conditions

- A. Up and downstream boundary condition start at the same time
- B. Delay in the upstream boundary condition
- C. Delay in the downstream boundary condition
- D. Delay in the down- and upstream boundary condition

Table 5-3 shows the test done for the boundary conditions.

Table 5-3 Tests 1 for the synthetic events for the boundary conditions

	Test set 1	Case	Synthetic event in boundaries		Delay in boundaries	
			Upstream	Downstream	Upstream	Downstream
			Q[m ³ /s]	h[m]	t ₀	t _h
Upstream boundary conditions	Test 1-1	A	Constant	0	0	0
	Test 1-1	B	Triangle	0	0	0
	Test 1-1	C	Parabolic	0	0	0
Downstream boundary conditions	Test 1-2	A	Small constant	Constant	0	0
	Test 1-2	B	Small constant	Tide	0	0
	Test 1-2	C	Small constant	Storm surge	0	0
	Test 1-2	D	Small constant	Storm surge and tide	0	0
Delay (timing) boundary conditions	Test 1-3	A	Parabolic	Storm surge and tide	0	0
	Test 1-3	B	Parabolic	Storm surge and tide	26	0
	Test 1-3	C	Parabolic	Storm surge and tide	0	26
	Test 1-3	D	Parabolic	Storm surge and tide	26	26

Per test only one variable is altered, keeping all other variables equal.

Figure 5-5 and Figure 5-6 show the values for the upstream boundary conditions (the discharges) and for the downstream boundary conditions (the water levels) for class C.

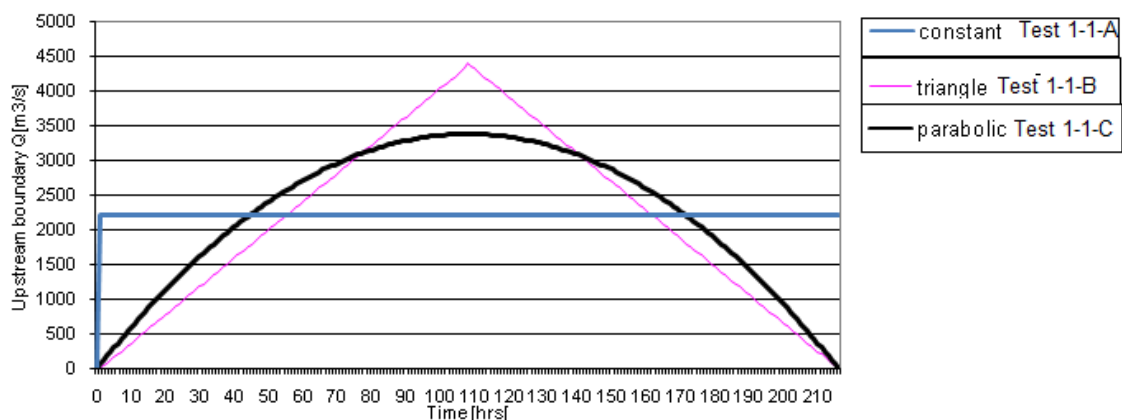


Figure 5-5 The different upstream discharges for tests 1 for class C

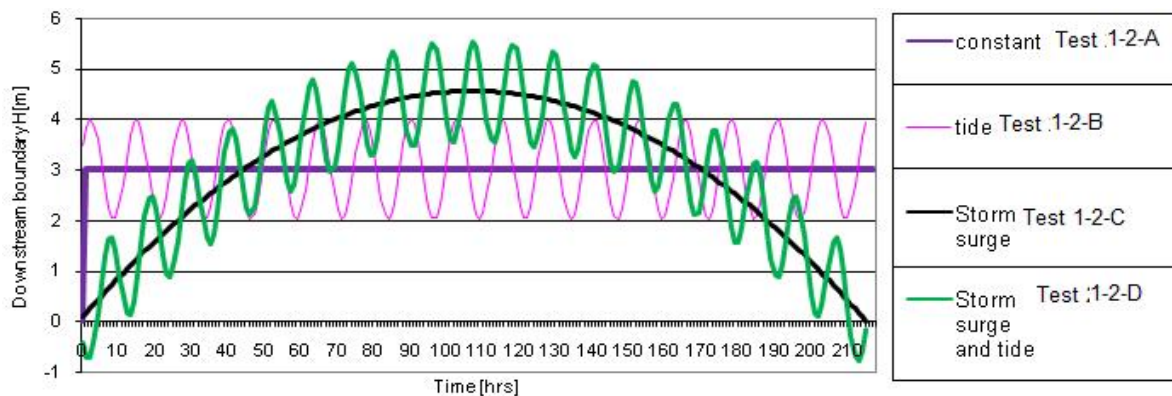


Figure 5-6 The different downstream water levels for tests 2 for class C

The discharges for the upstream boundary evolve differently over time but are of equal volume, when integrated over the simulation period. The values for the upstream boundary are derived from the bank full discharges, chapter 4.3.2.

The downstream boundary represents the sea with constant water level, a tidal water level, a storm surge and a combination of the latter two. For this boundary the different shapes are not the same as they represent a state and not a flux. This is a result of the dependence of water going through the downstream boundary.

The imposed water level is not the only factor that determines the flow through this boundary. The size and the direction of the flow depends mainly on the difference in water level of the imposed downstream boundary and the water level in the channel, imposed by the upstream boundary condition, see Figure 5-7.

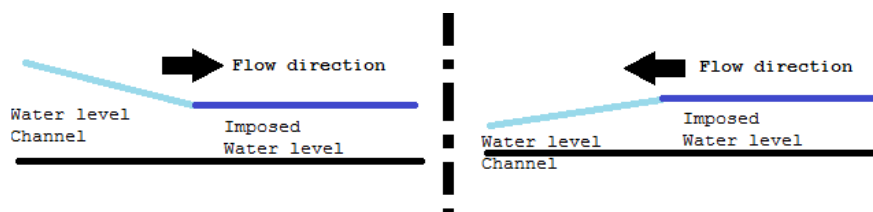


Figure 5-7 The discharge direction depends on the difference of the water level of the channel and the imposed water level of the downstream boundary

The water level in the channel is a function of the size of the discharge from the upstream boundary and the time of arrival at the downstream boundary. For this reason a number of tests are done with a certain phase difference in the start time of the discharge and the imposed water level. These are tests 1-3.

Slope in the direction perpendicular to the channel flow

The used classification of rivers and their surrounding areas, in chapter 4.3.2 gives a classification of rivers and areas on the basis of, among other things, the slope in the longitudinal direction of channel flow. The classification gives no insight into the slope in the direction perpendicular to channel flow.

In the test set 2, the impact of a slope in the direction perpendicular to the channel flow is examined. The altered variable in the test set 2 is the slope of 0.0001 in the perpendicular direction of the channel. Figure 5-8 shows the difference in the cross section of the area for the test set 1 and test set 2.



Figure 5-8 Cross section of the area with no slope and a small slope in the direction perpendicular to the channel flow

Table 5-4 gives information of the test set 2.

Table 5-4 Tests 2 for the slope in the direction perpendicular to the channel flow

Test set 2		Cases	Synthetic event in boundaries		Delay in boundaries	
Slope in the direction perpendicular to channel $i_b=0.0001$			Upstream	Downstream	Upstream	Downstream
			Q[m/s ³]	h[m]	t_0	t_h
Upstream boundary conditions	Test 2-1	A	Constant	0	0	0
	Test 2-1	B	Triangle	0	0	0
	Test 2-1	C	Parabolic	0	0	0
Downstream boundary conditions	Test 2-2	A	Small constant	Constant	0	0
	Test 2-2	B	Small constant	Tide	0	0
	Test 2-2	C	Small constant	Storm surge	0	0
	Test 2-2	D	Small constant	Storm surge and tide	0	0
Delay (timing) boundary conditions	Test 2-3	A	Parabolic	Storm surge and tide	0	0
	Test 2-3	B	Parabolic	Storm surge and tide	26	0
	Test 2-3	C	Parabolic	Storm surge and tide	0	26
	Test 2-3	D	Parabolic	Storm surge and tide	26	26

The output of the simulations of test set 2 is compared to the output of test set 1 to determine the influence on the output of the simulation, due to the altered slope in the direction perpendicular to the channel flow.

Varying parameters to characterize the floodplain and the channel

The parameters examined in the previous chapter, chapter 4 are similar to the parameters that are chosen in this section. The parameters that are investigated are the following:

- B_c : width of the channel
- n_c : Manning’s roughness coefficient of the channel
- z_b : the bed level of the channel
- n_f : Manning’s roughness coefficient of the flood plains

In the previous chapter the parameter are given a uniform distribution, where five values of each parameter are examined. In this section due to the large amount of simulations that would be needed for a test of five values for all the four parameters, only the minimum and the maximum values are tested, see Table 5-5.

Table 5-5 The minimum (test set 1 and test set 2) and maximum values (test set 3) for the parameters for class C and DA

Parameters	Class C		Class DA	
	Minimum	Maximum	Minimum	Maximum
Width of channel: B_c [m]	10	50	50	100
Roughness coefficient of channel: n_c [s/m ^{1/3}]	0.03	0.05	0.03	0.05
Roughness coefficient of floodplain: n_f [s/m ^{1/3}]	0.035	0.07	0.035	0.07
Bed level: z_b [m]	1	5	1	5

In test sets 1 and 2, discussed in the previous two sections, the minimum values for the parameters are used. In test set 3 the maximum values for the parameters are used for the simulations, while simulating the same altered variables as in test sets 1 and 2.

The output of the simulations of test sets 1 and 2 function as reference cases for test set 3. The resulting differences in the simulations between test set 3 and the reference cases determine the sensitivity of that parameter e.g. a small difference in the simulation between tests 3 and tests 1 (the upstream boundary conditions) for the parameter z_b indicates a small influence of the parameter z_b in combination with the variable upstream boundary conditions.

Due to the large amount of simulations, an example of tests 3 with the conditions of test 1 and test 2 for parameter B_c is shown in the Appendix XX. For each parameter 22 simulation are made, not all of them will be discussed in this chapter. The simulations with a large difference, meaning a large influence on the flood event are discussed.

Summary

The sensitivity of the following outputs, the water depth, the onset time of flooding and the flood extent, are examined in simulations using 1D/2D flow schematization. The changes in the output of the simulations caused by the varying event conditions and the varying channel and floodplain characteristics determine the sensitivity of the simulated varying conditions.

The size of the sensitivity is determined by using two methods, the visual examination and factor of differences. For an overview of all the simulations is in table I in the XX.

5.3 Results of the simulations

In this section only the simulations with significant results are discussed. The results of all the simulations can be found in the Appendix.

The results are discussed based on their influence on the output of the simulations, the water depth, the propagation of the flood and the flood extent. The combinations of the event conditions (boundary conditions), the characteristics of the area (the slope in the direction perpendicular to the channel flow) and the parameters (channel characteristics) show the most influence.

First the results of the simulations for the class C are discussed in section 5.3.1. Than the simulation results for the class DA are discussed in section 5.3.2. In the final section the differences between the two classes are discussed.

5.3.1 Results for class C

The water depth and the propagation of the flood

The result of the simulations for class C show that only the varying upstream boundary conditions have a high influence. This is determined by using the factor of difference and the visual examination, the results can be found in the Appendix.

The high influence of the upstream boundary conditions, is applicable for as well as the simulations with a slope (tests 2-1) and without a slope in the direction perpendicular to the channel flow (tests 1-1), see Figure 5-9.

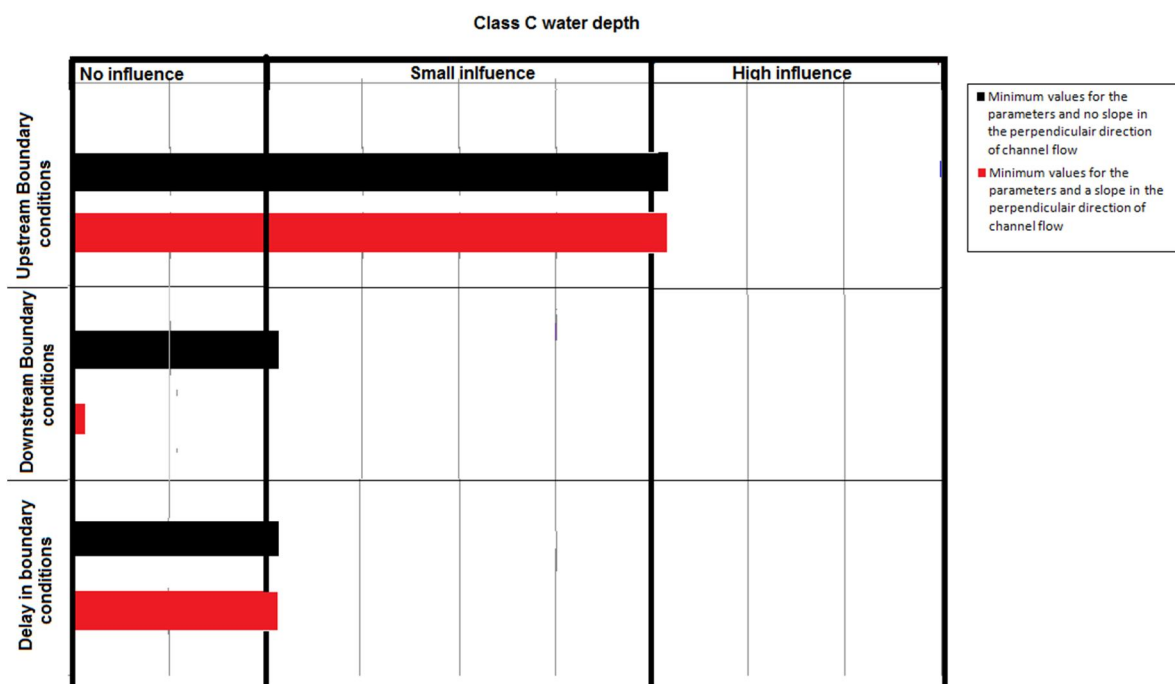


Figure 5-9 The influence on the water depth for class C of the simulations with varying conditions and characteristics of the flood event. The upstream boundary is the only event condition with a high influence.

The results of the water depth are exactly the same as the results found for the propagation of the flood, see Figure 5-10.

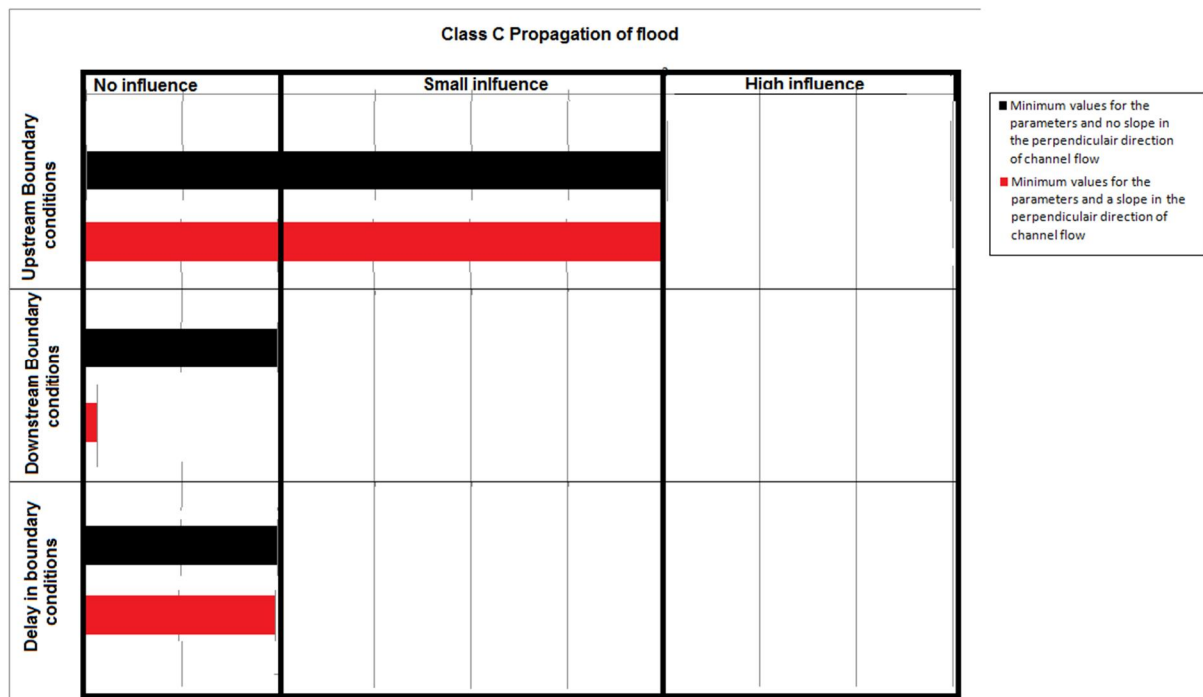


Figure 5-10 The influence on the propagation of the flood for class C of the simulations with varying conditions and characteristics of the flood event. The upstream boundary is the only event condition with a high influence.

The other simulations with the varying downstream boundary conditions (tests 1-2) and the varying delay in the boundary conditions (tests 1-3 and tests 2-3) show a small influence on the water depth and the propagation of the flood. Except for the simulations for the varying downstream boundary conditions with a slope in the direction perpendicular to the channel flow (tests 2-2), here there is no influence on the water depth and the propagation of the flood.

The influence of the varying conditions indicates the sensitivity of the outcome of the simulation due to the varying condition. This can also be interpreted as if there are uncertainties in the obtained data, when using wrong data in the upstream boundary conditions, this can lead to large uncertainties on the outcome of the simulation of the flood event. E.g. simulations of lower water depths for the prediction of a flood event than in the real flood event would occur. So the higher the sensitivity of a certain condition, the higher the chance is to have a wrong prediction of a flood event.

These simulations for the sensitivity for the water depth and the propagation of the flood show that priorities can be set on the information needed for a prediction of a flood event if the river and the floodplains can be classified as a class C.

The first priority, when only looking at the event conditions, is the upstream boundary conditions. The second priority depends on the type of area. If the area is relatively flat in the perpendicular direction of the channel flow (test set 1), the delay (or timing) of the boundary conditions and the downstream boundary conditions are of equal priority. If the area is not flat in the perpendicular direction of the channel flow (test set 2), the second priority goes to the delay (or timing) of the boundary conditions. The downstream boundary conditions have hardly any influence on the outcomes (the water depth and the propagation of the flood) and have thereby a low priority.

With these priorities set, it needs to be clarified, that these priorities are only of concern when there are limited resources (e.g. time and funds). If possible all the data for the conditions of the event should be collected.

The simulations of the parameters (test set 3) show how much certain parameters influence the water depth of the flood in combinations with the event conditions, see Figure 5-11.

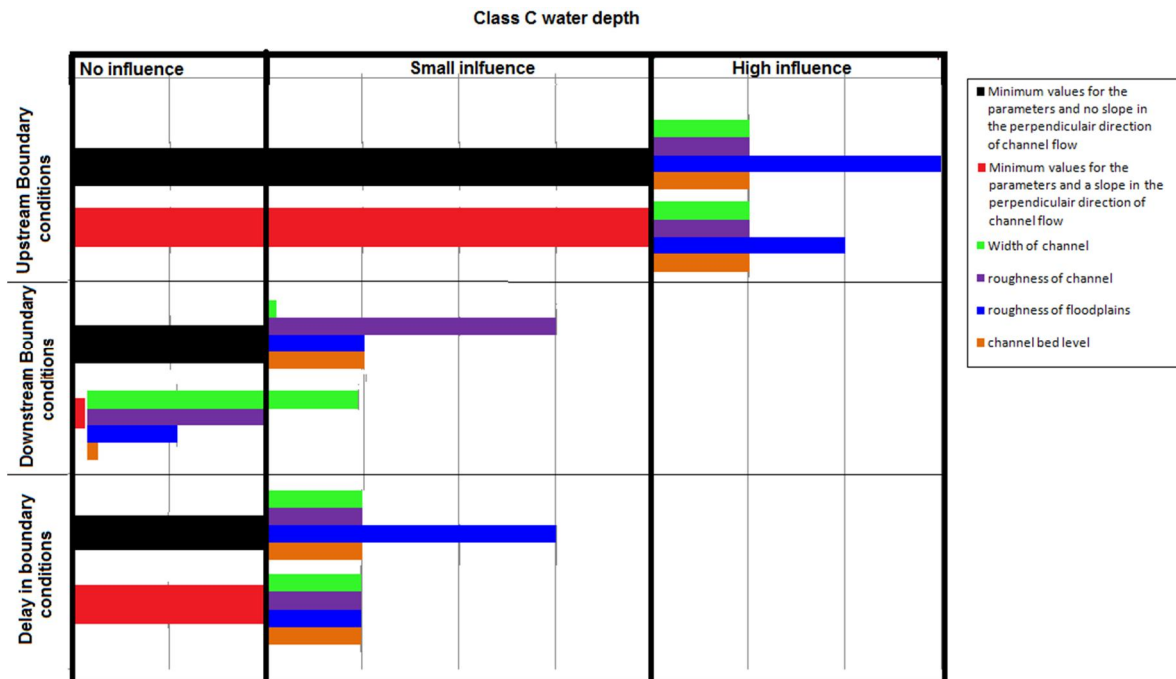


Figure 5-11 The influence on the water depth for class C for the simulations of the event conditions in combination with the parameters. For each event conditions the influence of each parameter is expressed in the increase of the influence of the event condition.

The outcome of the simulations for the water depth show that for four out of the six simulated event conditions, their sensitivity increased significantly by the influence of the roughness of the floodplains.

The simulations show that the first priority goes to the varying upstream boundary conditions (tests 1-1 and tests 2-1) in combination with the roughness coefficient.

The second priority is dependable on the type of area, with or without a slope in the perpendicular direction. If the latter case is applicable, the priority is to determine the delay (timing) of the boundary condition, this is only the case if the roughness coefficient of the floodplain is already determine in the first priority. Otherwise the priority is to obtain the combination of the upstream boundary conditions with the roughness of the channel.

Figure 5-12 shows the influence on the propagation of the flood for the parameters in combination with the varying event conditions.

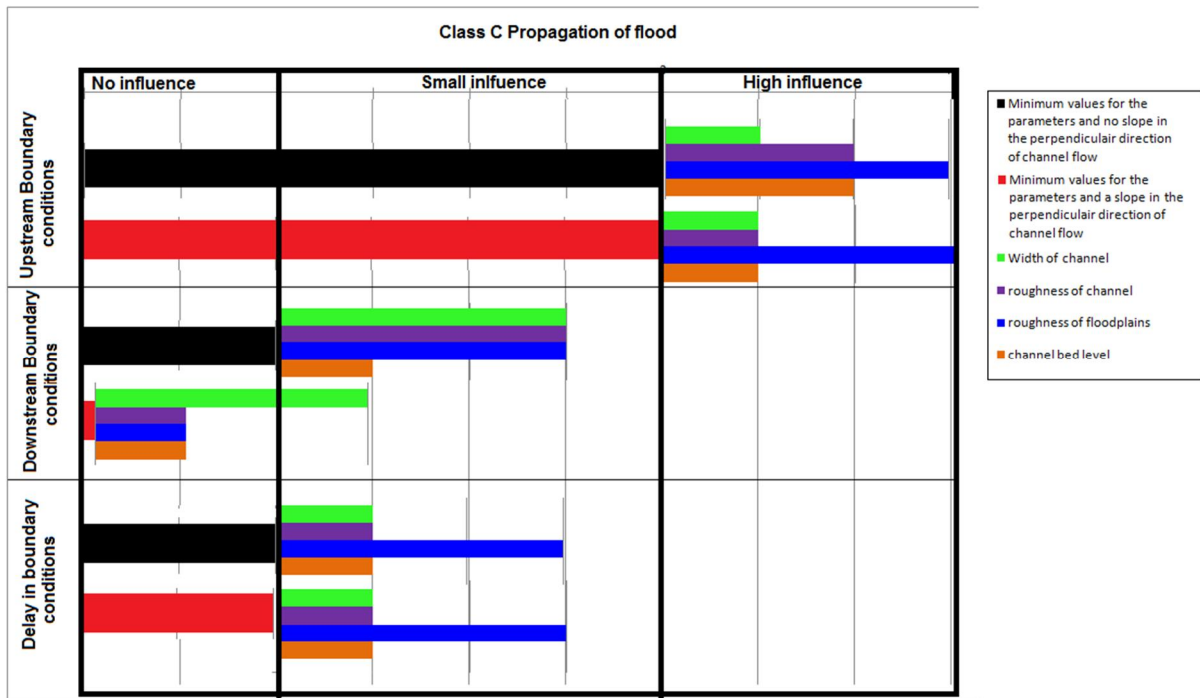


Figure 5-12 The influence on the propagation of the flood for class C for the simulations of the event conditions in combination with the parameters. For each event conditions the influence of each parameter is expressed in the increase of the influence of the event condition.

The roughness coefficient of the floodplains in combination with five out of six event conditions result in a higher sensitivity for the propagation of the flood. So the first priority is the upstream boundary conditions in combination with the roughness of the floodplains. This is the highest influence for the propagation of the flood, the second priority is less obvious. The next priorities depend on the area, with or without a slope in the direction perpendicular to the channel.

Flood extent

For the flood extent, the upstream boundary with no slope in the perpendicular direction (tests 1-1) are the only simulations showing influence, see Figure 5-13.

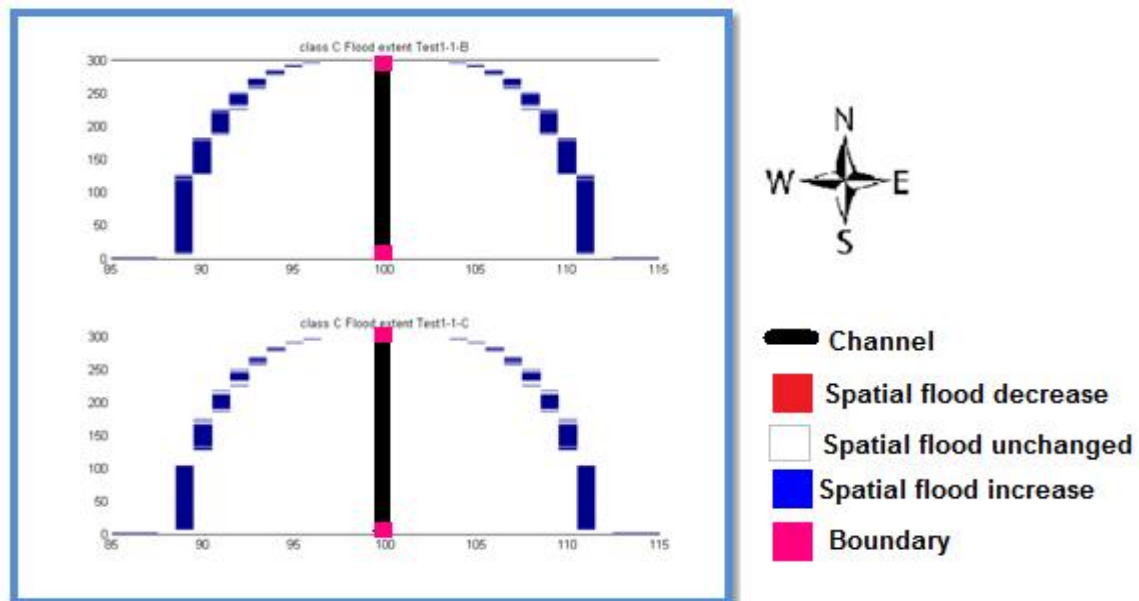


Figure 5-13 The differences in the spatial flood extent for the varying upstream boundary, zoomed into the flooded area. The simulation with a constant upstream boundary condition (test 1-1-A) is compared to the upstream boundary in the triangle shape (test 1-1-B) and the parabolic shape (test 1-1-C).

The upstream boundary conditions are the only conditions that have influence on the flood extent. The three tests done with varying upstream boundary show that the test with the highest peak (test 1-1-B, triangle shaped discharge) has the largest increase in the flood extent. Therefore the peak of the upstream discharge is the highest priority for the prediction of the flood extent.

The simulations with the parameters show none to small influence on the flood extent. The spatial plots for these simulations, like Figure 5-13, can be found in the Appendix.

Summary

Overall the upstream boundary conditions and the roughness coefficient of the floodplains are the first priority when a prediction of flood event needs to be simulated for an area classified as class C. This is the case for all the outcomes tested in these simulations, the water depth, the propagation of the flood and the flood extent.

5.3.2 Results for class DA

The water depth and the propagation of the flood

In the result of the simulations for class DA, none of the event conditions (the boundary conditions) give a high influence for the outputs. This is determined by using the factor of difference and the visual examination, the results can be found in the Appendix.

A small influence has been found for the water depth in the upstream boundary conditions and in the delay (timing) of the boundary conditions for as well as the simulations with a slope (tests 2-1 and tests 2-3) and no slope in the direction perpendicular to the channel flow (tests 1-1 and tests 1-3), see Figure 5-14. The tests 1-2 and 2-2 (simulations with the varying downstream boundary conditions) have no influence on the water depth.

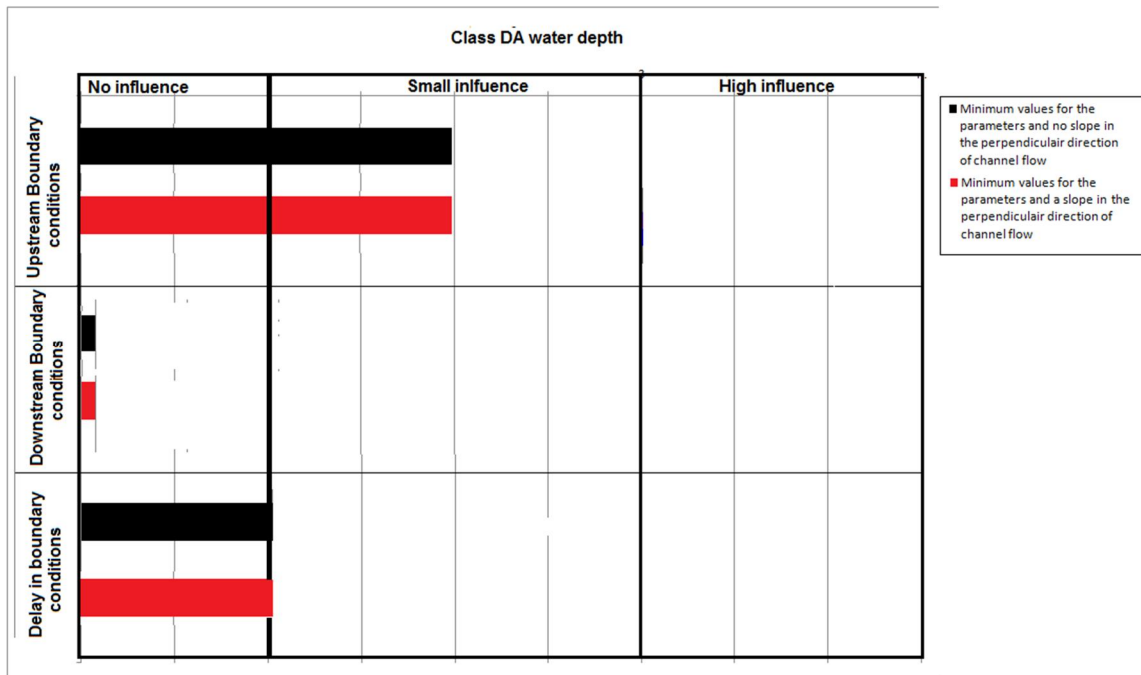


Figure 5-14 The influence on the water depth of the flood in class DA for the simulations with varying conditions and characteristics of the flood event. The upstream boundary conditions and the delay (timing) of the boundary conditions are the event conditions with a small influence. The downstream boundary conditions have no influence on the water depth

The propagation of the flood has similar small influence just as in the case of the water depth, except for the tests 2-2 (the varying downstream boundary conditions with a slope in the direction perpendicular to the channel flow). For this boundary event the influence on the propagation of the flood is small instead of no influence. Figure 5-15 shows the influence on the propagation of the flood.

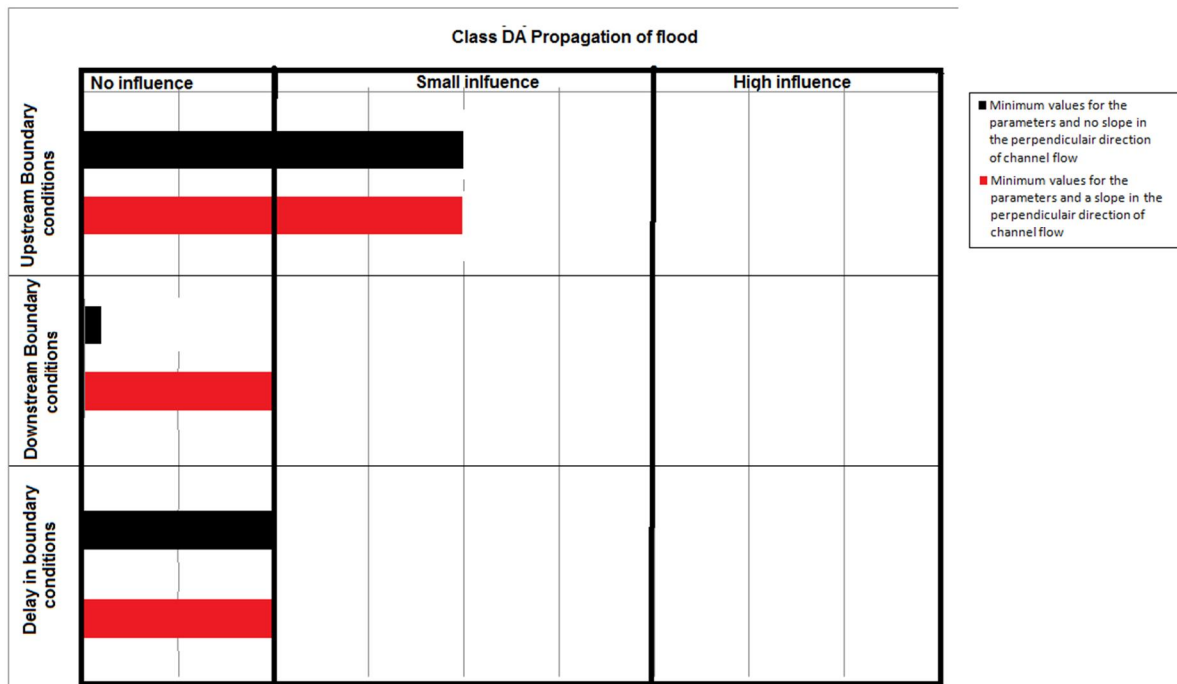


Figure 5-15 The influence on the water depth of the flood in class DA for the simulations with varying conditions and characteristics of the flood event. The downstream boundary conditions have no influence on the water depth. The other boundary conditions have a small influence on the propagation of the flood.

In class DA the largest influence on the water depth and the propagation are the upstream boundary conditions. This is still a small influence but it has more priority than the other two boundary events that are simulated.

The influences of the parameters are taken into account in combination with the event boundary conditions the sensitivity of the water depth in Figure 5-16.

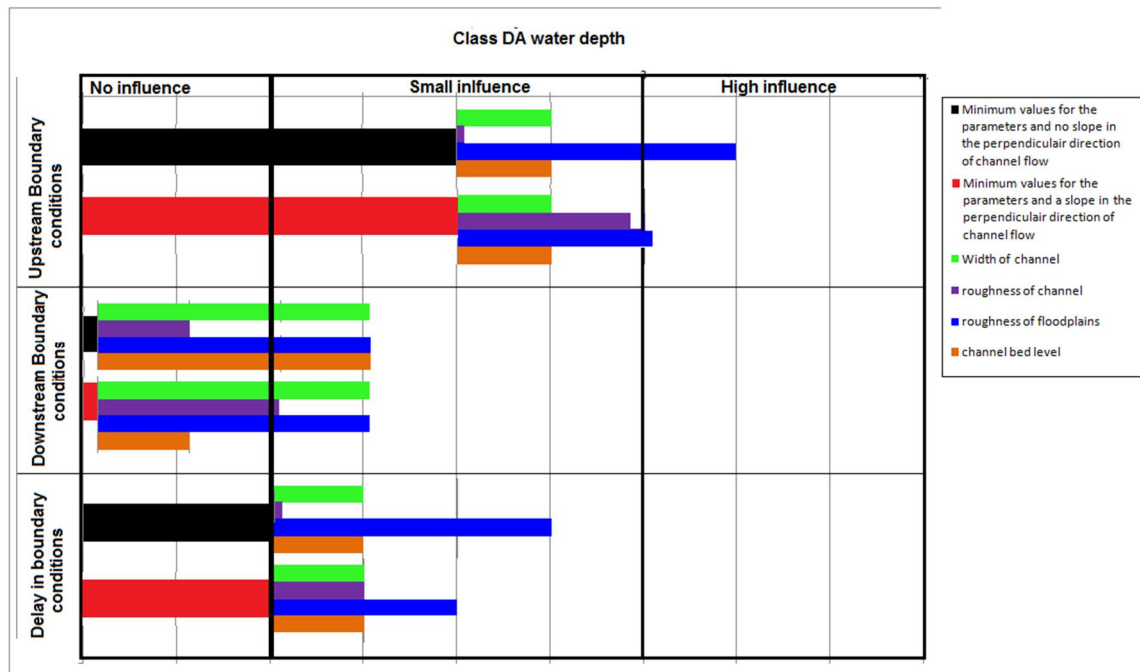


Figure 5-16 The influence on the water depth for class DA for the simulations of the event conditions in combination with the parameters. For each event conditions the influence of each parameter is expressed in the increase of the influence of the event condition.

The water depth in the tests 1-1 and tests 2-1 (the upstream boundary conditions without and with a slope in the direction perpendicular to the channel) move by the influence of the roughness coefficient of the flood plains from small to high influences. The other parameters only increase the sensitivity on the water depth of the tests 1-1 a little and do not change of influence classification. This can also be seen in the tests 1-3 and tests 2-3 (the delay (timing) of the boundary conditions). The roughness of the flood plains lifts these simulations to small influence instead of no influence. The simulations for the downstream boundary conditions (tests 1-2 and 2-2) have on their own no influence on the water depth. But with the parameters, channel width and roughness coefficient, the sensitivity increases to small influence. The sensitivity on the water depth due to the downstream boundary conditions is responsive to many parameters.

For the propagation of the flood the highest sensitivity lays with the upstream boundary conditions in combination with the parameters, the roughness of the floodplains and the width of the channel. Next is the roughness of the channel in combination with the downstream boundary for the areas with a slope in the direction perpendicular to the channel flow (tests 2-2) and the channel roughness in combination with the delay (timing) of the boundary conditions for the areas with a slope in the direction perpendicular to the channel flow (tests 2-3). The other simulations in combination with the parameters result in small and negligible change in the sensitivity on the propagation of the flood. The sensitivity of the propagation of the flood by the influence of the parameters in combination with the event boundary conditions are shown in Figure 5-18.

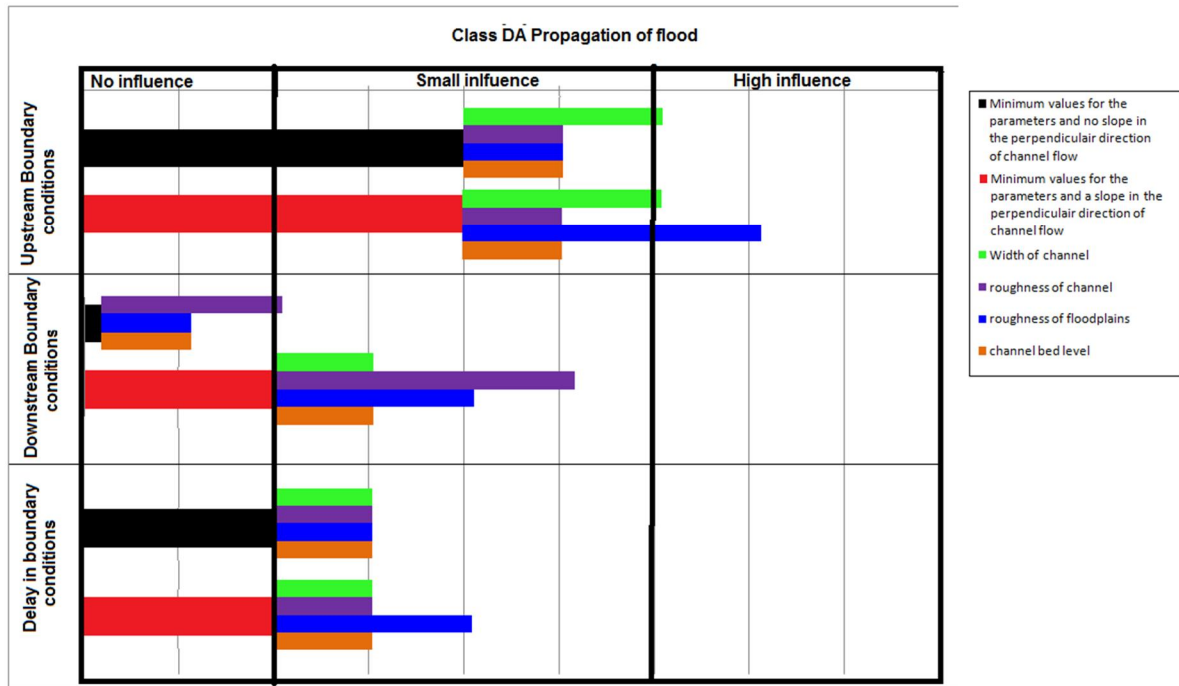


Figure 5-17 The influence on the propagation of the flood for class DA for the simulations of the event conditions in combination with the parameters. For each event conditions the influence of each parameter is expressed in the increase of the influence of the event condition.

Flood extent

The flood extent shows that the upstream boundary, the tests 1-1 and tests 2-1 (with no and a slope in the direction perpendicular to the channel flow) have the largest influence. The flood extent is increased in certain areas and decreases in other areas.

In Figure 5-18 the differences in the flood extent for the tests 1-1 are plotted spatially in two colors, blue for an increase and red for a decrease.

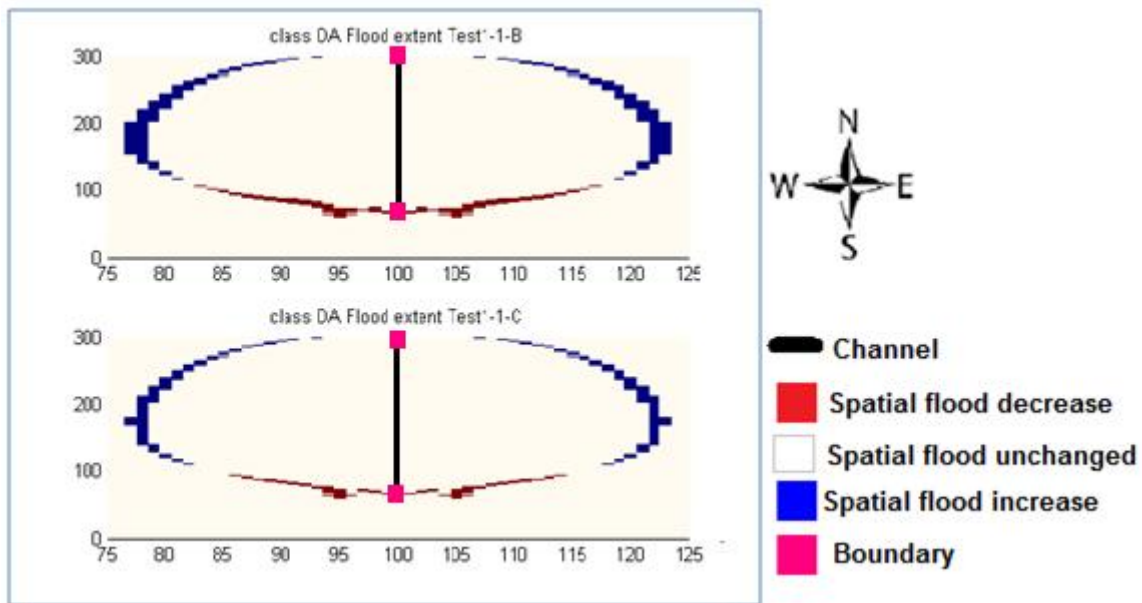


Figure 5-18 The difference in the flood extent for the class DA for the test 1-1-B (the triangle shaped upstream discharge) and the test 1-1-C (the parabolic shaped upstream discharge) compared to the test 1-1-A (constant upstream discharge).

The difference in the three simulations of tests 1-1 are the type of shape for the upstream discharge even though the three simulations are volumetric equal when integrated in the time, see Figure 5-5. So when the outcomes of the test 1-1-A (constant upstream discharge), the test 1-1-B (triangle shaped upstream discharge) and tests 1-1-C (parabolic shaped upstream discharge) are compared, two things stand out. The flood extent is increased in the west and east side of the channel and decreased in the south side of the river. The differences in the shape of the discharges can explain this. The increase in the west and east side is due to the size of the peak of the discharges. The test 1-1-B (triangle shaped) has the largest peak (4500 m³/s) and shows the largest increase in the flood extent in the west and east side of the channel in comparison to the test 1-1-C (parabolic shaped) where the largest peak is 3750 m³/s and the test 1-1-A with a constant discharge of 2500 m³/s

The decrease in flooded area in the south side can be explained by the shape of the discharges. In the last time steps of the simulation, the test 1-1-A (constant shaped discharge) has a larger volume when integrated over last 40 hours than the other two tests. Figure 5-19 shows the volume when integrated over the last 40 hours. Of the three simulations, the highest volume is for the constant shaped discharge (test 1-1-A), next the parabolic shaped discharge (test 1-1-B) and the last is the triangle shaped discharge. This is the same sequence as for the flood extent in the south side of the channel.

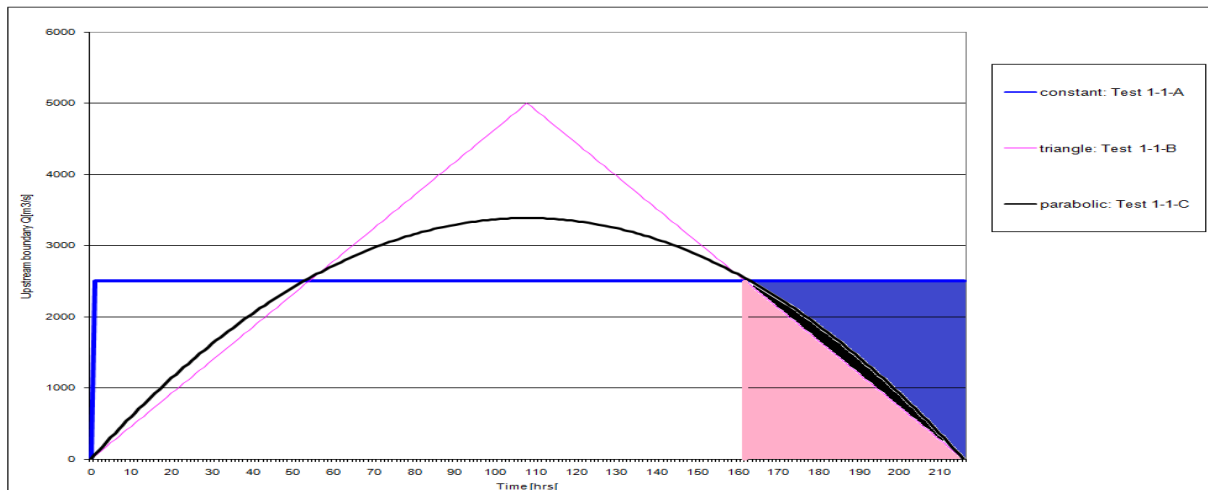


Figure 5-19 The three different shapes for the upstream discharge. The area under the three graphs for the last 40 hours of the simulation is colored with related color of the graph.

The same is found the simulations with a slope in the direction perpendicular to channel flow is presented, see Figure 5-20.

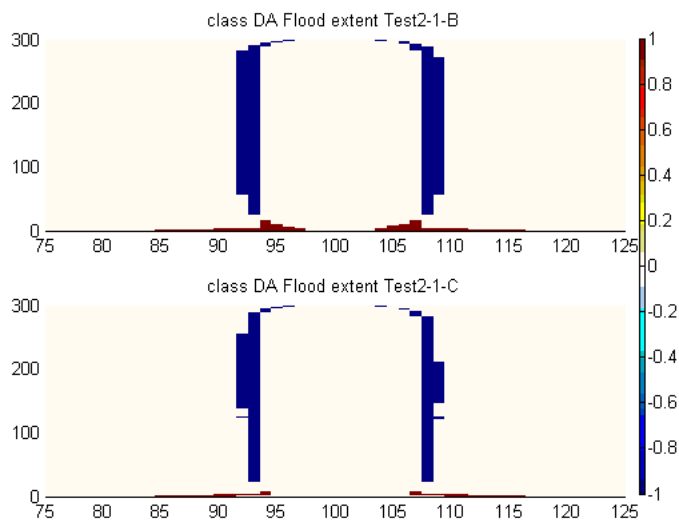


Figure 5-20 For the flood extent for the class DA, the simulation with a slope in the direction perpendicular to the channel flow, the test 2-1-B (the triangle shaped upstream discharge) and the test 2-1-C (the parabolic shaped upstream discharge) are compared to the test 2-1-A (constant upstream discharge)

The parameters in combination with the boundary conditions show no significant increase or decrease for the flood extent in class DA.

Overall the flood extent is sensitive for the upstream boundary conditions. The simulations showed that not only are the peak of the upstream discharge but also the shape (the volume of the discharge when integrated over the final simulation period) is of importance.

Summary

For class DA overall the upstream boundary conditions have the most influence on the water depth, the propagation of the flood and the flood extent. But in combination with the parameters there is a difference in the water depth and the propagation of the flood. For the water depth, the combination of the upstream boundary conditions with the roughness coefficient of the flood plains increases the sensitivity even more, for both tests 1-1 and 2-1 (with no and with a slope in the direction perpendicular to the channel flow). The sensitivity of the propagation of the flood is dependable on the upstream boundary conditions in combination with the two parameters, the roughness coefficient of the flood plains and the channel width.

For the flood extent the parameters have negligible influence, but the upstream boundary conditions have. For this type of flood information the shape and the size of the upstream boundary is of importance.

5.3.3 Differences between class C and class DA

In the previous sections the sensitivity of the outputs of the simulations, the water depth, the propagation of the flood and the flood extent, for the classes C and class DA are examined. Here the differences found in the sensitivity for the outputs of the simulations are discussed.

For class C the highest sensitivity of the water depth and the propagation of the flood come from the upstream boundary condition in combination with the roughness coefficient of the floodplains. The flood extent is also mostly influenced by the upstream boundary conditions. The peak of the

upstream discharge determines largely the flood extent and the shape of the upstream discharge had hardly no influence.

For class DA almost similar results were found. The upstream boundary conditions have for all the outcomes of the simulations the highest influence. But for each outcome of the simulations different aspects need to be included. For the water depth this is the parameter of the roughness coefficient of the flood plains. The influence of this combination leads to the highest sensitivity for the water depth. For the propagation of the flood, two parameters lead to high sensitivity, the combination of the upstream boundary and the parameters, the channel width and the roughness coefficient of the flood plains.

In class DA the flood extent has also a high sensitivity with the influence of the upstream discharge. The influence of the upstream discharge depends on the peak of the discharge and the type of shape of the discharge, especially the shape at the end of the simulation time.

The sensitivities for each class are actually the priorities of which data should be obtained first when a prediction for a flood event needs to be made. To give a clear view of which data should be obtained first a decision tree is made for the prediction of the water depth of the flood (Figure 5-21) and for the propagation of the flood (Figure 5-22).

Water depth

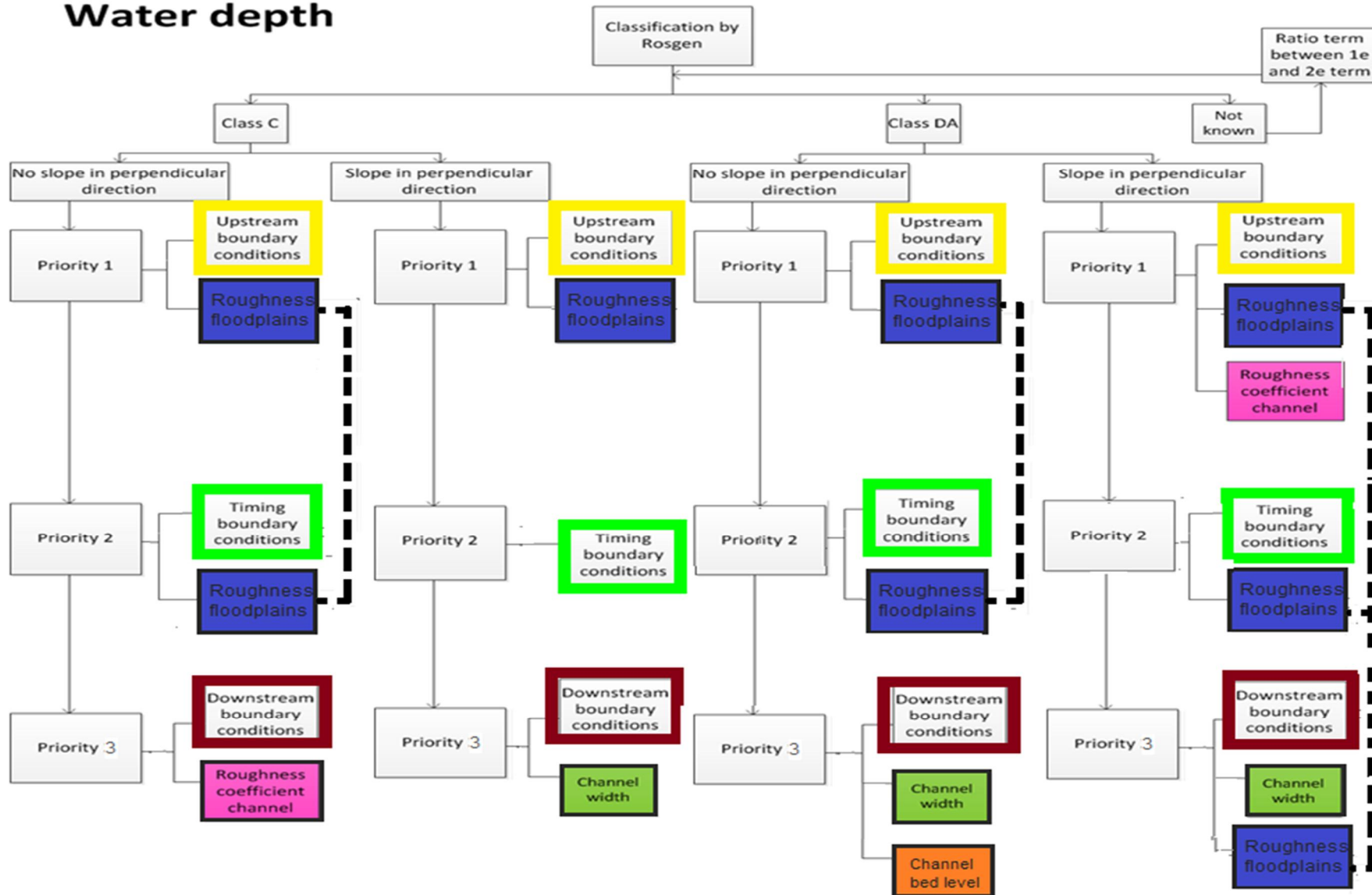


Figure 5-21 Decision tree for which data has priority to be obtained for the classes C and DA for the prediction of the water depth of the flood.

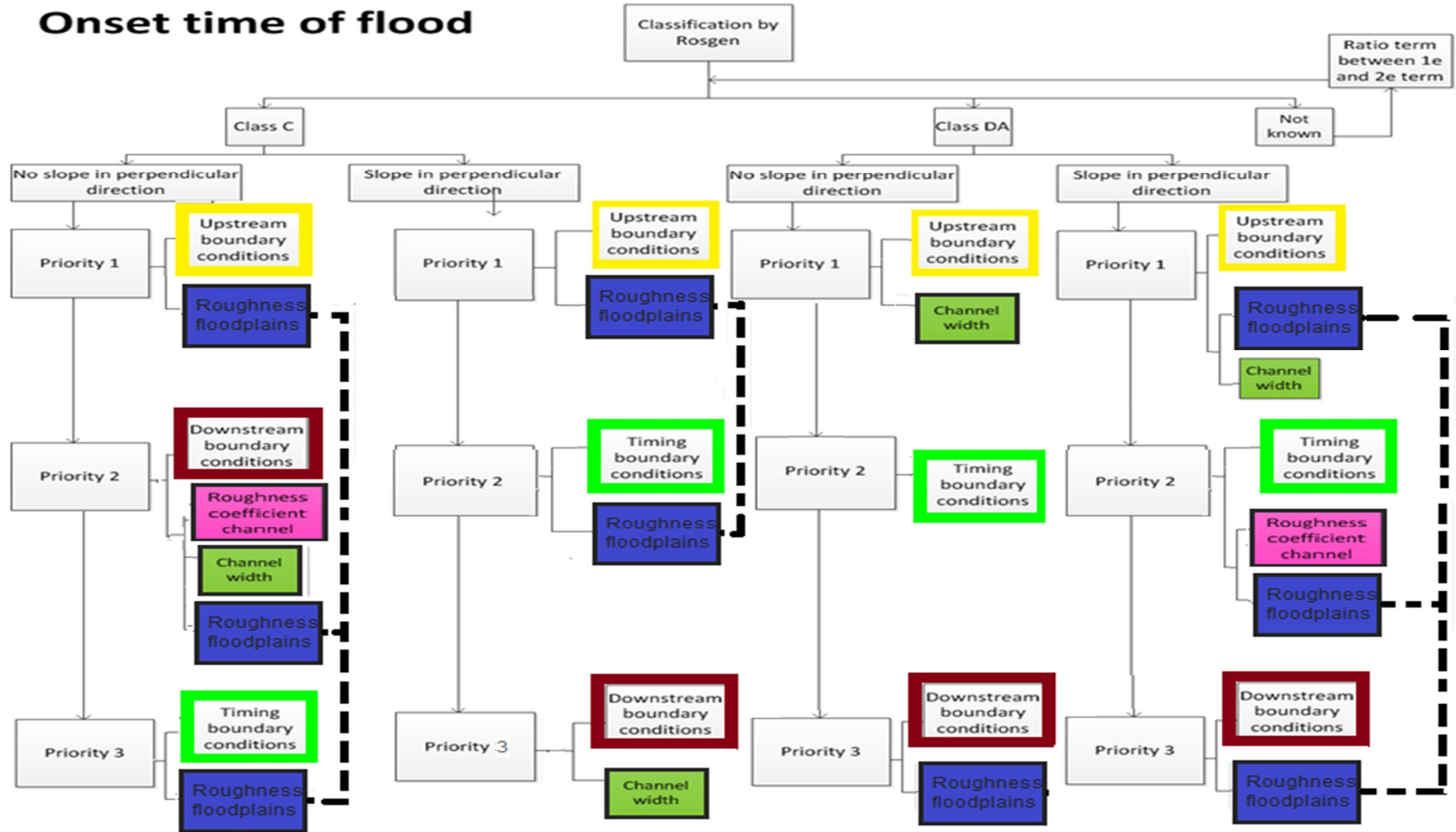


Figure 5-22 Decision tree for which data has priority to be obtained for the classes C and DA for the prediction of the propagation of the flood.

The prediction of the water depth of the flood has the same first priority for both classes. The first priority is the upstream boundary conditions in combination with the roughness coefficient of the floodplains. For the class DA with a slope in the direction perpendicular to the channel flow, the channel roughness needs to be taken into account.

The second priority is for the timing (delay) of the boundary conditions in combination with the roughness coefficient of the floodplains. Because this parameter is already needed in the first priority and now also for the second priority, it is a very important parameter.

For the third priority, the downstream boundary conditions are the data that needs to be obtained in combination with different parameters for each type of class and area. For most areas a combination with the channel width is needed.

When the prediction of the propagation of the flood needs to be determined, the first priority for both classes is the upstream boundary conditions. For class C this is for both areas in combination with the roughness coefficient of the floodplains. For class DA this is the channel width and for the area with a slope in the direction perpendicular to the channel flow the channel width and the roughness of the floodplains. For the second priority and third priority, the needed data varies for each class and area, Figure 5-22.

For the both classes the upstream boundary is the only conditions that influence the flood extent. For the prediction of the flood extent, there is a clear difference between class C and DA. For class C the peak of the discharge is important, while for the class DA the peak and the shape of discharge.

5.4 Conclusion

5.4.1 Comparison with 1D flow

The sensitivity of this 2D flow case study has examined the sensitivity for two classes. These results are compared to the results of the previous case study, chapter 4 Study case: 1D flow. Table 5-6 repeats the influence on the water depth and flood wave celerity of the parameters for the 1D flow from chapter 4.5.5.

Table 5-6 The influence of the parameters on the water depth of the flood plains on the flood wave celerity for the 1D flow case study.

1D flow	Classes	C	DA
	Influence		
Water depth of the flood plains	High	n_f, B_f, i_b	n_f, B_f, i_b
	Small		
	Negligible	B_c, n_c, z_b	B_c, n_c, z_b
Flood wave celerity	High	n_f, B_f, i_b	i_b
	Small		n_f, B_f
	Negligible	B_c, n_c, z_b	B_c, n_c, z_b

- *Water depth*

- In the 1D flow case study the same parameters for the sensitivity on the water depth were found for class C as for class DA. These are the parameters n_f (the roughness of the floodplains), B_f (the width of the floodplain) and i_b (slope of the channel bed).
- The high influence of the parameter the roughness of the floodplains is also found in the results for the 2D flow case study.

- In the 1D flow the parameters B_f (the width of the floodplain) and i_b (slope of the channel bed) have also a high influence on the water depth of the flood. In the 2D flow these parameters were not examined. But the simulations in the 2D flow case study with the slope in the direction perpendicular to the channel are an approximation for the B_f (the width of the floodplain). The slope in the direction perpendicular to the channel approximates a smaller width of the flood plains, see Figure 5-23.

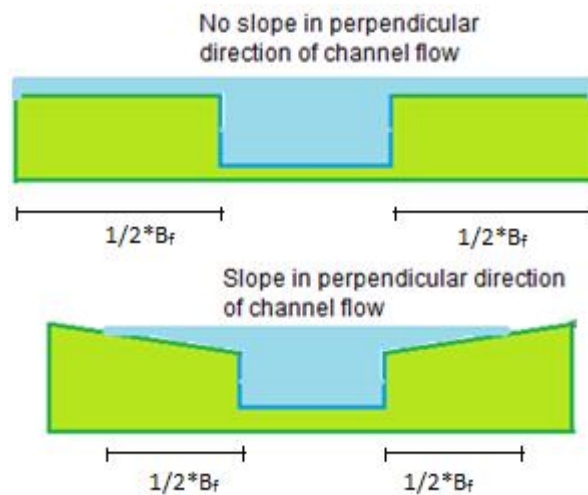


Figure 5-23 The slope in the direction perpendicular to the channel approximates a smaller width of the flood plains.

- The decision tree for the 2D flow case study in Figure 5-21 shows that for the water depth areas with a slope in the direction perpendicular to the channel have different priority than the areas where there is no slope in the direction perpendicular to the channel.
 - The negligible influence parameters in the 1D flow are the B_c (channel width), n_c (roughness coefficient of channel) and z_b (channel bed level). These parameters can be found in the 2D flow as the third priority. For the prediction of the water depth the case studies, the 1D flow in chapter 4 and the 2D flow chapter 5, give similar outcomes.
- *The flood wave celerity (For the 1D flow)/ the propagation of the flood (in the 2D flow)*
- *Class C:*
 - In the 1D flow the flood wave is highly influences by the parameters n_f (the roughness of the floodplains), B_f (the width of the floodplain) and i_b (slope of the channel bed).
 - In the 2D flow, the priority of the propagation of the flood is also the parameter n_f (the roughness of the floodplains)
 - The parameter B_f (the width of the floodplain) is not tested in the 2D flow, but the differences between the simulations with and without a slope in the direction perpendicular to the channel is an approximation for the B_f (the width of the floodplain). In the 2D flow the priority is different for these two simulations and points out the sensitivity of the B_f (the width of the floodplain) on the propagation of the flood.

- *Class DA:*
 - In the 1D flow the flood wave is highly influenced by the parameter i_b (slope of the channel bed). And the parameters n_f (the roughness of the floodplains) and B_f (the width of the floodplain) have a small influence.
 - In the 2D flow, the priority of the propagation of the flood is also the parameter n_f (the roughness of the floodplains)
 - In the 2D flow the priorities differ a little between the simulations with and without a slope in the direction perpendicular to the channel, similar to the small influence of the parameter B_f (the width of the floodplain).
 - In the 2D flow the parameter B_c (the channel width) has a high priority. This was not found in the 1D flow

5.4.2 Recommendations for the 2D flow

The influence of the parameters and the conditions in the 1D and 2D flow study cases show for some areas similarities and for other areas not. It is recommended to use the 2D flow decision tree, because in this case study the spatial and the time aspects are taken into account.

The 2D flow shows besides the influential parameters also that the conditions can have a large influence and especially in combination with the influential parameters. These conditions have not been tested for the other classes in the classification of rivers of Rosgen. It is my recommendation that these should be examined also on the influence of the combination of parameters and conditions on the prediction of a flood event.

6. Case study: the 2011 Thailand flood event

6.1 Introduction

In 2011 Thailand coped with floods in large parts of the country. The combination of long periods of intensive precipitation, the reservoirs being at maximum capacity and failing of embankments caused approximated total damage and losses of THB 1,425 Bn (US\$ 45.7 Bn) ("The World Bank Supports Thailand's Post-Floods Recovery Effort," 2011). The flood started in the north part of Thailand around July 2011 and spread down the Chao Phraya River to the south of Thailand. At the end of 2011 significant flooding had reached the south part of Thailand. The areas with large economic value were threatened by the potential flood. The main concern went to the capital, Bangkok, the airport and other industrial areas with multinational corporations.

In this chapter the 2011 Thailand flood event is simulated using publicly available data. In the previous chapters the sensitivity analysis of the properties of a flood model has been carried out for a 1D and a 2D flow schematization. The results in chapter 4 and 5 show certain sensitivity towards particular inputs for the flood model. As Thailand is characterized as an area that fits the description of class DA and C, the main sensitivity for this type of area are the roughness coefficient of the flood plains and the upstream boundary conditions.

There are a number of sources available to collect data for these sensitivities. In section 6.2 these data from different sources are discussed. In section 6.3 a selection of the data for the flood model are chosen based on the best fit of the flood in mid August. The selected data for the simulation for the mid August flood extent map is used to simulate the flood event from August till December. The results of these simulations are discussed in section 6.4. In section 6.5 the conclusions and discussion of the 2011 Thailand flood event.

6.2 Available data for 2011 Thailand flood event

In this section the available data for the simulation of the 2011 flood event in Thailand is discussed. Due to the sensitivity of the roughness of the flood plains and the upstream boundary conditions multiple data resources are researched for these conditions of the flood model. This section consists of the data obtained for the topographic information, the water systems and the precipitation. In the last section the observed data of the 2011 Thailand flood event to validate the flood model are discussed.

6.2.1 Topographic information

In chapter 4 and 5 the roughness of the flood plains was determined to have a high influence on the prediction of a flood event. In a real case like in Thailand, the roughness of the flood plains can not only be expressed in a roughness coefficient but also as obstacles for the water flow. These obstacles can be areas on higher ground and different types of areas.

Therefore the topographic information is used to determine the obstacles in the Thailand case study. The topographic information for the simulations consists out of three parts: The digital elevation model (DEM), the land use and forest cover map and the roads. These types of information have influence on the water flow in floodplains.

DEM

As a digital elevation model (DEM), the product of NASA/NGA Shuttle Radar Topography Mission (SRTM) is used. The SRTM data consists of elevation maps that are available publicly. The area of interest is available for tiles of 1 degree at a grid size close to 30 meter. The tile covering of Thailand

is an area of 300 by 200 km. The grid size is adjusted to be able to simulate the event in short amount of time in SOBEK. Two sizes are chosen, 1 km and 500 m. Figure 6-1 shows the digital elevation model for Thailand with a grid size of 1 km. The DEM is downloaded from the NASA website in grid sizes of approximate of 30 m before it is converted into two grid sizes of 1km and 500 m. The grids have been smoothed to remove noise with the use of Wavelet filter. In section 3.2.3 the use of Wavelet filter is explained. This was done with the Deltares prototype Rapid Flood Model Tool.

The DEM provided by SRTM is projected in WGS1984 in degrees. With the use ArcGIS this data is re-projected in to UTM zone 47North in meters.

Figure 6-1 shows the DEM map for the area of interest.

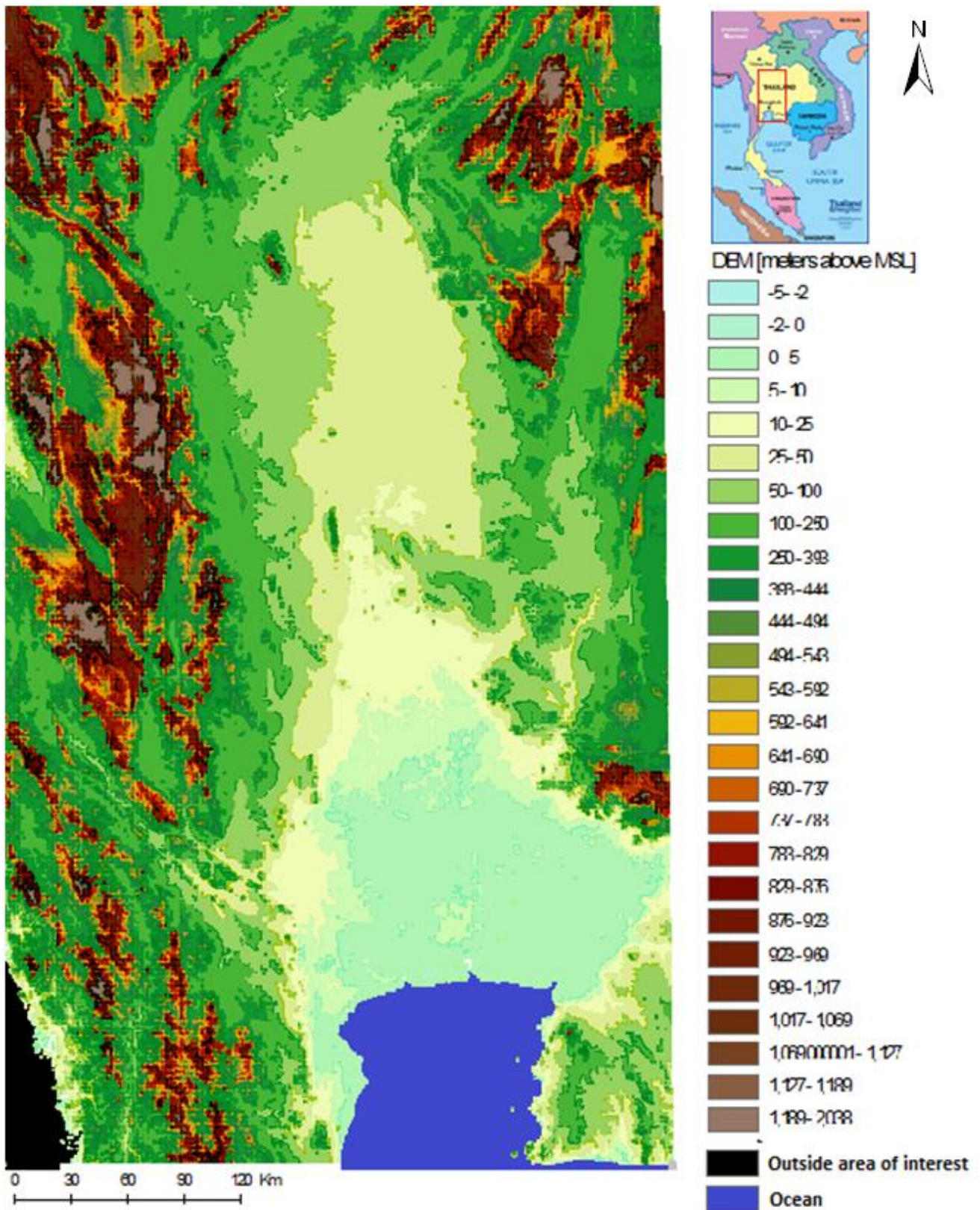


Figure 6-1 Digital elevation model from SRTM of Thailand with a grid size of 1km

The land use and forest cover map

In chapter 4 and 5 is determined that the roughness coefficient is an important parameter in a flood model.

The roughness coefficient depends amongst other things on the type of land use. An agriculture area will have a lower roughness than a forest area. To distinguish the different areas in Thailand, the 2000 Thailand land-use and forest cover map is used. This map is obtained from the website <http://www.rsgis.ait.ac.th/~souris/thailand.htm> (Souris, 2011).

Besides the forest areas the map gives different codes for different types of land use, which include among others agriculture, urban areas and savannah and grassland. The original map is for the whole of Thailand and comes in a raster shape with grid sizes of 500 m. The map is made from Landsat TM satellite images (30 m resolution) and is in geographic decimal degrees coordinate (long, lat), in INDIAN 1954 Datum (Ellipsoid is Everest Indian).

This map has been clipped to the area of interest. For the simulations with a grid size of 1 km the grids of the original map have been re-sampled to a size of 1 km. Figure 6-2 shows the original map which has been clipped and re-sampled to the area of interest with the grid size of 1 km.

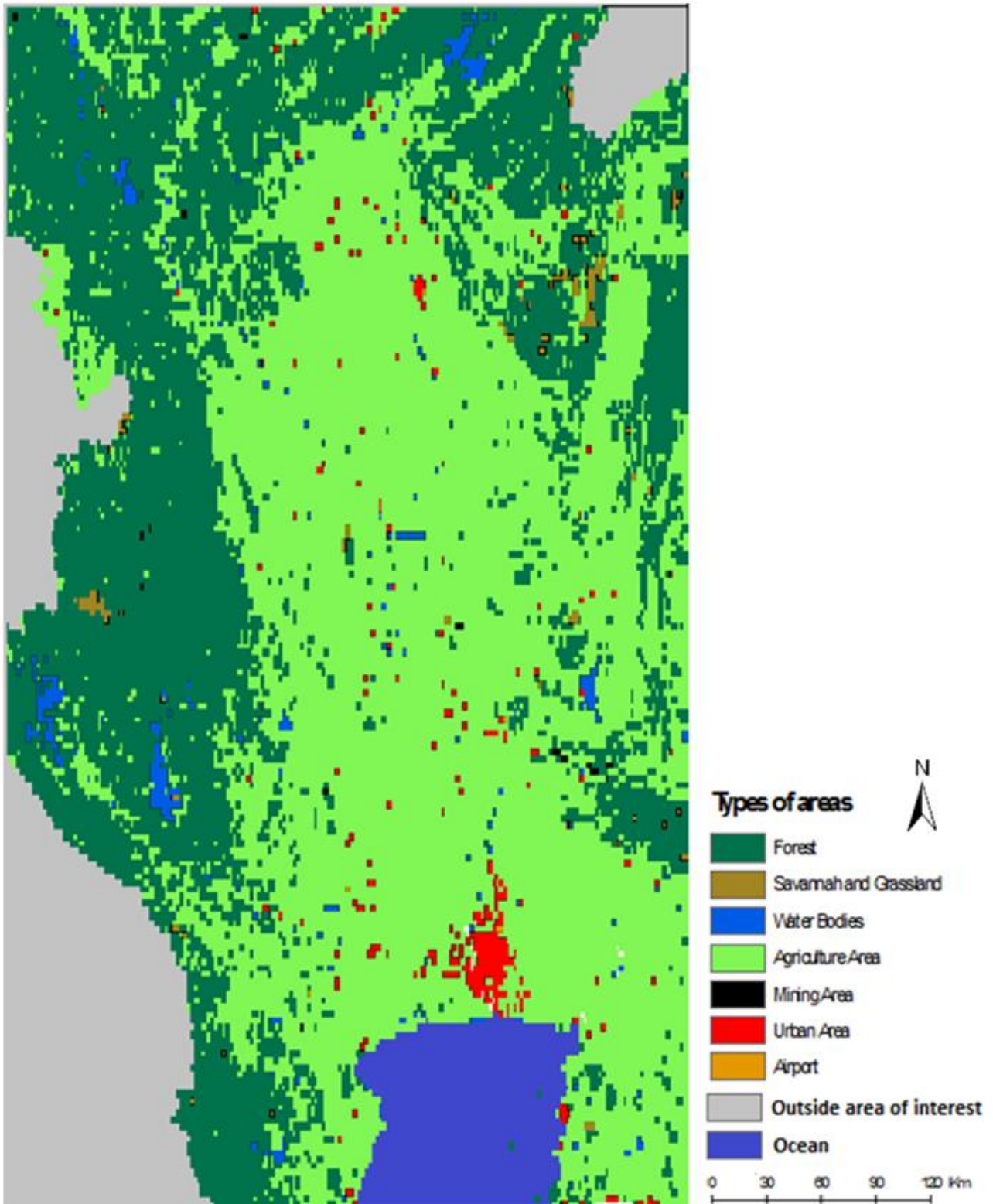


Figure 6-2 The land use and forest cover map in the area of interest in Thailand

In the original map the areas have codes which describe the type of area. For each area the corresponding Manning's coefficient is assigned to each type of areas by using the recommended design values of Manning roughness coefficient from the book '*Hydrologic analysis and design*' (McCuen, 2005). These values are presented in Table 6-1.

Table 6-1 Types of area with their original code and the assigned Manning's coefficient

Code	Type of areas	Manning's coefficient
111	Tropical Evergreen Forest	0.15
112	Dry Evergreen Forest	0.15
113	Hill Evergreen Forest	0.15
114	Pine Forest	0.15
115	Swamp Forest	0.15
116	Mangrove Forest	0.15
117	Inundated Forest	0.15
118	Beach Forest	0.15
121	Mixed Deciduous Forest	0.15
122	Dry Dipterocarp Forest	0.15
123	Bamboo Forest	0.15
131	Plantation	0.15
133	Eucalyptus Plantation	0.15
140	Secondary Forest	0.15
200	Agricultural Area	0.035
310	Urban	0.015
410	Savannah and Grassland	0.05
500	Water Bodies	0.04
610	Old Clearing, Encroachment and active Shifting Cultivation	0.035
700	Other Area	0.035
710	Golf Field	0.035
720	Airport	0.012
730	Mining Area	0.025

Roads

The SRTM data used to create the DEM for the area of interest is original a raster file with the grid size of 30 meters. On a grid of 30 m certain man made features can be left out due to the size of these features. These manmade features include high buildings and line elements like highways. These features are mostly filtered out in the SRTM data and average out when the SRTM data is re-sampled to 500 m and 1 km grids.

The line elements like the highways are usually elevated in real situations. For a flood event this type of elevated feature is an obstruction for the flood. For this reason the road elements are included into the DEM separately. From the OpenStreetMap (OSM) the locations of these roads can be obtained. Figure 6-8 shows the locations of the main and the secondary roads for the area of interest.

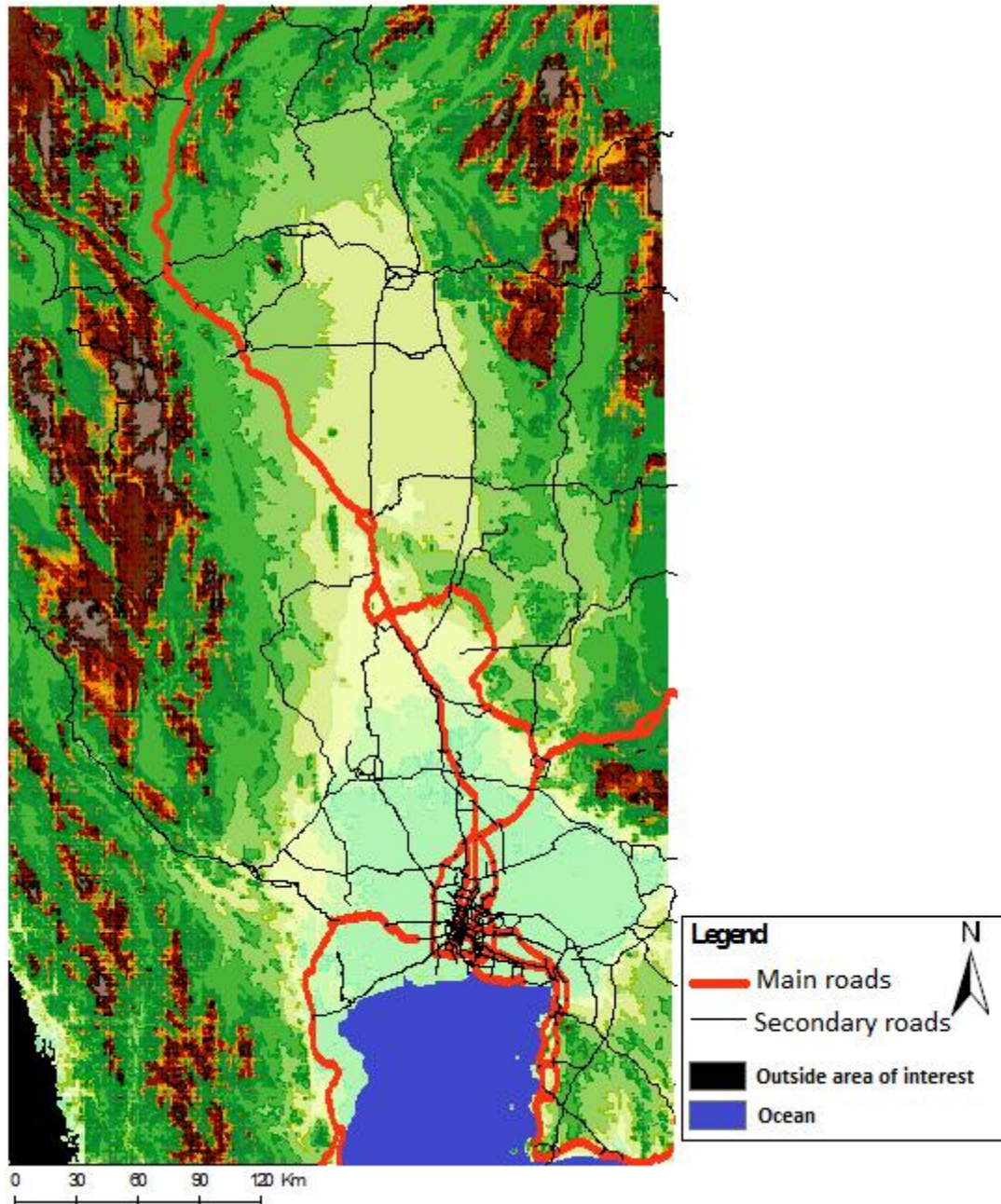


Figure 6-3 the main and secondary roads from OSM projected onto the DEM

The locations of the roads have been burned into the DEM, meaning the DEM has been elevated on the place where roads are. This was done with the Deltares prototype Rapid Flood Model Tool.

Based on the final report of *Post-flood field investigation in the lower Chao Phraya River Basin* (Jonkman et al., 2012), the estimation for the elevation of the main roads is 3m and the secondary road 2 m.

6.2.2 Water system

Rivers location

The location of the rivers is determined with the program PCRaster, which is called from the Deltares prototype tool. PCRaster determines automatically the drainage network from the DEM, using a similar model like the D8 model (Tribe, 1992) that is described in section 3.2.

The basis for this method is that water flows downwards on the surface in the direction of the steepest slope. When each grid cell has a flow direction, the drainage network is determined. Each flow direction has an order number consigned with the number of converging flows.

When a flow direction has no flows converging into his flow direction, this flow direction is assigned the first order. Second order flow is when two first order flows converge into one flow and third order flow is when two second order flows converge.

The number of order of a flow direction increases if two of the same orders converge. In the case of a high and a low order converging, the resulted flow order is the same as the highest order of the converged flows, see Figure 6-4.

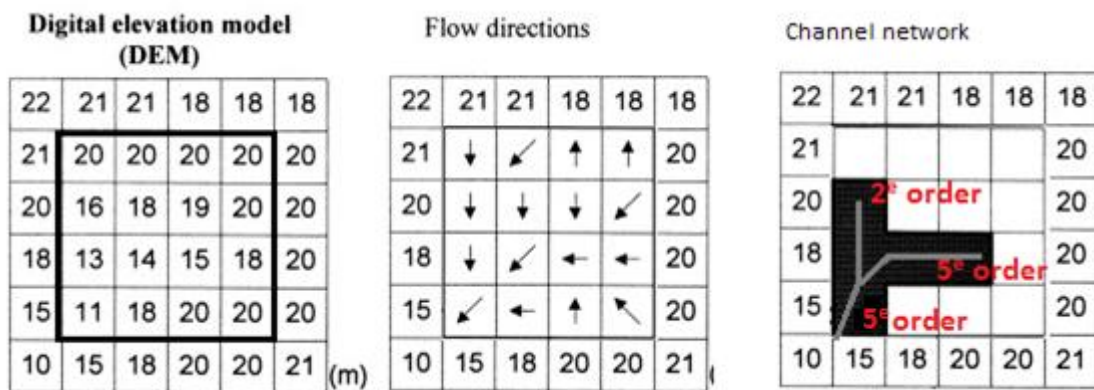


Figure 6-4 PCRaster uses the DEM to determine the flow directions and the drainage network

In the area of interest the amount of small rivers and channels is large. Figure 6-5 shows the river and stream network when chosen the five highest orders of the flow network. The rivers represent the 3 highest orders, while the streams are the 5 highest orders

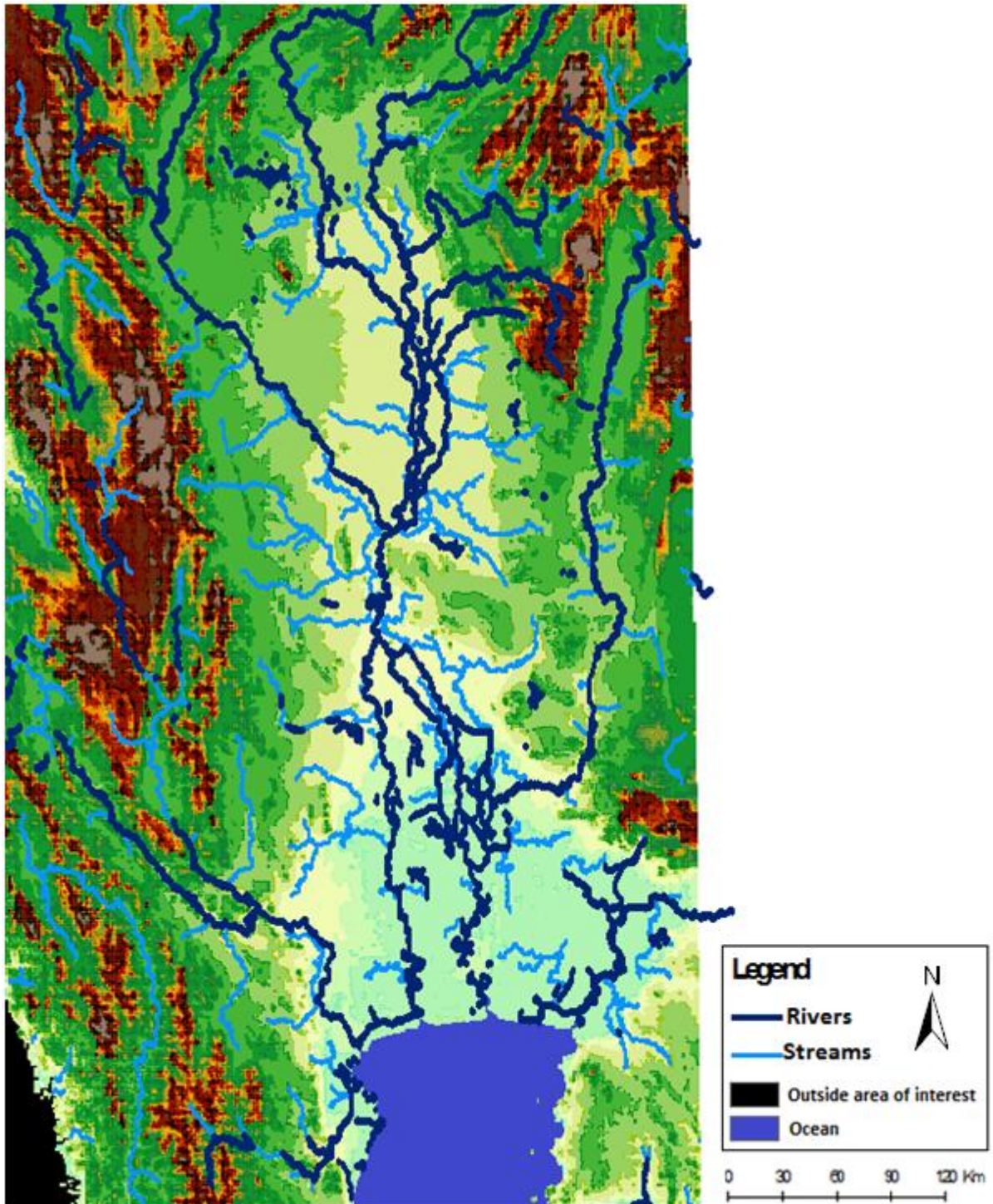


Figure 6-5 Rivers and streams determined with PCRaster

The choice here is to focus on the main rivers. For the simulation the three highest orders in the drainage network are chosen to be the river network. The locations of the rivers are validated visually by using OSM and Google maps.

River profiles

To determine rivers profiles, two methods have been used: the expression by Finnegan et al., 2005 and the Manning equation

To determine the width of the channels the expression from Finnegan et al., 2005 is used. For this equation the basis of the Manning equation and the basic mass conservation principles are used. The expression is:

$$W_i = [\alpha(\alpha + 2)^{2/3}]^{3/8} Q_i^{3/8} S^{-3/16} n^{3/8}$$

Where

W_i = Width of the river of river section i

α =width-to-depth ratio from classification of Rosgen, 1994 (50)

Q_i =discharge of river section i

S = channel slope (from DEM)

n =roughness coefficient

On average of 1 km for each river reach the width is calculated with this expression. The discharge depends on the order of converged flows into that point in the river reach determined by the PCRaster flow converging.

$$Q_i = A_{i,up}/A_{mapmaxup} * Q_{average}$$

$A_{i,up}$ = the total area converges to point i [m^2]

$A_{mapmaxup}$ = the total area converged [m^2]

$Q_{average}$ = annual average discharge [$170 m^3/s$ (Wikipedia)]

This expression makes sure that the points downwards of the river branches are wider than the upper point.

Similar approach is done for the depth of the rivers, but then using the Manning's equation and the maximum discharge.

$$H_i = \left[\frac{Q_i * n}{S^{0.5} * W} \right]^{3/5}$$

$$Q_i = A_{i,up}/A_{mapmaxup} * Q_{max}$$

H_i = Depth of the river of river section i

Q_{max} =maximum discharge [full bank discharge= $6000 m^3/s$]

With the expression of Finnegan et al., 2005 the rivers have profiles with a width and depth. The profiles are connected to the DEM, where the level of the DEM is the surface level and the level of the DEM minus depth is the bed level of the river.

River embankments

According to "The 2011 Thailand Floods Event Recap Report" (Impact Forecasting LLC, 2012) the embankments levels vary for each area. The industrial area has embankments up to 5 meters, while in other areas the embankment was less than 2.5 m. The DEM does not show any embankment due to the small size of the embankments. Because there is little information on where and where not the embankments are, two types of simulation are done, one simulation with and one without embankments. Both simulations are compared to the flood event and used to validate the inputs of the flood model.

To implement the embankments into the flood model, the depth of the rivers is adjusted. This is the same principle as was used in hypothetical case studies in chapter 4 and 5. By lowering the bed level of the rivers the implementation of the embankments in the flood model is simplified.

The alternative is to increase the tiles of the DEM around the rivers. But the size of the DEM tiles are 1 km/500 m, this would create a wall with the same size as the resolution of the DEM.

To validate the flood model inputs, two levels of the bed levels are simulated. The original bed level obtained from the expression from Finnegan et al., 2005 and a lowered bed level with 3 meters to simulated embankments along the rivers.

Ocean

One of the conclusions in chapter 5 is that the downstream boundaries have little influence on the flood extent, propagation and depth. But because this information is available online, the tidal data is used in the flood model.

The data used in this model is from the website from Hydrographic Department, Royal Thai Navy (<http://www.navy.mi.th/hydro/tide2011/BB2011H.xls>). The data are tidal charts for the Bangkok Bar from 2010 till 2013.

Any increase in the water level due to storm surges is not taken into account.

6.2.3 Precipitation

In this section the data for the precipitation and the methodology to implement the precipitation into the rapid flood model is discussed.

The methods are similar to the methods used to create the Hydro SHEDS products (Hydrological data and maps based on Shuttle Elevation Derivatives at multiple Scales). For Asia the Hydro SHEDS products were finished in March 2007 using the DEM of SRTM version 1 and 3.1. Since then the SRTM DEM has been updated to version 4.2, filling the voids and using improved interpolation techniques. For the rapid flood model the latest version of the SRTM DEM is used to determine the river network and also for the precipitation that flows into the river network.

Catchment areas

To determine the river locations, the PCRaster program is used to create a drainage network, which is considered now the river network. The three highest order rivers are chosen to be used as the rivers in the area of interest. As was explained in the previous section at River location, the lower order flows are not considered in the river network. When precipitation falls into these areas the water is drained towards the location of the rivers with the higher order. Therefore these lower order flows are considered the catchments areas for the higher order flows.

Figure 6-6 shows the 516 catchment areas (catchment polygons) with the related catchment points where the precipitation in the catchment area would come together. The precipitation that flows into these catchment points flow into another catchment area or into the river network. From the 516 catchment areas, 388 catchment points flow into the river network. These catchment points are considered a lateral inflow point for the rivers. The other 128 catchment points flow into another catchment area.

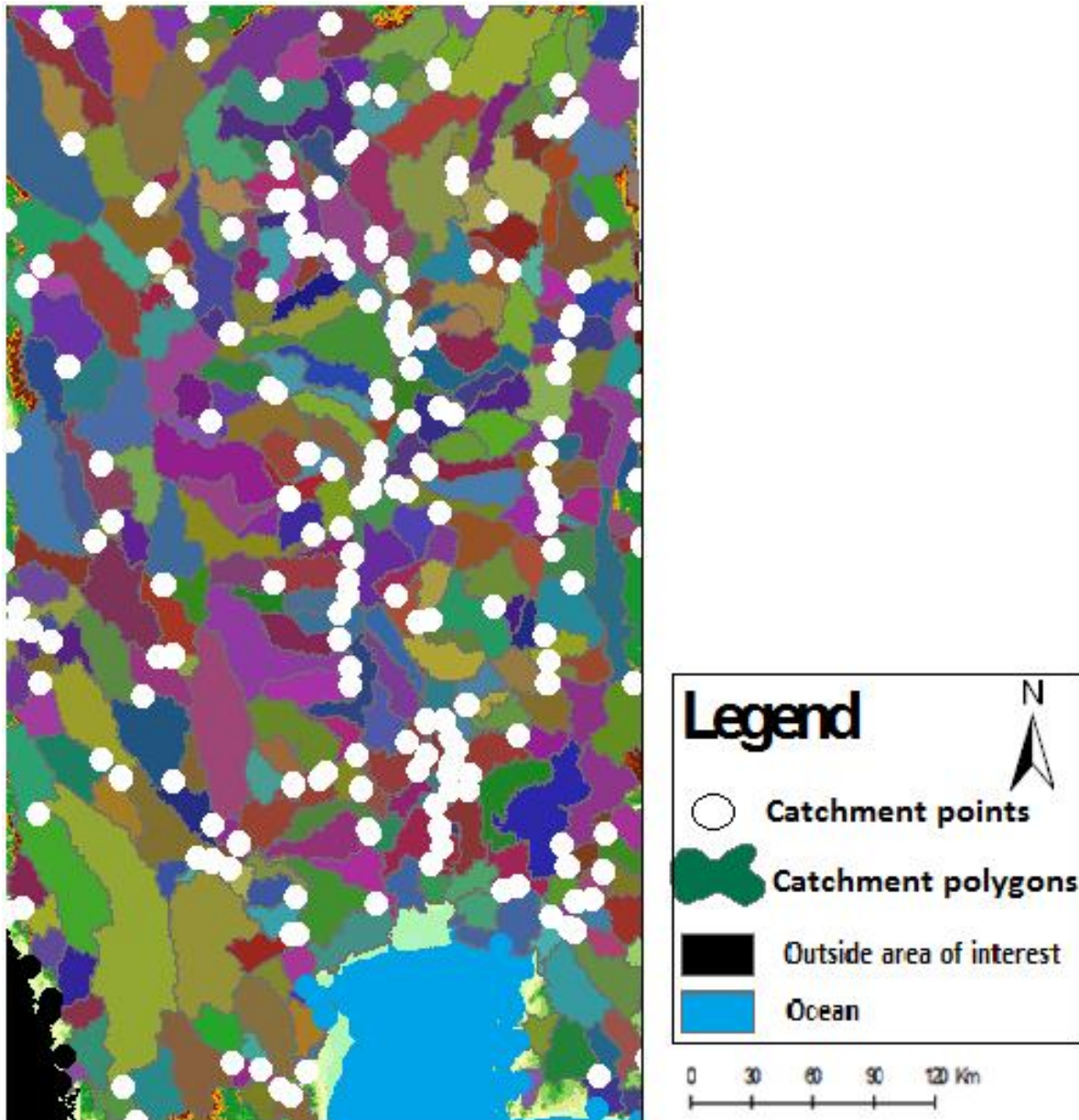


Figure 6-6 the area of interest divided into catchment areas. The catchment points are the points where the precipitation flows out of the catchment area into another catchment area or into the river . The total amount of catchment areas is 516.

The 388 catchment points are considered the lateral inflow points for the rivers. Each catchment point needs three types of information:

1. The surface area of the associated catchment area (catchment polygon).
2. The amount of precipitation in the associated catchment area.
3. The location of inflow into the river network.

This information is compiled with the use of ArcGIS.

The surface areas of the catchment polygons are connected to the associated catchment point. Each catchment point has the information on the total surface area that the flow would come from

The second information needed for each catchment point, is the amount of precipitation into a catchment area. The data used is GLDAS (Global Land Data Assimilation System) which provides among other information the precipitation data. The data are archived and distributed by the

Goddard Earth Science (GES) Data and Information Services Center (DISC) as part of the activities of NASA’s Science Mission Directorate.

The data can be downloaded from the website [http://hydro1.sci.gsfc.nasa.gov/thredds/catalog/GLDAS_NOAH025SUBP_3H/catalog.html] for the periods between 2000 en 2013. The data gives global three hourly outputs with a spatial resolution of 0.25 degrees (ellipsoid WGS-84). The data for the area of interest is downloaded and re-projected on the catchments area map (Figure 6-6). By re-sampling the GLDAS data from raster to the same shape of the polygons of the catchment areas, the total 3 hourly precipitation data for each catchment area is obtained.

The final step is to combine the surface area and precipitation in that area to catchment point. And the catchment point has the information on the size of the lateral inflow into the river network.

Precipitation data

The precipitation data from GLDAS contains three types of information that could be used for the flood model:

1. Rainfall rate
2. Surface runoff
3. Subsurface runoff

The rainfall rate is total amount of rain fallen into an area. The surface runoff is a percentage of rainfall rate that gets immediately runoff on the surface. The subsurface runoff is a percentage of the rainfall rate that infiltrates the ground and travels at shallow depths under the surface. Figure 6-7 shows the surface and subsurface runoff

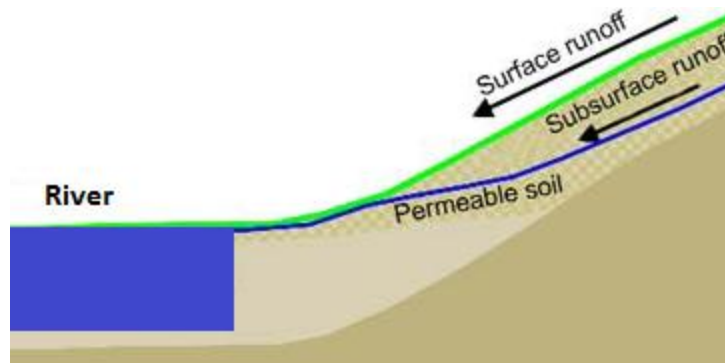


Figure 6-7 The relation between precipitation, surface and subsurface runoff

The rainfall rate is equal to the surface, subsurface runoff, the evaporation, the groundwater runoff and storage.

In chapter 2, Information for the simulation and prediction of a flood event, was decided not to consider a hydrological model. In a hydrological model amongst other things the infiltration and evaporation is taken into consideration.

Table 6-2 the rainfall runoff relation for the GLDAS data

	Rainfall runoff relation
min	0.39%
max	13.36%
average	3.22%

Instead only the three precipitation data types from GLDAS are used in combination with the rainfall-runoff relation. Annual evaporation losses are effectively constant, making the rainfall-runoff relation approximates a straight line(Pilgrim, 1983). The rainfall runoff relation depends on the amount of rain that falls. The more rain falls the higher the

percentage rain becomes surface runoff, varying from approximate 10% till 40%. For the GLDAS data the rainfall runoff relation is calculated by dividing the summed surface and the subsurface runoff by

the summed rainfall rate of six months for each catchment. Table 6-2 shows the minimum, maximum and average rainfall runoff relation from all the 388 catchments.

The values in table 6-2 are very low relative to the rainfall-runoff relation that approximates a straight line (Pilgrim, 1983). Therefore three types of precipitation are used to validate the inputs of the flood model. The 40% rainfall-runoff relations is an assumption.

1. Rainfall rate
2. Summed surface- and sub-surface runoff
3. 40% of rainfall rate

6.2.4 Overview of available data

In the previous sections the publicly available data for the rapid flood model to simulate the 2011 Thailand flood event are discussed. In Figure 6-3 an overview is shown for the information needed, the sources and the methods and equations formatting the data for the rapid flood model.

Table 6-3 Overview of publicly available data, sources and the tools to format the data for the rapid flood model

	Information needed	Source	Information from the source	Tools formatting data	Data for rapid flood model
Topographic information	Elevation	SRTM ¹	DEM (30 m grid size)	Wavefilter Resampling	DEM grid sizes: 1 x 1 km 500 by 500 m
	Land use	Souris, 2011 ²	Land use and forest cover map	Design values, McCuen, 2005	Manning roughness coefficient
	Line elements	OSM ³	Roads		Main roads Secondary roads
Water system	River location	SRTM ⁴	DEM (30 m grid size)	PCRaster D8 model, Tribe, 1992 Classification, Rosgen, 1994	River network
	River profiles	Wikipedia ⁵	Maximum and average discharges	Finnegan et al., 2005 Manning equation Classification, Rosgen, 1994	Width Depth
	River embankments			Assumptions	Along all rivers 3 m height
	Ocean conditions	Thailand navy ⁶	Tidal chart		Water levels
Precipitation	Catchment areas	GLDAS ⁷	Catchment areas	PCRaster	Lateral inflow points into river network
	Precipitation data	GLDAS	Rainfall rate Surface runoff	Rainfall-runoff relation, Pilgrim, 1983	40% Rainfall rate Surface runoff

¹ <http://dds.cr.usgs.gov/srtm>

² <http://www.rsgis.ait.ac.th/~souris/thailand.htm>

³ www.openstreetmap.org

⁴ <http://dds.cr.usgs.gov/srtm>

⁵ http://en.wikipedia.org/wiki/List_of_rivers_by_discharge

⁶ <http://www.navy.mi.th/hydro/tide2011/BB2011H.xls>

⁷ http://hydro1.sci.gsfc.nasa.gov/thredds/catalog/GLDAS_NOAH025SUBP_3H/catalog.html

6.2.5 Validation methodology and validation data

To be able to compare the simulated flood event with the real flood event, two methods are used.

The first method is to use satellite images to compare the extent of the flood and the propagation of the flood in the area in time.

The second method is to compare the discharges in the river of the simulation and the real event. These two methods are used to validate the simulated flood event.

Satellite images

The satellite images that are used to validate the flood model have been processed by UNITAR/UNOSAT with ArcGIS into a flood map. UNOSAT is a program of the United Nations Institute for Training and Research (UNITAR). The satellite data are a product of MODIS Aqua & Terra and NASA Rapid Response. The map presents a time series of the progression of flood waters from the central provinces of Thailand towards the capital city of Bangkok. The satellite data used for this are recorded from mid-August to mid-November 2011.

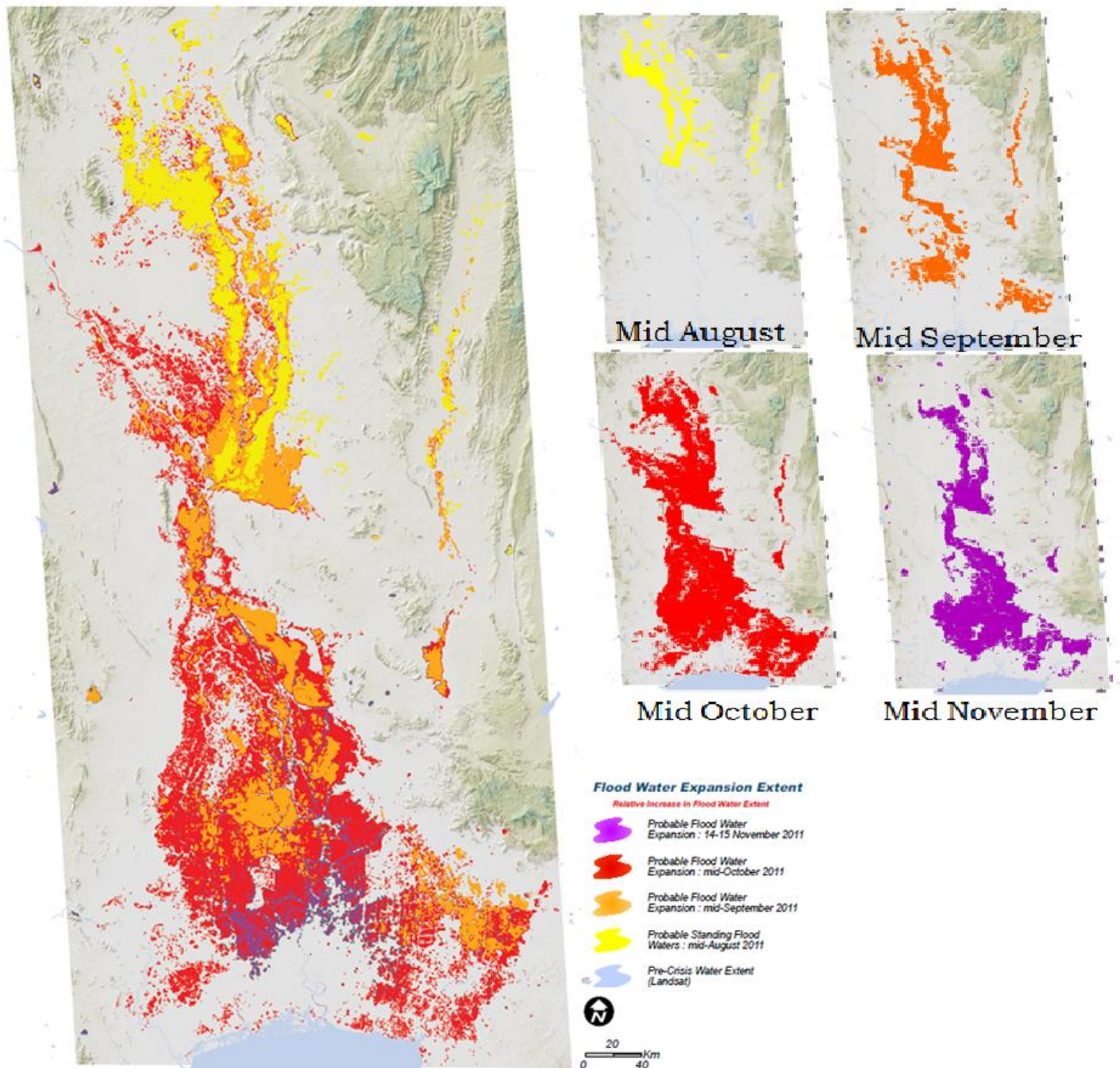


Figure 6-8 The flood extent and propagation from August till November 2011 (UNITAR_UNOSAT, n.d.)

The map in Figure 6-8 shows the flood extent for each month in a different color. These flood extent maps are layers on top of one another. With use of Adobe Illustrator the layers for the flood extent are separated and processed with ArcGIS to be used as validation maps. In the Appendix the maps for the flood extent for each month can be found.

Discharges in rivers:

The discharges for the rivers are, as is discussed in chapter 3, hard to obtain. The annual average and maximum discharges are available for the Chao Phraya River, but not for the other rivers in the river network. In addition the discharges during the flood are not available at the moment the rapid flood model needs to be used (during or before a flood occurs).

Nevertheless, this flood event has happened more than a year ago. There are several studies on this flood. One of the studies is from Deltares. Their model has been calibrated and validated. Only for the validation of this rapid flood model, the data from this model is used. This model gives for eleven rivers locations the discharge during the period August to November. Figure 6-9 gives the locations of the eleven river sections where the discharges are obtained from the calibrated and validated model of Deltares.

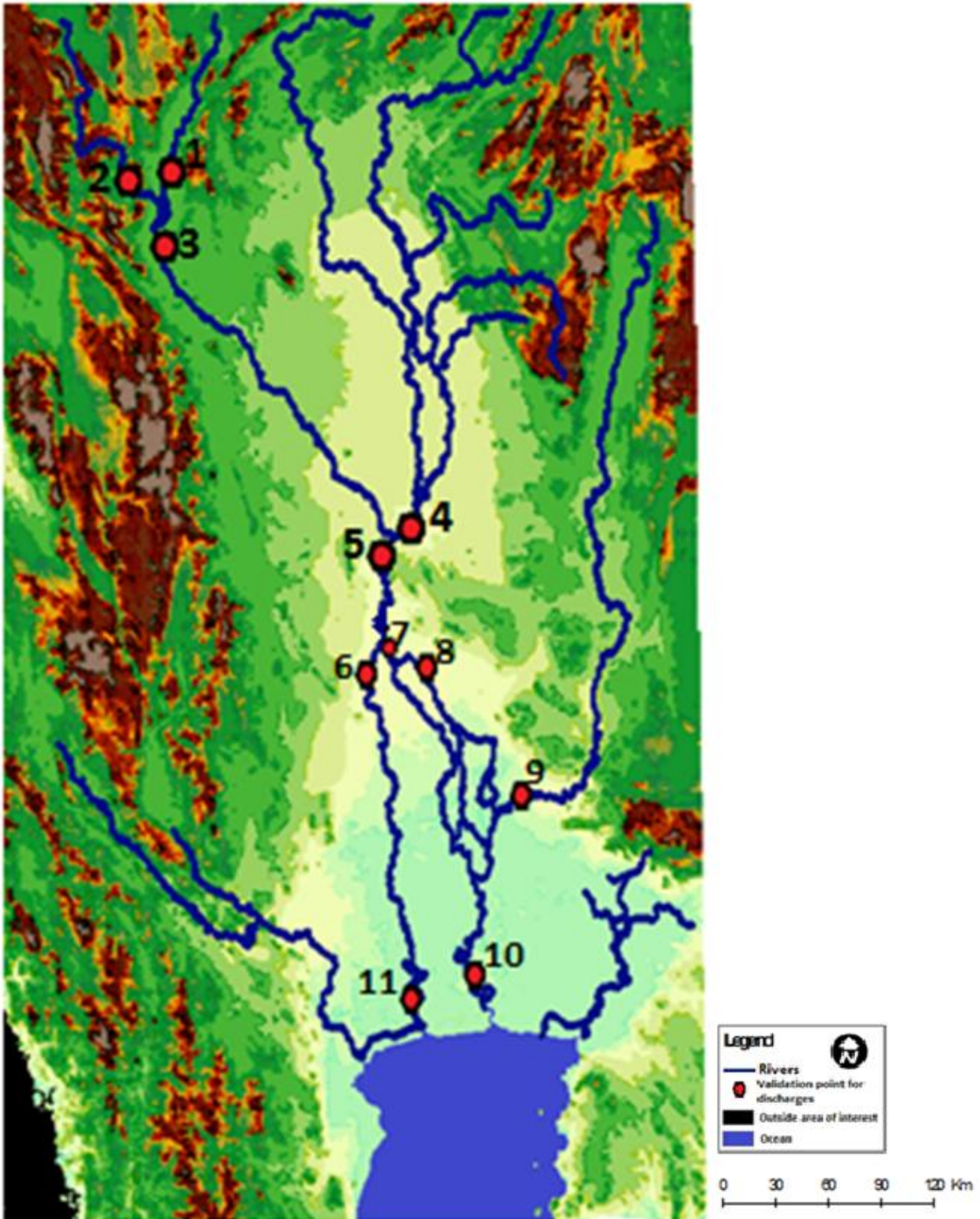


Figure 6-9 Map of the area of interest with the eleven places where the discharges are known

The discharge data will not be used to calibrate the model, only to validate the flood model. The objective of this study is to analyze the accuracy of a rapid flood model when using publicly available data. Therefore we assume in this case study that there is no data available to calibrate the model and only use this data to determine the accuracy of the used flood model.

The discharges from the model of Deltares are not considered as measured data. The comparison is done if differences are found in the simulated and the validation flood map, that can be explained by the selected data used for the simulation. In that case the discharges are compared relatively.

6.3 Selection of input data

6.3.1 Introduction

In the previous section the data for the input of the flood model are discussed. The input data for the flood model are schematization of the model and also flood characteristics. For some of the input there are multiple data sources or methods available to use for the flood model. These are the data options available:

- DEM
 - o Grid size
 - 1 km
 - 500 m
 - o friction
 - Constant: $n=0.04$
 - The land use and forest cover map (Souris, 2011)
 - o Roads
 - Only main roads
 - Main and secondary roads
- River profiles
 - o Bed level
 - Expression of Finnegan et al., 2005
 - Smoothed river beds
 - o Embankments
 - No embankments
 - Lowered bed level (3m)
- Precipitation
 - o Rainfall rate
 - o Sub- and surface runoff
 - o 40% of rainfall rate (rainfall runoff relation)

To be able to choose the right data source or method as input for the flood model, all combinations are simulated with the flood model for the period 1 July to mid-August. The flood extent map of mid-August is intended to serve as a validation map. The best combinations of the inputs selected from the list above are used to simulate the period of mid-August. The selection will be done visually by comparing the flood map derived from satellite images and the simulated flood map. Figure 6-10 shows the flood extent derived from the satellite image for mid-August.

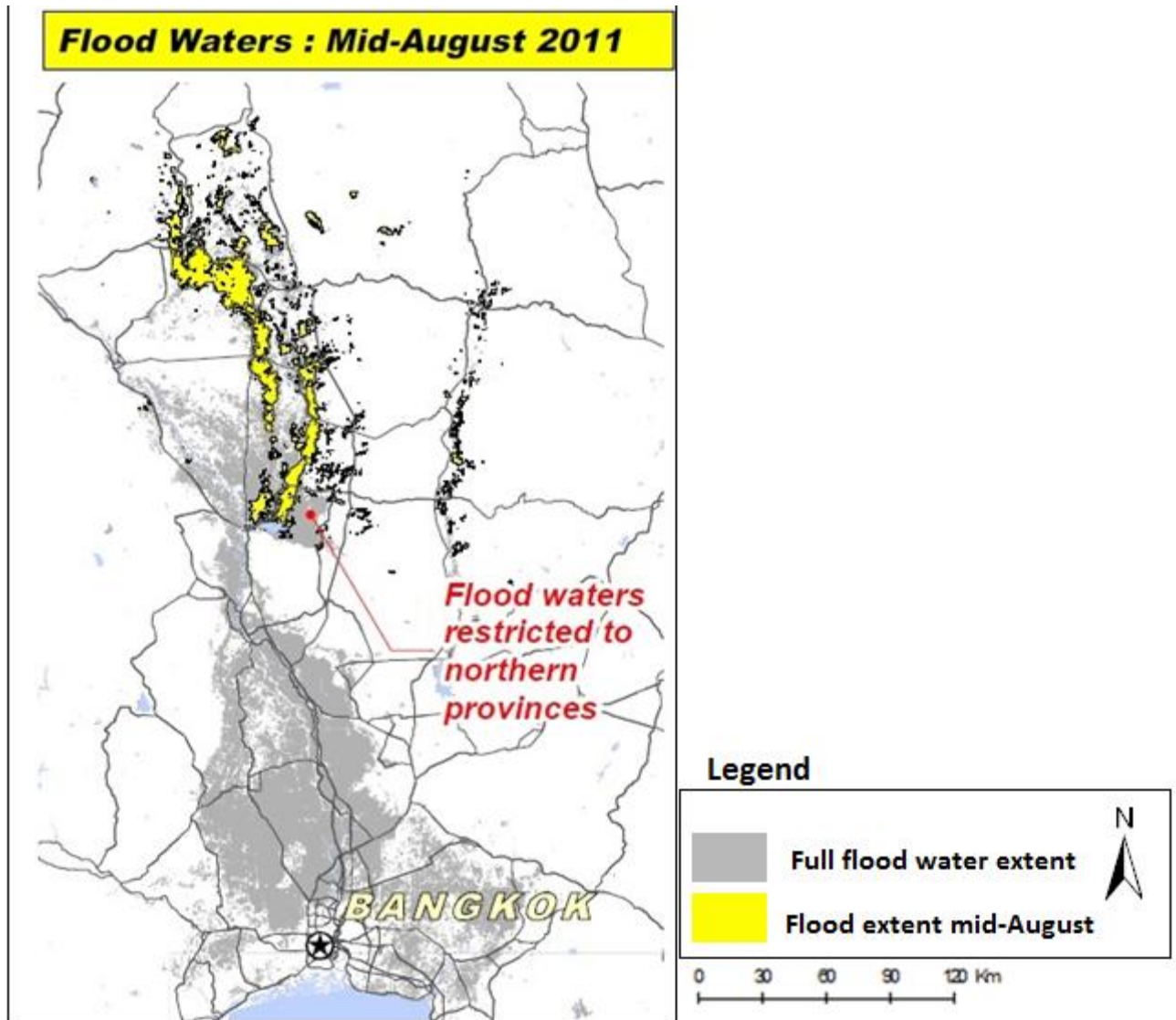


Figure 6-10 Flood extent in yellow for mid-August

The flood map derived from the satellite image for mid-August (Figure 6-10) shows that during this period the flood covered the north part of Thailand. It appears that the two rivers in the middle in the north are flooded.

For all the simulation with the varying input data, flood maps have been made to compare with the flood extent map of mid-August.

6.3.2 Selection of the data sources

In this section the different data for the inputs of the flood model, that are selected, are discussed.

DEM

The varying DEMs that can be used as input for the flood model have all been simulated. These are the selected options made for the DEM:

- Grid size: 1 km
- Friction: Land use and forest cover map (Souris, 2011)
- Roads: Main and secondary roads

Here below the motivation for the selected option are discussed.

The choice for which grid size to use, is based on the computation time of the simulations. With the use of 1 km the simulation for the period 1 July to mid-August took 1 hour and 30 minutes. With a grid size of 500 meters the simulation time increased with 9 hours. As this study is based on a rapid method to create a flood model, the grid size of 500 meters for this area takes too much computation time. The choice is to use the grid size that is less accurate but can be simulated in shorted amount of time.

The friction input for the DEM has two options, constant over the entire area or friction derived from the land use and forest cover map. The difference between the simulations with these two friction data is that with a constant friction, the water depth in the flood plains was larger and the propagation of the flood was faster. By comparing the flood extent maps from the simulations with the validation map of the mid-August flood extent, the simulation shows a good fit. The flood extent map simulated with the friction derived from land use and forest cover map, covered slightly more of the validation map of the mid-August flood extent.

Therefore the simulations for the other periods the friction derived from the land use and forest cover map is used.

Implementing the roads into the DEM shows an improvement of the flood extent map. Figure 6-11 shows flood extent for the simulations with and without the main road elevation of 3m, compared to the validation flood extent map of mid-August.

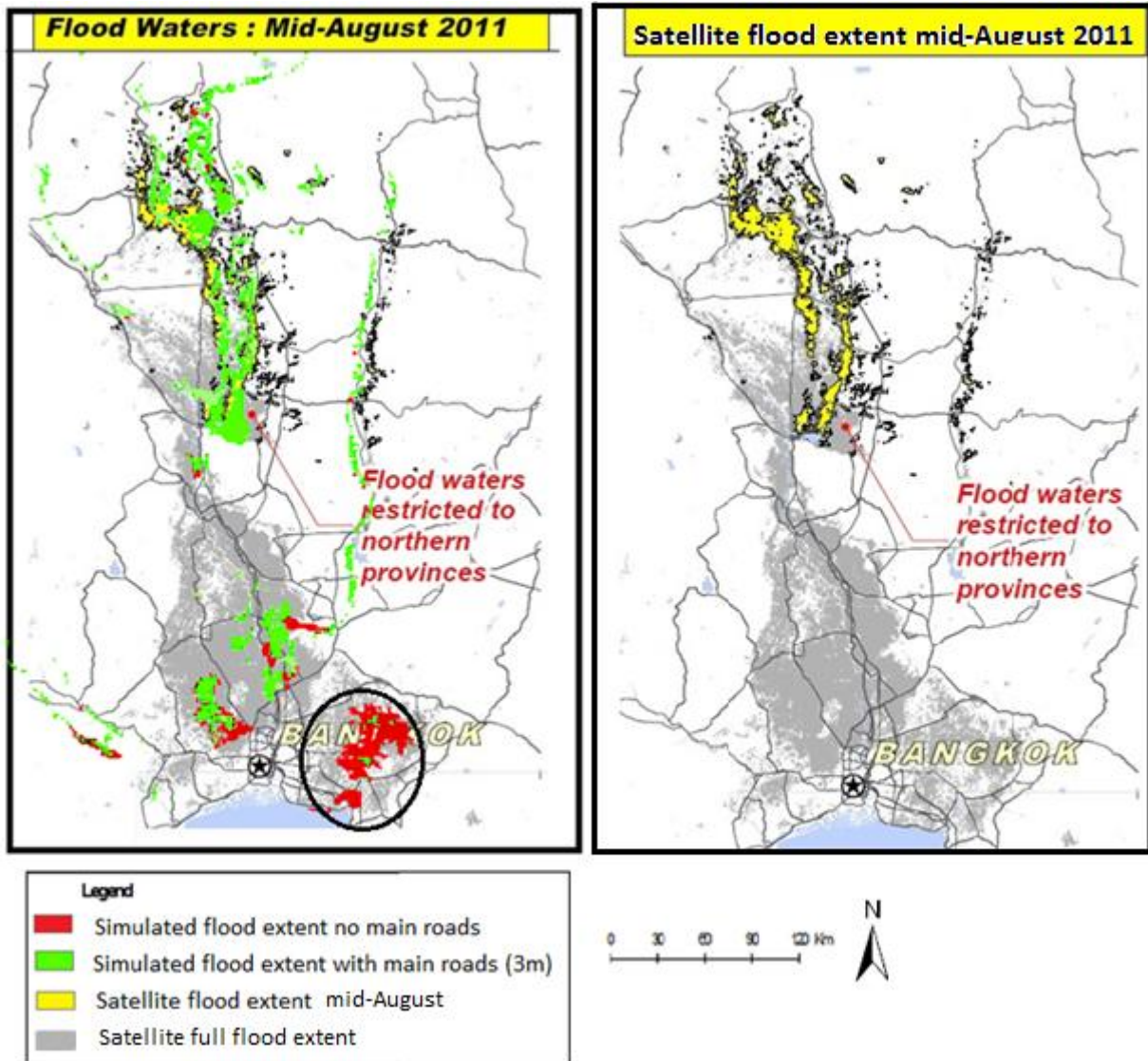


Figure 6-11 Flood extent for the simulations with and without main road and the validation flood extent map mid-August

In the north of Thailand the simulated flood extent with and without the main roads are similar. But in the south east, the simulated flood without the main roads causes flooding, which are not visible in the satellite image. This area is indicated with the black circle.

By implementing the main roads into the DEM the flood waters east of Bangkok are decreased. In the flood validation map (in yellow) this area is not flooded during August. By including the main roads the flood map fits better with the satellite map.

The implementation of the secondary roads shows hardly any differences for the flood extent during mid-August. But Figure 6-3 shows that the locations of the secondary roads are more concentrated in the south. The flooded area during mid-August is mainly in the north provinces of Thailand. During later periods this water starts to travel towards the south. The elevated line elements, like the secondary roads will have an influence on the propagation of the flood towards the south. Therefore the secondary roads are implemented into the DEM.

River profiles

The varying profiles that can be used as input for the flood model have all been simulated. These are the selected options for the profiles

- Bed level: Smoothed river beds
- Embankments: Lowered bed level (3m)

Here below the motivation for the selected option are discussed.

The profiles are derived from the expression of Finnegan et al., 2005. These profiles are submerged with the DEM, making the bed level of the rivers equal to the DEM level. This leads to problem in the flow direction of the rivers. At certain successive cross sections the slopes are extremely high. Figure 6-12 shows an example of bed levels before and after smoothing. The smoothing of the bed levels are done manually.

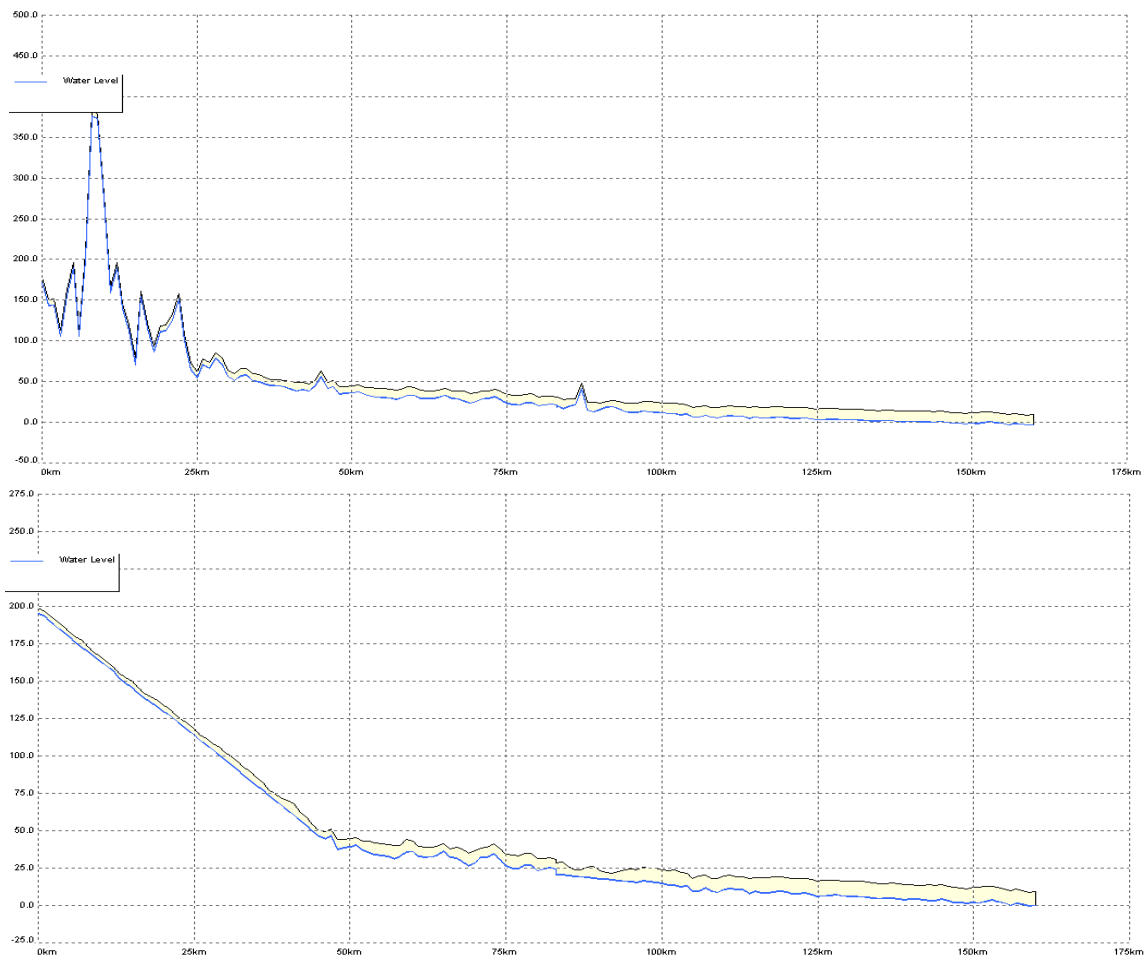


Figure 6-12 Side view of a river section before (upper view) and after smoothing (lower view)

Without the smoothing of the river bed levels, the water will build up at certain cross sections where the bed level of the following cross section lays much higher. This can lead to unrealistic high waters in the rivers. And in reality rivers do not have uphill jumps of 200 meters over a length of 5 km. Therefore the smoothed river profiles are selected as best option.

The simulations with no embankments show a flood extent that is not found in the validation map of mid-August, this area lays in the north-west, indicated with black circle. When implementing the embankments by lowering the bed level with 3 meters, the simulation of the flood extent is similar to the satellite map. Figure 6-13 shows the flooded areas with and without the implementation of the dykes.

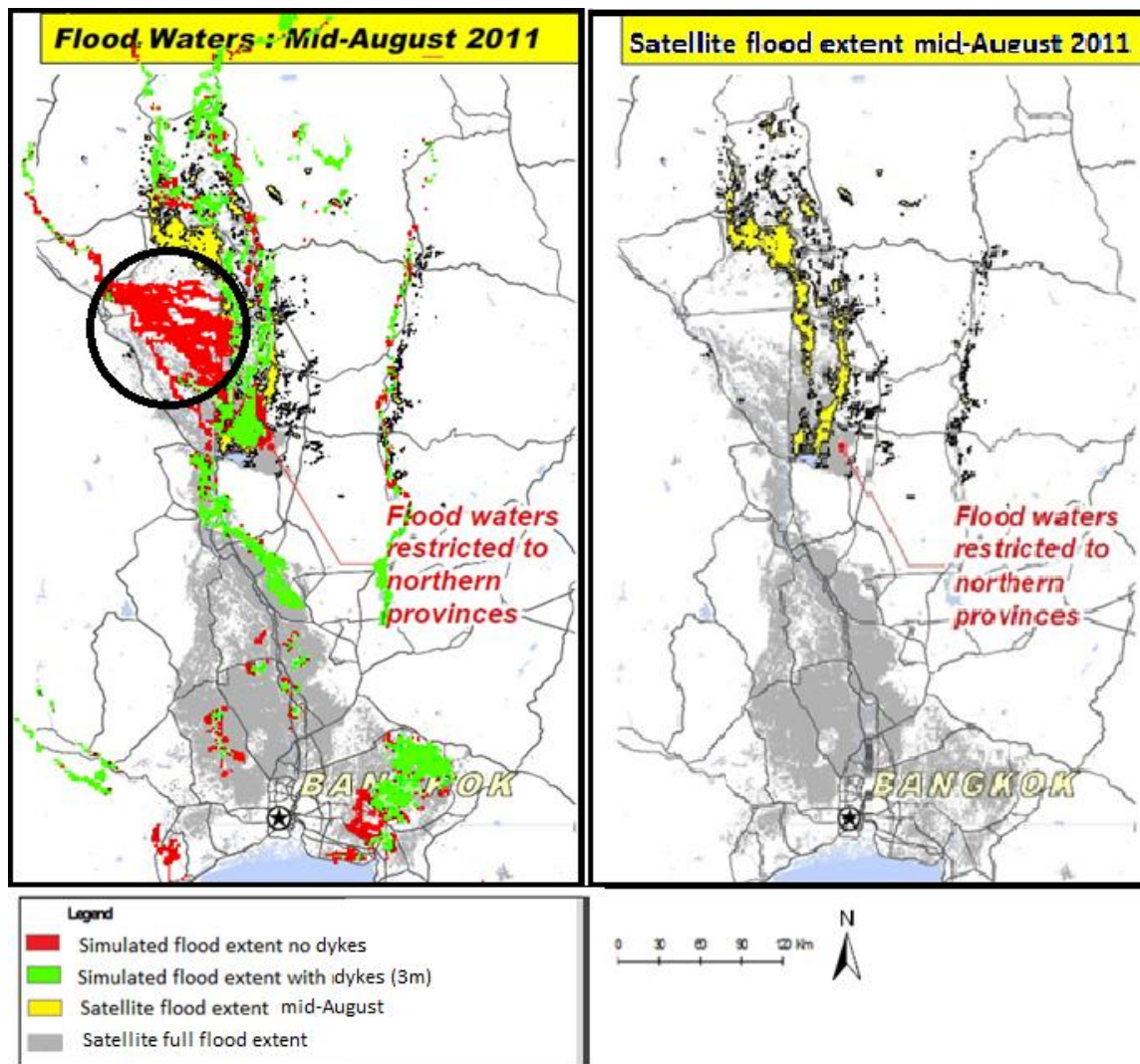


Figure 6-13 Flood extent for the simulations with and without dyke implementation and the validation map of mid-August displayed as layers on top of the area of interest.

As is shown in Figure 6-13 the simulation with the dyke implementation is a better fit for the validation map of mid-August.

Precipitation

The different options for the precipitation data that can be used as input for the flood model have all been simulated. The best results are obtained when using the following precipitation data:

- Precipitation: 40% of rainfall rate (rainfall runoff relation)

Here below the motivation for the selected option is discussed.

The flood map with the data from the rainfall rate showed an extreme large area flooded. Comparing this map to the validation map of mid-August, the conclusion is that the total amount of precipitation from the rainfall rate data is larger than what happened in the real event.

The sub- and surface runoff data for the precipitation, in contrast with the data from the rainfall rate, was too little. There were only small areas in the north flooded due to sub- and surface runoff.

The 40% of the rainfall rate data (rainfall-runoff relation) is the best fit in comparison to the other data. Figure 6-14 shows the flood maps for the three precipitation data in comparison the validation map of mid-August.

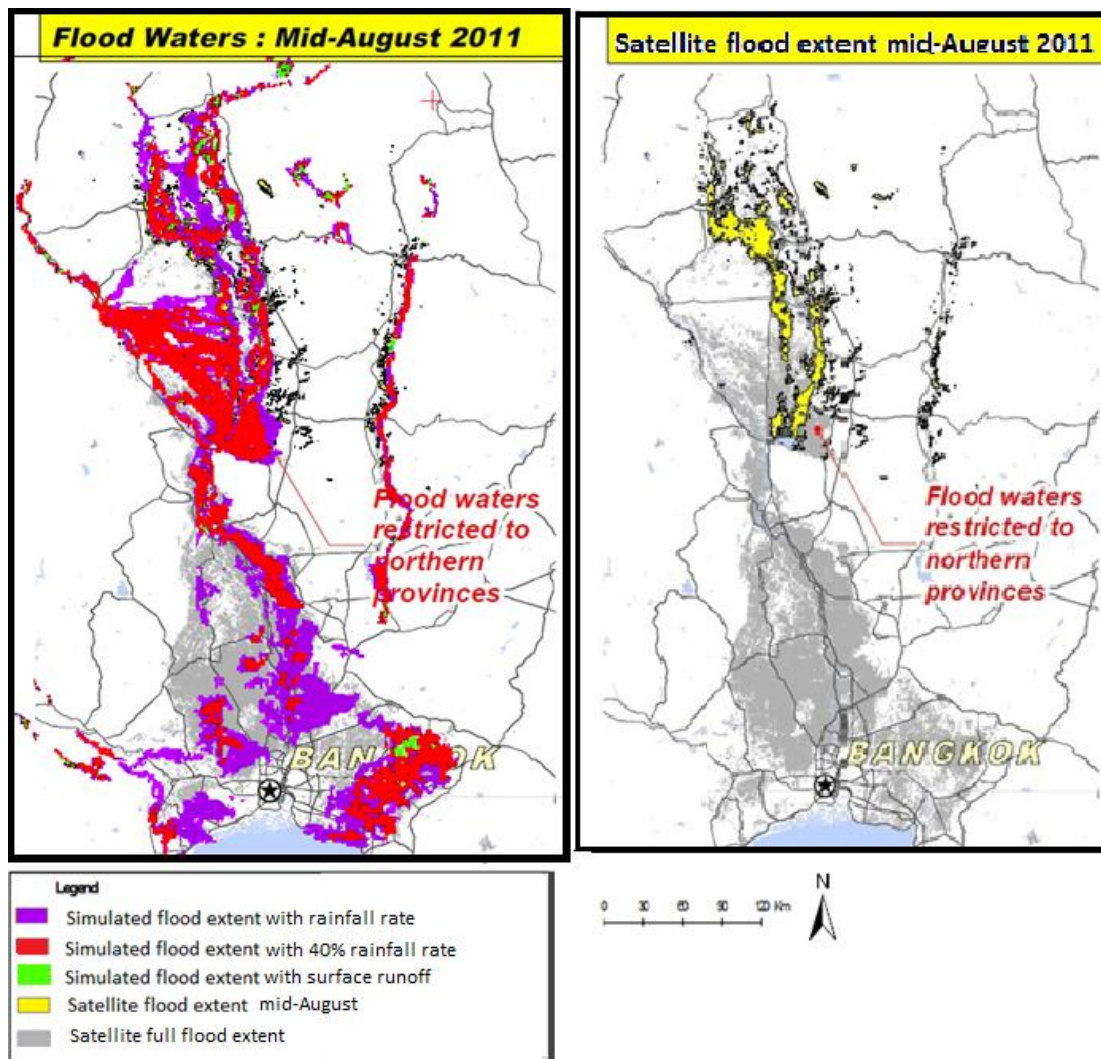


Figure 6-14 the flood extent map for the simulations with three precipitation data inputs and the validation map of mid-August, as layers on top of the area of interest.

6.3.3 Simulation with the combined selected data

From all the available data for the input of the flood model, these data are the best to fit with this flood model the flood extent for mid-August:

- DEM
 - o Grid size: 500 m
 - o Friction: Forest map (Souris, 2011)
 - o Roads: Main and secondary roads
- Profiles
 - o Bed level: Smoothed river beds
 - o Embankments: Lowered bed level (3m)
- Precipitation
 - o 40% of rainfall rate (rainfall runoff relation)

With these data as input for the flood for mid-August is simulated. Figure 6-15 displays simulated flood extent.

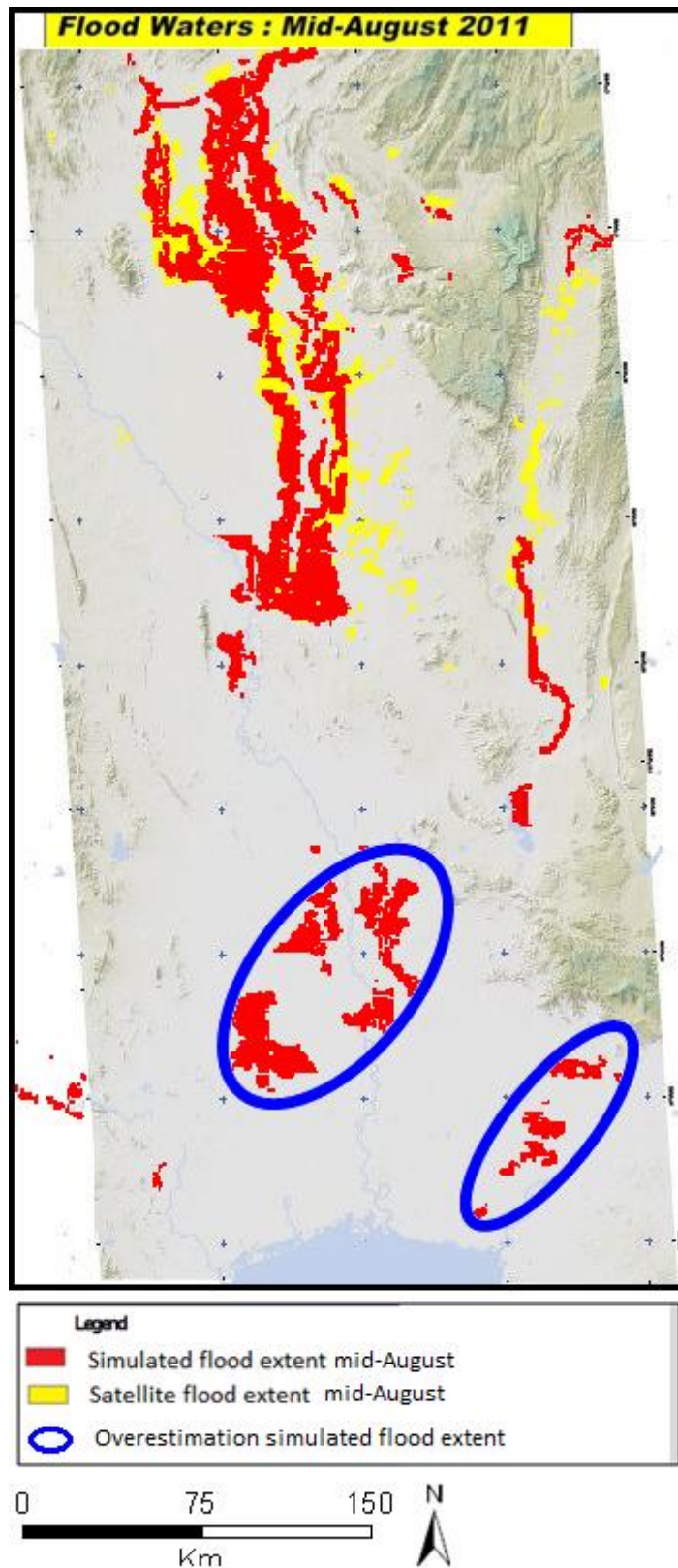


Figure 6-15 map of the simulated flood extent of mid-August is the red layer. The flood extent map from satellite image is the yellow layer. In blue circles the excessive simulated flood extent.

The flood extent fits the flood map derived from satellite image relatively good. Except for in the south, where there are flooded areas that not appear in the map derived from the satellite images. These excessive flooded areas are circled in blue in Figure 6-14.

6.4 Results of the rapid flood model for the three month period

The period from mid-August to mid-November have been simulated with the selected data from the previous section. For each month a flood map is made and will be compared to the flood map derived from the satellite image. Besides checking the fit of the flood extent maps visually, the discharges obtained from the calibrated and validated flood model of Deltares are also compared. The results are discussed for each month separately.

The flood maps from the simulations are not expected to fit the satellite images exactly, but the focus will be on the major differences and similarities between the two maps.

6.4.1 Simulation for mid-September

The flood map for the simulation of mid-September overlaying the flood map of the satellite images, is shown in Figure 6-16.

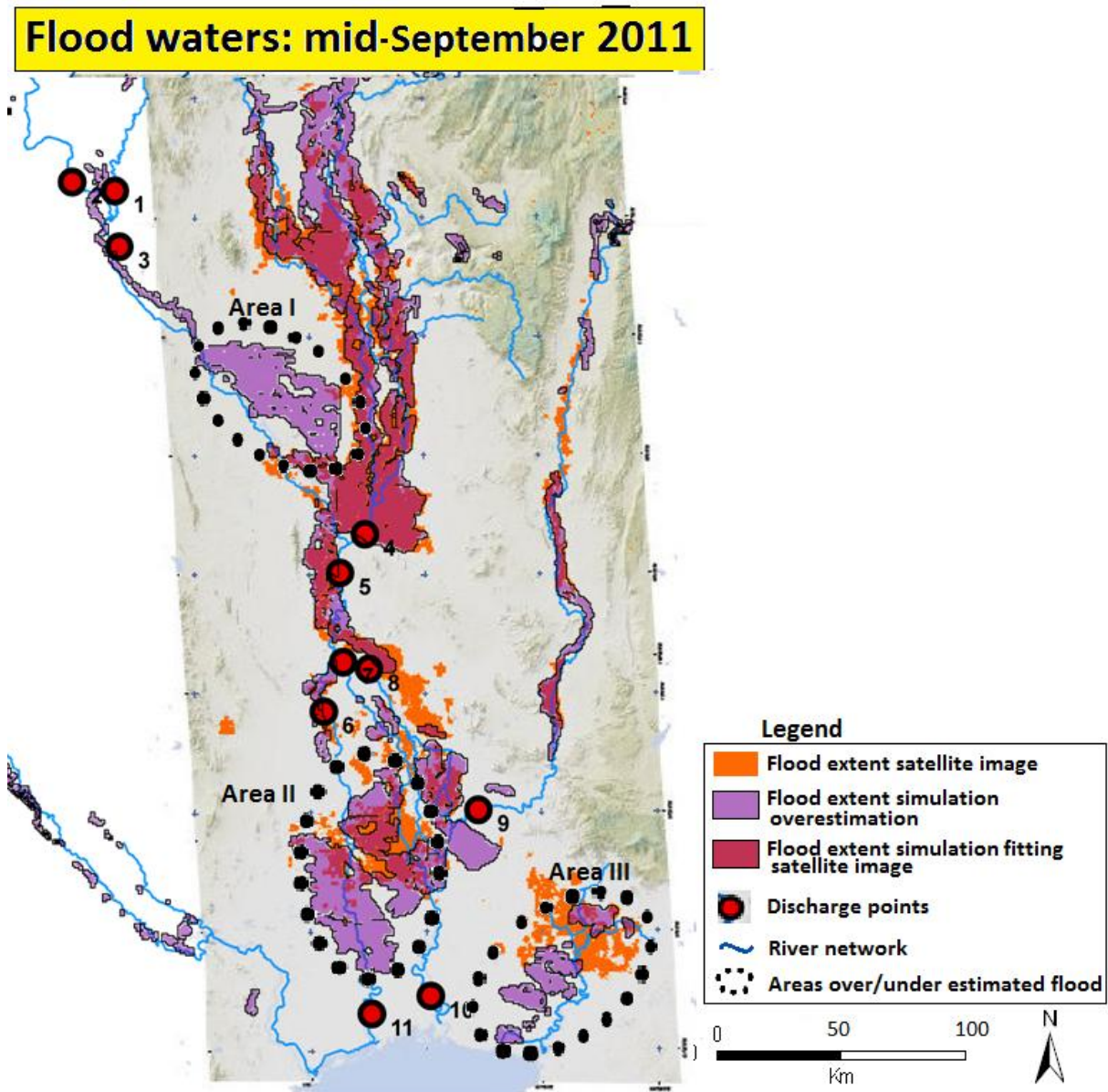


Figure 6-16 Flood extent map for mid-September of the simulation (in purple) and of the satellite image (in orange). In the black dotted circles are the three areas where the simulated flood exceeds the actual flood.

The flood map is reasonable good fit with the actual flood map. There are three areas where the simulated flood exceeds the satellite image. In areas I and II the flood is overestimated and in area III underestimated. By looking at points where the discharges are known in those areas, it can be determined if the overestimated areas are caused by wrong discharges in the flood model. In the Appendix the discharges of the rapid flood model and the calibrated and validated model of Deltares for all discharge points are presented.

Area I in the north west

In area I the simulation overestimates the flood extent. To be able to see if the discharges have an influence on the overestimation in area I, the up- and downstream discharge point in area I are compared. The upstream discharge points are 1, 2 and 3 and the downstream discharge point is 5.

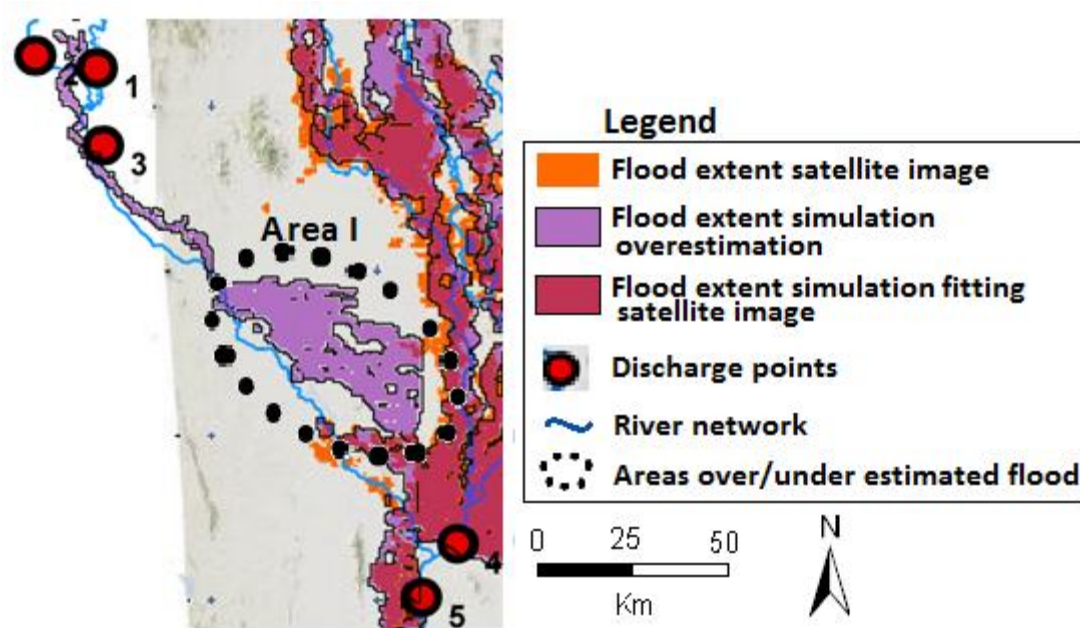


Figure 6-17 Overestimated flood in Area I

The graphs for the discharge points for area I from mid-August to mid-September are in Figure 6-18.

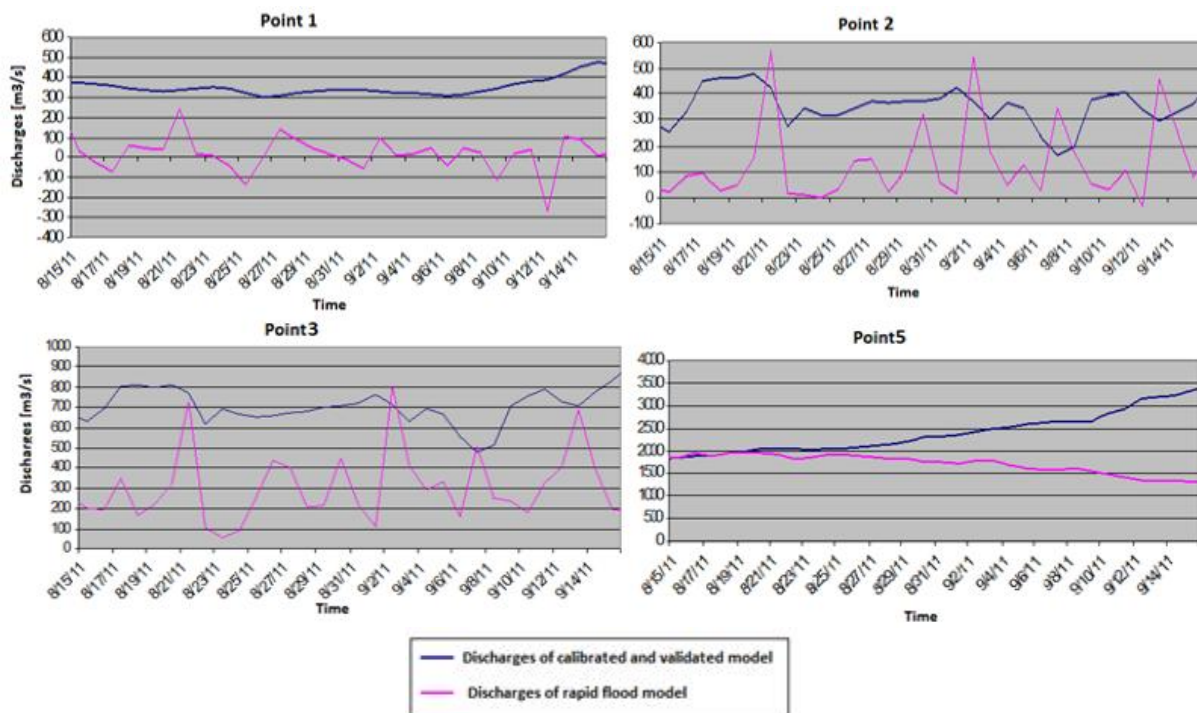


Figure 6-18 Discharges for the points 1,2 ,4 and 5 in the area I

In the upstream points, 1,2 and 3 the discharges in the rapid flood model are significant lower compared to the flood model of Deltares.

In the downstream point 5 the discharges start similar but as the discharge of the rapid model declines, the discharge of the flood model of Deltares increases.

The lower discharges in the rapid flood model can be explained by smaller the cross-sections. With smaller cross sections, lower discharges can cause an overestimation of the flood extent. The amount

of discharge that goes over the land is not known. This means that the total amount that was supposed to go through the river can be the same, but in the rapid flood model some of the water goes over land instead of going through the river.

The overestimated flood in area I indicates that the cross section derived from the expression of Finnegan et al., 2005 in this part of river network are underestimated.

In the point 1,2 and 3 are close to two catchment points. The lateral inflow from these catchment points makes the discharges in these points jump in sort amount of time. The discharges in point 2 in Figure 6-18, around 20 of August, show a jump from 50 m³/s to 550 m³/s. These high jumps in the discharges can be explained by the lack of delay in the precipitation. The precipitation that falls into the catchment area is immediately the lateral inflow into the river network. Real precipitation would have a certain delay and this would depend on the land use of the area. The land use in the rapid model is expressed in a roughness coefficient. However in the rapid flood model the roughness coefficient is only taken into account for the flood waters and not the precipitation.

Area I is also analyzed whether the other selected parameters to be derived from the data sources have influence on the overestimation of the flood. The locations of the main roads and secondary roads are checked in area I. Along the river in area I, the main road is located on the west of the river in the model. When this area is examined on Google maps, along the east side of the river another road is found which is not included into the DEM. It is not clear if this road is elevated but this could explain the flooded being only on the east side of the river in area I.

The overestimated flood extent in area I can be explained can be the result of significant smaller cross section and the lack of delay in the precipitation and the lateral inflow.

Area II in the south west

The two discharge points in the area II are point 6 (upstream) and point 11 (downstream). Figure 6-20 shows the discharges in point 6 and 11.

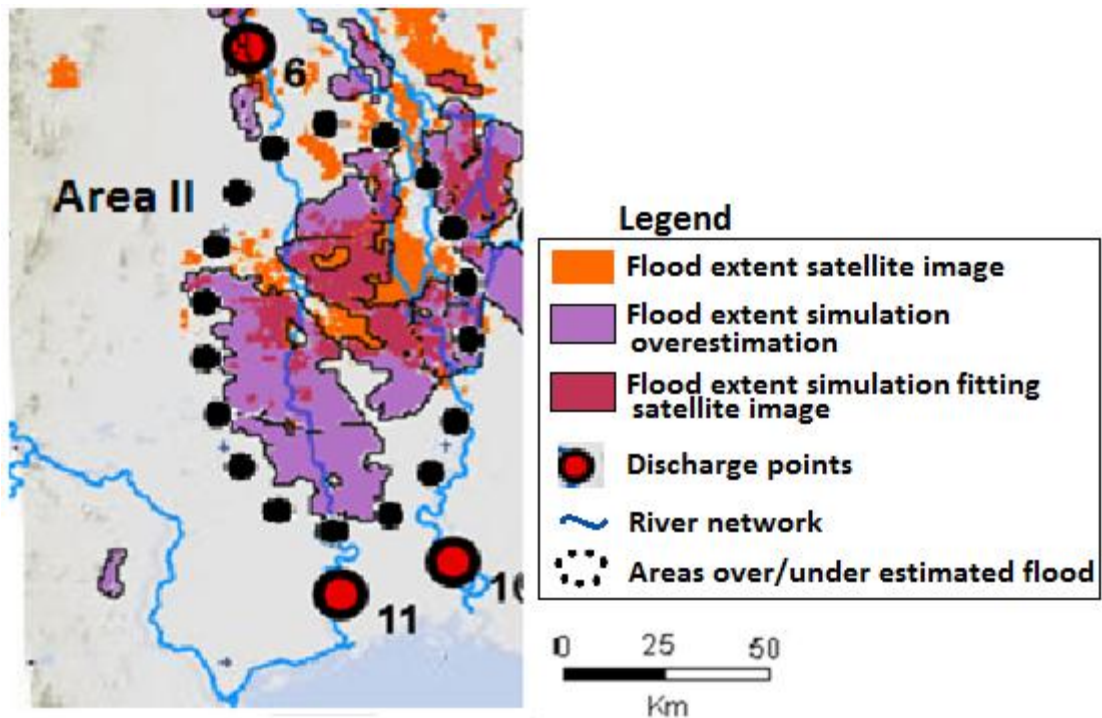


Figure 6-19 Overestimated flood in area II

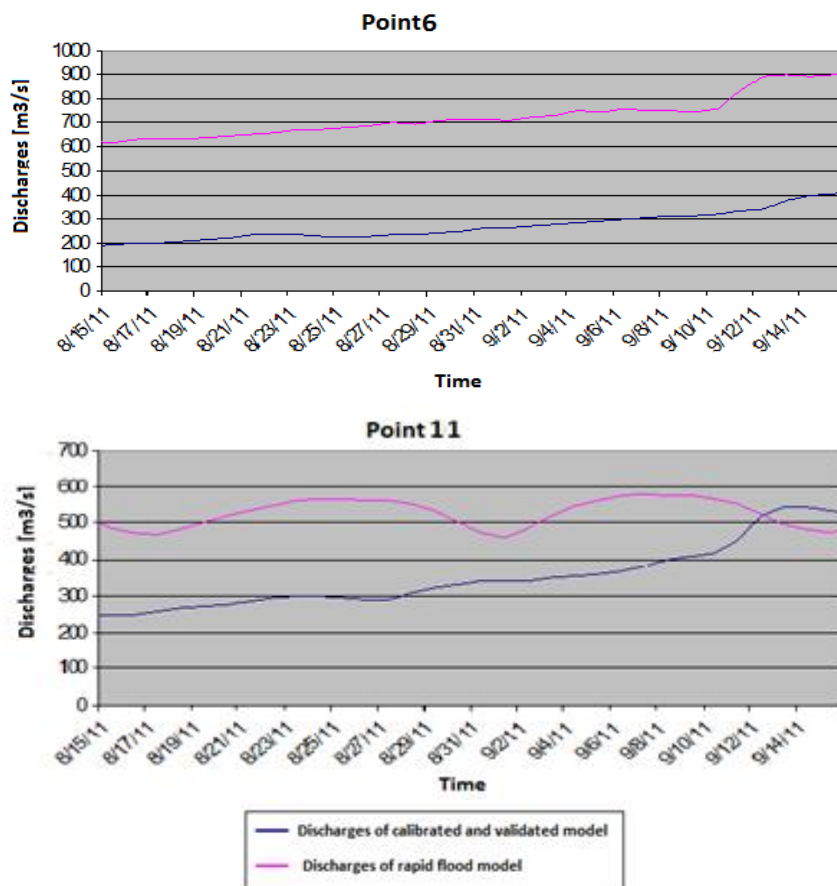


Figure 6-20 Discharges for point 6 and 11 in the area II for mid-September

The discharges in the rapid flood model in area II are larger than in the flood model of Deltares. The discharges in point 5 (Figure 6-18), upstream from point 6, are lower than in point 6. This means that between point 5 and 6 the lateral inflow from the catchment areas is so large that it increases the discharge in this part of the river network that causes flood overestimation.

The discharges in point 11 of the rapid flood model are higher and stay relative constant, while the discharge in the flood model of Deltares slightly increases in time. This indicates that the instant inflow of the precipitation in the catchment areas into the river network is not correct. The time that the precipitation in a certain catchment area needs to travel towards the river network is not taken into account.

The overestimation of the flood extent in area II can be the result of not including any delay into the time of precipitation and the time of inflow into the river network.

Area III in the south east

For area III there is no discharge point that can be compared with the simulated discharge. The flood extent from the simulation comes from the rivers, and not from flooded area upstream. This means that the water does not travel over the land. This exceeded flooded area can be explained with Figure 6-21.

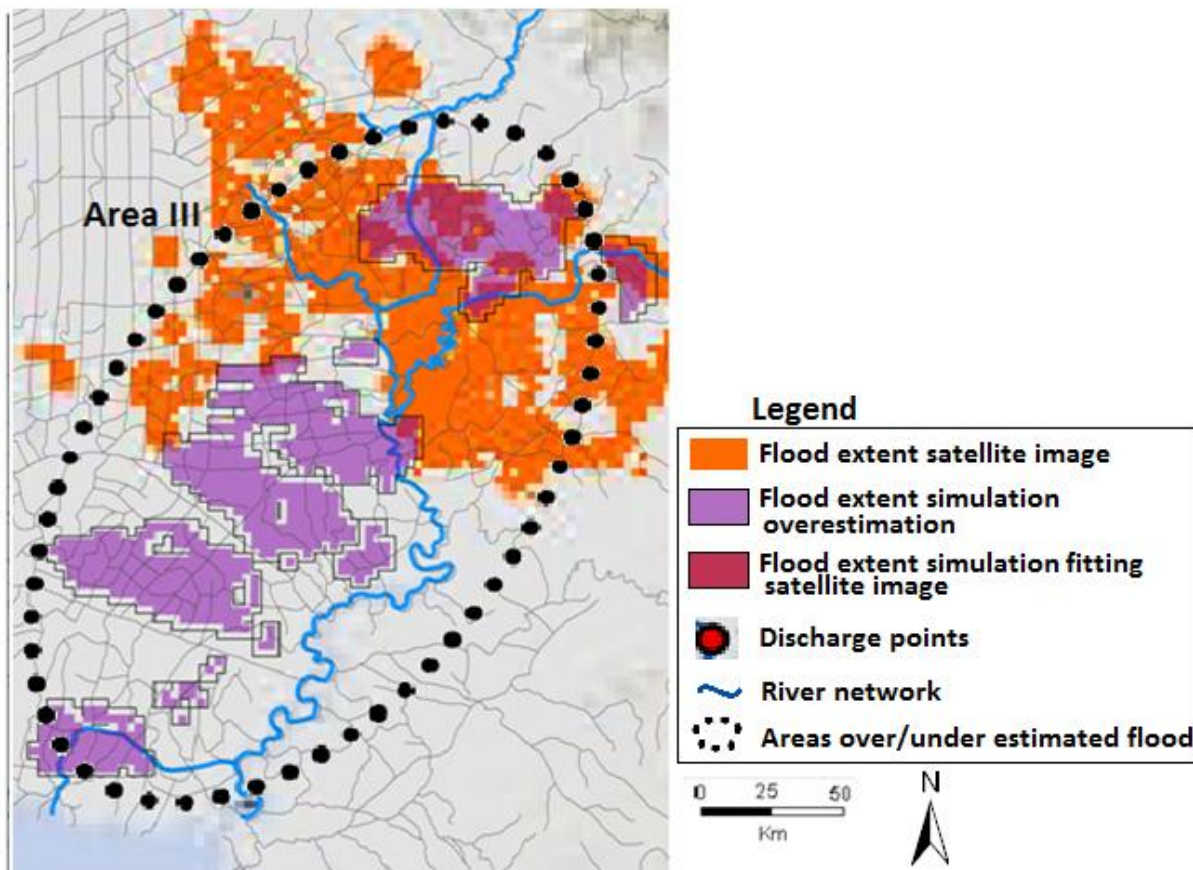


Figure 6-21 The flood extent in area III for mid-September with the river network and the canal network which is not included in the simulation.

Figure 6-21 displays all the rivers and canal in the area III. In red the river network which is used in the rapid flood model is displayed. The black lines are the lower order drainage network which were left out of the simulations. If the river network of lower order drainage network would have been included in the simulation this would allow the high waters to be distributed over all these canals.

Because these canals will have probably smaller cross-sections, they will flood faster than the large river.

6.4.2 Simulation for mid-October

In the simulation for mid-October, the flood extent is overall smaller than the satellite flood images. Figure 6-22 shows the flood extent maps.

Flood waters: mid- October 2011

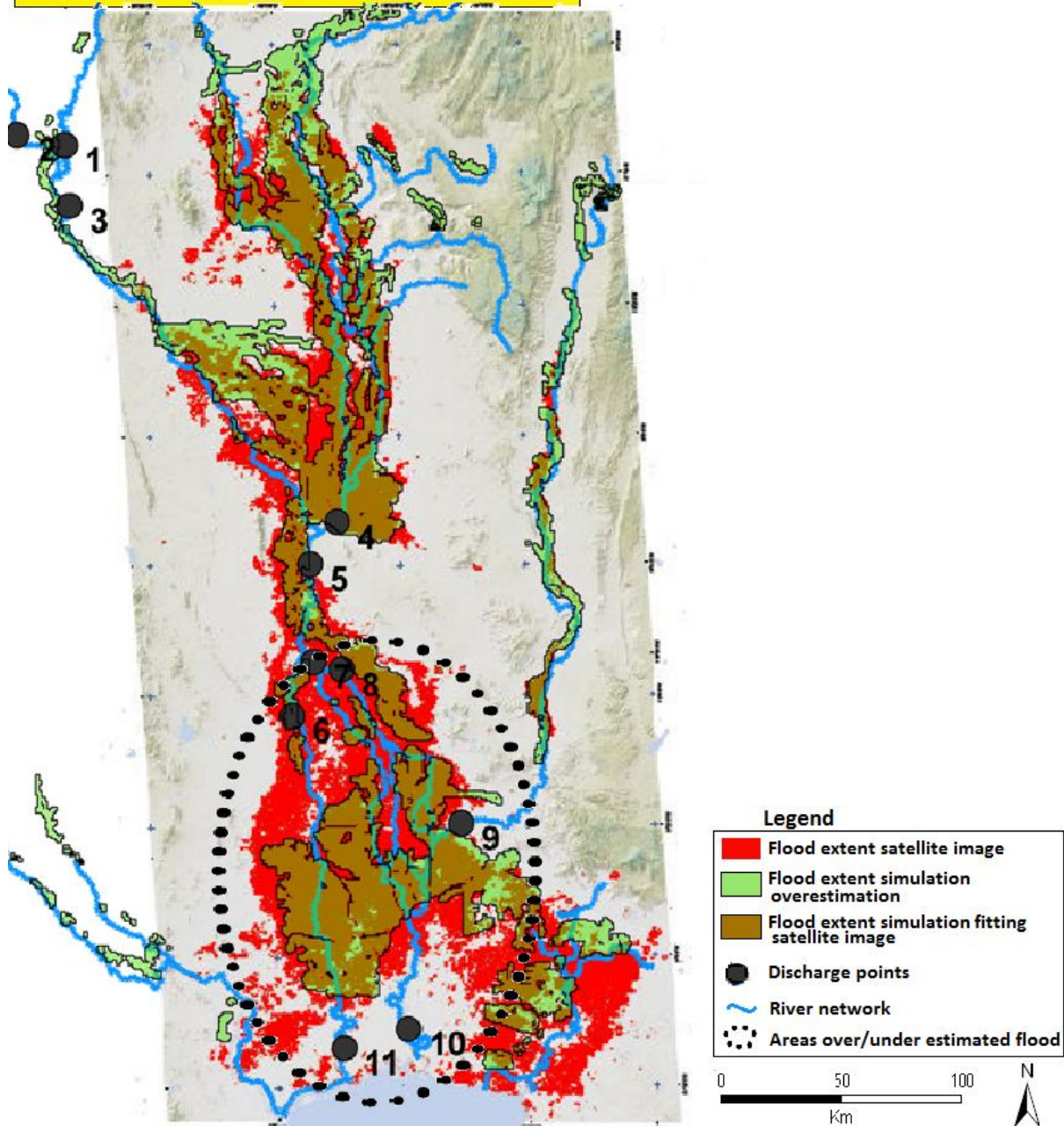


Figure 6-22 Flood extent map for mid-October of the simulation(in green transparent) and of the satellite image (in red). The river network is in blue. In the black dotted circle is the area where the simulated flood is significantly smaller than the satellite image.

Figure 6-22 shows a large area (area IV in the dotted circle) where the simulated flood extent does not fit the satellite image. Area IV shows overall underestimation of flood extent. The discharge points 6 and 11 are compared to each other and the points 7, 8, 9 and 10.

Westside of Area IV

The discharge point 6 is the upstream point and the discharge point 11 is the downstream point of the west side of area IV. Figure 6-23 shows the discharges of these points for the rapid flood model and the flood model of Deltares.

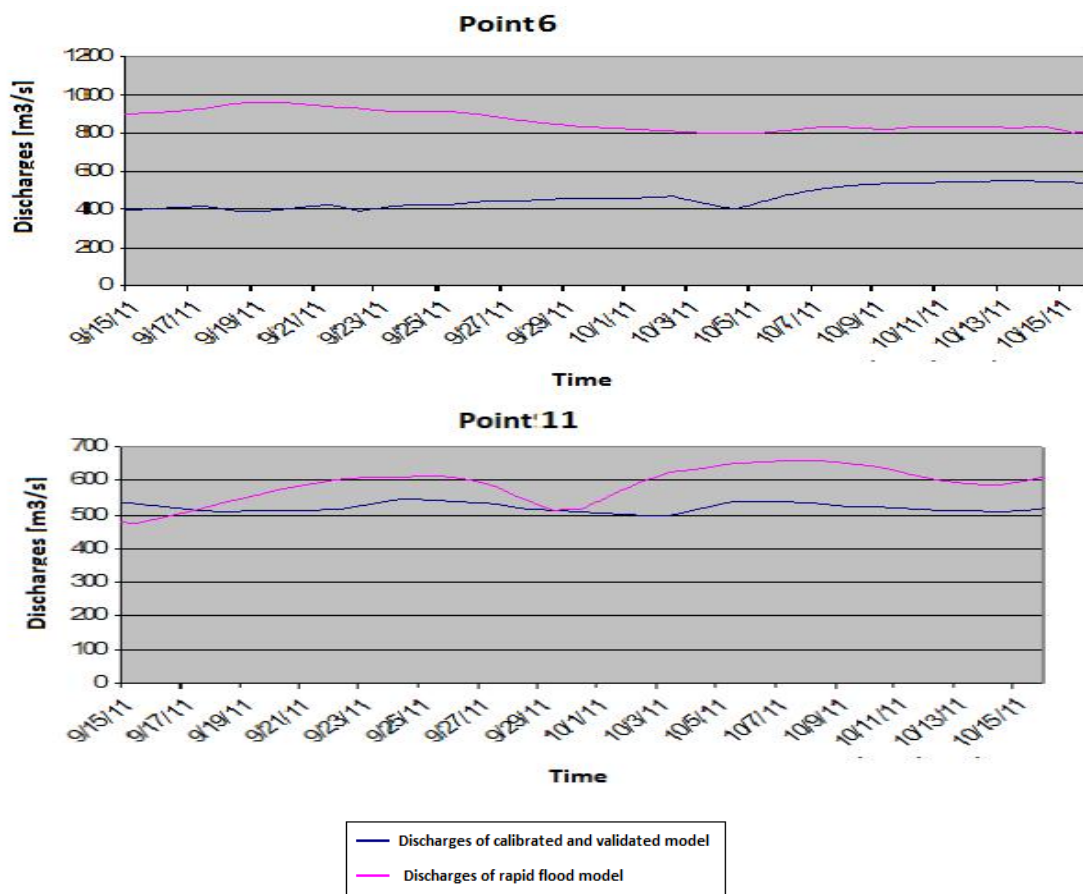


Figure 6-23 Discharges for point 6 and 11 from mid-September till mid-October

The upstream point 6 has relatively higher discharges in the rapid flood model than in the flood model of Deltares. While in the downstream point 11 the discharges are relatively similar. Even though the discharges are significantly higher in the upstream point the flood extent is underestimated with the rapid flood model. This can be an indication that the river cross sections in the rapid flood model are too large. In larger cross sections, even with larger discharges, can result in a flood extent that is smaller than in the satellite images.

It is also possible that the cross sections on the west side of area IV have the right dimensions, but the cross sections on the east side are too small. This would also lead to more water flowing through the river network on the west side of area IV.

Eastside of area IV

The discharge points 7, 8 and 9 are the upstream points and the discharge point 10 is the downstream point of the eastside of area IV. Figure 6-24 shows the discharges of these points for the rapid flood model and the flood model of Deltares.

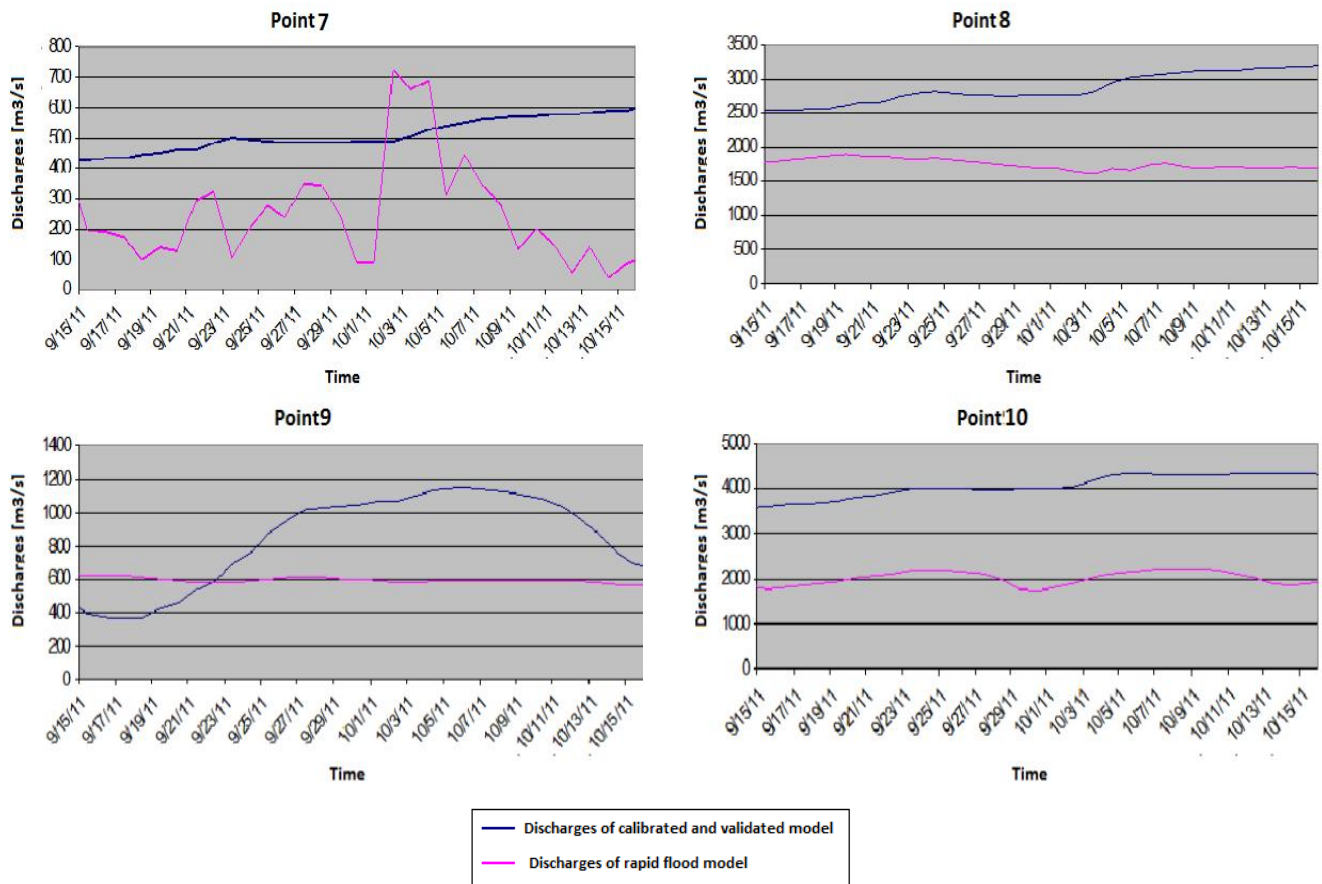


Figure 6-24 Discharges for points 7,8,9 and 10 from mid-September till mid-October

In the eastside of area IV the discharges are relatively lower in the rapid flood model.

Point 7 shows high jumps in the discharges. This indicates an irregular lateral inflow. This is similar findings found in area I from mid-September. The same as in mid-September, the lateral inflow pushes the large amount of precipitation straight into the river network without any delay.

The other three discharge points show relatively lower discharges that could result in the underestimated flood extent in this area.

So for area IV, most of the water goes through the Westside of the river network, causing relatively higher discharges. The indication that on the west side the cross sections in the river network are relative larger explains why the water flows through the west side instead of the east side.

Another explanation for the underestimated flood can be derived by comparing the DEM, flood extent from the rapid flood model and the satellite image. Figure 6-25 shows the DEM of area IV, with different maps on top of the DEM. The different maps are layer on top of the DEM in the following order: the satellite image (transparent), the flood extent from the rapid flood model, the secondary roads, the river network and the discharge points.

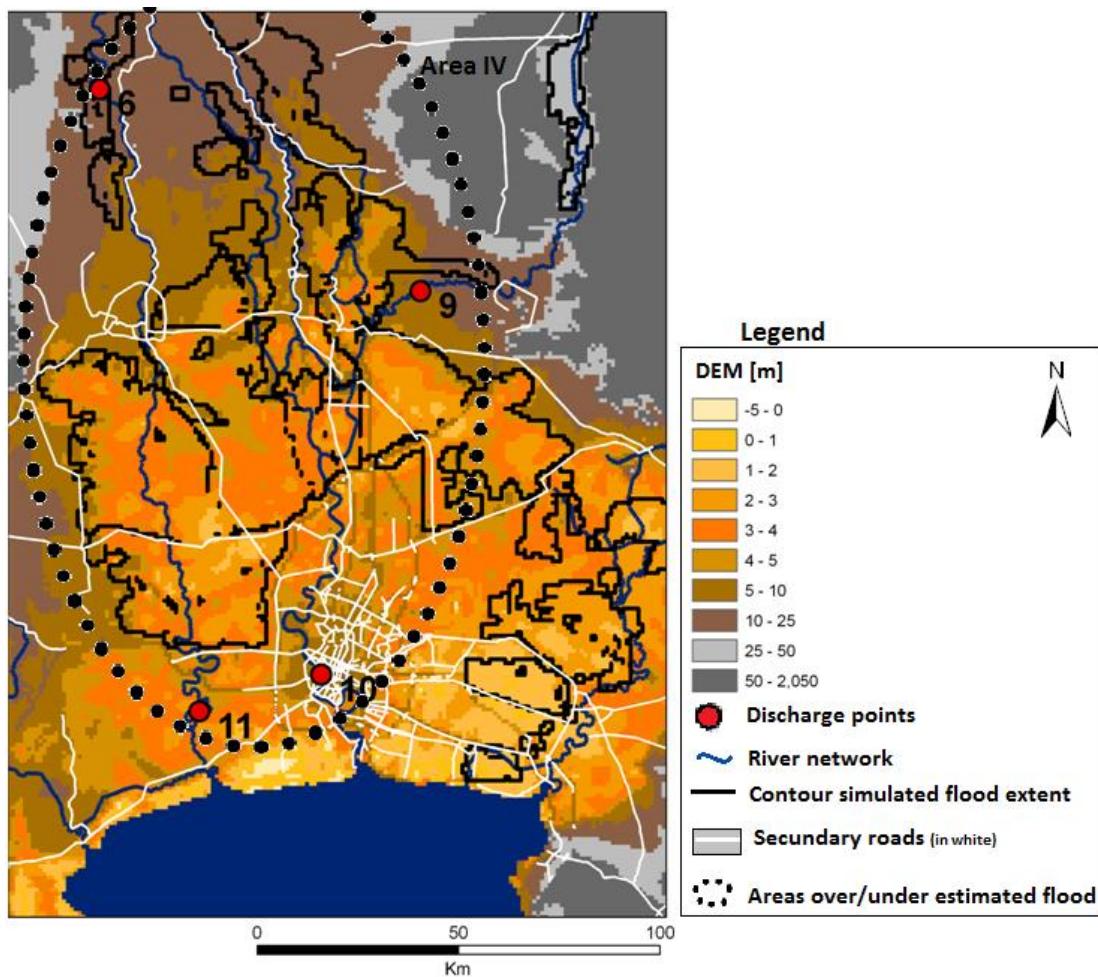
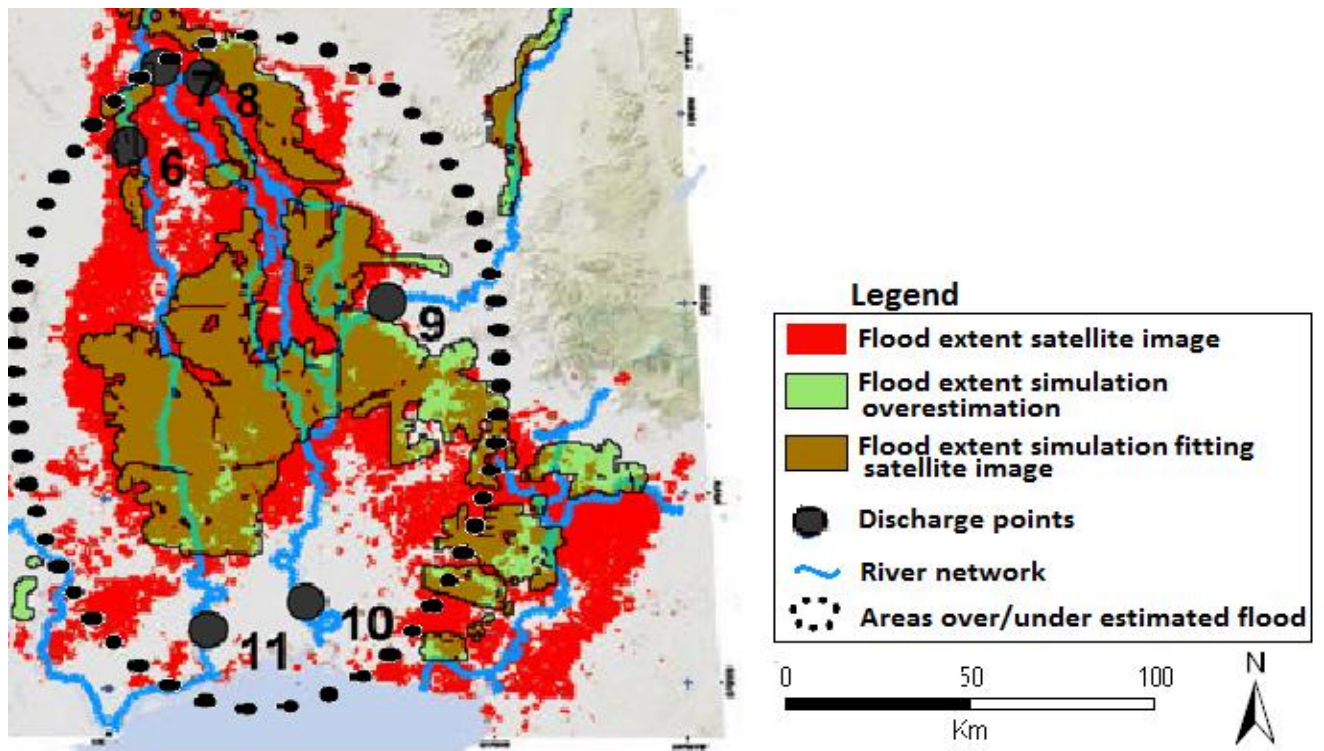


Figure 6-25 The DEM of area IV for mid-October, with layers of the satellite image and the flood extent of the rapid flood model, the secondary road layer and the river network layer on top of the DEM.

The difference between the flood extent of the rapid flood model (in green) and the satellite image (red shades) can be clarified by the DEM. The flood extent in the satellite image is red, but because of the large number layers, this image is made transparent, making the color of the satellite image in Figure 6-25 depend on the top layer. The satellite image is red shades, varying from purple to orange. The elevation difference in the DEM between 4 and 5 meters is marked with a light purple and darker purple.

Figure 6-25 shows that the flood extent of the rapid flood model is limited by two things. The gradual increase in the elevation in the DEM going north and the elevated line elements of the secondary roads. The contour of the flood extent of the rapid flood model goes together with either the line elements of the secondary roads or with the increase of the DEM from 4 to 5 meters.

For area IV for the mid-October flood, the simulated flood shows an underestimation of the flood. The analysis above indicates two reasons for this:

1. The cross sections of the river network on the west side of area IV are too large. Resulting in more water from upstream flowing into the west side river network and the causing smaller flood extent due to the larger storage in the river network. It can also be the case that the cross section in the eastside river network are too small, like was found in the simulations for mid-September.
2. The DEM is not precise enough in area IV. The increase in the elevation, going north is too large. And the elevated line elements of the secondary roads lead to compartmentalization of the flood waters.

6.4.3 Simulation for mid –November

The flood extent in mid-November has certain areas where the simulated flood is not exactly the same as the satellite image. These areas are the same areas discussed in the previous sections. The causes of the overestimation and underestimation of the flood extent in the same areas have the same explanations.

Mid-October has the largest flooded areas. The most notable in the mid-November flood extent of the satellite images is the difference between the mid-October and mid-November map. In the mid-November, the flood starts to retrieve and the flood extent becomes smaller. The retrieving parts, area I and V are circled with a black dotted line in Figure 6-26.

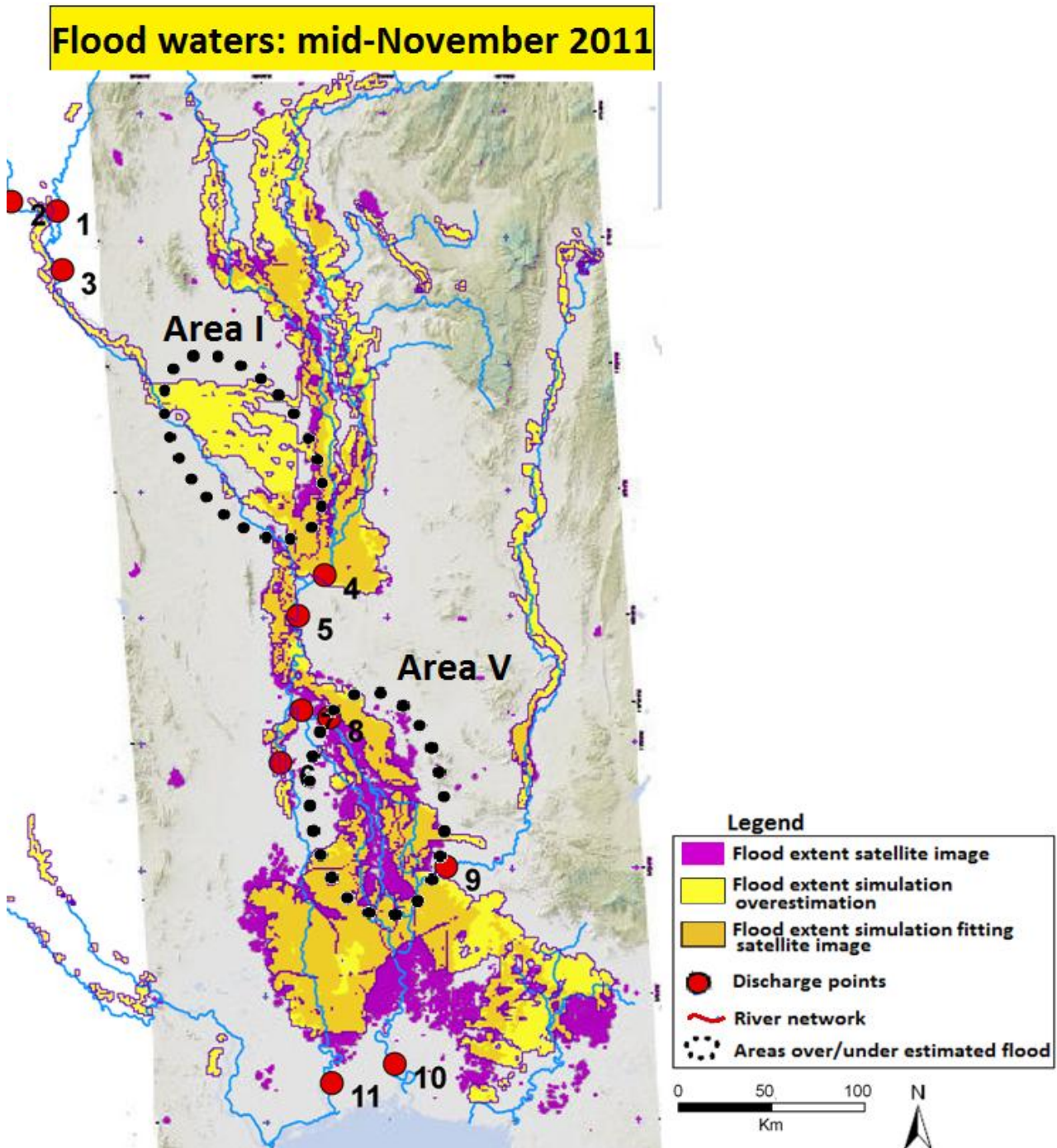


Figure 6-26 Flood extent map for mid-November of the simulation (in yellow transparent) and of the satellite image (in purple). The river network is in blue.

In area I the simulated flood is larger than the satellite image. For area I the flood extent map is similar for mid-October and mid-November. Only in mid-November the flood depth are significant lower than in mid-October. The flood depths in October are around 0.5 m and in November 0.005 m, this is only 5 mm. The flood simulation shows a retreat of the water just like in the satellite image. The retreat of the water in the simulation just goes much slower than in the real event. Especially because the simulation has been carried out till end of December. For the end December area I is still flooded, with a depth of 5 mm. This indicates that the water hardly retrieves from this area. Therefore the flood depth of 5 mm can be considered dry

In area V the flood extent shows that on the west side (between discharge point 6 and 11) the simulated flood extent is a really good fit. The simulated flood shows just like in the satellite image that flood water is retreating out of the flooded area.

In the flood model of Deltares and in the rapid flood model, the declining flood extent in November can be seen. There is a decreasing trend in all the discharge points, except for point 11. In both models the discharge point 11 shows a relative constant discharge.

The precipitation delay that is not included in the rapid flood model is discussed in the previous sections. In the previous sections by not including this delay, the sudden increase in the discharges could be explained. The rapidly decreasing discharge in point 6 can also be explained by excluding the delay of the precipitation into the lateral inflow, see Figure 6-27.

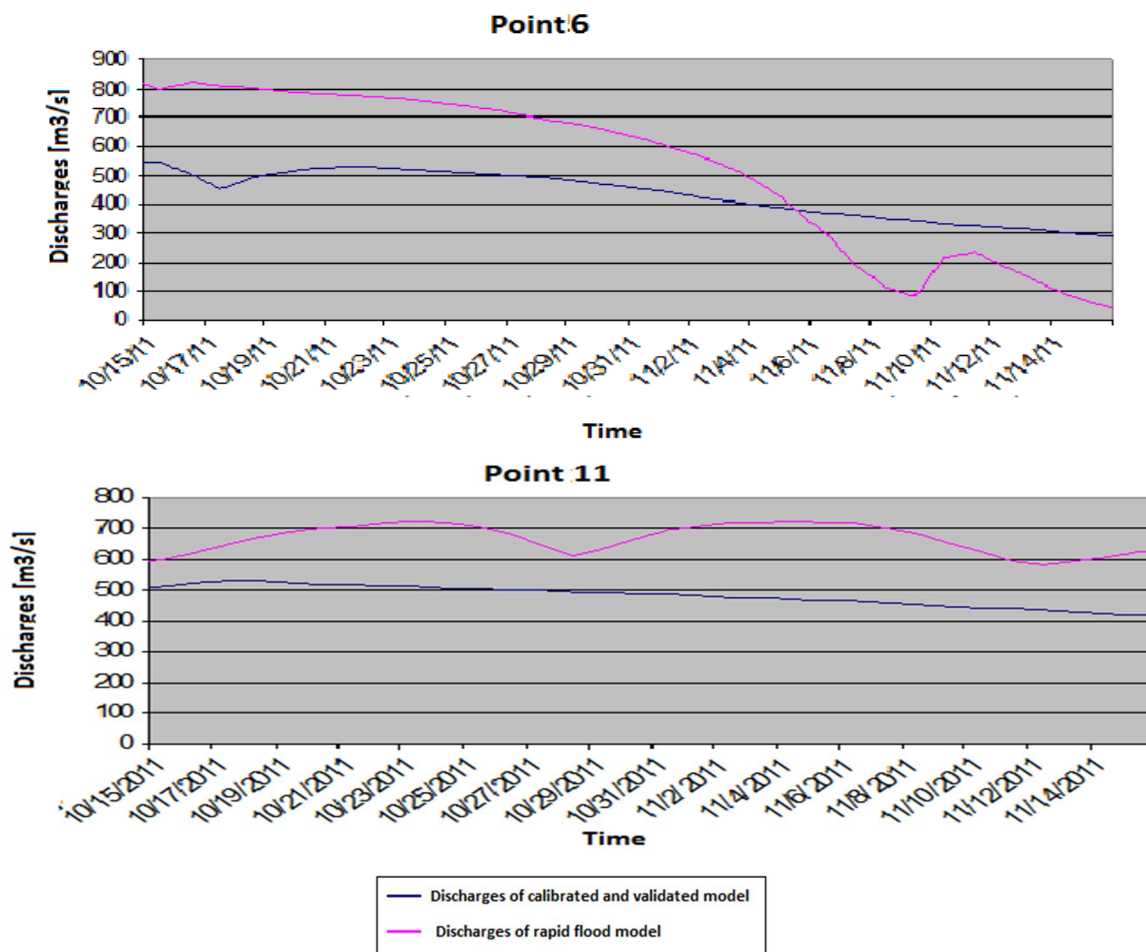


Figure 6-27 Discharge for mid-November in discharge point 6 and 11. The discharge decreases rapidly in point 6 due the exclusion of the delay in the precipitation and the later inflow.

In Figure 6-27 the rapid decreasing discharge is the result of the instantaneously relation between the precipitation and the lateral inflow. If the delay between the two was included, the high discharge was distributed more over the time.

The decrease in the discharge in point 6 has no influence on the flood extent in area V. This is also an indication that the water in the flooded area does not retrieve as fast as in the satellite images, just as was shown in area I.

The east side in area V shows again an underestimation of the flood. This is again indication that the cross section on the east side are smaller than they should be, causing the diverging of the river into the east and west , flowing more water towards the west side (which has larger cross sections) and less towards the east side. Figure 6-28 shows the lower discharges in the rapid flood model compared to the flood model of Deltares.

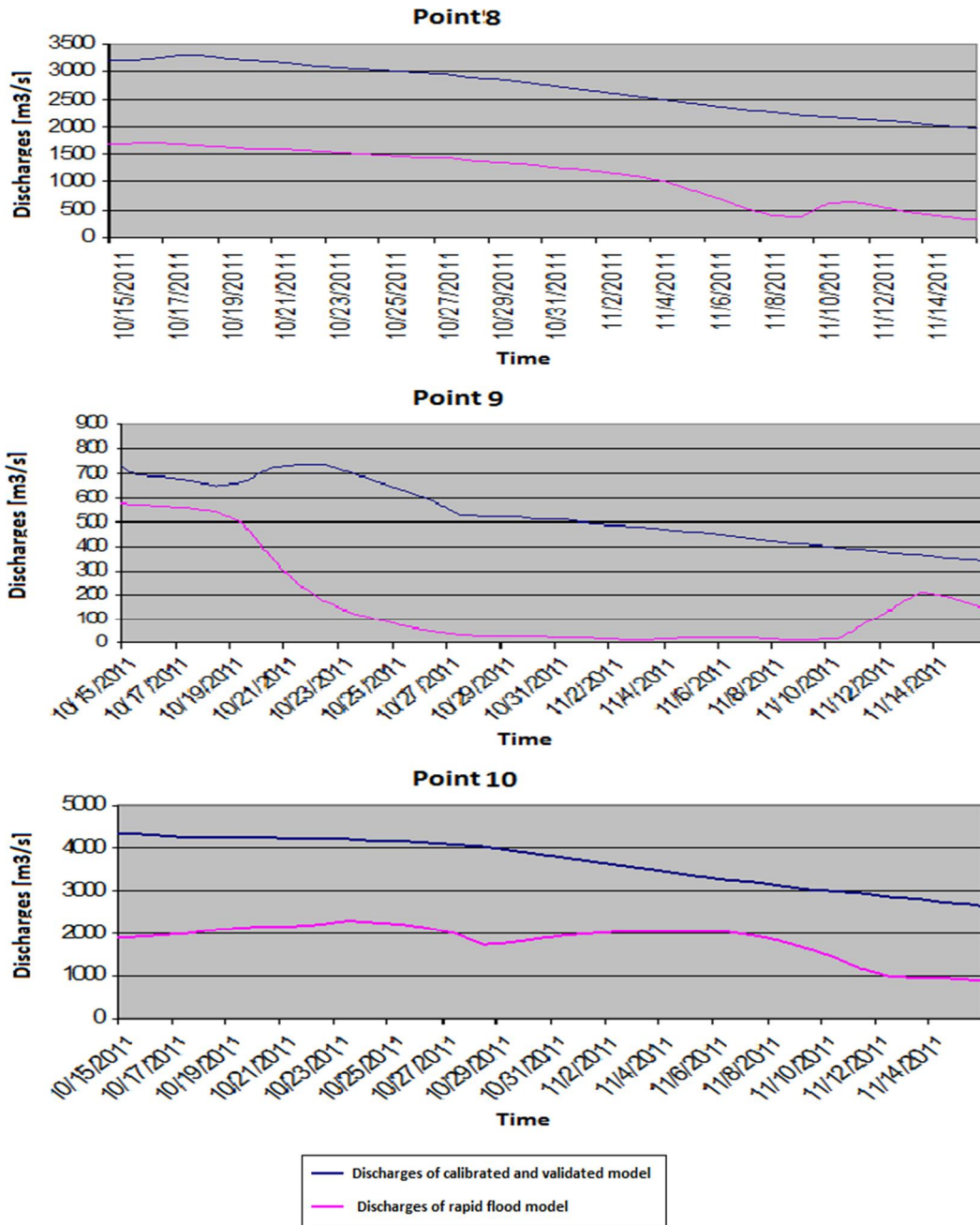


Figure 6-28 mid-November discharges in point 8, 9 and 10. The rapid flood model has much smaller discharges than the flood model of Deltares.

When the river diverges, the discharges are distributed over the two rivers, the west and east side of area V. This distribution is 1/3 towards the west and 2/3 towards the east side. The supplied discharges to the west side of river are larger than the flood model of Deltares and the east side is too low. Therefore this distribution should be different. In this case the distribution should be 1/6 to the west and 5/6 to east.

For mid-November the simulations show under and overestimated flood extent. The analyses of the result indicate these reasons for this:

1. The overestimated flood for mid-November is caused by water that retreats slower out of the flooded areas than in the satellite images. In certain areas the water does not retreat at all, but when the water depth is examined, this is so small that it can be considered dry.
2. The underestimated flood is an area that has not been flooded during the entire simulation period. The cause of this is the river diverging into two rivers and distributing the discharges over these two rivers.

6.5 Conclusions and discussion

The simulations with the rapid flood model for mid-September till mid-November are overall a good first indication of the flood extent and the propagation of the flood. The flood maps of the simulation do not fit the satellite images exactly. But that is also not the aim for this rapid flood model. This study evaluates the use of publicly available data for a rapid flood model. The aim of the rapid flood model is to produce the best prediction of a flood event in a short amount of time with limited available data.

This section is divided into two parts, first the main conclusion for the 2011 Thailand flood event study case and then the discussion on the results of this study case in comparison to the previous two study cases, the 1D and 2D flow.

6.5.1 Conclusion

The simulated flood shows a reasonably good fit with satellite images for the propagation and the flood extent.

Flood depth

The flood depth has not been examined in this case study. The absent of the real flood depths of the flood event makes it impossible to compare the simulated flood depth with anything. For this reason the flood depth has not been taking into account in this case study.

Propagation of flood

The propagation of the flood, in the simulated months, fits the satellite images. The satellite and the simulated flood start in mid-August concentrated in the north and during the month September the water starts traveling south. During mid-October the flood has the largest flood extent during the simulated period. In mid-November the satellite images shows a clear decreasing of the flooded area. In the simulated flood, the flood decreases slower.

Flood extent

For each month the areas that do not fit the satellite images have been analyzed in the previous section. These are the four main conclusions found for the over- and underestimation of the flood extent.

1. Delay in lateral inflow
In the rapid model the precipitation is directly the lateral inflow in the river network. Even though the precipitation falls on catchment areas that are kilometers away from the lateral inflow point. By using the precipitation as direct inflow, the discharges in the river network

increase and decrease rapidly. This can cause the river network to exceed its capacity causing flooding.

2. The cross sections derived from Finnegan et al.(2005)

The cross section have been obtained from the expression derived from Finnegan et al.(2005). In the simulations for mid-September and mid-October the cross section in certain areas are not correct causing over- and underestimation of the flood.

In the simulation for September the cross sections in area I are considered too small, causing large amount of water to go into the flooded areas instead of going through the river network.

In the simulation for October the cross section are either too small on the east side of area IV or too large on the west side of area IV. Causing less discharge going through the river section with smaller cross sections.

In the rapid model there are certain areas where the cross sections appear to be too small causing an overestimation of the flood extent.

3. Diverging rivers

When a river diverges into two river streams the discharges get distributed over the two river streams. In the simulations for this case study the distribution is based the 1D schematization of the river streams, the cross section, the water level downstream, the slope and the roughness of the river streams. The 2D effects are neglected, e.g. bends that cause velocity difference in the cross section. This leads to more discharge into one river stream, which can cause an overestimated flood extent and underestimation of the flood in the another river stream.

4. Coarse DEM

In the last simulated month, mid-November, the flood starts to decrease compared to mid-October in certain areas. The simulations with the rapid flood model, show that the water in the river network is decreasing, but the flood extent decreases much slower.

The accuracy of the DEM can be the cause of this. The choice to use a grid size of 1 km is based in computation time. The downside of using a 1 km grid is that it's less accurate. Due to coarse grid resolution, the elevation difference between two grids can be larger than with 500 m grid size. The simulation for mid-October shows that in the south part of the area this is the one of causes that the flood extent is underestimated.

The secondary roads, that have been elevated in the DEM cause compartmentalization of flooded areas. This causes the water not to be able to leave in the flooded areas. This can be seen in the simulation for mid-November, where the water is retreating much slower than in the satellite images.

6.5.2 Discussion

In the previous section the conclusions show that the rapid flood model gives a good indication of the propagation and the flood extent but it is not a perfect fit compared to the satellite images. The aim of a rapid flood model is to produce the best prediction of a flood event in a short amount of time. In this section the causes for the miss fits of the flood maps are discussed with solutions that are fitting for the rapid flood model.

Before the four main causes and the solutions are discussed, it needs to be mentioned that there is not one cause for the over- and underestimation of the flood extent. The combination of all four previous mentioned causes can contribute to a better prediction of a flood event. Here the causes and the previous results found in the 1D and 2D flow are discussed.

1. Delay in lateral inflow

The conclusions of the previous chapters, the 1D and 2D flow, showed that the roughness coefficient of the flood plains and the upstream boundary conditions have the highest influence on the prediction of a flood event. This can also be seen in the Thailand study case. The lateral inflow derived from the precipitation falling in the catchments should include a certain time delay depending on the distance between the catchment area and the lateral inflow point. To determine this delay not only should the distances be taken into account also the roughness coefficient of the catchment areas.

2. The cross sections derived from Finnegan et al. (2005)

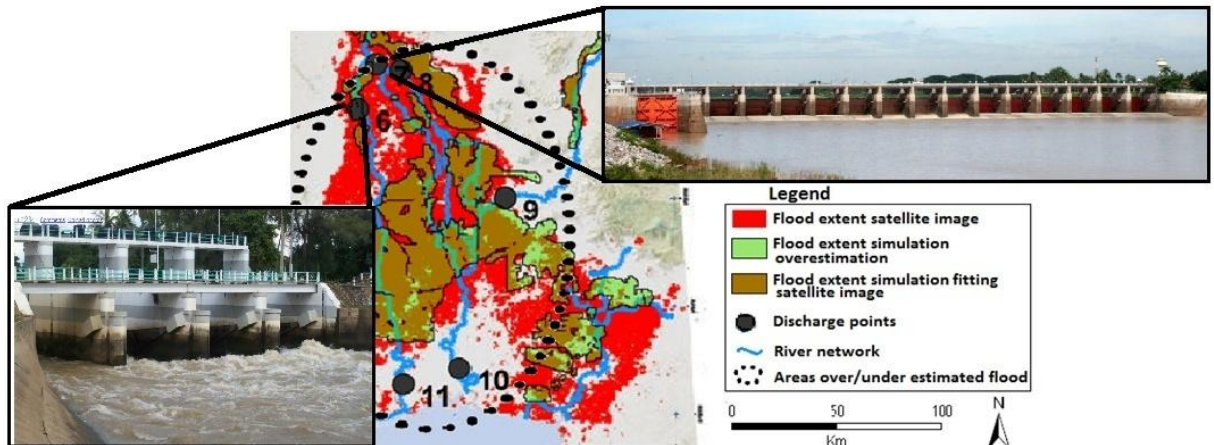
In the 1D flow study case the Chao Phraya River had been classified as a class C/DA by the ratio term (section 4.5.3). The largest difference between these two classes is the slope and the width-depth ratio. These two parameters can also be found in derivation of the cross sections from the expression of Finnegan et al. (2005). The slope has been derived from the DEM for each river network separately, varying in the north with a larger slope to the south with a smaller slope. But the width-depth ratio is fixed for the entire river network. This should also vary like the slope, being smaller in the north and larger in the south of Thailand. In the Deltares prototype Rapid Flood Model Tool, the river cross sections are not smoothed. This needs to be done manually. For the future, it is recommended to implement this into the Deltares tools of the rapid flood model.

3. Diverging rivers, ratio of splitting

The diverging rivers in the river network are difficult to implement in the rapid flood model. The distribution of the discharges is simulated in a 1D schematization, neglecting the 2D effects of diverging river.

In the rapid flood model the diverging river in the middle, discussed in the simulation mid-November, the distribution is 1/3 to the west and 2/3 to the east side. The best fit would be more in the 1/6 and 5/6.

It is surprising to see that although the distribution of the diverging river is not correct the flood is reasonable good fit. Especially because on exactly that location two barriers can be found on Google maps.



The used distribution of the discharges of 1/3 and 2/3 is not a bad estimation. The number of doors can be seen in the pictures but also on Google maps, in the west side river is 4 and of the east side 16. This is close to the distribution of the discharges derived from the cross section. The depth should also be taken into account, but it gives an insight into the real size difference between the two river arms.

4. Coarse DEM

The simulation for the mid-October and mid-November show an underestimation of the flood in the south area. This is probably linked amongst other causes to the coarse DEM. Decreasing the DEMs grid size for the entire area is not an option due to the computation time (1,5 hour for 1 km grids and 9,5 hours for 200 m grids). But because in the south of the area it is a more populated area and with more details it would be better to use a smaller grid size in this area.

In the DEM the embankments were not included. The embankments were incorporated into the rapid flood model by lowering the bed level of the rivers. The problem with this approach is that dyke breaches cannot be simulated. And this is exactly what happened in the south area. In *the Post-flood field investigation in the Lower Chao Phraya River Basin 23 – 27 January 2012* (Jonkman et al., 2012) ten breaches are reported in the southern area.

7. Conclusions and recommendations

This study contributes to the knowledge and evaluation of the usability of a rapid flood model. In this final chapter the conclusions of this study are summarized and discussed. In section 7.1 the main conclusions are listed. The main conclusions are motivated by answering the research questions in section 7.2. Suggestions to further improve the model are listed in section 7.3.

7.1 Summarized main conclusions

The current rapid flood model consists of these inputs:

Figure 7-1 Data used in the current rapid flood model

	Information needed	Source	Information from the source	Tools formatting data	Data for rapid flood model
Topographic information	Elevation	SRTM ⁸	DEM (30 m grid size)	Wavefilter Resampling	DEM grid sizes: 1 x 1 km 500 by 500 m
	Land use	Souris, 2011 ⁹	Land use and forest cover map	Design values, McCuen, 2005	Manning roughness coefficient
	Line elements	OSM ¹⁰	Roads		Main roads Secondary roads
Water system	River location	SRTM ¹¹	DEM (30 m grid size)	PCRaster D8 model, Tribe, 1992 Classification, Rosgen, 1994	River network
	River profiles	Wikipedia ¹²	Maximum and average discharges	Finnegan et al., 2005 Manning equation Classification, Rosgen, 1994	Width Depth
	River embankments			Assumptions	Along all rivers 3 m height
	Ocean conditions	Thailand navy ¹³	Tidal chart		Water levels
Precipitation	Catchment areas	GLDAS ¹⁴	Catchment areas	PCRaster	Lateral inflow points into river network
	Precipitation data	GLDAS	Rainfall rate Surface runoff Subsurface runoff	Rainfall-runoff relation, Pilgrim, 1983	40% Rainfall rate Surface runoff Subsurface runoff

- The current rapid flood model can be set up to give a prediction for a flood in one or two days. The time to produce a prediction depends on the level of details in the model, and

⁸ <http://dds.cr.usgs.gov/srtm>

⁹ <http://www.rsgis.ait.ac.th/~souris/thailand.htm>

¹⁰ www.openstreetmap.org

¹¹ <http://dds.cr.usgs.gov/srtm>

¹² http://en.wikipedia.org/wiki/List_of_rivers_by_discharge

¹³ <http://www.navy.mi.th/hydro/tide2011/BB2011H.xls>

¹⁴ http://hydro1.sci.gsfc.nasa.gov/thredds/catalog/GLDAS_NOAH025SUBP_3H/catalog.html

hence the desired accuracy of the prediction. In case more details (data) are used to increase the accuracy, the disadvantage is that the computation and simulation and data processing time of the model also increases.

The use of the Deltares Rapid Flood Model tool automatically downloads and process a number of the data. This takes half of a day. Certain data needs to be manually be processed for the rapid flood model. The time to process the data manually depends on the expertise of the modeler with the rapid flood model and the data processing skills.

- There is an abundance of publicly available data for the rapid flood model. Most of the data needs to be processed and formatted with different methods and equations before they can be used for the rapid flood model. The rapid flood model can potentially be applied for any flood prone area in the world as data used are publicly and globally available
- The terrain type has a large influence on the usability of the rapid flood model. The classification of rivers and areas by Rosgen, 1994 is used to identify these areas into mountainous, slightly hilly, delta small slope and deltas with flat areas. The applicability of the model depends on which type of river area, the area of interest belongs to. Which methods are suitable for the data and which variables have the most influence on the prediction, depends on the type of river and area. For the four classes tested in this study, the data for the most influential parameters and conditions are available publicly.

7.2 Answering research question

In this section, the research questions are answered. These are the elaborated motivations for the main conclusion listed here above.

In this study the possibilities to make a rapid prediction of a flood event based on publicly available data for any flood prone area in the world are examined. The objective of this study is:

‘Evaluation of the usability of a rapid flood model’

The three main research questions are answered in the following sections:

1. Which publicly available data and methods can be used for the simulation and prediction of a flood event?

1.1 What kind of information is required for the simulation and prediction of a flood event?

The study focuses on river flooding and is geared to the use of a rapid flood model in crisis management. The river flooding was simulated in a SOBEK 1D-2D model, because it offered a good compromise between a complex 2D model (computation time) and a simple altitude model (accuracy). These choices reduce the amount of information needed to the following:

- Origin of the flood event
 - o High discharges
 - o Intensive precipitation
 - o Sea conditions
- Type of terrain
 - o Slope
 - o Land use
- River characteristics
 - o Location
 - o Geometry (width, depth, slope etc.)

Crisis management benefits from the use of flood danger maps. The flood danger map consists of these types of information:

- the flood extent
- the propagation of flood
- the flood depth

For further details on the information required for simulation and prediction of a flood, see chapter 2.

1.2 Which publicly available data sources can provide the required information for the simulation and prediction of a flood event?

A large number of data sources are found that can provide the required information for the simulation and prediction of a flood event. Most of the publicly available data need to be processed first in order to provide the entire required information. Several methods to format the publicly available data are reviewed. Table 7-1 shows a selection of the publicly available data sources and the methods to format the data for the rapid flood model. For more details on the publicly available data see chapter 3.

Table 7-1 Selection of the public data sources available online for the rapid flood model

Type of information		Source	Information	Method formatting data
Origin flood event	Discharges	Wikipedia	Maximum discharges Average discharges	River classification (Rosgen, 1994) Expression of Finnegan (2005)
	Precipitation	GLDAS	Rainfall rate Subsurface runoff Surface runoff	Rainfall-runoff relation
	Sea conditions	Surfforecast.com	Tidal charts	Wind set-up
Type of terrain	Terrain slope	SRTM ASTERGDEM	Digital elevation map (DEM)	Wavelet Filter
	Land use	OpenStreetMap SRTM ASTERGDEM	Differentiate land use types	Manning roughness coefficient (McCuen, 2005)
River information	Geometry	Wikipedia	Maximum and average depth and width	River classification of Rosgen [1994] Expression of Finnegan [2005]
	Location	OpenStreetMap Google Maps	Coordinates	D8 model (Tribe, 1992)

2 Which parameters and conditions have the largest influence on the simulation and the prediction of a flood event?

To determine the parameters with the largest influence, four types of terrain are investigated. The four types of terrains are mountainous, slightly hilly, delta with small slope and delta with relatively flat terrain. The river classification scheme of Rosgen, 1994 is used as a tool to identify the types of

river areas and their characteristics The four types of classes examined in this study are class Aa, B, C and DA. These river areas vary in the width-depth ratio, the sinuosity, entrenchment and dominant slope range. The influences of the parameters and conditions are studied for three types of flood maps, the flood extent, flood depth and propagation of the flood. In the next subsection the results from the 1D flow case and followed by the results of the 2D flow case are discussed.

2.1 Which sets of data have the largest influence on the simulation and the prediction of flood event using 1D flow schematization?

The influence of the parameters to be derived from the data sources in the 1D schematization is determined for two characteristics of flood events, the flood depth and the propagation of the flood. The parameters that have been studied are the river and the floodplain characteristics.

Table 7-2 shows which parameters have a high influence on the predicted flood propagation and flood depth. These parameters with a high influence indicate that the accuracy of the prognosis of a flood event depends highly on the accuracy of these parameters.

Table 7-2 The parameters with a high influence on the flood prediction for the classes Aa+, B, C and DA

Type of terrain	Mountainous	Slightly hilly	Relatively flat delta	Flat areas
Classes	Aa+	B	C	DA
Water level in the flood plains	<ul style="list-style-type: none"> Floodplain roughness Width channel 	<ul style="list-style-type: none"> Floodplain roughness Bed level of channel 	<ul style="list-style-type: none"> Floodplain roughness Width floodplain Slope of terrain 	<ul style="list-style-type: none"> Floodplain roughness Width floodplain Slope of terrain
Flood wave celerity	<ul style="list-style-type: none"> Floodplain roughness Width floodplain Slope of terrain 	<ul style="list-style-type: none"> Floodplain roughness Width floodplain Bed level of channel 	<ul style="list-style-type: none"> Floodplain roughness Width floodplain Slope of terrain 	<ul style="list-style-type: none"> Slope of terrain

There are three parameters that show a negligible to small influence on the flood depth and the propagation of the flood for almost all areas, the channel roughness, the channel width and the bed level of the channel. The other three parameters, the roughness coefficient and width of the floodplain and the slope of terrain have a large influence on the flood depth and the propagation of the flood for most of the areas.

2.2 Which sets of data have the largest influence on the simulation and the prediction of flood event using a 2D flow schematization?

For the 2D schematization the influence on the flood extent, flood depth and propagation of the flood is only analyzed for the delta areas with a small slope and relatively flat terrain, classes C and DA. These areas represent the Thailand area. Concentrating on only these two classes made it possible to study more variables than in the 1D flow schematization. Besides the parameters in the 1D flow also varying conditions, e.g. up- and downstream boundary conditions and slope in perpendicular slope direction, were tested.

Table 7-3 shows the result of the most influential parameters and conditions for 2D flow.

Table 7-3 Parameters and conditions with a high influence on the prediction of a flood event for class DA.

Type of river area	Delta terrain with small slope		Delta with relatively flat terrain	
Classes	C		DA	
Slope perpendicular to the	No slope	Small slope	No slope	Small slope

channel			
Water depth	<ul style="list-style-type: none"> • Upstream boundary condition • Floodplain roughness 	<ul style="list-style-type: none"> • Upstream boundary condition • Floodplain roughness 	<ul style="list-style-type: none"> • Upstream boundary condition • Floodplain roughness • Channel roughness
Propagation of the flood	<ul style="list-style-type: none"> • Upstream boundary condition • Floodplain roughness 	<ul style="list-style-type: none"> • Upstream boundary condition • Width channel 	<ul style="list-style-type: none"> • Upstream boundary condition • Floodplain roughness • Width channel
Flood extent	<ul style="list-style-type: none"> • Peak upstream boundary condition 	<ul style="list-style-type: none"> • Tail upstream boundary condition 	

A delta with small sloped terrain, identified as class C, has the same two parameters with high influence. Both the propagation of the flood and the flood depth are highly influences by the combination of the upstream boundary conditions and the floodplain roughness.

A delta with flat terrain , class DA, shows for both the flood depth and the propagation of the flood, the highest dependency on the upstream boundary conditions and the slope perpendicular to the channel.

The flood extent was not highly sensitive to any of the parameters and conditions. Only the discharge peak showed some influence. The higher the peak of the upstream discharge, the larger the flood extent becomes. But for the area with flat terrain, class DA, not only is the discharges peak important but also the 'tail' of the discharges (rate at which the discharge reduces after the peak). It appears that in this type of area, the river area has a certain capacity, not depending on the peak discharge but more on the total volume discharged. When the capacity is reached, the peaks of the subsequent discharge causes an increase in the flood extent.

The Thailand area has been classified as a delta area, with small slopes and relatively flat terrain, class C and DA. Even though in the 1D flow the influential parameters were similar for class C and DA, the 2D flow shows that these areas can behave differently and have different influential parameters and conditions for the prediction of a flood.

3 Are the rapid flood models a feasible tool to be used for urgent prediction of a flood event for the purpose of crisis management?

The 2011 Thailand flood is the case study used to answer the final research question. The area of the Thailand case study is classified as combination of C and DA and is assumed to have the same influential parameters and conditions.

3.1 *Is a prediction with a rapid flood model possible in a short amount of time?*

The current rapid flood model can produce a prediction of a flood event in relatively short time. The current rapid flood model can be set up in 1 or 2 days by an experienced modeler. The time to produce a prediction depends on the amount of model detail. In case more details (data) are used to increase the accuracy, the disadvantage is that the computation and simulation time of the model also increases.

3.2 *Is there enough data publicly available in real time to be able to use rapid flood models in crisis management?*

There is a large amount of publicly available data online that can be used for the prediction of a flood event. Most of the data needs to be processed before it can serve as input for the rapid flood model. If the data is correctly processed, the rapid flood model is able to give a good indication of flood prediction.

In the Thailand case, there are certain data that could not be found online, like information about the locks, sluices and other hydraulic structures. Applying these data as input for the model can improve the prediction of a flood.

The flood extent from the simulations gives a good first indication of the flood extent, but does not fit the satellite images exactly. To improve the prediction of a flood these four aspects of the rapid flood model are discussed:

1. Delay in lateral inflow

In the study case of Thailand, the instant lateral inflow of the precipitation into the river network causes highly fluctuating discharges. This results in overestimations of the flood extent due to the exceedance of discharge capacity in the rivers. The same is found in the 2D flow case study, the flood extent that is highly influenced by the peak of the discharge in the delta areas with a small slope (class C). The distance and the land use of the catchment area should be used to estimate the delay of the precipitation into the river network.

2. The river cross sections

The cross sections have been obtained from using the expression derived by Finnegan et al. (2005). In the simulations in the rapid flood model the cross section in certain areas are not correct causing mainly overestimation of the flood extent. In these areas the river network has usually smaller cross sections than in reality allowing the capacity of the river to be exceeded in the simulation.

3. Diverging rivers

The diverging rivers in the river network are difficult to implement in the rapid flood model. The distribution of the discharges is simulated in a 1D schematization, neglecting the 2D effects of diverging river. This can cause more discharge into one river stream, which causes an overestimated flood extent and an underestimation of the flood in another river stream.

4. DEM

The choice to use a grid size of 1 km is based on computation time. The downside of this choice is that it's less accurate and that the elevation difference between two grids is larger than with a smaller grid size. This effect can especially be seen in the south area in the Thailand case which contains a lot of detail because it is a populated area. These details are averaged out due to the coarse DEM and can be the explanation for the weakness of the rapid flood model in this area.

Another effect due to the coarse DEM is the slow retreat of the flood. In the last simulated period, mid-November, the flood starts to retreat in southern areas compared to mid-October. The simulations with the rapid flood model correctly show that the discharges in the river network are decreasing, but the flood extent decreases much slower compared to the satellite images. One of the reasons for this can be the implementation of the secondary roads, which have been elevated in the DEM, causing compartmentalization of flooded areas. This traps the water in the flooded areas.

3.3 Is the rapid flood model applicable for any flood prone area in the world?

The rapid flood model can be applied for the two types of river areas that are investigated in this study. Due to the publicly and globally available data used, the model could potentially be applied for any flood prone area in the world. However the online data that are used, are processed with the methods and equations to be used as input for the rapid flood model. The data processing and the most influential parameters depend highly on the type of river area. For the processing methods and equations, the type of the area is used for assumptions. If an area is wrongly identified, this can lead

to wrong assumptions and the focus on the wrong parameters. This will not improve the prediction of the flood.

Therefore the type of the area has a large impact on the prognosis of the flood event. The identification of the type of river area, with the classification, is an important aspect.

7.3 Recommendations

The rapid flood model with the use of publicly available data gives a good indication of the flood event in Thailand of 2011. In this section the possible improvements and future developments of the rapid flood model are discussed.

This section is sorted into three sections:

- Improving the current rapid flood model
- Including new data sets into the rapid model
- Further developments of the rapid flood model

7.3.1 Improving the current rapid flood model

In the previous section is concluded that some of the data needed modification. It is important to note that the weaknesses of the prediction of the flood event might be fixed by improving multiple data sets or just one. The area of Thailand is a delta area with a small slope and a relatively flat terrain. This area is classified as class C and DA, based on the ratio between the forcing term (bank-full discharge and the slope of the terrain) and the river characteristics term (width and depth). If separate models were made for each area, the rapid model would perform better. For that reason it is recommended to split the rapid flood model into one model for each distinct area. The weaknesses of the prediction can be seen as two different problems for the north and the south. By using different simulations for the two areas the prediction of a flood event can be improved.

In the north in the Thailand case, the main problem is the high fluctuations in the discharges due to the instant inflow of precipitation into the river network. The lateral inflow needs a certain delay to realistically represent the precipitation into the river network. The 2D flow results show that the flood extent depends on the peak of the discharges, in an area with a small slope, class C.

It is recommended to not only take the distance between the catchment area and the inflow point into account but to also include the land use over which the precipitation needs to travel towards the lateral inflow point. This information is already in the rapid flood model, as the floodplain roughness. This was only used for the flood waters and not to the precipitation.

By delaying the lateral inflow the discharges in the river will not fluctuate that much, but will be smoothed over time. This will hopefully result in discharges that do not exceed the river capacity in an unrealistic manner. It is possible that this can even solve the problems with the established small cross section that are found with the expression of Finnegan et al. (2005).

Besides the delay in the lateral inflow, in the south in the Thailand case, the main problems are the dimensions of the cross sections and the coarse DEM.

A different method to derive the cross section, which is more suitable for a flat terrain, class DA, e.g. another width-depth ratio, could possibly result in more realistic cross sections. Comparing to the computation method used in this study, applying a larger width-depth ratio to this type of area, will result in wider cross sections and relatively higher discharge capacities. This can also be a solution for the difficulties with modeling the discharge entering the arms of a diverging river. When larger cross sections are assigned to the rivers in the south the distribution of the discharges will also change.

The miss fits of the prediction due to the coarse DEM have little to do with the type of river area. The southern area is an area with more development, like roads and urban areas. To improve the prediction in these areas more elevation details are needed. These details disappear in the coarse grid size. Splitting the area up into the northern and southern area opens up the possibility to increase the level of detail in the southern area without increasing the computation time excessively by choosing a finer grid size for the entire area.

In the current rapid flood model, the simulated flood maps are compared visually with the satellite images. In the 2D flow case study, a visual and a quantitative method was used to identify the difference in the simulations. This method or another method should be used to identify error type I and II(section 2.3.5) to give a better insight into the errors of the prediction with the rapid flood model.

7.3.2 Including new data into the rapid flood model

In this case study, the main missing data in the rapid flood model are the hydraulic structures and in particularly the barriers, e.g. sluices and locks. These barriers regulate the discharges of a river and have large influence on a flood event.

The other structure type that is missing, are the embankments. The embankments are actually implemented in the model in a simplified manner, by increasing the wet surface of the cross section by lowering the bed level. Due to this simplification, the breaching of the embankments cannot be simulated.

Gathering the data on hydraulic structures is difficult and sometimes even impossible (e.g. prediction of a dyke breach). But the inclusion into the rapid flood model should be feasible when this information is available. It is surprising that without including the hydraulic structures, the rapid flood model nonetheless produces a good first indication of the prediction of a flood. But the implementation of these structures can improve the prediction of a flood event for other areas. It can be possible that it works for this flood event, due to the large flood waters over land, and for another flood event, these structures are more significant.

7.3.3 Further developments of the rapid flood model

At the moment, the rapid flood model gives an indication of the flood propagation (when the flooding will occur), the flood extent (where the flooding will occur) and the flood depth (the severity of the flood). For further development of the rapid model the testing of measures against floods would be of added value. So instead of giving only a prediction of a flood, the rapid flood model would also be able to test measures against the flood. The measurements to prevent or reduce the consequences of a flood event would be helpful for crisis management. The type of measurements can be a bypass, retention areas, reinforcing weak links in the dykes or evacuating areas.

Figure 2-1 Origins of flood events	5
Figure 2-2 A call to 911 to report flooding	7
Figure 2-3 Flood extent map from DEM all levels below 20 m are inundation areas	15
Figure 3-1 Distance to next downstream gauging station. Darker color means closer stations, while the lighter colors means increasing distance to the nearest downstream stations, which blends into the white colored unmonitored landmass (Fekete and Vörösmarty, 2002)	18
Figure 3-2 Station measuring sea water levels ("Sea Level Trends," 2012)	18
Figure 3-3 A bottom profile (black line) with the absolute and relative accuracy errors (brown, grey and red line)	21
Figure 3-4 Normal distribution of the vertical accuracy	21
Figure 3-5 Longitudinal, cross-sectional and plan views of stream types (Rosgen, 1994)	22
Figure 3-6 Classification of channels with the important parameter, the bed material (Rosgen, 1994)	23
Figure 3-7 Entrenchment ratio for class A, B and C (Rosgen, 1994)	23
Figure 3-8 Cross section of a river with dykes in the Netherlands	24
Figure 3-9 The entrenchment ratio is ratio between flood-prone width and the bank-full width	25
Figure 3-10 Wind set-up by storm surge (Molenaar et al., 2008)	26
Figure 3-11 Space-wave length tiles for a) Fourier basis functions b) Wavelet basis functions	26
Figure 3-12 Using a DEM to determine the flow directions and the channel network	27
Figure 3-13 Virtual stations, the red rectangles, based on the intersection between the channel, in black, and the satellite orbits, the white lines	27
Figure 3-14 Width to depth ratio with bank-full width [http://www.fgmorph.com/fg_3_19.php]	28
Figure 3-15 Buffer zone for the Upper Negro River	28
Figure 4-1 Schematization of the cross section of a river and flood plain area	31
Figure 4-2 Values of first term on the vertical axes, $Q_{tot} b^{12}$ and second term on the horizontal axes, $Bc * z b * 1nC * Rc^{23}$ of Equation 4-10 for all classes	38
Figure 4-3 The Meuse river at Maastricht	39
Figure 4-4 View of the Rhine from the source till the estuary. The yellow section is the Middle Rhine.	39
Figure 4-5 The Nile River, with in blue the upper-middle part between Aswan and Edfou	39
Figure 4-6 Example of the angle of the water depth in the floodplains	42
Figure 4-7 The angle of the components	43
Figure 4-8 The effect of a uniform distribution of the components on the water level of the floodplains for class Aa+.	43
Figure 4-9 The effect of a uniform distribution of the components on the water level of the floodplains for class B.	44
Figure 4-10 The effect of a uniform distribution of the components on the water level of the floodplains for class C.	45
Figure 4-11 The effect of a uniform distribution of the components on the water level of the floodplains for class DA.	46
Figure 4-12 The effect of a uniform distribution of the components on the flood wave celerity of the floodplains for class Aa+	48
Figure 4-13 The effect of a uniform distribution of the components on the flood wave celerity of the floodplains for class B	49
Figure 4-14 The effect of a uniform distribution of the components on the flood wave celerity of the floodplains for class C	50
Figure 4-15 The effect of a uniform distribution of the components on the flood wave celerity of the floodplains for class DA	51
Figure 5-1 Schematization in SOBEK of the area of 200 by 300 km with a slope from north to south of 0.005; the channel situated in the middle in blue, the boundaries at the north and south side of the channel in the pink squares and the black lines dividing the grid cells.	57

- Figure 5-2 Example of two tests; test X (the reference simulation) and test Y; The grid cells indicate if they are flooded (1) or not (0). The difference of the tests X and Y indicate if in both simulations the grid is flood (0 and white), only flooded in test X (1 and red) or only flooded in test Y (-1 and blue). 58
- Figure 5-3 An example of the spatially plotted water depth of two simulations. And the spatially plotted difference of reference simulation X1 and simulations X2, X3 and X4. Each grid cell has a water level with related shade of blue or red. 59
- Figure 5-4 an example for the cumulative distribution of the four examples 60
- Figure 5-5 The different upstream discharges for tests 1 for class C 63
- Figure 5-6 The different downstream water levels for tests 2 for class C 64
- Figure 5-7 The discharge direction depends on the difference of the water level of the channel and the imposed water level of the downstream boundary 64
- Figure 5-8 Cross section of the area with no slope and a small slope in the direction perpendicular to the channel flow 65
- Figure 5-9 The influence on the water depth for class C of the simulations with varying conditions and characteristics of the flood event. The upstream boundary is the only event condition with a high influence. 67
- Figure 5-10 The influence on the propagation of the flood for class C of the simulations with varying conditions and characteristics of the flood event. The upstream boundary is the only event condition with a high influence. 68
- Figure 5-11 The influence on the water depth for class C for the simulations of the event conditions in combination with the parameters. For each event conditions the influence of each parameter is expressed in the increase of the influence of the event condition. 69
- Figure 5-12 The influence on the propagation of the flood for class C for the simulations of the event conditions in combination with the parameters. For each event conditions the influence of each parameter is expressed in the increase of the influence of the event condition. 70
- Figure 5-13 The differences in the spatial flood extent for the varying upstream boundary, zoomed into the flooded area. The simulation with a constant upstream boundary condition (test 1-1-A) is compared to the upstream boundary in the triangle shape (test 1-1-B) and the parabolic shape (test 1-1-C). 71
- Figure 5-14 The influence on the water depth of the flood in class DA for the simulations with varying conditions and characteristics of the flood event. The upstream boundary conditions and the delay (timing) of the boundary conditions are the event conditions with a small influence. The downstream boundary conditions have no influence on the water depth 72
- Figure 5-15 The influence on the water depth of the flood in class DA for the simulations with varying conditions and characteristics of the flood event. The downstream boundary conditions have no influence on the water depth. The other boundary conditions have a small influence on the propagation of the flood. 72
- Figure 5-16 The influence on the water depth for class DA for the simulations of the event conditions in combination with the parameters. For each event conditions the influence of each parameter is expressed in the increase of the influence of the event condition. 73
- Figure 5-17 The influence on the propagation of the flood for class DA for the simulations of the event conditions in combination with the parameters. For each event conditions the influence of each parameter is expressed in the increase of the influence of the event condition. 74
- Figure 5-18 The difference in the flood extent for the class DA for the test 1-1-B (the triangle shaped upstream discharge) and the test 1-1-C (the parabolic shaped upstream discharge) compared to the test 1-1-A (constant upstream discharge). 74
- Figure 5-19 The three different shapes for the upstream discharge. The area under the three graphs for the last 40 hours of the simulation is colored with related color of the graph. 75

Figure 5-20 For the flood extent for the class DA, the simulation with a slope in the direction perpendicular to the channel flow, the test 2-1-B (the triangle shaped upstream discharge) and the test 2-1-C (the parabolic shaped upstream discharge) are compared to the test 2-1-A (constant upstream discharge)	76
Figure 5-21 Decision tree for which data has priority to be obtained for the classes C and DA for the prediction of the water depth of the flood.	78
Figure 5-22 Decision tree for which data has priority to be obtained for the classes C and DA for the prediction of the propagation of the flood.	79
Figure 5-23 The slope in the direction perpendicular to the channel approximates a smaller width of the flood plains.	81
Figure 6-1 Digital elevation model from SRTM of Thailand with a grid size of 1km	85
Figure 6-2 The land use and forest cover map in the area of interest in Thailand	87
Figure 6-3 the main and secondary roads from OSM projected onto the DEM	89
Figure 6-4 PCRaster uses the DEM to determine the flow directions and the drainage network	90
Figure 6-5 Rivers and streams determined with PCRaster	91
Figure 6-6 the area of interest divided into catchment areas. The catchment points are the points where the precipitation flows out of the catchment area into another catchment area or into the river . The total amount of catchment areas is 516.	94
Figure 6-7 The relation between precipitation, surface and subsurface runoff	95
Figure 6-8 The flood extent and propagation from August till November 2011 (UNITAR_UNOSAT, n.d.)	98
Figure 6-9 Map of the area of interest with the eleven places where the discharges are known	99
Figure 6-10 Flood extent in yellow for mid-August	101
Figure 6-11 Flood extent for the simulations with and without main road and the validation flood extent map mid-August	103
Figure 6-12 Side view of a river section before (upper view) and after smoothing (lower view)	104
Figure 6-13 Flood extent for the simulations with and without dyke implementation and the validation map of mid-August displayed as layers on top of the area of interest.	105
Figure 6-14 the flood extent map for the simulations with three precipitation data inputs and the validation map of mid-August, as layers on top of the area of interest.	106
Figure 6-15 map of the simulated flood extent of mid-August is the red layer. The flood extent map from satellite image is the yellow layer. In blue circles the excessive simulated flood extent.	107
Figure 6-16 Flood extent map for mid-September of the simulation(in purple) and of the satellite image (in orange). In the black dotted circles are the three areas where the simulated flood exceeds the actual flood.	109
Figure 6-17 Overestimated flood in Area I	110
Figure 6-18 Discharges for the points 1,2 ,4 and 5 in the area I	110
Figure 6-19 Overestimated flood in area II	112
Figure 6-20 Discharges for point 6 and 11 in the area II for mid-September	112
Figure 6-21 The flood extent in area III for mid-September with the river network and the canal network which is not included in the simulation.	113
Figure 6-22 Flood extent map for mid-October of the simulation(in green transparent) and of the satellite image (in red). The river network is in blue. In the black dotted circle is the area where the simulated flood is significantly smaller than the satellite image.	114
Figure 6-23 Discharges for point 6 and 11 from mid-September till mid-August	115
Figure 6-24 Discharges for points 7,8,9 and 10 from mid-September till mid-October	116
Figure 6-25 The DEM of area IV for mid-October, with layers of the satellite image and the flood extent of the rapid flood model, the secondary road layer and the river network layer on top of the DEM.	117
Figure 6-26 Flood extent map for mid-November of the simulation(in yellow transparent) and of the satellite image (in purple). The river network is in blue.	119

Figure 6-27 Discharge for mid-November in discharge point 6 and 11. The discharge decreases rapidly in point 6 due the exclusion of the delay in the precipitation and the later inflow. 120

Figure 6-28 mid-November discharges in point 8, 9 and 10. The rapid flood model has much smaller discharges than the flood model of Deltares. 121

Table 0-1 The most influential parameters for the 1D flow case study per type of river area	vi
Table 0-2 the most influential parameters for the 2D flow case study.....	vii
Table 2-1 Different users of flood maps, their purposes and an example.....	8
Table 2-2 Systematic flood mapping increasing information down table (Merz et al., 2007) [give examples with pictures].....	8
Table 2-3 Spatial scales for a flood map	9
Table 2-4 Time scales for a flood map	10
Table 2-5 Real flood event compared to the prediction of flood event.....	10
Table 2-6 Comparison 'predictive' models with modeling flood inundation and standard hydraulic models. Complexity increases down table (Bates and De Roo, 2000).....	13
Table 2-7 Steps to setup and run a flood model	14
Table 2-8 Type of choices for the flood map for this study	16
Table 3-1 Overview of available on-line data	20
Table 3-2 Accuracy of the SRTM and ASTER GDEM data ("SRTM Statistics," 2012 and <i>ASTER Validation Team</i> , 2011).....	20
Table 4-1 Classification for types of area varying in slope, width-depth ratio and cross-section [draw better pictures]	31
Table 4-2 Values for the components of the flow for the channel and flood plains in the schematization	35
Table 4-3 Example of calculations of Class Aa+ with average values of the components and varying values of i_b	35
Table 4-4 Ratio of the first and the second term for all classes.....	38
Table 4-5 Values for the first and second term (Equation 4-10) and the ratio (Equation 4-16) of these two terms for the three real rivers.....	40
Table 4-6 The values for the water level of the floodplain due to change in values of the components for class Aa+	44
Table 4-7 The values for the water level of the floodplain due to change in values of the components for class B	45
Table 4-8 The values for the water level of the floodplain due to change in values of the components for class C	46
Table 4-9 The values for the water level of the floodplain due to change in values of the components for class DA.....	47
Table 4-10 All classes with the difference in the water level of the floodplain for the uniform distribution of the components and the angle of the components.....	47
Table 4-11 The values for the flood wave celerity due to change in values of the components for class Aa+ ..	49
Table 4-12 The values for the flood wave celerity due to change in values of the components for class B	50
Table 4-13 The values for the flood wave celerity due to change in values of the components for class C	51
Table 4-14 The values for the flood wave celerity due to change in values of the components for class DA... ..	52
Table 4-15 The difference in the flood wave celerity for varying values of the components for call classes ...	52
Table 4-16 For each class the components are divided into three groups according to their influence on the water level of the floodplains and their influence on the flood wave celerity.....	53
Table 5-1 an example of the normal distribution: he median, the angle, the factor of difference and the factor of influence for five normal distributions.....	61
Table 5-2 Differences between the classes C and DA with the range in values for the parameters.....	61
Table 5-3 Tests 1 for the synthetic events for the boundary conditions	63
Table 5-4 Tests 2 for the slope in the direction perpendicular to the channel flow.....	65
Table 5-5 The minimum (test set 1 and test set 2) and maximum values (test set 3) for the parameters for class C and DA.....	66
Table 5-6 The influence of the parameters on the water depth of the flood plains on the flood wave celerity for the 1D flow case study.	80

Table 6-1 Types of area with their original code and the assigned Manning’s coefficient..... 88

Table 6-2 the rainfall runoff relation for the GLDAS data 95

Table 6-3 Overview of publicly available data, sources and the tools to format the data for the rapid flood model 96

Table 7-1 Selection of the public data sources available online for the rapid flood model 128

Table 7-2 The parameters with a high influence on the flood prediction for the classes Aa+, B, C and DA ... 129

Table 7-3 Parameters and conditions with a high influence on the prediction of a flood event for class DA. 129

References

- An Introduction to Wavelets: Wavelet versus Fourier Transforms [WWW Document], n.d. URL www.amara.com/IEEEwave/IW_wave_vs_four.html (accessed 7.13.12).
- Apel, H., Aronica, G.T., Kreibich, H., Thieken, A.H., 2008. *Flood risk analyses—how detailed do we need to be?* *Natural Hazards* 49, 79–98.
- ASTER Global Digital Elevation Model Version 2 – Summary of Validation Results (ASTER GDEM Validation Team), 2011. . Compiled by Dave Meyer on behalf of the NASA Land Processes Distributed Active Archive Center and the Joint Japan-US ASTER Science Team.
- Bates, P.D., De Roo, A.P.J., 2000. *A simple raster-based model for flood inundation simulation*. *Journal of Hydrology* 236, 54–77.
- Belknap, J.K., Mitchell, S.R., O'Toole, L.A., Helms, M.L., Crabbe, J.C., 1996. *Type I and type II error rates for quantitative trait loci (QTL) mapping studies using recombinant inbred mouse strains*. *Behavior Genetics* Vol. 26, 149–160.
- Booth, D.B., Jackson, C.R., 1997. *URBANIZATION OF AQUATIC SYSTEMS: DEGRADATION THRESHOLDS, STORMWATER DETECTION, AND THE LIMITS OF MITIGATION*. *Journal of the American Water Resources Association* 33, 1077–1090.
- Cook, A., Merwade, V., 2009. *Effect of topographic data, geometric configuration and modeling approach on flood inundation mapping*. *Journal of Hydrology* 377, 131–142.
- de Moel, H., van Alphen, J., Aerts, J.C.J.H., 2009. *Flood maps in Europe – methods, availability and use*. *Natural Hazards and Earth System Science* 9, 289–301.
- Deckers, P., Kellens, W., Reyns, J., Vanneuville, W., Maeyer, P., 2009. A GIS for Flood Risk Management in Flanders, in: Showalter, P.S., Lu, Y. (Eds.), *Geospatial Techniques in Urban Hazard and Disaster Analysis*. Springer Netherlands, Dordrecht, pp. 51–69.
- Duckstein, L., Kisiel, C.C., 1971. *EFFICIENCY OF HYDROLOGIC DATA COLLECTION SYSTEMS ROLE OF TYPE I AND II ERRORS*. *Journal of the American Water Resources Association* 7, 592–604.
- European Environment Agency, 2010. *Mapping the impacts of natural hazards and technological accidents in Europe : an overview of the last decade*. The Agency, Copenhagen, Denmark.
- EXCIMAP, 2007. Handbook on good practices for flood mapping in Europe, European exchange circle on flood mapping.
- Fekete, B.M., Vörösmarty, C.J., 2002. The current status of global river discharge monitoring and potential new technologies complementing traditional discharge measurements. Presented at the PUB Kick-Off Meeting, Brasilia.
- Finnegan, N.J., Roe, G., Montgomery, D.R., Hallet, B., 2005. Controls on the channel width of rivers: Implications for modeling fluvial incision of bedrock. *Geology* 33, 229.
- Frey, H., Paul, F., 2012. On the suitability of the SRTM DEM and ASTER GDEM for the compilation of topographic parameters in glacier inventories. *International Journal of Applied Earth Observation and Geoinformation* 18, 480–490.
- Hirt, C., Filmer, M.S., Featherstone, W.E., 2010. Comparison and validation of the recent freely available ASTER-GDEM ver1, SRTM ver4.1 and GEODATA DEM-9S ver3 digital elevation models over Australia. *Australian Journal of Earth Sciences* 57, 337–347.
- Horritt, M.S., Bates, P.D., 2002. Evaluation of 1D and 2D numerical models for predicting river flood inundation. *Journal of Hydrology* 268, 87–99.
- Hoss, F., Jonk, S.N., Maaskant, B., 2011. A comprehensive assessment of multilayered safety (meerlaagsveiligheid) in flood risk management - TU Delft Discover. Presented at the 5th International Conference on Flood Management, Tokyo, Japan.
- Impact Forecasting LLC, 2012. 2011 Thailand Floods Event Recap Report.

- Jonkman, S.N., Vardhanabhuti, B., Blommaart, P., Hardeman, B., Kaensap, K., van der Meer, M., Schweckendiek, T., Vrijling, J.K., 2012. Post-flood field investigation in the Lower Chao Phraya River Basin 23 – 27 January 2012 (No. Final report). ENW.
- Kellenberg, D.K., Mobarak, A.M., 2008. Does rising income increase or decrease damage risk from natural disasters? *Journal of Urban Economics* 63, 788–802.
- Kiss, R., n.d. Determination of drainage network in digital elevation models, utilities and limitations [WWW Document]. URL www2.sci.u-szeged.hu/foldtan/geomatematikai_szakosztaly/JHG/default.htm (accessed 7.11.12).
- Koudijs, M., 2012. USING ICESAT/GLAS LASER ALTIMETRY FOR WATER LEVEL ESTIMATIONS IN THE MEKONG RIVER. Technical University Delft, Delft.
- Leon, J.G., Calmant, S., Seyler, F., Bonnet, M.-P., Cauhopé, M., Frappart, F., Filizola, N., Fraizy, P., 2006. Rating curves and estimation of average water depth at the upper Negro River based on satellite altimeter data and modeled discharges. *Journal of Hydrology* 328, 481–496.
- List of rivers by discharge - Wikipedia, the free encyclopedia [WWW Document], n.d. URL http://en.wikipedia.org/wiki/List_of_rivers_by_discharge (accessed 11.7.12).
- Mc Gahey, C., Samuels, P.G., Knight, D.W., O'Hare, M.T., 2008. Estimating river flow capacity in practice. *Journal of Flood Risk Management* 1, 23–33.
- McCuen, R.H., 2005. *Hydrologic analysis and design*, 3rd ed. ed. Pearson Prentice Hall, Upper Saddle River, N.J.
- Merz, B., Thielen, A.H., Gocht, M., 2007. Flood Risk Mapping At The Local Scale: Concepts and Challenges, in: Begum, S., Stive, M.J.F., Hall, J.W. (Eds.), *Flood Risk Management in Europe*. Springer Netherlands, Dordrecht, pp. 231–251.
- Middle Rhine - Wikipedia, the free encyclopedia [WWW Document], 2012. URL www.en.wikipedia.org/wiki/Middle_Rhine (accessed 11.5.12).
- Molenaar, W.F., van Baars, S., Kuijper, H.K.T., 2008. *Manual Hydraulic structures*.
- Nicholls, R., Hoozemans, F., Marchand, M., 1999. Increasing flood risk and wetland losses due to global sea-level rise: regional and global analyses. *Global Environmental Change* 9, S69–S87.
- Nile River [WWW Document], n.d. URL www.aldokkan.com/geography/nile.htm (accessed 11.5.12).
- Nirupama, N., Simonovic, S.P., 2006. Increase of Flood Risk due to Urbanisation: A Canadian Example. *Natural Hazards* 40, 25–41.
- Pilgrim, D.H., 1983. Some problems in transferring hydrological relationships between small and large drainage basins and between regions. *Journal of Hydrology* 65, 49–72.
- Priestnall, G., Jaafar, J., Duncan, A., 2000. Extracting urban features from LiDAR digital surface models. *Computers, Environment and Urban Systems* 24, 65–78.
- Reuter, H.I., Neison, A., Strobl, P., Mehl, W., Jarvis, A., 2009. A first assessment of Aster GDEM tiles for absolute accuracy, relative accuracy and terrain parameters. *IEEE*, pp. V–240–V–243.
- Romanowicz, R., Beven, K.J., Tawn, J., 1996. Bayesian calibration of flood inundation models, in: Anderson, M.G., Walling, D.E., Bates, P.D. (Eds.), *Floodplain Processes*. Wiley, pp. 333–350.
- Rosgen, D.L., 1994. A classification of natural rivers. *CATENA* 22, 169–199.
- Sanders, B.F., 2007. Evaluation of on-line DEMs for flood inundation modeling. *Advances in Water Resources* 30, 1831–1843.
- Schumann, G., Matgen, P., Hoffmann, L., Hostache, R., Pappenberger, F., Pfister, L., 2007. Deriving distributed roughness values from satellite radar data for flood inundation modelling. *Journal of Hydrology* 344, 96–111.
- Sea Level Trends [WWW Document], 2012. URL <http://tidesandcurrents.noaa.gov/sltrends/sltrends.shtml> (accessed 11.9.12).
- Shuttle Radar Topography Mission Statistics [WWW Document], n.d. URL www2.jpl.nasa.gov/srtm/statistics.html (accessed 11.7.12).
- Souris, M., 2011. GIS data of Thailand [WWW Document]. URL <http://www.rsgis.ait.ac.th/~souris/thailand.htm> (accessed 5.1.13).

- Spaargaren, G.R., 2002. Grensmaasproject: veiligheid, natuurontwikkeling en delfstoffen :: TU Delft Institutional Repository (Master Thesis). Technical University Delft.
- Surf Forecast and Surf Reports Worldwide | Surf-forecast.com [WWW Document], n.d. URL www.surf-forecast.com/ (accessed 11.7.12).
- The World Bank Supports Thailand's Post-Floods Recovery Effort [WWW Document], 2011. URL <http://www.worldbank.org/en/news/feature/2011/12/13/world-bank-supports-thailands-post-floods-recovery-effort> (accessed 4.15.13).
- Tribe, A., 1992. Automated recognition of valley lines and drainage networks from grid digital elevation models: a review and a new method. *Journal of Hydrology* 139, 263–293.
- UNITAR_UNOSAT, n.d. Time Series Analysis of Thailand Flooding 2011 V2 [WWW Document]. URL <http://www.unitar.org/unosat/maps/THA> (accessed 4.15.13).
- Williams, G.P., 1978. Bank-full discharge of rivers. *Water Resources Research* 14, 1141.
- Workshop on Flood Maps, 2006. . Flood Awareness & Prevention Policy in border areas, Berlin.

